Politecnico di Milano
Department of Mathematics
Doctoral Programme in
Mathematical Models and Methods in Engineering

STEADY NAVIER-STOKES EQUATIONS IN DOMAINS WITH OBSTACLE AND APPLICATIONS TO THE STABILITY OF SUSPENSION BRIDGES

Doctoral Dissertation of:
Gianmarco Silvio Sperone Martí

Supervisor:
Professor Filippo Gazzola

Tutor:
Professor Riccardo Sacco

The Chair of the Doctoral Programme:
Professor Irene Maria Sabadini

2019 - Cycle XXXII

ABSTRACT

Vortex shedding is the phenomenon observed when a fluid hits a rigid structure immersed in the fluid, causing the formation of vortices on the downwind side of the obstacle. Indeed, vortices are shed alternately from one side to the other giving rise to the *von Kármán vortex street*. Shifting low-pressure zones are then created on the leeward side of the structure which, in turn, generate a fluctuating force that acts orthogonally to the flow direction; we shall refer to this force as the *lift*. When the structure considered is the deck of a suspension bridge and the fluid flow is the wind, a consequence of the von Kármán vortex street is the oscillating movement of the deck towards the low-pressure zone, a tremor known in the literature as *vortex-induced vibration*. Naturally, if the input of energy from the wind into the deck grows unsteadily, violent lift forces will appear, possibly leading to the collapse of the suspension bridge. In this chaotic situation, the whole structure oscillates and both the cables and the hangers generate unexpected behaviors of the deck, such as torsional movements. The **main general goal** of the present research is to understand, analyze and quantify (in a suitable manner) the existing relationship between the fluid velocity, the resulting lift, and, ultimately, the attainment of the thresholds for hanger slackening and cable shortening.

This thesis is organized as follows. The Introduction (Chapter 1) serves as a summary and is taken from [39], where we survey some of the existing (and sometimes contradictory) results on turbulence, fluids and structures, and suggest several natural questions whose answers would increase the mathematical understanding of these phenomena. In Chapter 2, following [126], we focus our attention on the structure: the **Melan equation** for suspension bridges is derived by assuming small displacements of the deck and inextensible hangers. We determine the thresholds for the validity of the Melan equation when the hangers slacken, thereby violating the inextensibility assumption. To this end, we preliminarily study the possible shortening of the cables: it turns out that there is a striking difference between even and odd vibrating modes since the former never shorten. These problems are studied both on beams and plates. For the remaining parts of this work we analyze exclusively the hydrodynamic component of the fluid-structure interaction problem considered. In Chapter 3, taken from [127], a variational formulation for a class of mixed and nonstandard boundary conditions (based on the vorticity, pressure, normal and tangential components of the velocity field) on a smooth obstacle is discussed for the Stokes equations. Possible boundary data are then derived through separation of variables of biharmonic equations in a planar region having an internal concave corner. Explicit singular solutions show that, at least qualitatively, these conditions are able to reproduce vortices over the leeward wall of the obstacle. Then, Chapter 4 (whose results are contained in the preprint [124]) is devoted to the study of planar viscous flows governed by the stationary Navier-Stokes equations with inhomogeneous Dirichlet boundary data in non simply connected domains. In a symmetric framework the appearance of forces is strictly related to non-uniqueness of the solution. Explicit bounds on the data ensuring uniqueness are then sought and several functional inequalities (concerning relative capacity, Sobolev embedding, the continuity constant of the Bogovskii operator) are analyzed in detail: explicit bounds are obtained. The case of "almost symmetric" frameworks is also considered. An **explicit universal threshold** on the Reynolds number ensuring that the flow generates no lift is obtained regardless of the shape and the nature of the obstacle. A shape optimization problem, aiming to minimize the impact of forces, is then addressed numerically. Connections of the results with elasticity and mechanics are also emphasized. Finally, several concluding remarks, open problems and future perspectives are the main content of Chapter 5.

ACKNOWLEDGMENTS

On a personal level, my most sincere acknowledgments are directed to my parents Silvio and María Isabel, my sisters María Stefania and María Melania, and all my family. I thank you not only for having supported, guided and accompanied me in the most constant and loving way during all these years as a PhD student, but also for all those teachings that have allowed me to grow as a human being, both professionally and emotionally. My deepest gratitude goes to my parents, who have always driven me to follow my convictions and to set high goals in life, indicating me the right path to achieve them. In this same context, I cannot fail to mention my closest friends (Héctor and Trinidad, Lucas and Montserrat, Tomás, Santiago and Elisa, Juan Pablo and Amanda), whose invaluable and unconditional friendship has given me the strength to overcome times of adversity and the joy to enjoy the countless moments of fun. Despite the distance in these three years of separation that we have lived, all of you, family and friends, have continued to bring happiness, light and wisdom into my life, specially during periods that I lacked of all three of them.

On an academic level, I begin by expressing my admiration to all the teachers, colleagues and administrative staff of the Department of Mathematics of the Polytechnic University of Milan, for their professionalism and good will. I would like to underline my recognition to professors Monica Conti, Filippo Dell'Oro, Maurizio Garrione, Maurizio Grasselli, Gabriele Grillo, Vittorino Pata, Nicola Soave, Franco Tomarelli and Gianmaria Verzini for all the knowledge they transmitted to me through courses, seminars or just friendly discussions. Professor Irene Sabadini deserves my special appreciation for managing the administrative aspects of the doctoral programme in the most proficient way. Outside the Polytechnic University of Milan, the same tribute applies to professors Denis Bonheure (Brussels), Manuel del Pino (Bath), Eduard Feireisl (Prague), Andrei Fursikov (Moscow), Giovanni Paolo Galdi (Pittsburgh) and Sebastian Schwarzacher (Prague).

Finally, but of greater importance, my most profound gratitude is directed to Professor Filippo Gazzola. Not only his vision, leadership and expertise (in many areas of mathematical analysis) are primarily responsible for the achievements contained in this PhD thesis, but also his constant dedication, kindness and patience that guided me through this quest. Furthermore, his prudence and countless advices, which transcended the professional field, permitted me to mature both as a mathematician and as person, and therefore I consider him not only a teacher, but a mentor: from every meeting we held, whether it was a lecture, a seminar or a friendly talk, I could extract a valuable lesson. From the very first day he believed and trusted in me, and this attitude remained immovable over these three years, despite of my endless mistakes; for this I will always be grateful to him. My biggest desire is that the end of this PhD research will represent another important step in a fruitful and long-lasting collaboration and relationship.

Contents

Chapter 1

Introduction - Some mathematical questions on fluids and structures

Nessuna certezza delle scienze è dove non si pò applicare una delle scienze matematiche, ovver che non sono unite con esse matematiche.

Leonardo da Vinci (1452-1519)

Strong blowing winds, especially when they hit an obstacle, generate air turbulence with subsequent appearance of vortices behind the obstacle. The first documented and surviving realization of vortices is usually attributed to some sketches by Leonardo da Vinci, see Figure 1.1. Nowadays, wind tunnel
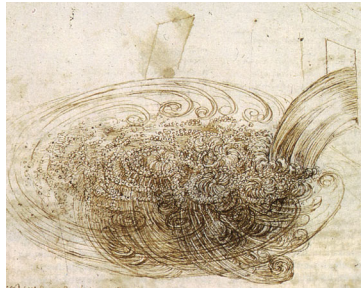
Figure 1.1: Drawing of water vortex by Leonardo da Vinci, ca. 1510-1513.

experiments artificially blow air flows and give precise pictures of turbulence and of the dependence of the vortex shedding on the parameters of the flow [91, 139, 215, 216], see e.g. the left picture in Figure 4.7. Vortex shedding is the cause of so-called vortex-induced vibrations [11, 86, 87, 268, 269, 271], namely oscillatory motions of the obstacle. Thanks to the huge progresses of the numerical analysis of fluid flows and the increasing computer capacities, turbulence may also be detected by refined numerics using Computational Fluid Dynamics (CFD), see e.g. [98, 103, 109, 223]. However, the current knowledge of turbulence is still foggy with frequent updates. We refer to [105] for a general introduction and to [20] for

> *the most recent advances in attacking these questions* [the fundamental questions in turbulence] *using rigorous mathematical tools.*

Helmholtz [140] published the foundation of the theory 160 years ago, followed by Stokes (1845), Strouhal (1878), Prandtl (1904), Bénard (1908), von Kármán (1912) and, nowadays, according to [216, Section 1.1],

> *it is not only that the accumulated knowledge is vast, but also that the accretion of knowledge and experience on the topic continues to grow unabated, perhaps exponentially.*
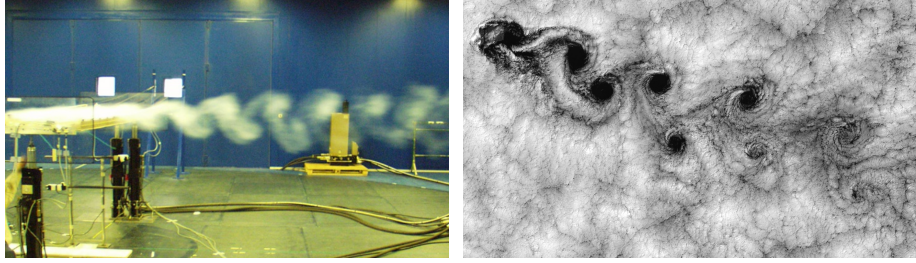
Figure 1.2: Left: vortices around the deck of a scaled bridge obtained experimentally in the wind tunnel of the Politecnico di Milano. Right: clouds off the Chilean coast showing Kármán vortex streets (Landsat 7 image-NASA).

The vortex formation within a flow surrounding an object is the basic observation that laid the foundations of aerodynamics. Complicated phenomena were quickly observed, and the important parameters were identified. A general understanding of viscosity effects began to emerge during the mid-nineteenth century, particularly in the works of Stokes [249, 250], followed later by Prandtl [210] who introduced his *boundary layer theory*. Prandtl claims that the no-slip condition holds even for very small viscosity, but its influence is confined to a small region along the body, the so-called boundary layer. Within this layer the velocity of the fluid rapidly changes from zero on the surface of the body to the free-stream velocity of the flow. In presence of high curvature of the obstacle surface, the flow can be interrupted entirely and the boundary layer may detach from the surface: this phenomenon is called *separation*.

The separation process depends on viscosity and stream velocity whose important influence is collected in the Reynolds number Re that expresses the ratio between inertial forces and viscous forces of the flow. In the year 1883, Reynolds [226] investigated which factors determine whether the motion of water in a pipe is direct or sinuous, thereby introducing the dimensionless parameter

$$\mathrm{Re} = \frac{\rho u L}{\mu} = \frac{uL}{\nu},$$

where ρ is the density of the fluid, u is its velocity, μ is its dynamic viscosity, ν is the kinematic viscosity and L is the diameter of the pipe. Reynolds was interested in the transition from laminar to turbulent regime: a flow is called *laminar* or *streamlined* if it follows parallel layers, with no disruption between the layers, whereas it is called *turbulent* if it undergoes irregular fluctuations or mixing, see Figure 1.3. In a
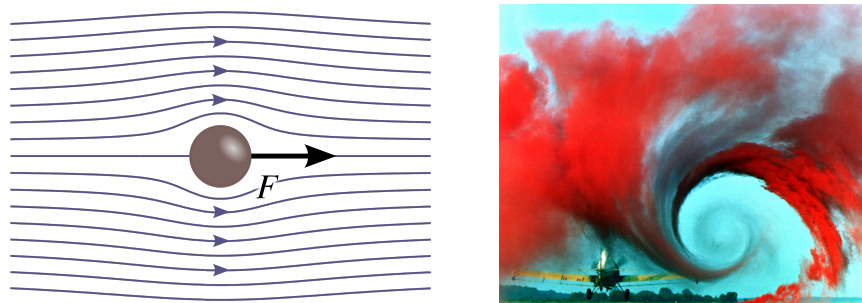
Figure 1.3: Left: laminar flow around a bluff body. Right: turbulent flow from an airplane wing (NASA-Photo ID: EL-1996-00130).

turbulent flow, the speed of the fluid is widely changing both in magnitude and direction. Experiments and numerics show that for Re $\ll$ 1, the flow is laminar. For a Reynolds number in the range between 1 and 100, the flow exhibits a complicated (chaotic) structure, while for Re $\gg$ 100, the flow is turbulent, displaying a complex pattern formed by the velocity field. Quoting [99]:

2

While much of the hemodynamics in a healthy human body has low Reynolds number, resulting in laminar flow, relatively high Reynolds number flow is observed at some specific locations [...] For instance, the peak Reynolds number in the human aorta has been measured to be approximately 4000 [163].

Besides a blood flow in arteries, other turbulent flows include most natural rivers which have Reynolds numbers well above 2000, lava flow, atmosphere and ocean currents, wind-turbines wake, boat and building wakes or aircraft-wing tips. The Reynolds number for the air surrounding an aircraft during flight varies from about 2×10^6 for small slow-speed airplanes to 2×10^7 for large high-speed airplanes.

According to Batchelor [22, Section 5.11], in practice, the most significant feature of a flow past a fixed body (fully immersed in a steady stream that is constant at infinity), is the force exerted on the body by the fluid, which is usually decomposed into two components: the drag force F_D parallel to the flow direction and the lift force F_L perpendicular to the flow. In practice, these forces are computed through the formulas

$$F_D = \frac{C_D}{2} \rho A_f W^2, \qquad F_L = \frac{C_L}{2} \rho A_p W^2, \tag{1.1}$$

where ρ is the fluid density, W is the upstream velocity, A_f is the frontal area (the projected area seen by an observer looking towards the object from a direction parallel to the upstream velocity), and A_p is the planform area (the projected area seen by an observer looking towards the object from a direction normal to the upstream velocity). In (4.135), C_D and C_L denote, respectively, the drag and lift coefficients, giving dimensionless forms of the drag and lift forces. They are usually determined by help of a simplified analysis, some numerical procedures or empirical rules based on (e.g. wind tunnel) experiments. We refer to [204, Chapter 9] for more details and to [88, 139] in the particular case of suspension bridges. The lift force is intimately related to the vortex shedding process: when asymmetric vortices appear behind the bluff body, the asymmetry generates a forcing lift which starts the vortex-induced vibrations. The vortex shedding in the wake of a structure may also achieve one of its natural frequencies, resulting in a vortex-induced resonance, with subsequent vibrations of the structure. A large variety of models were used to phenomenologically study vortex shedding and vortex-induced vibrations but a unified theory seems lacking: from [216] we quote

literature on vortex-induced vibrations is vast and continuously growing, both on fundamental issues and on methods for their prediction in engineering, where applications are numerous. [...] In fact, because of the practical and theoretical importance of vortex-induced vibrations, models have been developed and used since the 1960s. Reviews show not only a large number of them, but also significant differences in the fundamental aspects of their formulations.

For instance, the aerodynamic forces acting on the deck of a suspension bridge vary with respect to many parameters. It is therefore important to study the aerodynamic derivatives which measure how those forces and moments change as other parameters (such as airspeed, angle of attack, etc.) related to stability are perturbed. The aerodynamic derivatives have been so far determined experimentally, and given the complexity of the vortex shedding phenomena and vortex-induced vibrations, one needs a huge amount of experimental data before attempting a theoretical analysis. Still concerning suspension bridges, we quote [216]:

some recent effort has gone into obtaining the aerodynamic derivatives using numerical methods. For example, Larsen [175] uses a discrete vortex method to obtain the aerodynamic derivatives for two different cross-sections. A comparison between his results and the experimental data of Scanlan-Tomko [232] shows the numerical data to be reasonably good, but probably not good enough to obtain accurate stability predictions.

The study of vortex shedding is intimately related to vortex dynamics for which a huge literature is available from the physical, engineering and mathematical communities, see for instance [9, 21, 157, 185, 186, 189, 193, 208, 224, 225, 227] and the numerous citations therein. Vortices appear in a great

variety of Ginzburg-Landau theories, models in fluid-mechanics, superconductivity and superfluidity [10, 29, 155, 214, 239, 256, 267].

The unforced incompressible Euler equations

$$u_t + (u \cdot \nabla)u + \nabla p = 0, \qquad \nabla \cdot u = 0 \qquad (x, y, z) \in \Omega, \quad t > 0 \qquad (1.2)$$

play a central role in theoretical fluid mechanics and even in mathematical physics, not only because they model adiabatic and inviscid flows, but also because they can be seen, in some particular situations, as the inviscid limit of the Navier-Stokes system [189, 191] or as the limit of other model equations in some asymptotical regime, see for instance [47, 240]. Nevertheless, if one wishes to model turbulence, there are several reasons not to consider (1.2). One is that vortices do not only appear in high Reynolds regimes (e.g. for small viscosity), for which (1.2) would be a good approximation; indeed, vortices can also be generated at low Reynolds, for instance by singularities in the domain and, in particular, by possible obstacles in the flow. Another one is the celebrated d'Alembert paradox [179, 180, 181, 182], see next section, which shows that the Euler equations (1.2) are not appropriate to directly describe the lift and drag exerted from fluids on bluff bodies.

1.1 Why do airplanes fly?

On the authority NASA website [1] one may read:

> *There are many explanations for the generation of lift found in encyclopedias, in basic physics textbooks, and on Web sites. Unfortunately, many of the explanations are misleading and incorrect. Theories on the generation of lift have become a source of great controversy and a topic for heated arguments for many years. [...] To truly understand the details of the generation of lift, one has to have a good working knowledge of the Euler equations.*

The conclusion is a quite strong mathematical statement. So, let us start modelling an incompressible non-viscous fluid in $\mathbb{R}^3 \setminus B$, where B is a solid ball, with the Euler equations (1.2). We suppose that the stream velocity is constant at infinity, i.e. there exists $u_\infty \in \mathbb{R}^3$ such that $u(x) \to u_\infty$ as $|x| \to \infty$. Denoting by R the radius of the ball and assuming that it is centered at the origin, it is readily seen that the potential

$$U(x, y, z) = \left(1 + \frac{R^3}{2(x^2 + y^2 + z^2)^{3/2}}\right)x \qquad (1.3)$$

yields a steady state solution $u = \nabla U$ of (1.2) in $\mathbb{R}^3 \setminus B$ with constant velocity $u_\infty = (1, 0, 0)$ at infinity and such that u is tangent to ∂B, by which we mean that $u \cdot n = 0$ on ∂B. Due to the symmetry of the field $u = \nabla U$, one easily checks that the flow pressure on the boundary of the ball is zero, i.e.

$$\int_{\partial B} p\hat{n} \, d\sigma = -\frac{1}{2} \int_{\partial B} |u|^2 \hat{n} \, d\sigma = 0,$$

which means that the fluid neither produces a drag, nor a lift. This obviously contradicts everyday experience. Moreover, this theoretical paradox is not a consequence of the symmetry of the obstacle B (that induces the symmetry of u). Indeed, in the 18th century, d'Alembert [179, 180, 181, 182] proved a surprising result about stationary solutions of the Euler equations:

> *Après avoir ainsi développé mes principes, j'examine une hypothèse dont plusieurs auteurs d'hydro-dynamique se sont servis jusqu'ici, & je fais voir que si on suivait une telle hypothèse pour déterminer la résistance d'un fluide, cette résistance se trouverait nulle, ce qui est contraire à toutes les expériences.*

This result, nowadays known as the *d'Alembert paradox* has been and still is a source of debate. In modern terminology, the d'Alembert paradox may be stated as follows.

Theorem 1.1 ([179, 180, 181, 182]). *Let $D \subset \mathbb{R}^3$ be a compact smooth set and let $\hat{n}$ be the inward unit normal vector to ∂D. Let $u = u(x)$ ($x \in \Omega = \mathbb{R}^3 \setminus D$) be a smooth field over the closure of Ω, divergent-free, tangent to ∂D, and constant at infinity. If u is irrotational, then u is a stationary solution of (1.2) in Ω and the fluid force on the obstacle is zero, that is,*

$$F = \int_{\partial D} p \hat{n} \, ds = 0 \, .$$

The proof of Theorem 1.1 is based on classical tools from potential theory and on the Divergence Theorem, see e.g. [135, Theorem 2.1], [192, Theorem 4.3] or [265, Section 8.2]. Some comments about the irrotational assumption on the flow are in order. A physical justification of this assumption is based on the fact that, at very large distances from the obstacle, the flow may be seen as uniform ($u \equiv$ constant) so that it is indeed irrotational. But whether this condition remains true all over $\mathbb{R}^3 \setminus D$ is a delicate matter. In fact, by the vorticity-transport formula [189, Proposition 1.8, p.20], the behavior of the vorticity at infinity is transported in all the domain, provided the particle trajectories are smooth and invertible, which would justify the assumption of irrotational flows in Theorem 1.1, see also [114]. Even though this was already a concern of Birkhoff [32] (see below), it is still an open problem whether (1.2) admits steady rotational solutions.

We refer to [60, 136, 190, 247] and the numerous references therein for further discussions on the paradox. As shown by Theorem 1.1, although the Euler equations (1.2) provide a good model of reality for many problems of fluid dynamics, they cannot directly account for the lift force. Since only a viscous fluid satisfies the no-slip condition of its particles on the surface of the body immersed in the flow, it is nowadays commonly accepted that viscosity is needed to generate a lift, as first suggested by Saint-Venant [81]. However, any rigorous physical justification or mathematical proof remains far out of reach [135, 265]. Birkhoff [32, p.21] conjectured the drag could be the result of an instability of potential flows:

> *the paradoxes of ideal fluid theory may be, in part, paradoxes of topological oversimplification [by which he meant that there is no valid mathematical reason to consider potential flows only]. [...] Though Dirichlet flows and other steady flows are mathematically possible, there is no reason to suppose that any steady flow is stable. It is perfectly conceivable that, in an "ideal" fluid, initially departing slightly from Dirichlet flow, irregularly varying turbulent "eddies" are built up mathematically in the "wake" of an obstacle-reproducing mathematically what is observed physically at large Reynolds' numbers R. [...] To admit this possibility, we must reject the idea that there is a necessary tendency towards symmetry in natural phenomena, and admit the possibility that a symmetrically stated problem may not have any stable symmetric solution.*

Birkhoff was violently criticised by Stoker [248], especially for invoking instability, and he did not insist more on this idea. Even more, in the second version of Birkhoff's book [33], these thoughts disappeared. More recently, Hoffman and Johnson [146] reconsidered Birkhoff's attempt to explain the paradox. Part of the conclusion in [146] says:

> *We have presented a resolution of d'Alembert's paradox based on analytical and computational evidence that a potential solution with zero drag is illposed as a solution of the Euler equations, and under perturbations develops into a wellposed turbulent solution with substantial drag in accordance with observations.*

In a followup paper based on this explanation, Hoffman-Jansson-Johnson [144] presented a new mathematical theory of flight, see also [145], which is fundamentally different from the theory by Prandtl-Kutta-Zhukovsky [34, 262, 264]. Quoting the authors:

> *The new theory shows that the miracle of flight is made possible by the combined effects of (i) incompressibility, (ii) slip boundary condition and (iii) 3d rotational slip separation, creating a flow around a wing which can be described as (iv) potential flow modified by 3d rotational separation.*

The basic novelty of the theory is expressed in (iii) as a fundamental 3d flow phenomenon only recently discovered by advanced computation and analysed mathematically, and thus is not present in the classical theory. Finally, (iv) can be viewed as a realization in our computer age of Euler's original dream to in his equations capture an unified theory of fluid flow.

The paper curiously starts with an *Editorial Foreword* which states:

The special character of this article requires some comments by the editors on the purpose of its publication. Though, its mathematical content does not meet the degree of mathematical rigor usually expected by articles in this journal, the implications of the argument and the accompanying novel numerical computations are of such far reaching importance for technical fluid dynamics, particularly for the computation of certain features in turbulent flow, that it deserves serious considerations. The main purpose of this publication is therefore to stimulate critical discussion among the experts in this area about the relevance and justification of the view taken in this article and its possible consequences for modelling and computation of turbulent flow.

It is surprising that this paper has not received much attention and did not stimulate neither public criticism nor interest so far, see however the (publicly revealed) private debate on Johnson's blog [154]. Birkhoff's doubt on the instability is, at least mathematically, quite natural: it is well-known that symmetric problems can simultaneously have unstable symmetric solutions and non symmetric stable solutions. Among others, Tang and Aubry [255] have numerically studied Föppl's vortex model [102, 171, 227] which aims to describe an incompressible fluid past a cylinder. Tang and Aubry analysed the symmetry breaking instability leading to vortex shedding:

It is well known that if a circular cylinder starts moving from rest in an incompressible fluid, twin vortices spinning in opposite directions form behind the cylinder soon after motion begins. These vortices grow and become more and more elongated as time increases until they reach their maximal size. After that time, the bubble of vortices remains steady at low Reynolds numbers, develops into a time-dependent oscillating wake regime in which the bubble remains attached to the body at about Re 48−50 or breaks down into a Kármán vortex street at higher Reynolds numbers. It is interesting to notice that if the initial condition is symmetric, the solution formally remains symmetric at all later times. In other words, the subspace of symmetric solutions is an invariant subspace of the Navier-Stokes equations [see Proposition 1.1 below] subject to the boundary conditions considered here. The fact that the flow goes away from this subspace beyond the critical Reynolds number in both physical and numerical experiments means that the symmetric bubble becomes unstable beyond the critical Reynolds number. It remains, nevertheless, a solution at all Reynolds numbers. This observation led Föppl [102] to investigate whether one can find steady solutions in the form of twin vortices and study their stability property. Föppl represented the system by building a two-dimensional, incompressible potential flow consisting of a uniform oncoming flow, a pair of point vortices symmetrically located with respect to the centerline behind the cylinder, and inner vortices placed to satisfy the boundary condition on the body [see e.g. [171, 227]]. He found fixed points i.e., steady flows for which the twin vortices can indeed maintain their locations relative to the cylinder. Such equilibrium positions are located on two symmetric curves starting from the rear stagnation point of the bubble. Föppl, who also studied the stability of the equilibrium, showed that the vortices are stable to all symmetric perturbations and unstable to some asymmetric perturbations. However, there was a mistake in Föppl's analytical results which was later detected and corrected by Smith [243] who showed that the equilibrium is only marginally stable to all symmetric perturbations instead of being stable as originally found by Föppl.

The symmetry breaking is well documented by experimental works, see e.g. [67, 68, 69]. Jackson [153] and Zebib [273] computationally tackled the symmetry breaking instability from the Navier-Stokes equations

$$u_t - \nu\Delta u + (u \cdot \nabla)u + \nabla p = 0 \qquad \nabla \cdot u = 0, \tag{1.4}$$

where, as usual, $\nu > 0$ is the kinematic viscosity, in the neighbourhood of the critical Reynolds number. The transition is marked by a Hopf bifurcation which is not fully understood as the Navier-Stokes equations yield an infinite-dimensional dynamical system.

Even if a direct connection cannot be established with a symmetry breaking instability of a steady state of the Euler equations, it is certainly worth mentioning the following striking theoretical result due to Bardos et. al [19] that somehow suggests that Birkhoff's feeling is maybe not unreasonable:

Proposition 1.1 ([19]). *Let u_0 be a function of (x, y) only, then the weak solution of the 3D Euler equations (1.2) might become spontaneously a function of (x, y, z). If the initial data is axi-symmetric or helical symmetric, the weak solutions of the Euler equations might spontaneously break the symmetry. On the contrary, if u_0 is a function of (x, y), then the Leray-Hopf weak solution of the 3D Navier-Stokes equations (1.4) remains a function of (x, y) only. For axi-symmetric initial data, or helical initial data, the symmetry is also preserved.*

In fact, the wild weak solutions of the Euler equations that do not obey the two-dimensional symmetry of the initial data should be ruled out because they cannot be obtained as vanishing viscosity limit solutions of the Navier-Stokes equations (1.4). The existence of weak solutions of the Navier-Stokes equations has been treated in pioneering works [149, 169, 183, 187] in cylindrical domains. In the case of a non-cylindrical, but a priori known domain, weak solutions were first studied in [106] for the case of homogeneous Dirichlet boundary conditions. For further details, we refer to some classics [7, 63, 115, 194, 257].

Having in mind obstacles modelling suspension bridges, we consider the case where the fluid is enclosed in a *bounded box* of $\mathbb{R}^3$ and we assume that the obstacle is a cylinder, namely a 2D object times an interval. More precisely, we consider

$$\Omega = \{(-L, L)^2 \times (0, \Lambda)\} \setminus \{\overline{K} \times (0, \Lambda)\}$$

for some $L, \Lambda > 0$ and some 2D obstacle K with $D = K \times (0, \Lambda)$. Since our purpose is to analyse the drag and lift forces acting on the obstacle D, it is sometimes convenient (especially for the lift) to restrict the attention to a 2D section of the box, for instance at the midpoint. The domain Ω and its intersection Σ with the plane $z = \frac{\Lambda}{2}$ are represented in Figure 1.4 (not in scale!), together with a sketch of the flow and the appearance of vortices. The rectangular shape of the cross section K of the obstacle D has been chosen here for simplicity of the picture; this model was first suggested in [38, 125] and subsequently applied in [127] for a study of non-standard boundary conditions for the planar Stokes equations inducing vortices around concave corners.
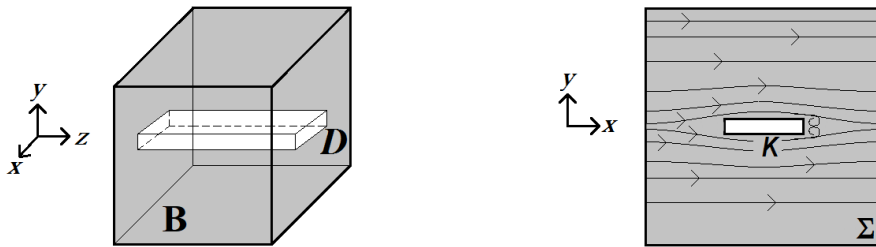
Figure 1.4: The domain Ω and its intersection Σ with the plane $z = \frac{\Lambda}{2}$.

We next discuss the computation of the drag and lift forces exerted on an obstacle by the flow of a viscous fluid. The rate of strain tensor σ and the stress tensor $\mathbb{T}$ of any viscous incompressible fluid are given by (see [173, Chapter 2]):

$$\sigma(u) = \nabla u + \nabla^T u, \quad \mathbb{T}(u, p) = -p\mathbb{I} + \nu\sigma(u), \tag{1.5}$$

where $\mathbb{I}$ is the identity matrix (either 2×2 or 3×3, according to the space dimension). As expressed by (4.123), in a viscous fluid, in addition to the pressure drag, one needs to take into account the skin friction so that the total force exerted by the fluid over the obstacle D is given by the vector field

$$F_D = -\int_{\partial D} \mathbb{T}(u, p) \cdot \hat{n}, \tag{1.6}$$

where the minus sign is due to the fact that the outward unit normal n to Ω is directed towards the interior of D. Assuming that the inflow is horizontal, namely the only nonzero component of the boundary velocity is the x-component on the boundary of the box $(-L, L)^2 \times (0, \Lambda)$, the horizontal component in (4.124) is the drag force, while the orthogonal component is the lift force. For smooth obstacles $D \subset \mathbb{R}^3$ the drag force may also be written as

$$\frac{\nu}{2} \int_{\Omega} |\sigma(u)|^2. \tag{1.7}$$

see e.g. [25] for the details. It is clear that while the drag force is always acting in the direction of the flow and hence in a one-dimensional direction, the lift force is orthogonal to the drag and has two degrees of freedom in a 3D setting; this is the precise reason why it may be convenient to focus on 2D cross sections of the obstacle, especially when the obstacle is a cylinder aiming to model the deck of a bridge as in Figure 1.4. In this case, for the drag force in (1.7), the integral must be computed over the cross-section Σ.

It is possible to derive exact formulas for the drag exerted by a creeping flow over bodies displaying special symmetries like spheres, ellipsoids and cylinders. In 1851, Stokes [250] addressed the problem of the steady flow of a viscous fluid (having constant density ρ and a constant free-stream velocity equal to $u_0 \in \mathbb{R}^3$) surrounding a rigid sphere of radius R. By neglecting, with respect to viscosity, the convective term $(u \cdot \nabla)u$ appearing in the Navier-Stokes equations, he explicitly computed the velocity field of the flow and provided the following formula for the drag over the sphere:

$$F_D = 6\pi\rho\nu R|u_0|, \tag{1.8}$$

a result that remained in history as the *Stokes law*, see [174, Chapter 6]. Similar expressions for an ellipsoid, a circular disk moving broadside-on, or a circular disk moving edge-ways can be found in the book of Lamb [171, Article 339] (the first edition of this work was published in 1879), from where we quote:

> The formula of Stokes (1.8) for the resistance experienced by a slowly moving sphere has been employed in physical researches of fundamental importance, as a means of estimating the size of minute globules of water, and thence the number of globules contained in a cloud of given mass. Consequently the conditions of its validity have been much discussed both from the experimental and from the theoretical side.

A rigorous refutation of the validity of Stokes law was performed by Oseen in 1910, see [213], where it was proven that the convective term may be neglected only at a sufficiently short distance from the sphere, precisely when $|x| \ll \nu/|u_0|$. Far away from the body one may approximate u with u_0, and subsequently $(u \cdot \nabla)u$ with $(u \cdot \nabla)u_0$, by means of which Oseen presented the following linear model for the far-field velocity:

$$-\nu\Delta u + (u_0 \cdot \nabla)u + \frac{1}{\rho}\nabla p = 0 \qquad \nabla \cdot u = 0, \tag{1.9}$$

usually known as the *Oseen equations*, which constitute an intermediate step between the linear Stokes system and the fully non-linear Navier-Stokes system. An exact resolution of (1.9) yields an improvement of Stokes law given by:

$$F_D = 6\pi\rho\nu R|u_0|\left(1 + \frac{3R|u_0|}{8\nu}\right),$$

as well as the following expression for the drag, by unit length, applied over an infinite-length cylinder of radius R that is being held orthogonally to the stream, see [173, Chapter II]:

$$F_D = \frac{4\pi\rho\nu|u_0|}{\frac{1}{2} - \gamma - \log\left(\frac{R|u_0|}{4\nu}\right)},$$

where $\gamma = 0.57721...$ is the Euler-Mascheroni constant.

1.2 Fluid-structure interaction: where do we stand?

Most of the current fluid-structure interaction models that are used in practical applications rely on experimental and numerical tools. In the case of wind-bridge interaction, these tools, that are nowadays consolidated, are fairly simple and are based on the following assumptions: the wind is considered ergodic and stationary, the bridge behaviour is considered linear, the aerodynamic loads are governed by linear laws. As explained in [39, Section 5], see also [167], the assumption of linear behaviour of bridges is unreasonable. In the Engineering literature, the studies started from the approaches used in the aeronautical field almost one century ago since the works of Küssner [164], Sears [234, 235], Wagner [266] and Theodorsen [258], and later applied to wind engineering by Davenport [77], Scanlan [230, 231] and others. The aeroelastic problem was initially studied on simple geometries like flat plates, where simplified analytical solutions are achievable, and then extended to more complex shapes like airfoils or deck bridges through semi-empirical methodologies. In the Mathematical literature, most of the contributions to fluid-structure interactions are numerical. The reason is that even simple models give rise to extremely difficult problems: already well-posedness turns out to be quite challenging. Let us survey some of the existing models and results.

After the seminal paper of Serre [241], the breakthrough theoretical results on fluid-structure interaction appeared around 2000, see [62, 134, 147, 148]. For a finite number of rigid bodies and incompressible as well as compressible fluid models, we refer to Desjardins and Esteban [84, 85]. We recall here the simpler case of one spherical body following Conca, San Martín and Tucsnak [62]. Let $A \subset \mathbb{R}^3$ be an open bounded set representing the domain occupied by both the fluid and the body, assumed to be a moving ball of radius 1. Denote, respectively, by $\Omega_t \subset A$ and $B_t = A \setminus \Omega_t$ the parts of A occupied by the fluid and the body at a given instant t. Then the system of equations modelling this fluid-structure interaction reads

$$\begin{cases} u_t - \nu\Delta u + (u \cdot \nabla)u + \nabla p = 0, \quad \nabla \cdot u = 0 \quad \text{in } \Omega_t, \ t > 0, \\ u = 0 \quad \text{on } \partial A, \ t > 0, \quad u = h'(t) - \omega(t) \wedge \hat{n} \quad \text{on } \partial B_t, \ t > 0, \\ Mh''(t) = -\int_{\partial B_t} \sigma\hat{n}, \ t > 0, \quad J\omega'(t) = \int_{\partial B_t} \hat{n} \wedge \sigma\hat{n}, \ t > 0, \\ u(x,0) = u_0(x) \quad \text{in } \Omega_0, \quad h'(0) = h_1 \in \mathbb{R}^3, \quad \omega(0) = \omega_0 \in \mathbb{R}^3. \end{cases} \tag{1.10}$$

In the above system, the unknowns are $u(x,t)$, $h(t)$ and $\omega(t)$, namely the velocity field of the fluid, the position of the center of the ball and the angular velocity of the ball, respectively. Therefore, the second identity in $(1.10)_2$ imposes the no-slip condition at the fluid-solid interface whereas $(1.10)_3$ expresses the conservation of linear and angular momentum for the body (as in (4.123), σ denotes the rate of strain tensor of the fluid). The existence of weak solutions, up to collision, for problem (1.10) is established in the following theorem.

Theorem 1.2. [62] *Assume that the open set $\widetilde{A} = \{x - y \mid x, y \in A\}$ has smooth boundary. Given $h_0 \in A$ such that $\mathrm{dist}(h_0, \partial A) > 1$, suppose that (u_0, h_1, ω_0) is an element of the following space:*

$$\mathbb{H}_{h_0} = \{(v, \ell, k) \in L^2(\widetilde{A}) \times \mathbb{R}^3 \times \mathbb{R}^3 \mid \nabla \cdot v = 0 \text{ in } \widetilde{A}, \ v \cdot \hat{n} = 0 \text{ on } \partial\widetilde{A}, \ v|_{B_1}(y) = \ell + k \times y, \ v|_{E_{h_0}} = 0\},$$

9

where B_1 is the unit ball of $\mathbb{R}^3$ and $E_{h_0} = \widetilde{A} \setminus (A - h_0)$. Then, there exists $T_0 > 0$ such that the problem (1.10) has a weak solution (U, h, w) for any $T < T_0$. Moreover, one of the following alternatives holds true:

$$T_0 = +\infty \qquad or \qquad \lim_{t \to T_0} dist(B(t), \partial A) = 0. \tag{1.11}$$

The "no-contact" assumption is crucial. Starovoitov [246] proved that there exist at least two generalised solutions to the problem if collisions of the body with the boundary of the flow region are allowed. These solutions are distinguished by the behaviour of the body after collision with the boundary: in the first solution, the body moves away from the boundary after the collision while in the second solution, the body and the boundary remain in contact. Also, in the case of a compressible fluid, Feireisl [94] constructed a solution in which a ball remains attached to the top surface of the cavity A regardless of the intensity of the gravity force, thus showing that collisions may lead to non-physical situations in a standard mathematical framework. The problem discussed in Theorem 1.2 was also tackled for the Euler equations [212]. For further developments, we refer to [45, 54, 70, 89, 95, 116, 117, 118, 138, 207, 209, 229, 253] and the references therein. A uniqueness result has been obtained by Glass and Sueur [133] (both when the fluid is governed by the Euler equations or the Navier-Stokes equations). It is also worth mentioning that fluid-structure interaction problems have been considered for compressible fluids in [41, 42, 43, 46] and stabilisation or control issues have been tackled e.g. in [15, 16, 44, 254].

Related to the unrealistic situation discovered in [94] lies the *no-collision paradox*, firstly encountered by O'Neill et al. [64, 65, 82, 211] during the 1960s. By considering a rigid sphere, immersed in a stationary Stokes flow and falling over a flat wall, they showed that the drag over the body diverges rapidly as it approaches the ramp, thus impeding the sphere from touching the wall in finite time. The paradox was later extended to the case of a Navier-Stokes flow, first in 2D and subsequently in 3D [141, 142]. Only frontal collisions are taken into account in those papers. In the 3D setting, as shown in [143], grazing collisions between smooth bodies can occur. Here we just recall a result by Gérard-Varet and Hillairet [129] who, in an attempt to explain the no-collision paradox, consider a general solid body $S_t \subset A$ and take into account that if the distance between ∂A and ∂S_t becomes very small (less than 10^{-6}m), the no-slip condition is no longer accurate and must be replaced by the following Navier condition:

$$\begin{cases} (u - u_S) \cdot \hat{n} = 0, \quad (u - u_S) \wedge \hat{n} = -2\alpha(\sigma \cdot \hat{n}) \wedge \hat{n} \quad \text{on} \;\; \partial S_t \\ u \cdot \hat{n} = 0, \quad u \wedge \hat{n} = -2\beta(\sigma \cdot \hat{n}) \wedge \hat{n} \;\; \text{on} \;\; \partial A, \end{cases} \tag{1.12}$$

where $u_S(x, t) = h'_S(t) + \omega(t) \wedge (x - h(t))$ is the velocity, at every point x of the solid body S_t, whose center of mass is in position $h(t) \in \mathbb{R}^3$ at time $t > 0$. In (1.12), impermeability is ensured by imposing that the normal component of the relative velocity of the fluid is zero, whereas the coefficients $\alpha, \beta > 0$ are the so-called slip lengths (note that the tangential component of the relative velocity may exhibit discontinuities). The existence of weak solutions, up to collision, for problem (1.10)-(1.12) (exchanging B_t by S_t) is established in the following:

Theorem 1.3. [129] *Let $S \subset A$ be two $C^{1,1}$ bounded domains of $\mathbb{R}^3$. Let $u_0 \in \overline{\mathcal{D}(A)}^{L^2(A)}$, with $\mathcal{D}(A)$ being the subspace of solenoidal vector fields belonging to $C_0^\infty(A)$, and assume that there exist $V, W \in \mathbb{R}^3$ such that $u_0^S(x) = V + W \wedge (x - h(0))$, for every $x \in \partial S$. Furthermore, suppose that $(u_0 - u_0^S) \cdot \hat{n} = 0$ on ∂S. Then, there exists $T_0 \in (0, +\infty]$ and a weak solution of (1.10)-(1.12) over $[0, T)$ associated to the initial data u_0 and u_0^S. Moreover, such a weak solution exists up to collision, that is, the alternative (1.11) holds.*

Further theoretical results are related to models with a linear elastic hyperbolic-type equation describing the dynamics of the solid, by the Euler equations [57] or the Navier-Stokes equations [17, 18] or the Stokes equations [176] for the dynamic of the fluid, and by suitable Neumann-type transmission boundary conditions (see also [152] for the case of a non-Newtonian fluid). A major difficulty is then to deal with the mismatch between parabolic and hyperbolic regularity and, so far, only very few satisfactory regularity results have been obtained [13, 18, 176], thereby proving that the setting is correct.

Nonlinear plates interacting with fluids have also been studied [56, 84, 203]. In fact, there are further models, with nonstandard interface conditions [178], with mechanical damping [177] or stochastic forcing [59]. Finally, let us mention the survey [58] where a variety of models mathematically describing the interaction between flows and oscillating structures are discussed.

Chapter 2

Thresholds for hanger slackening and cable shortening in the Melan equation for suspension bridges

In the present chapter we consider a simplified fluid-structure interaction problem given by the oscillation of the deck of a suspension bridge as a consequence of the wind action; we focus our attention on the fluctuation of the structure after the fluid flow has input a large amount of energy into it.

In 1888, the Austrian engineer Josef Melan [198] introduced the so-called deflection theory and applied it to derive the differential equation governing a suspension bridge, modeled as a combination of a string (the sustaining cable) and a beam (the deck), see Figure 2.1. The beam and the string are connected through hangers. Since the spacing between hangers is usually small relative to the span, the set of the hangers is considered as a continuous membrane connecting the cable and the deck.
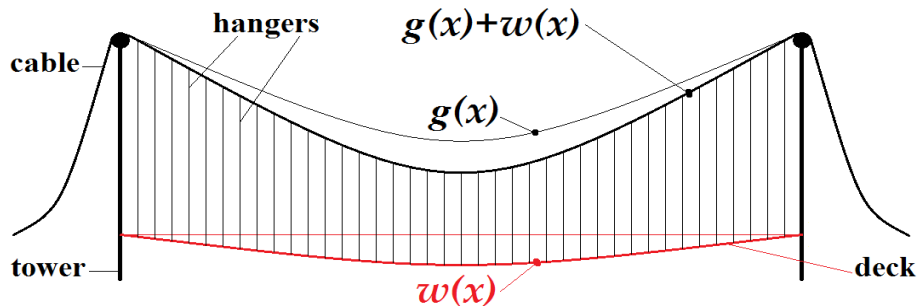
Figure 2.1: Beam (red) sustained by a cable (black) through parallel hangers.

Let us quickly outline how the Melan equation is derived; we follow here [263, VII.1]. We denote by
L the length of the beam at rest (the distance between towers) and $x \in (0, L)$ the position on the beam;
$p = p(x)$ the live load and $-q < 0$ the dead load per unit length applied to the beam;
$g = g(x)$ the displacement of the cable due to the dead load $-q$;
L_c the length of the cable subject to the dead load $-q$;
A the cross-sectional area of the cable and E_c its modulus of elasticity;
H the horizontal tension in the cable, when subject to the dead load $-q$ only;
EI the flexural rigidity of the beam;
$w = w(x)$ the displacement of the beam due to the live load p;
$h = h(w)$ the additional tension in the cable produced by the live load p.

12

When the system is only subject to the action of dead loads, the cable is in position $g(x)$ while the unloaded beam is in the horizontal position $w \equiv 0$, see Figure 2.1. The cable is adjusted in such a way that it carries its own weight, the weight of the hangers and the weight of the deck (beam) without producing a bending moment in the beam, so that all additional deformations of the cable and the beam due to live loads are small. The cable is considered as a perfectly flexible string subject to vertical dead and live loads. The string is subject to a downwards vertical constant dead load $-q$ and the horizontal component $H > 0$ of the tension remains constant. If the mass of the cable is neglected, then the dead load is distributed per horizontal unit. The resulting equation simply reads $Hg''(x) = q$ (see [263, (1.3),VII]) so that the cable takes the shape of a parabola with a $\cup$-shaped graph. If the endpoints of the string (top of the towers) are at the same level $\gamma > 0$ (as in suspension bridges, see again Figure 2.1), then the solution g and the length L_c of the cable are given by:

$$g(x) = \gamma + \frac{q}{2H} x(x - L), \quad g'(x) = \frac{q}{H}\left(x - \frac{L}{2}\right), \quad g''(x) = \frac{q}{H}, \quad \forall x \in (0, L), \tag{2.1}$$

$$L_c = \int_0^L \sqrt{1 + g'(x)^2}\, dx. \tag{2.2}$$

The elastic deformation of the hangers is usually neglected, so that the function w describes both the displacements of the beam and of the cable from its equilibrium position g. This classical assumption is justified by precise studies on linearized models, see e.g. [188]. When the live load p is added, a certain amount p_1 of p is carried by the cable whereas the remaining part $p - p_1$ is carried by the bending stiffness of the beam. In this case, it is well-known [198, 263] that the equation for the displacement w of the beam is

$$EI\, w''''(x) = p(x) - p_1(x) \qquad \forall x \in (0, L). \tag{2.3}$$

At the same time, the horizontal tension of the cable is increased to $H + h(w)$ and the deflection w is added to the displacement g. Hence, according to (2.1), the equation which takes into account these conditions reads

$$\big(H + h(w)\big)\big(g''(x) + w''(x)\big) = q - p_1(x) \qquad \forall x \in (0, L). \tag{2.4}$$

Then, by combining (2.1)-(2.3)-(2.4), we obtain

$$EI\, w''''(x) - \big(H + h(w)\big) w''(x) - \frac{q}{H} h(w) = p(x) \qquad \forall x \in (0, L), \tag{2.5}$$

which is known in literature as the **Melan equation** [198, p.77]. The beam representing the bridge is hinged at its endpoints, which means that the boundary conditions to be associated to (2.5) are

$$w(0) = w(L) = w''(0) = w''(L) = 0. \tag{2.6}$$

Theoretical results on the Melan equation (2.5) are quite demanding [122, 128] and this is the reason why it has attracted the attention of numerical analysts [236, 237, 238, 270]. In this chapter, which is based on the published article [126], we analyze and quantify the two main nonlinear (and challenging) behaviors of (2.5). The first one is the additional tension of the cable, $h(w)$ which is a nonlocal term and is proportional to the length increment of the cable. Depending on the deflection of the beam, the cable may vary its shape and tension, and such phenomenon is studied in Section 2.1 where we compute the exact thresholds of shortening, depending on the deflection w. In Theorem 2.1 we show that there is a striking difference between the even and odd vibrating modes of the beam. The second source of nonlinearity is the possible slackening of the hangers which, however, is not considered in (2.5) due to the assumption of inextensibility of the hangers. Indeed, w in (2.5) aims to represent both the deflections of the beam and of the cable, implying that the cable reaches the new position $g + w$. But since the hangers do not resist to compression, they may slacken so that the cable and the beam move

13

independently and w will no longer represent the displacement of the cable from its original position. This phenomenon is analyzed in detail in Section 2.2 where we suggest an improved version of (2.5) which also takes into account the slackening of the hangers, see (2.15). In Section 2.3 we extend this study to a partially hinged rectangular plate aiming to model the deck of a bridge and thereby having two opposite edges completely free: we view these free edges as beams sustained by cables and governed by the Melan equation. The results are complemented with some enlightening figures.

2.1 Thresholds for cable shortening in a beam model

A given displacement of the deck $w \in C^1([0, L], \mathbb{R})$ generates an additional tension $h(w)$ in the cable that is proportional to the increment of length of the cable $\Gamma(w)$, that is,

$$h(w) = \frac{E_c A}{L_c} \Gamma(w) \quad \text{where} \quad \Gamma(w) = \int_0^L \left[\sqrt{1 + \left(w'(x) + g'(x)\right)^2} - \sqrt{1 + g'(x)^2} \right] dx \,. \tag{2.7}$$

Definition 2.1. *We say that a displacement w **shortens** the cable if $\Gamma(w) < 0$.*

There are at least three rude ways to approximate $h(w)$, by replacing $\Gamma(w)$ with

$$-\frac{q}{H} \int_0^L w(x)dx, \quad -\frac{q}{H} \int_0^L w(x)dx + \int_0^L \frac{w'(x)^2}{2} dx, \quad -\frac{q}{H} \int_0^L \frac{w(x)}{\left[1 + \frac{q^2}{H^2}\left(x - \frac{L}{2}\right)^2\right]^{3/2}} dx.$$

These approximations are obtained through an erroneous argument. While introducing (2.5), Biot-von Kármán [263] warn the reader by writing *whereas the deflection of the beam may be considered small, the deflection of the string, i.e., the deviation of its shape from a straight line, has to be considered as of finite magnitude.* However, they later decide to *neglect $g'(x)^2$ in comparison with unity.* A similar mistake with a different result is repeated by Timoshenko [259, 260]. These approximations may lead to an average error of about 5% for $h(w)$. Around 1950 the civil and structural German engineer Franz Dischinger emphasized the dramatic consequences of bad approximations on the structures and 5% turns out to be a too large error. Moreover, since related numerical procedures are very unstable, see [122, 236, 237, 238], also from a mathematical point of view one should analyze the term $h(w)$ with extreme care.

Since the displacement of the deck w, created by a live load p, is the solution of the Melan equation (2.5), we study here which loads yield a shortening of the cable. In particular, we analyze the fundamental modes of vibration of the beam so that we consider the following class of live loads:

$$p_n(x) = \rho \left(\frac{n\pi}{L}\right)^2 \left\{ \left(\frac{n\pi}{L}\right)^2 EI + H + h\left(\rho \sin\left(\frac{n\pi x}{L}\right)\right) \right\} \sin\left(\frac{n\pi x}{L}\right) - \frac{q}{H} h\left(\rho \sin\left(\frac{n\pi x}{L}\right)\right) \quad \forall n \in \mathbb{N}, \tag{2.8}$$

for varying values of $\rho \in \mathbb{R}$. The load p_n consists of a negative constant part $-\frac{q}{H} h\left(\rho \sin\left(\frac{n\pi x}{L}\right)\right)$ and a part that is proportional to the fundamental vibrating modes of the beam $\sin\left(\frac{n\pi x}{L}\right)$, which are the eigenfunctions of the following eigenvalue problem:

$$v''''(x) = \lambda v(x) \quad (0 < x < L), \qquad v(0) = v(L) = v''(0) = v''(L) = 0 \,. \tag{2.9}$$

The reason of this choice for p_n is that, after some computations, one sees that the resulting displacement w_n (solution of (2.5)) is proportional to a vibrating mode:

$$w_n(x) = \rho \sin\left(\frac{n\pi x}{L}\right) \quad \forall x \in [0, L]. \tag{2.10}$$

Whence, $|\rho|$ measures the amplitude of oscillation of the vibrating mode w_n. For every $n \in \mathbb{N}$, we put $\Gamma_n(\rho) := \Gamma(w_n)$ and from (2.7) we infer that

$$\Gamma_n(\rho) = \int_0^L \sqrt{1 + \left[\frac{q}{H}\left(x - \frac{L}{2}\right) + \frac{n\pi}{L}\rho\cos\left(\frac{n\pi x}{L}\right)\right]^2}\, dx - L_c \quad \forall \rho \in \mathbb{R}. \tag{2.11}$$

In the next result we emphasize a striking difference between even and odd modes.

Theorem 2.1. *Assume that $\frac{q}{H} < \frac{2}{5}$.*
- *If $n \geq 1$ is even, then $\Gamma_n(\rho) \geq 0$ for all ρ; therefore, an even vibrating mode cannot shorten the cable.*
- *If $n \geq 1$ is odd, then there exists a (unique) critical value $\rho_n^* > 0$ such that $\Gamma_n(\rho_n^*) = 0$ and $\Gamma_n(\rho) < 0$ for all $\rho \in (0, \rho_n^*)$; therefore, odd vibrating modes shorten the cable when their amplitude of oscillation ρ is within this interval.*

Theorem 2.1 is proved in Section 2.4. The assumption $q/H < 2/5$ in Theorem 2.1 is verified in the vast majority of real suspension bridges. For instance, for the numerical data employed in [270], it happens that $q/H = 1.739 \times 10^{-3}\,[m^{-1}]$. Moreover, as reported in [221, Section 15.17], the sag-span ratio in a suspension bridge always lies in the range $(\frac{1}{12}, \frac{1}{8})$. In view of (2.1), this means that

$$\frac{L}{12} < g(0) - g\left(\frac{L}{2}\right) < \frac{L}{8} \quad \text{or, equivalently,} \quad \frac{2}{3L} < \frac{q}{H} < \frac{1}{L}.$$

Therefore, the assumption $\frac{q}{H} < \frac{2}{5}$ is valid for any suspension bridges with a span of at least $2.5\,[m]$! In any case, numerical results seem to show that the assumption $\frac{q}{H} < \frac{2}{5}$ is not necessary for the validity of Theorem 2.1.

Related to ρ_n^*, as characterized by Theorem 2.1, we introduce the quantity

$$\xi_n^* = \rho_n^*\left(\frac{n\pi}{L}\right)^2\left\{\left(\frac{n\pi}{L}\right)^2 EI + H + \frac{E_c A}{L_c}\Gamma\left(\rho_n^* \sin\left(\frac{n\pi x}{L}\right)\right)\right\} \quad \forall n \in \mathbb{N}, \tag{2.12}$$

which is the amplitude of oscillation of the live load p_n in (2.8) that generates the critical oscillation $w_n^*(x) = \rho_n^* \sin(\frac{n\pi x}{L})$. Throughout this chapter, as far as numerical data are needed, we use the parameters taken from [270]:

$$L = 460\,[m], \quad EI = 57 \times 10^6\,[kN \cdot m], \quad E_c A = 36 \times 10^6\,[kN], \quad \frac{q}{H} = 1.739 \times 10^{-3}\,[m^{-1}]. \tag{2.13}$$

Table 2.1 shows the critical values of ρ_n^* and ξ_n^* (according to Theorem 2.1 and (2.12)), as functions of some odd values of $n \in \mathbb{N}$.

n	1	3	5	7	9	11	13	15	17	19
ρ_n^*	94.807	3.056	0.657	0.239	0.112	0.061	0.037	0.024	0.016	0.011
ξ_n^*	444.016	156.115	125.811	124.578	132.962	145.676	160.734	177.192	194.559	212.620

Table 2.1: Critical coefficients for cable shortening in odd-vibrating modes.

As stated in Theorem 2.1, even modes never shorten the cable. This *does not* mean that odd modes are "worse" or more prone to elongate the cable. On the contrary, thinking of a periodic-in-time oscillation proportional to a vibrating mode (2.10), that is,

$$\rho(t)\sin\left(\frac{n\pi x}{L}\right) \quad \forall x \in [0, L], \quad \forall t > 0,$$

with $\rho(t)$ varying between $\pm\overline{\rho}$, we reach the opposite conclusion. To see this, in Figure 2.2 we plot the graphs of Γ_2 and Γ_3 and we see that

$$\max\{\Gamma_3(\overline{\rho}), \Gamma_3(-\overline{\rho})\} > \max\{\Gamma_2(\overline{\rho}), \Gamma_2(-\overline{\rho})\} = \Gamma_2(\overline{\rho}).$$

Therefore, even if the cable shortens when $\rho(t) \in (0, \rho_3^*)$ for the third mode, the cable itself elongates more than for the second mode when $\rho(t) < 0$. We come back to this issue in Section 2.3.
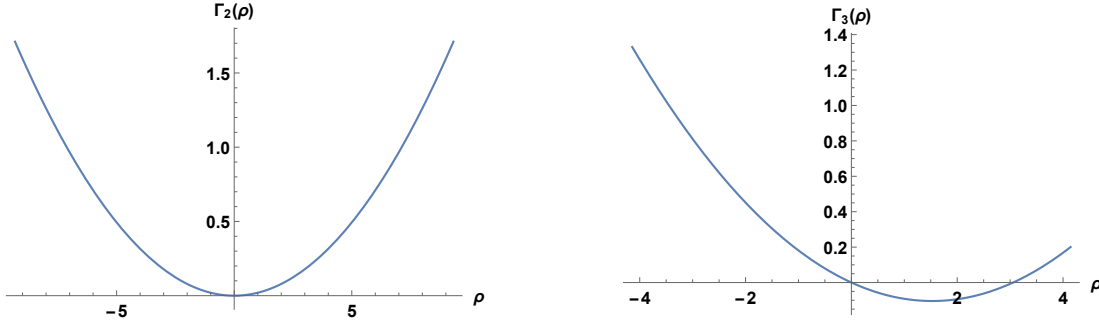

Figure 2.2: Increment of cable length in the second (left) and third (right) vibrating modes.

2.2   Thresholds for hangers slackening in a beam model

In this section we estimate the thresholds that provoke the slackening of some hangers. Since the hangers resist to extension but not to compression, if the deck goes too high above its equilibrium position, then *the hangers may no longer be considered as rigid inextensible bars.* In particular, they will not push upwards the cable in such a way that it loses convexity: the general principles governing the deformation of a finite-length cable under the action of a downwards vertical load (see [263, (1.3), VII]) indicate that the cable remains convex. This means that if $g + w$ is not convex, then it *does not* describe the position of the cable anymore.

In order to explain how the Melan equation (2.5) should be modified in case of hanger slackening we briefly recall the concept of *convexification* which can be formalized in several equivalent ways, see [92, (3.2), I] for full details.

Let $I \subset \mathbb{R}$ be a compact interval. The convexification f^{**} of a continuous function $f : I \to \mathbb{R}$ is:

- the pointwise supremum of all the affine functions everywhere less than f;
- the pointwise supremum of all the convex functions everywhere less than f;
- the largest convex function everywhere less than or equal to f;
- the convex function whose epigraph is the closed convex hull of the epigraph of f;
- the second Fenchel conjugate of f, that is,

$$f^{**}(x) = \sup_{y \in \mathbb{R}}\{xy - f^*(y)\} \quad \forall x \in I, \quad \text{where} \quad f^*(y) = \max_{x \in I}\{yx - f(x)\} \quad \forall y \in \mathbb{R}.$$

This notion enables us to give the following:

Definition 2.2. *We say that a displacement w **slackens** the hangers in some (nonempty) interval $(a, b) \subset [0, L]$ if the graph of*

$$z := g + w \tag{2.14}$$

*lies strictly above that of its convexification z^{**} in (a, b). Then, the **slackening region** $\mathcal{S} \subset [0, L]$ is the union of all the slackening intervals, that is,*

$$\mathcal{S} = \{x \in (0, L) \mid z(x) > z^{**}(x)\}.$$

In the slackening region, not only the Melan equation (2.5) is incorrect but also (2.3) fails since *the whole amount of live load is carried by the beam*: one has $p_1(x) = 0$ for all $x \in \mathcal{S}$. Therefore (2.5) should be replaced with the more reliable equation

$$EI\, w''''(x) + \left(\chi_{\mathcal{S}}(w) - 1\right)\left(\left(H + h(w)\right) w''(x) + \frac{q}{H}\, h(w)\right) = p(x) \qquad \forall x \in (0, L) \tag{2.15}$$

16

where $\chi_{\mathcal{S}}(w)$ is the characteristic function (that depends on w) of the slackening region $\mathcal{S}$, see Definition 2.2. We summarize these results in the following statement.

Proposition 2.1. *In absence of slackening ($\mathcal{S} = \emptyset$) the two equations (2.5) and (2.15) coincide; in this case, the solution w represents the displacement of the beam whereas z in (2.14) represents the position of the cable.*

In presence of slackening ($\mathcal{S} \neq \emptyset$) the correct equation is (2.15) and the position of the cable is described by z^{**}.

The term $(\chi_{\mathcal{S}}(w) - 1)$ adds a further nonlinearity to the Melan equation (2.5). As far as we are aware, there is no general theory to tackle equations such as (2.15). It would therefore be interesting to study its features in detail.

Although the exact slackening region is difficult to determine, it is clear that the non-convexity intervals of z in (2.14) represent proper subsets of these regions. Therefore, we have

Proposition 2.2. *Let w be the solution of (2.15) and let z be as in (2.14). If $\mathcal{S} \neq \emptyset$, then*

$$\{x \in (0, L); \, z''(x) \leq 0\} \subsetneq \mathcal{S}.$$

We now apply Proposition 2.1 to the case of the loads p_n in (2.8).

Proposition 2.3. *Let p_n and w_n be as in (2.8) and (2.10). Let*

$$C_n^* := \frac{q}{H}\left(\frac{L}{n\pi}\right)^2 \qquad \forall n \in \mathbb{N}. \tag{2.16}$$

Slackening occurs if and only if

$$\rho > C_1^* \text{ when } n = 1, \qquad |\rho| > C_n^* \text{ when } n \geq 2; \tag{2.17}$$

in this case, the position of the cable is described by z_n^{**} (with $z_n = g + w_n$).

The proof of Proposition 2.3 is fairly simple. The slackening region of w_n is nonempty if and only if there exists $x \in (0, L)$ such that $z_n''(x) < 0$, where

$$z_n(x) = g(x) + w_n(x) = \gamma + \frac{q}{2H}x(x - L) + \rho\sin\left(\frac{n\pi x}{L}\right) \qquad \forall x \in [0, L].$$

This property translates into

$$\exists x \in (0, L) \quad \text{such that} \quad \rho\sin\left(\frac{n\pi x}{L}\right) > C_n^*,$$

which is equivalent to (2.17).
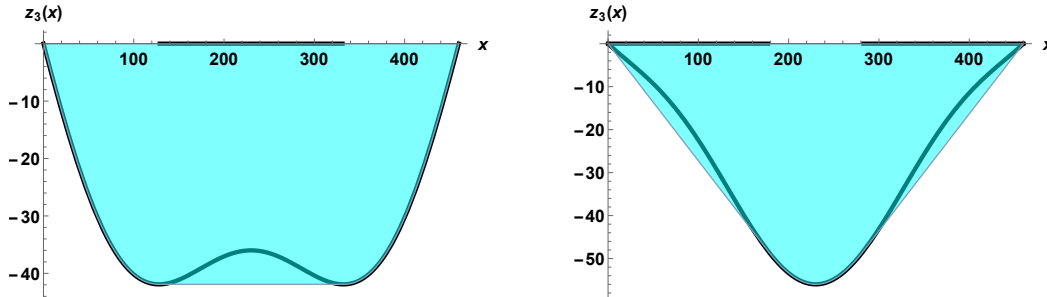

Figure 2.3: Slackening of the third vibrating mode when $\rho_3 < -C_3^*$ (left) and when $\rho_3 > C_3^*$ (right).

Since it is by far nontrivial to determine explicitly the convexification of z_n and the slackening region $\mathcal{S}_n$, we follow a numerical-geometrical approach, that is, we plot the closed convex hull of the epigraph of z_n. We take again the numerical values (2.13). In order to illustrate the procedure, consider the function z_3 (with $\gamma = 0$, since we are only interested in the shape of the curve), whose slackening threshold is $C_3^* \approx 4.1426$. By putting amplitudes of $\rho_3 = \pm 10$, we obtained the graphs of z_3 in Figure 2.3 where the slackening intervals have been highlighted over the horizontal axis, and the closed convex hull of the epigraph of z_3 has been shaded. Similarly, by putting amplitudes of $\rho_5 = \pm 5$, we obtained the plots displayed in Figure 2.4 for the graphs of z_5 (for which $C_5^* \approx 1.4913$):
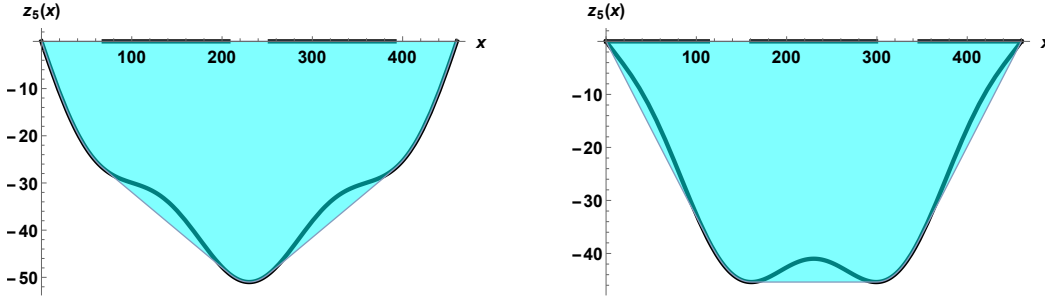

Figure 2.4: Slackening of the fifth vibrating mode when $\rho_5 < -C_5^*$ (left) and when $\rho_5 > C_5^*$ (right).

It is worthwhile noticing that the hangers slackening in even modes occurs asymmetrically with respect to the center of the beam but, at the same time, symmetrically with respect to the value of ρ_n. To clarify this point, in Figure 2.5 we display the graphs of z_2 (where $C_2^* \approx 9.3208$) when $\rho_2 = -20$, and of z_4 (where $C_4^* \approx 2.3301$) when $\rho_4 = 8$. The remaining figures when $\rho_2 > C_2^*$ or $\rho_4 < -C_4^*$ may be obtained by simply reflecting the curves with respect to the center of the beam.
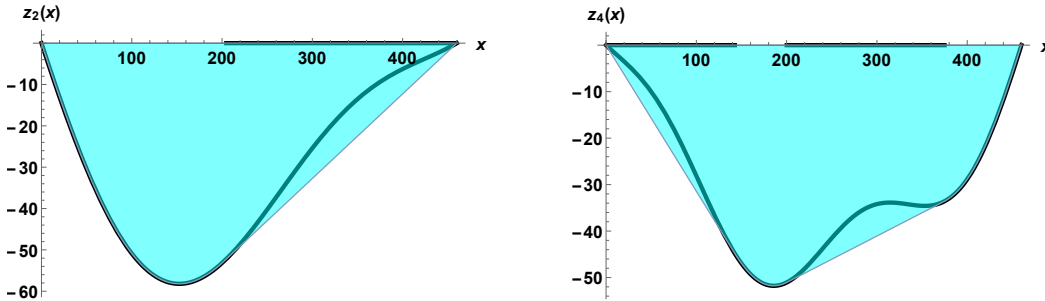
Figure 2.5: Slackening of the second vibrating mode when $\rho_2 < -C_2^*$ (left), and of the fourth vibrating mode when $\rho_4 > C_4^*$ (right).

The numerical values of C_n^* for $n \leq 10$ are reported in Table 2.2 where we used the parameters as in (2.13).

One last issue must be addressed. In some of the pictures in Figures 2.3, 2.4 and 2.5 we observe that the endpoints of the deck $x = 0$ and $x = L$ actually belong to the slackening region $\mathcal{S}_n$. This is clearly a physically impossible situation since the hangers are not expected to slacken at the endpoints of the beam. Geometrically, one expects instead that the tangent lines to the curve at the endpoints of the beam lie strictly below the graph of z_n in $(0, L)$, that is:

$$z_n(x) > \max\{z_n'(0)x, \ z_n'(L)(x - L)\} \quad \forall x \in (0, L), \quad \forall n \in \mathbb{N}. \tag{2.18}$$

Clearly, condition (2.18) is not satisfied for large values of $|\rho_n|$, but it remains valid even when $|\rho_n|$ is slightly larger than the slackening (and convexity) threshold (2.16). For the first ten vibrating modes, we numerically computed the threshold ρ_n^{**} that ensures condition (2.18), when $|\rho_n| \leq \rho_n^{**}$ (if n is even) and $\rho_n \leq \rho_n^{**}$ (if n is odd), with the parameters as in (2.13). We obtained the second line in Table 2.2.

18

n	1	2	3	4	5	6	7	8	9	10
C_n^*	37.283	9.321	4.143	2.330	1.491	1.035	0.761	0.582	0.460	0.372
ρ_n^{**}	58.564	14.641	6.507	3.660	2.342	1.626	1.195	0.915	0.723	0.585

Table 2.2: Thresholds for non-convexity and hangers slackening in the first ten vibrating modes.

2.3   Behavior of cables and hangers in a plate model

The deck of a real bridge cannot be described by a simple (one-dimensional) beam since it fails to display torsional oscillations. In this section we take advantage of the results so far obtained in order to analyze the vibrating modes of a rectangular plate $\Omega = (0, \pi) \times (-\ell, \ell)$ ($2\ell > 0$ is the width of the plate and $2\ell \ll \pi$); for simplicity, we take here $L = \pi$. Specifically, we consider a partially hinged plate whose elastic energy is given by the Kirchhoff-Love functional, see [206, 251] for discussions on the boundary conditions and updated derivation of the corresponding Euler-Lagrange equation. From [97] we know that the vibrating modes of the plate Ω are obtained by solving the following eigenvalue problem

$$\begin{cases} \Delta^2 u = \lambda u & \text{for } (x, y) \in \Omega \\ u = u_{xx} = 0 & \text{for } (x, y) \in \{0, \pi\} \times (-\ell, \ell) \\ u_{yy} + \sigma u_{xx} = u_{yyy} + (2 - \sigma)u_{xxy} = 0 & \text{for } (x, y) \in (0, \pi) \times \{-\ell, \ell\}, \end{cases} \tag{2.19}$$

where $\sigma \in \left(0, \frac{1}{2}\right)$ is the Poisson ratio. The boundary conditions for $x = 0$ and $x = \pi$ show that the short edges of the plate are hinged, while the conditions for $y = \pm \ell$ show that the plate is free on the long edges. Problem (2.19) is the two-dimensional counterpart of (2.9). From [97] we also know that the eigenvalues of (2.19) may be ordered in an increasing sequence of strictly positive numbers diverging to $+\infty$. Correspondingly, the eigenfunctions are identified by two indices $m, k \in \mathbb{N}_+$ and they have one of the following forms:

$$W_{m,k}(x, y) = \varphi_{m,k}(y) \sin(mx) \quad \text{with corresponding eigenvalue } \nu_{m,k},$$

$$\overline{W}_{m,k}(x, y) = \psi_{m,k}(y) \sin(mx) \quad \text{with corresponding eigenvalue } \mu_{m,k}.$$

The $\varphi_{m,k}$ are odd while the $\psi_{m,k}$ are even and this is why the $W_{m,k}$ are called *torsional* eigenfunctions while the $\overline{W}_{m,k}$ are called *longitudinal* eigenfunctions. The main difference between these two classes is precisely that $\overline{W}_{m,k}(x, \ell) = \overline{W}_{m,k}(x, -\ell)$ so that the free edges $y = \pm \ell$ are in the same position for longitudinal vibrations, while $W_{m,k}(x, \ell) = -W_{m,k}(x, -\ell)$ so that the free edges are in opposite positions for torsional vibrations.

We first deal with the slightly more complicated case of torsional vibrating modes. Then the eigenvalues $\nu_{m,k}$ are the (ordered) solutions $\lambda > m^4$ of the following equation:

$$\sqrt{\lambda^{1/2} - m^2}[\lambda^{1/2} + (1-\sigma)m^2]^2 \tanh(\ell\sqrt{\lambda^{1/2} + m^2}) = \sqrt{\lambda^{1/2} + m^2}[\lambda^{1/2} - (1-\sigma)m^2]^2 \tanh(\ell\sqrt{\lambda^{1/2} - m^2}),$$

while the function $\varphi_{m,k}$ may be taken as

$$\varphi_{m,k}(y) = [\nu_{m,k}^{1/2} - (1-\sigma)m^2] \frac{\sinh\left(y\sqrt{\nu_{m,k}^{1/2} + m^2}\right)}{\sinh\left(\ell\sqrt{\nu_{m,k}^{1/2} + m^2}\right)} + [\nu_{m,k}^{1/2} + (1-\sigma)m^2] \frac{\sin\left(y\sqrt{\nu_{m,k}^{1/2} - m^2}\right)}{\sin\left(\ell\sqrt{\nu_{m,k}^{1/2} - m^2}\right)},$$

see [97]. In particular, $\varphi_{m,k}(\ell) = 2\sqrt{\nu_{m,k}} = -\varphi_{m,k}(-\ell)$.

We view both the free edges of the plate $y = \pm \ell$ as beams connected to a cable and governed by the modified Melan equation (2.15). Then we take the following function as a solution of (2.15):

$$w_{m,k}(x) := \alpha W_{m,k}(x, \ell) = \alpha \varphi_{m,k}(\ell) \sin(mx) = 2\alpha\sqrt{\nu_{m,k}} \sin(mx) \quad \forall x \in [0, \pi], \tag{2.20}$$

19

for $m, k \in \mathbb{N}$ and $\alpha \in \mathbb{R}$, a function that belongs to the family of eigenfunctions of (2.9), see (2.10), assuming that $L = \pi$. As already mentioned, together with $w_{m,k}$ in (2.20), for torsional modes one needs to consider also its companion $-w_{m,k}$.

For longitudinal modes, one has to replace $w_{m,k}$ in (2.20) with

$$\overline{w}_{m,k}(x) := \alpha \overline{W}_{m,k}(x, \ell) = \alpha \psi_{m,k}(\ell) \sin(mx) \quad \forall x \in [0, \pi], \tag{2.21}$$

where $\psi_{m,k}(\ell)$ depends on the longitudinal eigenvalue $\mu_{m,k}$ of (2.19); see [97] for the precise characterization of $\mu_{m,k}$. For longitudinal modes, the behavior is the same on the two opposite edges.

The above discussion, combined with Theorem 2.1, yields the following statement.

Proposition 2.4. *Assume that $\frac{q}{H} < \frac{2}{5}$.*
- *If $m \geq 1$ is even, then the vibrating mode (either torsional or longitudinal) cannot shorten the cable.*
- *If $m \geq 1$ is odd and the mode is longitudinal, then there exists a (unique) critical value $\alpha^* = \alpha^*_{m,k} > 0$ such that for $\alpha \in (0, \alpha^*)$ both the cables are shortened while for other values of α no cable is shortened.*
- *If $m \geq 1$ is odd and the mode is torsional, then there exists a (unique) critical value $\alpha^* = \alpha^*_{m,k} > 0$ such that for $0 < |\alpha| < \alpha^*$ one and only one cable is shortened, while for other values of α no cable is shortened.*

Following the guideline of Section 2.1, one may then determine the exact critical values $\alpha^*_{m,k}$ (for odd m). It suffices to consider the critical values ρ^*_n from Theorem 2.1 and to take

$$\alpha^*_{m,k} = \frac{\rho^*_m}{\varphi_{m,k}(\ell)} \quad \text{or} \quad \alpha^*_{m,k} = \frac{\rho^*_m}{\psi_{m,k}(\ell)},$$

depending on whether the vibration is torsional or longitudinal.

Regarding slackening and the loss of convexity, the above discussion, combined with Propositions 2.2 and 2.3, yields the following statement.

Proposition 2.5. *Let w be the solution of (2.15) and assume that one of the free edges of Ω is in position w. Let z be as in (2.14). If $\mathcal{S} \neq \emptyset$, then*

$$\{x \in (0, L); z''(x) \leq 0\} \subsetneq \mathcal{S}.$$

In particular, if $w_{m,k}$ in (2.20) (resp. $\overline{w}_{m,k}$ in (2.21)) is the position of one of the free edges of Ω, then slackening of the hangers on that edge occurs if and only if

$$\alpha_1 > \frac{q}{H\varphi_{1,k}(\ell)} \quad \text{when } m = 1, \qquad |\alpha_m| > \frac{q}{Hm^2\varphi_{m,k}(\ell)} \quad \text{when } m \geq 2$$

$$\left(\text{resp. } \alpha_1 > \frac{q}{H\psi_{1,k}(\ell)} \quad \text{when } m = 1, \qquad |\alpha_m| > \frac{q}{Hm^2\psi_{m,k}(\ell)} \quad \text{when } m \geq 2 \right);$$

in this case, the position of the cable is described by $z^{**}_{m,k}$ (with $z_{m,k} = g + w_{m,k}$, resp. $z_{m,k} = g + \overline{w}_{m,k}$).

The final step consists in considering the evolution equation modeling the vibrations of the partially hinged rectangular plate Ω. According to [97], this leads to the following fourth-order wave-type equation:

$$\begin{cases} u_{tt} + \Delta^2 u = 0 & \text{for } (x, y, t) \in \Omega \times \mathbb{R}_+ \\ u = u_{xx} = 0 & \text{for } (x, y, t) \in \{0, \pi\} \times (-\ell, \ell) \times \mathbb{R}_+ \\ u_{yy} + \sigma u_{xx} = u_{yyy} + (2 - \sigma)u_{xxy} = 0 & \text{for } (x, y, t) \in (0, \pi) \times \{-\ell, \ell\} \times \mathbb{R}_+. \end{cases} \tag{2.22}$$

We wish to analyze here the evolution of the cable shortening and of the hanger slackening for the torsional vibrating modes $W_{m,k}$ of (2.19); as for the stationary case, the behavior of the longitudinal modes $\overline{W}_{m,k}$ is simpler. Therefore, we associate to (2.22) the following initial conditions

$$u(x, y, 0) = BW_{m,k}(x, y), \quad u_t(x, y, 0) = 0 \quad \forall(x, y) \in \Omega, \tag{2.23}$$

for some $B \in \mathbb{R}$. The problem (2.22)-(2.23) may be solved by separating variables and the solution is

$$u_{m,k}(x,y,t) = B\cos\left(\sqrt{\nu_{m,k}}\,t\right)W_{m,k}(x,y) \qquad \forall(x,y,t) \in \Omega \times \mathbb{R}_+. \tag{2.24}$$

Again, we view both the free edges of Ω as beams connected to a cable and governed by the modified Melan equation (2.15). Therefore, we consider the restriction to the free edge $y = \ell$ (the case $y = -\ell$ being similar) of the function $u_{m,k}$ in (2.24):

$$v_{m,k}(x,t) := u_{m,k}(x,\ell,t) = B\cos\left(\sqrt{\nu_{m,k}}\,t\right)\varphi_{m,k}(\ell)\sin(mx) \qquad \forall(x,t) \in (0,\pi)\times\mathbb{R}_+, \tag{2.25}$$

see (2.20). Similarly, for the longitudinal modes, we consider the function

$$\overline{v}_{m,k}(x,t) := B\cos\left(\sqrt{\mu_{m,k}}\,t\right)\psi_{m,k}(\ell)\sin(mx) \qquad \forall(x,t) \in (0,\pi)\times\mathbb{R}_+, \tag{2.26}$$

see (2.21). We are interested in determining the conditions under which the cables shorten their length (in odd vibrating modes) or when the hangers slacken. Unlike the preceding situations, such conditions will now be observed over a space-time region, because the coefficients representing the amplitude of the expressions (2.25) and (2.26) are periodic functions in time.

Concerning the shortening of the cables, we introduce some notations. Let $\alpha^*_{m,k} > 0$ be as in Proposition 2.4. If $m \geq 1$ is odd and the mode is longitudinal, put

$$I_S = \{t \geq 0;\ 0 < B\cos(\sqrt{\mu_{m,k}}\,t) < \alpha^*_{m,k}\}, \quad I_N = \mathbb{R}_+ \setminus I_S.$$

If $m \geq 1$ is odd and the mode is torsional, put

$$I^S = \{t \geq 0;\ 0 < |B\cos(\sqrt{\nu_{m,k}}\,t)| < \alpha^*_{m,k}\}, \quad I^N = \mathbb{R}_+ \setminus I^S.$$

Note that all these sets are nonempty, although I^N may have null measure: this happens if $|B| \leq \alpha^*_{m,k}$. Then, from Proposition 2.4 we deduce the following statement.
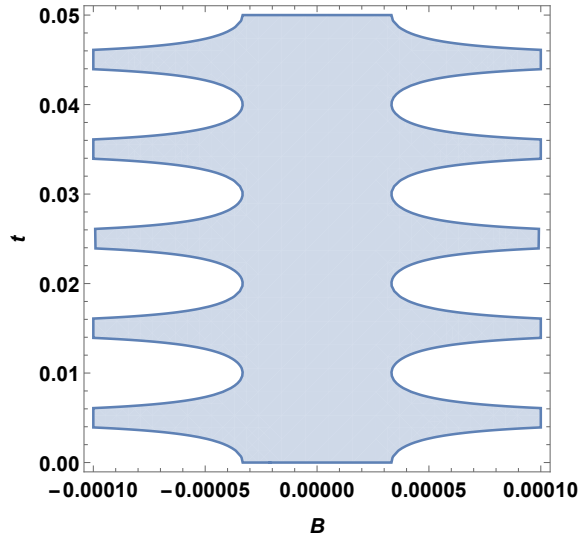
Figure 2.6: For $B \in [-0.0001, 0.0001]$, values of $t \in I^S$ (shaded) provoking cable shortening in the third torsional mode.

Proposition 2.6. *Assume that $\frac{q}{H} < \frac{2}{5}$.*
• *If $m \geq 1$ is even, then the vibrating mode (either torsional or longitudinal) does not shorten the cables for any $t > 0$.*
• *If $m \geq 1$ is odd and the mode is longitudinal, then both the cables are shortened if $t \in I_S$ whereas no cable is shortened if $t \in I_N$.*
• *If $m \geq 1$ is odd and the mode is torsional, then one and only one cable is shortened when $t \in I^S$ whereas no cable is shortened if $t \in I^N$.*

Once more we emphasize the striking difference between odd and even modes. Proposition 2.6 is illustrated in Figure 2.6 by shading the sub-regions of the rectangle $(B, t) \in [-0.0001, 0.0001] \times [0, 0.05]$ in which $t \in I^S$ for the third torsional mode. It turns out that for $0 < |B| \lesssim 0.000032$, for almost every $t > 0$ one (and only one) cable is shortened, whereas for larger values of $|B|$ the white regions (no shortening) have positive measure.

Also the slackening of the hangers (and the loss of convexity) in all the vibrating modes is now observed in a space-time region which periodically-in-time reproduces itself. In order to discuss together the longitudinal and torsional cases, we use the same notation to denote the function to be convexified:

$$z_{m,k}(x, t) = g(x) + v_{m,k}(x, t) \quad \left(\text{resp. } z_{m,k}(x, t) = g(x) + \overline{v}_{m,k}(x, t) \right) \qquad \forall (x, t) \in (0, \pi) \times \mathbb{R}_+, \quad (2.27)$$

where $v_{m,k}$ and $\overline{v}_{m,k}$ are as in (2.25) and (2.26). Concerning the non-convexity regions, for a given $B \in \mathbb{R}$ they are characterized by the points $(x, t) \in [0, \pi] \times [0, \infty)$ that satisfy the inequality:

$$\frac{\partial^2 z_{m,k}}{\partial x^2}(x, t) \leq 0$$

or, equivalently, by the points $(x, t) \in [0, \pi] \times [0, \infty)$ in which:

$$Bm^2 \varphi_{m,k}(\ell) \cos\left(\sqrt{\nu_{m,k}}\, t\right) \sin(mx) \geq \frac{q}{H} \quad \left(\text{resp. } Bm^2 \psi_{m,k}(\ell) \cos\left(\sqrt{\nu_{m,k}}\, t\right) \sin(mx) \geq \frac{q}{H} \right). \quad (2.28)$$

Notice that inequality (2.28) defines a region of $\mathbb{R}^2$ of positive measure only when $|B| > C^*_{m,k}$, where the convexity threshold is now given by:

$$C^*_{m,k} = \frac{q}{Hm^2 \varphi_{m,k}(\ell)} \text{ for the torsional modes,} \quad C^*_{m,k} = \frac{q}{Hm^2 \psi_{m,k}(\ell)} \text{ for the longitudinal modes,}$$

for every integers $m, k \geq 1$. Precisely, given $B \in \mathbb{R}$ and integers m and k, let us put:

$$\alpha_{m,k}(t) = B \cos\left(\sqrt{\nu_{m,k}}\, t\right) \quad \left(\text{resp. } \alpha_{m,k}(t) = B \cos\left(\sqrt{\mu_{m,k}}\, t\right) \right) \quad \forall t \geq 0.$$

Then, as a consequence of Proposition 2.5, we obtain the following statement.

Proposition 2.7. *Let u be the solution of (2.22) and assume that one of the free edges of Ω is in position $v_{m,k}$ as in (2.25) or $\overline{v}_{m,k}$ as in (2.26). Let $z_{m,k}$ be as in (2.27), depending on the vibrating mode considered. If $|B| > C^*_{m,k}$, then $\mathcal{S} \neq \emptyset$. Furthermore, whenever $|\alpha_{m,k}(t)| > C^*_{m,k}$ we have:*

$$\left\{ x \in (0, \pi) \mid \frac{\partial^2 z_{m,k}}{\partial x^2}(x, t) \leq 0 \right\} \subsetneqq \mathcal{S}.$$

More precisely, if $|B| > C^*_{m,k}$ and if $v_{m,k}$ in (2.25) (resp. $\overline{v}_{m,k}$ in (2.26)) is the position of one of the free edges of Ω, then slackening of the hangers on that edge occurs for all $t > 0$ such that:

$$\alpha_{1,k}(t) > \frac{q}{H \varphi_{1,k}(\ell)} \text{ when } m = 1, \quad |\alpha_{m,k}(t)| > \frac{q}{Hm^2 \varphi_{m,k}(\ell)} \text{ when } m \geq 2$$

$$\left(\text{resp. } \alpha_{1,k}(t) > \frac{q}{H \psi_{1,k}(\ell)} \text{ when } m = 1, \quad |\alpha_{m,k}(t)| > \frac{q}{Hm^2 \psi_{m,k}(\ell)} \text{ when } m \geq 2 \right);$$

in this case, the position of the cable is described by $z^{**}_{m,k}$, with $z_{m,k} = g + v_{m,k}$ as in (2.27).

Proposition 2.7 defines the slackening regions in the (x, t)-plane. Since these are difficult to determine explicitly, we focus our attention on the non-convexity regions. As a first example, we take the second torsional mode, whose convexity threshold is $C^*_{2,1} \approx 1.52 \times 10^{-4}$. In this case, setting $B = \pm 2 \times 10^{-4}$ and considering the rectangle $(x, t) \in [0, \pi] \times [0, 0.035]$, we obtained Figure 2.7.
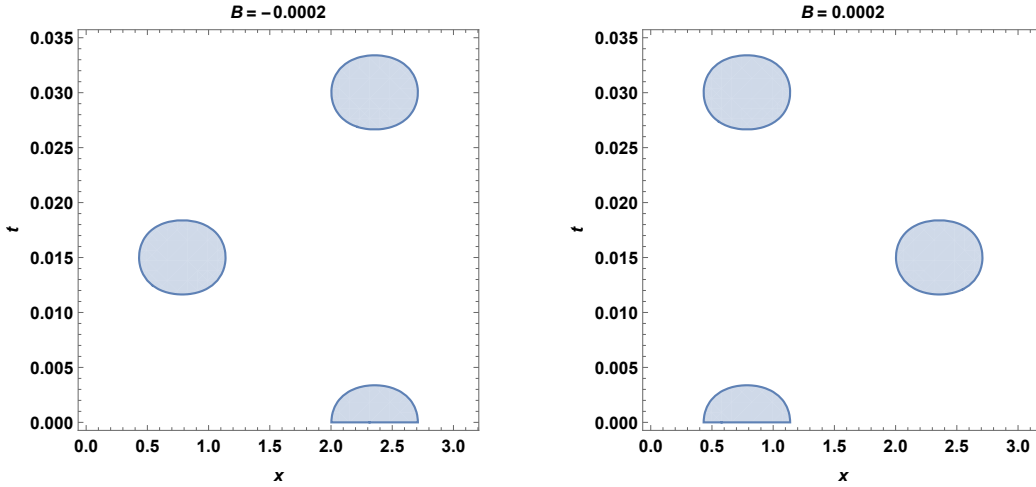
Figure 2.7: Non-convexity region of the second torsional mode for a time-varying amplitude.

Similar plots are obtained for the function $z_{3,1}$, whose convexity threshold is $C^*_{3,1} \approx 4.5 \times 10^{-5}$. By taking $B = \pm 1 \times 10^{-4}$, we get the following sub-region of the space-time rectangle $(x,t) \in [0,\pi] \times [0, 0.025]$ defined by Proposition 2.7:
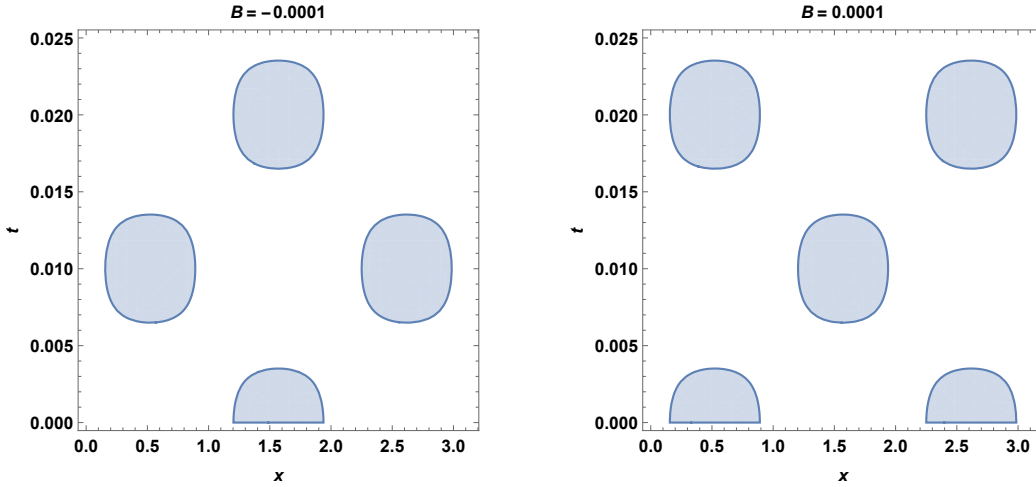
Figure 2.8: Non-convexity region of the third torsional mode for a time-varying amplitude.

All these plots may also be read by assuming that the right and left pictures represent simultaneously the non-convexity intervals for each cable, as far as torsional vibrations are involved: for any given $t > 0$ one should cross horizontally the two pictures in order to find which part of the interval $(0, \pi)$ of the two cables would be non-convex. In fact, the non-convexity regions are proper subsets of the slackening regions, see Proposition 2.7. Hence, the slackening regions are slightly wider in the x-direction than the "ellipses" in the above plots. This fact is illustrated in Figure 2.9 where we compare the non-convexity and slackening regions in the third torsional mode.

2.4   Proof of Theorem 2.1

The first step is a technical lemma which involves hyper-geometric integrals:
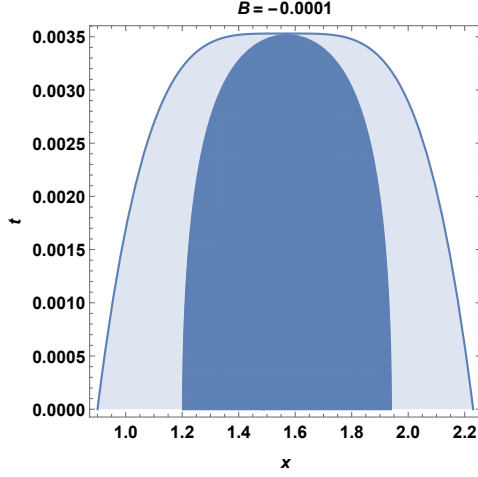
Figure 2.9: Slackening region for the third torsional mode

Lemma 2.1. *For odd $n \in \mathbb{N}$ and $0 < \mu < \frac{2}{5}$ we have*

$$G_n := \int_0^{\pi/2} \frac{t \sin(nt)}{\sqrt{1 + (\mu t)^2}} \, dt \quad \begin{cases} > 0 & \text{if } n \equiv 1 \pmod 4 \\ < 0 & \text{if } n \equiv 3 \pmod 4. \end{cases} \tag{2.29}$$

Proof. For $t \in \mathbb{R}$ such that $|t| < \dfrac{1}{\mu}$, the following power expansion is valid:

$$\frac{1}{\sqrt{1 + (\mu t)^2}} = \sum_{k=0}^{\infty} \binom{-1/2}{k} (\mu t)^{2k}.$$

Therefore, since $\mu < \frac{2}{5}$, for all $t \in \left[0, \dfrac{\pi}{2}\right]$ we can write:

$$G_n = \sum_{k=0}^{\infty} \binom{-1/2}{k} I_{n,k} \, \mu^{2k} \quad \forall n \in \mathbb{N}, \quad \text{where} \quad I_{n,k} = \int_0^{\pi/2} t^{2k+1} \sin(nt) \, dt \quad \forall n, k \in \mathbb{N}. \tag{2.30}$$

Since we are considering odd values of $n \in \mathbb{N}$, after integrating by parts twice $I_{n,k}$ in (2.30) we obtain:

$$I_{n,k} = -\frac{2k(2k+1)}{n^2} I_{n,k-1} + \delta(n) \frac{2k+1}{n^2} \left(\frac{\pi}{2}\right)^{2k} \quad \forall k \geq 1,$$

with $I_{n,0} = \dfrac{\delta(n)}{n^2}$, for every odd $n \in \mathbb{N}$, and:

$$\delta(n) = \begin{cases} 1 & \text{if } n \equiv 1 \pmod 4 \\ -1 & \text{if } n \equiv 3 \pmod 4. \end{cases} \tag{2.31}$$

An inductive argument over $k \geq 1$ allows then to deduce

$$I_{n,k} = \delta(n) \sum_{j=0}^{k} \frac{(-1)^{k+j}}{n^{2(k+1-j)}} \frac{(2k+1)!}{(2j)!} \left(\frac{\pi}{2}\right)^{2j} \quad \forall k \geq 1. \tag{2.32}$$

24

Our first claim is that $I_{n,k} > 0$ when $n \equiv 1 \pmod 4$, and that $I_{n,k} < 0$ when $n \equiv 3 \pmod 4$, for all $k \in \mathbb{N}$. But, according to (2.31) and the form of expression (2.32), it suffices to show that:

$$J_{n,k} := (-1)^k \sum_{j=0}^{k} \frac{(-1)^j}{(2j)!} \left(\frac{n\pi}{2} \right)^{2j} > 0 \quad \forall n \in \mathbb{N} \text{ odd}, \ k \geq 1. \tag{2.33}$$

In order to prove (2.33), we distinguish two cases.

• **Case (A):** $k > \dfrac{\sqrt{1+(n\pi)^2} - 7}{4}$. Since $n \in \mathbb{N}$ is odd, we know that

$$0 = \cos \left(\frac{n\pi}{2} \right) = \sum_{j=0}^{k} \frac{(-1)^j}{(2j)!} \left(\frac{n\pi}{2} \right)^{2j} + \sum_{j=k+1}^{\infty} \frac{(-1)^j}{(2j)!} \left(\frac{n\pi}{2} \right)^{2j}. \tag{2.34}$$

We put $a_j = \dfrac{1}{(2j)!} \left(\dfrac{n\pi}{2} \right)^{2j}$ and observe that, for every $j \geq 1$,

$$\frac{a_j}{a_{j-1}} = \frac{(n\pi)^2}{8j(2j-1)} < 1 \quad \Longleftrightarrow \quad j > \frac{\sqrt{1+(n\pi)^2}+1}{4}.$$

Hence, the Leibniz criterion can be applied to the *tail* series $\sum_{j=k+1}^{\infty}(-1)^j a_j$ if $j > \frac{\sqrt{1+(n\pi)^2}+1}{4}$. But since the first ratio to be considered is a_{k+2}/a_{k+1}, the Leibniz criterion may be applied whenever

$$k + 2 > \frac{\sqrt{1+(n\pi)^2}+1}{4} \quad \Longleftrightarrow \quad k > \frac{\sqrt{1+(n\pi)^2}-7}{4},$$

which is precisely the case considered. Therefore, the tail series $\sum_{j=k+1}^{\infty}(-1)^j a_j$ has the same sign as $(-1)^{k+1}$. In view of (2.34), the finite sum $\sum_{j=0}^{k}(-1)^j a_j$ has the sign of $(-1)^k$, that is, the opposite sign of the tail series. In turn, $J_{n,k} > 0$ in this case, for all odd values of $n \in \mathbb{N}$.

• **Case (B):** $k < \frac{\sqrt{1+(n\pi)^2}-7}{4}$. We distinguish here further between odd and even values of k. For even $k \in \mathbb{N}$, we may write

$$J_{n,k} = 1 + \sum_{i=1}^{k/2} (a_{2i} - a_{2i-1})$$

and, since $2i \leq k$, all the terms in the sum are positive in view of the assumption of case B. Therefore, $J_{n,k} > 0$ for even k.

For odd $k \in \mathbb{N}$, we may write

$$J_{n,k} = \sum_{i=0}^{\frac{k-1}{2}} (a_{2i+1} - a_{2i})$$

and, since $2i+1 \leq k$, all the terms in the sum are positive in view of the assumption of case B. Therefore, $J_{n,k} > 0$ also for odd k.

Inequality (2.33) is so proved for all n and k. Let us now fix an integer $n \equiv 1 \pmod 4$ (the case when $n \equiv 3 \pmod 4$ follows a completely analogous procedure). As a consequence of (2.33), we obtain the upper bound:

$$I_{n,k} = -\frac{2k(2k+1)}{n^2} \frac{(2k-1)!}{n^{2k}} J_{n,k-1} + \frac{2k+1}{n^2} \left(\frac{\pi}{2} \right)^{2k} < \frac{2k+1}{n^2} \left(\frac{\pi}{2} \right)^{2k} \quad \forall k \geq 1. \tag{2.35}$$

Back to (2.30), we may write:

$$G_n = \frac{1}{n^2} + \sum_{k=1}^{\infty} \binom{-1/2}{k} \left[\sum_{j=0}^{k} \frac{(-1)^{k+j}}{n^{2(k+1-j)}} \frac{(2k+1)!}{(2j)!} \left(\frac{\pi}{2} \right)^{2j} \right] \mu^{2k}. \tag{2.36}$$

We observe that the binomial coefficient $\binom{-1/2}{k}$ is negative when k is odd and positive otherwise. Furthermore, if we put

$$b_k := \left| \binom{-1/2}{k} \right| \quad \forall k \geq 1,$$

then one has that

$$\frac{b_{k+1}}{b_k} = \frac{2k+1}{2k+2} < 1 \quad \forall k \geq 1, \tag{2.37}$$

so that $b_k \leq b_1 = 1/2$ for all $k \geq 1$. Since in (2.36) all the terms in the sum over $j \in \{0, \ldots, k\}$ are strictly positive as a consequence of (2.33), by exploiting (2.35) and (2.37) we obtain

$$G_n > \frac{1}{n^2} - \sum_{\substack{k=1 \\ k \text{ odd}}}^{\infty} \frac{1}{2} \frac{2k+1}{n^2} \left(\frac{\mu\pi}{2}\right)^{2k} = \frac{1}{n^2} \left[1 - \frac{1}{2} \sum_{p=0}^{\infty} (4p+3) \left(\frac{\mu\pi}{2}\right)^{4p+2} \right].$$

For every $x \in (-1, 1)$, the geometric series can be differentiated term by term, that is,

$$\frac{d}{dx} \left(\sum_{p=0}^{\infty} x^{4p+3} \right) = \sum_{p=0}^{\infty} (4p+3) x^{4p+2} = \frac{d}{dx} \left(\frac{x^3}{1-x^4} \right) = \frac{x^6 + 3x^2}{(1-x^4)^2} \quad \forall x \in (-1, 1).$$

Hence, we finally infer that

$$G_n > \frac{1}{n^2} \left[1 - \frac{\left(\frac{\mu\pi}{2}\right)^6 + 3\left(\frac{\mu\pi}{2}\right)^2}{2\left[1 - \left(\frac{\mu\pi}{2}\right)^4\right]^2} \right]. \tag{2.38}$$

Some computations show that the right-hand side of (2.38) is strictly positive (at least) when $\dfrac{\mu\pi}{2} < 0.65$, so in particular, when $\mu < 0.4$. This concludes the proof. $\qquad \square$

For the sake of illustration, in Table 2.3 we give the numerical approximation of G_n, for odd values of $n \in \mathbb{N}$ up to $n = 19$, when $\mu = 1.739 \times 10^{-3}$ (as in (2.13)):

n	1	3	5	7	9	11	13	15	17	19
G_n	0.9999	-0.1111	0.0399	-0.0204	0.0123	-0.0082	0.0059	-0.0044	0.0034	-0.0027

Table 2.3: Numerical values of the integral G_n in (2.29), for some odd values of $n \in \mathbb{N}$.

In fact, for every $\mu \geq 0$ we know that $G_n \longrightarrow 0$ as $n \longrightarrow \infty$, as a direct consequence of the Riemann-Lebesgue Theorem. This is quite visible also in Table 2.3.

Our second technical result gives a qualitative property of the graph of $\Gamma_n(\rho)$.

Lemma 2.2. *For all integer $n \geq 1$, the map $\rho \mapsto \Gamma_n(\rho)$ is strictly convex.*

Proof. It suffices to analyze the case when $L = \pi$, and so:

$$\Gamma_n(\rho) = \int_0^\pi \sqrt{1 + \left[\frac{q}{H} \left(x - \frac{\pi}{2} \right) + n\rho \cos(nx) \right]^2} \, dx - L_c \quad \forall \rho \in \mathbb{R}, \quad \forall n \in \mathbb{N}.$$

After differentiating under the integral sign we obtain the following:

$$\Gamma_n'(\rho) = \int_0^\pi \frac{n \cos(nx) \left[\frac{q}{H} \left(x - \frac{\pi}{2} \right) + n\rho \cos(nx) \right]}{\sqrt{1 + \left[\frac{q}{H} \left(x - \frac{\pi}{2} \right) + n\rho \cos(nx) \right]^2}} \, dx, \tag{2.39}$$

26

$$\Gamma_n''(\rho) = \int\limits_0^\pi \frac{[n\cos(nx)]^2}{\left[1 + \left(\frac{q}{H}\left(x - \frac{\pi}{2}\right) + n\rho\cos(nx)\right)^2\right]^{3/2}} \, dx,$$

for $\rho \in \mathbb{R}$ and $n \in \mathbb{N}$. Therefore, $\Gamma_n''(\rho) > 0$, for every $n \geq 1$ and $\rho \in \mathbb{R}$, so that Γ_n is a strictly convex function all over $\mathbb{R}$. $\qquad\square$

In view of (2.39), we see that

$$\Gamma_n'(0) = \frac{nq}{H} \int\limits_0^\pi \frac{\left(x - \frac{\pi}{2}\right)\cos(nx)}{\sqrt{1 + \left(\frac{q}{H}\right)^2\left(x - \frac{\pi}{2}\right)^2}} \, dx. \tag{2.40}$$

If n is even, then the integrand in (2.40) is skew-symmetric with respect to $x = \pi/2$ and hence

$$\Gamma_n'(0) = 0 \qquad \text{for even } n. \tag{2.41}$$

If n is odd, then we make the substitution $t = x - \frac{\pi}{2}$ and we note that

$$\cos\left(nt + \frac{n\pi}{2}\right) = \begin{cases} -\sin(nt), & \text{if } n \equiv 1 \pmod 4 \\ \sin(nt), & \text{if } n \equiv 3 \pmod 4, \end{cases}$$

for all $n \geq 1$ and $t \in \left[-\frac{\pi}{2}, \frac{\pi}{2}\right]$. Therefore, after setting $\mu = \frac{q}{H}$, we see that $\Gamma_n'(0) = -2\mu n \delta(n) G_n$ if n is odd. From (2.31) and Lemma 2.1 we then infer that

$$\Gamma_n'(0) < 0 \qquad \text{for odd } n. \tag{2.42}$$

Since $\Gamma_n(0) = 0$ for all n, Theorem 2.1 follows by combining Lemma 2.2 with (2.41) and (2.42).

Chapter 3

Boundary conditions for planar Stokes equations inducing vortices around concave corners

For the remaining parts of this work we analyze exclusively the hydrodynamic component of the fluid-structure interaction problem considered: the obstacle is assumed to remain static and we study the interaction between the fluid and the rigid walls of the domain.

Experimental evidence (see, e.g. [35, 78, 87, 272]) shows that, when a fluid hits a bluff body, its flow is modified and creates vortices around the body (behind it), see Figure 4.1. Vortices may also be
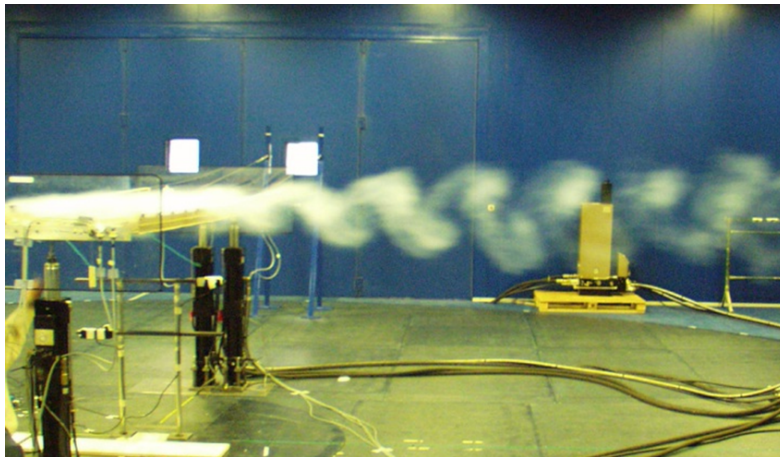
Figure 3.1: Vortices obtained in wind tunnel experiments at the Politecnico di Milano.

detected numerically [103, 109]. Depending on the geometry of the body, a symmetrical or asymmetrical rotating flow is periodically developed in that hidden part. A detailed description of this phenomenon is given in [233] but, even in the case of a perfectly circular cylinder, instabilities in the vortex shedding pattern may appear, see [210, Section 4.2.6]. In the vortex formation, flow separations and reattachments strongly depend on the Reynolds number through fairly complicated rules (see e.g. [103]), which makes the analytical and the numerical treatments very challenging. So far, the mathematical modeling of these phenomena is rather poor and totally unsatisfactory for engineers [139]. A viscous fluid past a rigid body immersed in the fluid is usually tackled under (no-slip) homogeneous Dirichlet boundary conditions for the velocity field on the surface of the obstacle, see [169, Chapter 2, Section 2] and [173, Chapter 2]. But since in the long term we have in mind to study an obstacle representing a suspension bridge which undergoes oscillations (moving obstacle) [38], an interactive motion of the obstacle should

also be studied with different boundary conditions, as in [62]. Mixed boundary conditions (based on the normal velocity, tangential velocity, vorticity and pressure) arise naturally in a network of pipes [195], in fluid-structure models in hemodynamics [53] and in the thermoelectromagnetic flow of a viscous fluid [6]. These nonstandard boundary conditions for the Stokes and Navier-Stokes equations were introduced by Conca et al. [30, 31, 61] (see also [26, 49, 76, 119, 131] for subsequent developments), suggesting an alternative variational formulation for problems of fluids around an obstacle. Having in mind to explain the vortex shedding generated by the wind acting on the deck of an oscillating suspension bridge, in this chapter (which is based on the published article [127]) we pursue a double objective: we discuss nonstandard variational formulations for the Stokes equations in domains with an obstacle and we determine possible boundary data which give rise to vortices.

For the first purpose we consider the stationary Stokes equations in a bounded domain $Q \subset \mathbb{R}^3$:

$$- \eta \Delta u + \nabla p = f \,, \quad \nabla \cdot u = 0 \qquad \text{in } Q \,, \tag{3.1}$$

where $\eta > 0$ denotes the kinematic viscosity, $u : Q \to \mathbb{R}^3$ is the velocity field, $p : Q \to \mathbb{R}$ is the scalar pressure, $f : Q \to \mathbb{R}^3$ is an external force. The domain Q is not simply connected, it contains an obstacle $D \subset \mathbb{R}^3$ representing the bridge. It is clear that *linear equations* such as (3.1) may not be suitable to describe turbulent regimes and it is by far more realistic to stick to *nonlinear equations* such as the Euler equations or the full Navier-Stokes equations, see [189]. Therefore, this chapter should just be seen as a first attempt to derive some information from the boundary behavior of the solution, possibly applicable to more sophisticated models: in fact, by assuming a constant transversal behavior of the force f, we further simplify the study by reducing to a planar domain. This chapter is also a first contribution to a research project [38], submitted to the Thelam Fund (Belgium) in March 2018. The variational formulation in [31] is based on the vorticity instead of the gradient of the velocity and this suggests to impose boundary conditions on the vorticity itself. In the present chapter, we revisit the procedure in [31] and we extend it to a slightly more general context, see Section 3.1.1 where we reduce the 3D problem to a 2D problem and we explain in detail the physical model. The well-posedness of the considered problem is established in Theorem 3.1 in Section 3.1.2. Its proof is based on a nontrivial application of the Lax-Milgram Theorem. The ellipticity of the related bilinear form depends on the regularity and the topology of the domain. If a domain with $\mathcal{C}^2$-boundary is not simply-connected, Foias-Temam [101] showed that the subspace of irrotational vector fields is nontrivial (its dimension is equal to the number of cuts needed to make the domain simply-connected). In [61, Appendix A], the authors managed to prove the ellipticity of the bilinear form when the domain is a convex polyhedron or when its boundary is of class $\mathcal{C}^{1,1}$. Although our domain is neither convex, nor a polyhedron, nor of class $\mathcal{C}^{1,1}$, nor simply-connected, we are still able to demonstrate the ellipticity of the bilinear form by combining some results contained in [132].

The second purpose of this chapter is to determine boundary conditions and data which yield solutions of the Stokes equations (3.1) displaying vortices. Obviously, any change in the boundary data strongly modifies the behavior of the solution. We identify boundary conditions compatible with the considered variational formulation, although the "optimal choice" of the boundary data remains unclear. We focus our attention on an unbounded, simply connected planar region having a concave right angle. If on the one hand simple connectivity enables us to show the existence of a *stream function* satisfying a biharmonic equation (see [75] and Section 3.3), on the other hand it is known [137, 197] that existence and regularity results may fail in nonsmooth domains even if the data are smooth. A variety of methods have been developed in order to solve biharmonic equations in planar regions [80, 158, 159, 199, 200, 206]. The singularities of solutions in the neighborhood of a concave corner are described through functional spaces with weighted norms. In most cases, these singularities are of power type (see Borsuk-Kondrat'ev [40, Chapter 5]), but in the present chapter the singularity will be represented by the composition between trigonometric and logarithmic functions, see Theorem 3.2 below, and thus characterized by chaotic oscillations near the angle. In Section 3.4 we determine some boundary conditions and data that highlight vortices within the explicit solution, in separated-variable form, of (3.1). These boundary

conditions impose a null normal component of the velocity field (in both faces of the concave angle) and some value for the scalar vorticity. Our boundary data are also justified by the regularity properties of the solution: we introduce *singular* solutions, see Definition 3.2, and we choose data giving rise to this kind of solutions.

This chapter is organized as follows. In Section 3.1.1 we describe in detail the domain Q, together with its two-dimensional projection Ω; the nonstandard boundary conditions for the Stokes equations to be solved in Ω are presented in Section 3.1.2, whose main core is the corresponding existence and uniqueness result, see Theorem 3.1. In Section 3.2, a review of the method of separation of variables is carried out for the biharmonic equation in polar coordinates in an unbounded domain $\Lambda \subset \mathbb{R}^2$ having a concave right angle. A class of separated-variable solutions is obtained in Theorem 3.2 that allows us to characterize, in Section 3.3, singular solutions of the Stokes equations in Λ, see Definition 3.2. Finally, in Section 3.4 we give explicit singular solutions of the Stokes system in Λ. This is done by considering two families of boundary conditions: for laminar inflow and for oriented velocity, see Sections 3.4.1 and 3.4.2, respectively. The results are complemented with some figures.

3.1 The Stokes equations with nonstandard boundary conditions

3.1.1 From the three-dimensional problem to the planar problem

In the space $\mathbb{R}^3$ we consider the deck of the bridge to be a thin plate defined by

$$D = (0, \pi) \times (-\ell, \ell) \times (-d, d), \tag{3.2}$$

where $d \ll \ell \ll \pi$. To have an idea, one could take $\ell = \pi/150$ and $d = \pi/1000$ (a deck of length 1km, with the width of about 13m, whose thickness is about 1m). Then we consider the region where the air surrounds the deck

$$Q = (0, \pi) \times (-L, L)^2 \setminus D, \tag{3.3}$$

where $L \gg \pi$, for instance $L = 100\pi$ (100km, an approximation of an unbounded region). The domains Q and D, as well as their intersections Ω and K with the plane $x = \frac{\pi}{2}$, are represented in Figure 3.2 (not in scale).
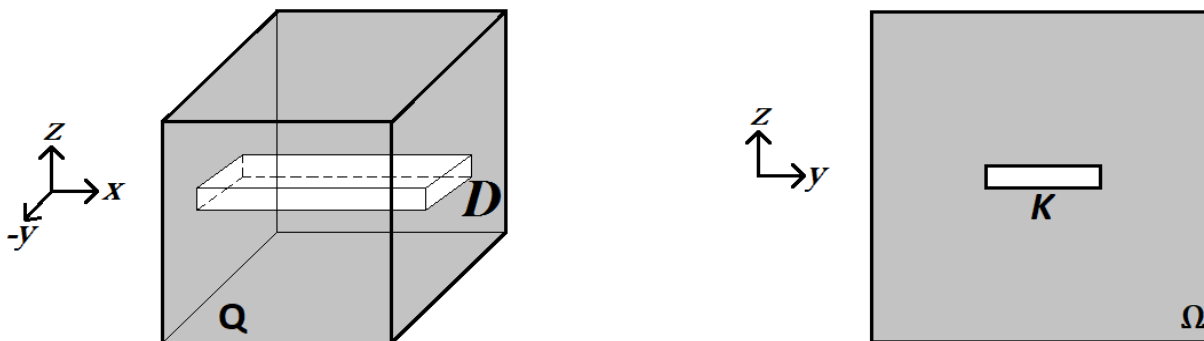
Figure 3.2: The domains Q and D (left) and their intersections Ω and K with the plane $x = \frac{\pi}{2}$.

We are interested in solving (3.1) with nonstandard and mixed boundary conditions on the different parts of ∂Q, depending on the velocity, vorticity and pressure. This is a particular inflow-outflow problem in a rectangular cylinder (with obstacle) [123]. We model the case where the wind is blowing only in the y-direction, so that it is reasonable to analyze the planar section of this configuration, as represented in the right picture of Figure 3.2. Neither the 3D domain Q nor the 2D domain Ω are simply connected. From now on, all the two-dimensional vector fields will be considered as three-dimensional vector fields,

assuming that they do not depend on the first variable and that their first component is identically null. We are so led to study the planar problem of a flow around the rectangle K.

In fact, in this planar setting we consider a *smooth rectangular obstacle* of width 2ℓ and height $2d$, still denoted by K, whose corners are smoothened by small quarters of circles, as in the left picture of Figure 3.3. Therefore, $K \subset (-\ell, \ell) \times (-d, d)$, while the open domain $\Omega = (-L, L)^2 \setminus \overline{K}$ is the region where the air surrounds the obstacle K: they are both represented, not in scale, in the right picture of Figure 3.3.
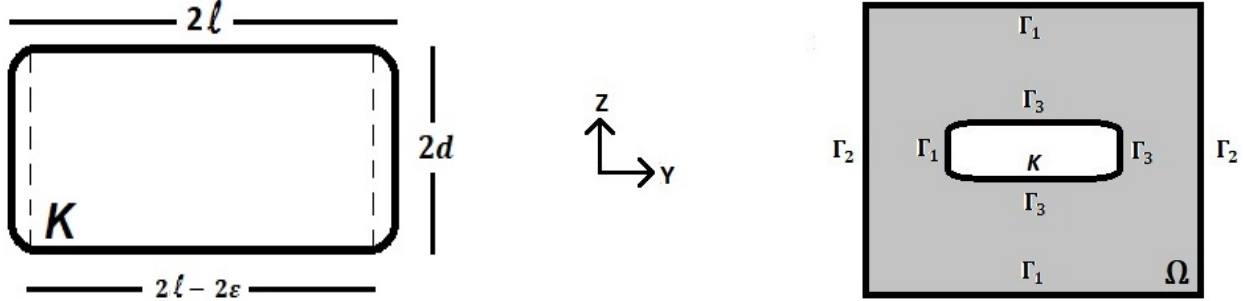
Figure 3.3: The obstacle K (left) and the domain Ω (right).

For our purposes, it will be convenient to decompose the boundary of Ω as:

$$\partial\Omega = \overline{\Gamma_1} \cup \overline{\Gamma_2} \cup \overline{\Gamma_3},$$

where:

$$
\begin{aligned}
\Gamma_1 &= \{(y, z) \in \partial K \mid -\ell \leq y < -\ell + \varepsilon\} \, \cup \, \{(y, z) \in \mathbb{R}^2 \mid y \in (-L, L),\ z \in \{-L, L\} \}, \\
\Gamma_2 &= \{(y, z) \in \mathbb{R}^2 \mid y \in \{-L, L\},\ z \in (-L, L) \}, \\
\Gamma_3 &= \{(y, z) \in \partial K \mid -\ell + \varepsilon < y \leq \ell\},
\end{aligned}
\tag{3.4}
$$

so that the rounded corners on the left side of K belong to Γ_1. Therefore, Ω is an open, bounded and connected set, with a locally Lipschitz boundary and with the interior boundary ∂K of class $\mathcal{C}^{1,1}$. Consequently, the outward unit normal $\hat{n}$ is defined almost everywhere on $\partial\Omega$, as a Lipschitz-function on each connected component of $\partial\Omega$. This model was first suggested in the research project [38, 125].

3.1.2 An existence and uniqueness result

We model the situation in which a constant wind blows in the y-direction, so that the forcing term f and its potential F read

$$f = f(y, z) = (w, 0), \qquad F(y, z) = wy \qquad \forall (y, z) \in \Omega, \tag{3.5}$$

being $w > 0$ the scalar wind velocity. In this setting, the cross product of two planar vectors (in the plane spanned by $\{\hat{\mathbf{j}}, \hat{\mathbf{k}}\}$) and the curl of a two-dimensional vector field is a three-dimensional vector field whose only non-null component is the one parallel to $\hat{\mathbf{i}}$:

$$u(y, z) = u^1(y, z)\hat{\mathbf{j}} + u^2(y, z)\hat{\mathbf{k}} \qquad \Longrightarrow \qquad \nabla \times u = \left(\frac{\partial u^2}{\partial y} - \frac{\partial u^1}{\partial z}\right)\hat{\mathbf{i}} \qquad \forall u \in \mathcal{C}^1(\Omega)^2.$$

The stationary Stokes equations are analyzed over the domain Ω:

$$-\eta\Delta u + \nabla p = f, \quad \nabla \cdot u = 0 \quad \text{in } \Omega, \tag{3.6}$$

where, again, $u : \Omega \to \mathbb{R}^3$ is the velocity field (but with null first component) and $p : \Omega \to \mathbb{R}$ is the scalar pressure while $\eta > 0$ is the kinematic viscosity. Given $u_0 \in H^{1/2}(\Gamma_1)^2$, $p_0 \in H^{-1/2}(\Gamma_2)$ and $h \in H^{-1/2}(\Gamma_3)^2$, to (3.6) we associate the following generalized boundary conditions:

$$u = u_0 \ \text{on } \Gamma_1, \qquad u \times \hat{n} = 0,\ p = p_0 \ \text{on } \Gamma_2, \qquad u \cdot \hat{n} = 0,\ (\nabla \times u) \times \hat{n} = h \times \hat{n} \ \text{on } \Gamma_3. \tag{3.7}$$

The first condition in (3.7) prescribes the velocity field in all parts of Γ_1 (nonhomogeneous Dirichlet boundary condition), according to the expected physical properties of the problem. The second condition in (3.7) imposes that the flow is normal on the parts of $\partial\Omega$ where the flow is entering and exiting and, therefore, the pressure will be constant with opposite signs in correspondence of the inflow or outflow parts. The third condition in (3.7) states that the flow is tangential on Γ_3. From a physical point of view, it would be reasonable to assume that $h = 0$ on the upper and lower faces of the obstacle K; nevertheless, we will consider general data $h \in H^{-1/2}(\Gamma_3)^2$. On the opposite side of the deck (leeward wall), the velocity u is tangential as well as the vorticity. This last boundary condition is crucial if one intends to model the shedding of vortices.

Next, we introduce two functional spaces:

$$V(\Omega) \doteq \{v \in H^1(\Omega)^2 \mid \nabla \cdot v = 0 \text{ in } \Omega; \quad v = 0 \text{ on } \Gamma_1; \quad v \times \hat{n} = 0 \text{ on } \Gamma_2; \quad v \cdot \hat{n} = 0 \text{ on } \Gamma_3\},$$

$$H(\Delta, \Omega) \doteq \{q \in L^2(\Omega) \mid \Delta q \in L^2(\Omega)\}.$$

Since the trace operator is linear and continuous from $H^1(\Omega)$ to $H^{1/2}(\partial\Omega)$, we infer that $V(\Omega)$ is a closed subspace of $H^1(\Omega)^2$ and therefore it constitutes a Hilbert space under the usual scalar product of $H^1(\Omega)^2$, defined as:

$$(u, v)_{H^1(\Omega)^2} \doteq (u^1, v^1)_{H^1(\Omega)} + (u^2, v^2)_{H^1(\Omega)} \quad \forall u, v \in H^1(\Omega)^2.$$

As explained in [31, Théorème 1.9], all the functions of $H(\Delta, \Omega)$ possess a trace belonging to $H^{-1/2}(\partial\Omega)$.

We also need to introduce the continuous bilinear form $A : H^1(\Omega)^2 \times H^1(\Omega)^2 \to \mathbb{R}$ defined by

$$A(u, v) = \eta \int_\Omega (\nabla \times u) \cdot (\nabla \times v) \, dx \quad \forall u, v \in H^1(\Omega)^2; \tag{3.8}$$

note that the last two components of $\nabla \times u$ and $\nabla \times v$ are identically null and that

$$(\nabla \times u) \cdot (\nabla \times v) = \left(\frac{\partial u^2}{\partial y} - \frac{\partial u^1}{\partial z} \right) \left(\frac{\partial v^2}{\partial y} - \frac{\partial v^1}{\partial z} \right) \quad \forall u, v \in H^1(\Omega)^2.$$

Finally, we will also need the continuous linear functional $L : H^1(\Omega)^2 \to \mathbb{R}$ defined by

$$L(v) = \int_\Omega f(x) \cdot v(x) \, dx - \langle p_0, v \cdot \hat{n} \rangle_{\Gamma_2} + \eta \langle h \times \hat{n}, v \rangle_{\Gamma_3} \quad \forall v \in H^1(\Omega)^2, \tag{3.9}$$

where $\langle \cdot, \cdot \rangle_{\Gamma_i}$ denotes the duality product between $H^{-1/2}(\Gamma_i)$ and $H^{1/2}(\Gamma_i)$ ($i \in \{1, 2, 3\}$).

As in [31] (see also [61]), for the boundary datum u_0 we assume that:

$$\exists U_0 \in H^1(\Omega)^2 \quad \text{such that} \quad \begin{cases} \nabla \cdot U_0 = 0 & \text{in } \Omega \\ U_0 = u_0 & \text{on } \Gamma_1 \\ U_0 \times \hat{n} = 0 & \text{on } \Gamma_2 \\ U_0 \cdot \hat{n} = 0 & \text{on } \Gamma_3. \end{cases} \tag{3.10}$$

Notice that the existence of such U_0 depends on $u_0 \in H^{1/2}(\Gamma_1)^2$ through the Divergence Theorem: hence, (3.10) is an assumption on u_0. More precisely, consider the space X of solutions of the (incomplete) problem

$$\nabla \cdot V = 0 \text{ in } \Omega, \quad V \times \hat{n} = 0 \text{ on } \Gamma_2, \quad V \cdot \hat{n} = 0 \text{ on } \Gamma_3.$$

Then the space of admissible u_0 coincides with the traces over Γ_1 of functions $V \in H^1(\Omega)^2 \cap X$.

In this functional framework, and under assumption (3.10), we consider the following variational formulation (suggested in [61, (1.25)]) for the boundary-value problem (3.6)-(3.7):

$$\text{find } u \in H^1(\Omega)^2 \text{ such that: } (u - U_0) \in V(\Omega), \quad A(u, v) = L(v) \text{ for every } v \in V(\Omega). \tag{3.11}$$

The next result is the main core of the present section: the existence of a unique solution of the variational (or weak) problem (4.103) is stated, together with the equivalence between this variational formulation and the boundary-value problem (3.6)-(3.7), which justifies the validity of the weak formulation (4.103):

Theorem 3.1. *If $p_0 \in H^{-1/2}(\Gamma_2)$ and $h \in H^{-1/2}(\Gamma_3)^2$, the variational problem (4.103) has a unique solution $u \in H^1(\Omega)^2$. The solution u is such that $(\nabla \times u) \in H(\Delta, \Omega)^3$ and there exists $p \in H(\Delta, \Omega)/\mathbb{R}$ such that u and p are solutions of the boundary-value problem (3.6)-(3.7) in the following sense:*

- $-\eta \Delta u + \nabla p = f$ *and* $\nabla \cdot u = 0$ *in* Ω, *in distributional sense.*

- u *satisfies (3.7) over* Γ_1, Γ_2 *and* Γ_3 *in the sense of traces of functions belonging to* $H^1(\Omega)^2$, *whereas* p *and* $(\nabla \times u)$ *satisfy (3.7) over* Γ_2 *and* Γ_3 *in the following sense:*

$$\int_\Omega (-\eta \Delta u + \nabla p) \cdot v(x) \, dx - \eta \int_\Omega (\nabla \times u) \cdot (\nabla \times v) \, dx = \langle p_0, v \cdot \hat{n} \rangle_{\Gamma_2} - \eta \langle h \times \hat{n}, v \rangle_{\Gamma_3} \quad \forall v \in V(\Omega). \quad (3.12)$$

Furthermore, if $\nabla \times (\nabla \times u) \in L^2(\Omega)^3$, *then (3.12) implies that:*

- $p = p_0$ *over* Γ_2 *in the sense of* $H^{-1/2}(\Gamma_2)/\mathbb{R}$ *and* $(\nabla \times u) \times \hat{n} = h \times \hat{n}$ *over* Γ_3, *in the sense of* $H^{-1/2}(\Gamma_3)^3$.

Finally, if $u \in \mathcal{C}^2(\overline{\Omega}; \mathbb{R}^2)$ *and* $p \in \mathcal{C}^1(\overline{\Omega}; \mathbb{R})$ *are classical solutions of the boundary-value problem (3.6)-(3.7), then* u *is also a solution of the variational problem (4.103).*

The proof of Theorem 3.1 follows closely [61] and a hint is given below. We first make precise what we intend by $V(\Omega)$-ellipticity:

Definition 3.1. *We say that the bilinear form* $A : H^1(\Omega)^2 \times H^1(\Omega)^2 \to \mathbb{R}$ *is* $V(\Omega)$-**elliptic** *if there exists* $\gamma > 0$ *(which depends only on the domain* Ω *and its boundary) such that:*

$$A(v, v) = \eta \int_\Omega |\nabla \times v|^2 \, dx \geq \gamma \|v\|^2_{H^1(\Omega)^2} \quad \forall v \in V(\Omega). \quad (3.13)$$

If the bilinear form A is $V(\Omega)$-elliptic, then the Lax-Milgram Theorem allows us to deduce that the variational problem (4.103) has a unique solution. To this end, the following results contained in [132, Chapter I, Section 2 and Section 3] need to be recalled:

Lemma 3.1. *Let* $\Phi \subset \mathbb{R}^2$ *be an open bounded set, with a locally Lipschitz boundary. If* Φ *is a convex polygon or if its boundary is of class* $\mathcal{C}^{1,1}$, *then:*
- *the space*

$$U(\Phi) := \{v \in L^2(\Phi)^2 \mid \nabla \cdot v \in L^2(\Phi); \quad \nabla \times v \in L^2(\Phi)^3; \quad v \cdot \hat{n} = 0 \text{ on } \partial\Phi\}, \quad (3.14)$$

is continuously embedded into $H^1(\Phi)^2$ *and there exists* $C > 0$, *depending only on* Φ, *such that:*

$$\|v\|_{H^1(\Phi)^2} \leq C\{\|v\|^2_{L^2(\Phi)^2} + \|\nabla \cdot v\|^2_{L^2(\Phi)} + \|\nabla \times v\|^2_{L^2(\Phi)^3}\}^{1/2} \quad \forall v \in U(\Phi); \quad (3.15)$$

- *the space*

$$W(\Phi) := \{v \in L^2(\Phi)^2 \mid \nabla \cdot v \in L^2(\Phi); \quad \nabla \times v \in L^2(\Phi)^3; \quad v \times \hat{n} = 0 \text{ on } \partial\Phi\}, \quad (3.16)$$

is continuously embedded into $H^1(\Phi)^2$ *and there exists* $C > 0$, *depending only on* Φ, *such that:*

$$\|v\|_{H^1(\Phi)^2} \leq C\{\|v\|^2_{L^2(\Phi)^2} + \|\nabla \cdot v\|^2_{L^2(\Phi)} + \|\nabla \times v\|^2_{L^2(\Phi)^3}\}^{1/2} \quad \forall v \in W(\Phi). \quad (3.17)$$

33

As in [31, 61], we consider the following subspace of $L^2(\Omega)^2$:

$$\Psi(\Omega) = \{v \in L^2(\Omega)^2 \mid \nabla \times v \in L^2(\Omega)^3; \; \nabla \cdot v = 0 \text{ in } \Omega; \; v \times \hat{n} = 0 \text{ on } \Gamma_1 \cup \Gamma_2; \; v \cdot \hat{n} = 0 \text{ on } \Gamma_1 \cup \Gamma_3\}. \quad (3.18)$$

This functional space is well-defined since, if $v \in L^2(\Omega)^2$ is such that $\nabla \times v \in L^2(\Omega)^3$ and $\nabla \cdot v \in L^2(\Omega)$, then its tangential and normal traces exist, respectively, in the boundary spaces

$$v \times \hat{n} \in H^{-1/2}(\partial\Omega)^3; \qquad v \cdot \hat{n} \in H^{-1/2}(\partial\Omega).$$

Moreover, $\Psi(\Omega)$ is a Hilbert space when endowed with the scalar product

$$\langle v, w \rangle_{\Psi(\Omega)} = \int_\Omega v \cdot w \, dx + \int_\Omega (\nabla \times v) \cdot (\nabla \times w) \, dx \quad \forall v, w \in \Psi(\Omega),$$

with corresponding norm $\|v\|_{\Psi(\Omega)} = \langle v, v \rangle_{\Psi(\Omega)}^{1/2}$. Note that if $v \in \Psi(\Omega)$, then $v = 0$ on Γ_1, since $v \times \hat{n} = v \cdot \hat{n} = 0$ on Γ_1. It is also clear that the space $V(\Omega)$ (endowed with the standard norm of $H^1(\Omega)^2$) is continuously embedded into $\Psi(\Omega)$. Actually, the following result holds; the proof follows the same line as [61, Theorem A.1] in a slightly different geometric context (a planar domain, neither convex nor with a $\mathcal{C}^{1,1}$ boundary).

Lemma 3.2. *The space $\Psi(\Omega)$ is continuously embedded into $V(\Omega)$, and therefore $\Psi(\Omega) = V(\Omega)$ (algebraically and topologically).*

Proof. We employ a localization argument, similar to the one in [61, Appendix A]. Since $\overline{\Omega} \subset \mathbb{R}^2$ is compact, it can covered by a finite number of open disks $\{\theta_i\}_{i=1}^m$, for some $m \geq 1$:

$$\overline{\Omega} \subset \bigcup_{i=1}^m \theta_i.$$

By reducing the radius of the disks $\{\theta_i\}_{i=1}^m$ (if necessary), we may assume that, if $i \in \{1, \ldots, m\}$ is such that $\theta_i \cap \partial K \neq \emptyset$, then θ_i does not intersect any of the faces of $\overline{\Omega}$ contained in the lines $y = \pm L$ or $z = \pm L$. Next, we introduce a partition of unity subordinate to the open cover $\{\theta_i\}_{i=1}^m$, that is, we consider a family of functions $\{\alpha_i\}_{i=1}^m \subset \mathcal{C}_0^\infty(\mathbb{R}^2)$ such that:

$$\alpha_i \in \mathcal{C}_0^\infty(\theta_i), \quad 0 \leq \alpha_i(x) \leq 1 \text{ for every } x \in \overline{\Omega}, \qquad \forall i \in \{1, \ldots, m\},$$
$$\sum_{i=1}^m \alpha_i(x) = 1 \text{ for every } x \in \overline{\Omega}.$$

Therefore, for every function $v \in \Psi(\Omega)$ we can write:

$$v(x) = \sum_{i=1}^m \alpha_i(x)v(x) \quad \forall x \in \overline{\Omega},$$

and $\Psi(\Omega)$ is continuously embedded into $V(\Omega)$ provided that:
– $\alpha_i v \in H^1(\Omega)^2$, for every $v \in \Psi(\Omega)$ and for every $i \in \{1, \ldots, m\}$;
– there exist $C > 0$ (depending only on Ω, $\{\theta_i\}_{i=1}^m$ and $\{\alpha_i\}_{i=1}^m$), such that:

$$\|\alpha_i v\|_{H^1(\Omega)^2} \leq C\|v\|_{\Psi(\Omega)} \quad \forall v \in \Psi(\Omega), \quad \forall i \in \{1, \ldots, m\}.$$

Having these targets in mind, let $v \in \Psi(\Omega)$ and $i \in \{1, \ldots, m\}$ and let us distinguish two different cases.
● **Case (A):** $\theta_i \cap \partial\Omega = \emptyset$, or $\theta_i \cap \partial\Omega \neq \emptyset$ but $\theta_i \cap \overline{K} = \emptyset$. In this case, since $\partial\Omega$ is a union of sets having Lipschitz-continuous boundaries and since α_i has compact support in θ_i, it is not restrictive to assume that the function $\alpha_i v$ is defined in an open and convex subset of $\theta_i \cap \Omega$, which we shall denote by ζ_i (see

34

Figure 3.4: Construction of the open set $\zeta_i \subset (\theta_i \cap \Omega)$.

Figure 4.6). Then ζ_i is a convex polygon and $\mathrm{supp}(\alpha_i) \cap \Omega \subset \zeta_i$. On the other hand, since $v \in \Psi(\Omega)$, we infer that $\alpha_i v \in L^2(\zeta_i)^2$, $\nabla \cdot (\alpha_i v) \in L^2(\zeta_i)$, $\nabla \times (\alpha_i v) \in L^2(\zeta_i)^3$ and that $(\alpha_i v) \times \hat{n} = 0$ in $\partial \zeta_i$. By applying Lemma 3.1, we then deduce that $\alpha_i v \in H^1(\zeta_i)^2$ and that there exists $C_i > 0$ (depending only on ζ_i) such that

$$\|\alpha_i v\|_{H^1(\zeta_i)^2} \le C_i \{\|\alpha_i v\|_{L^2(\zeta_i)^2}^2 + \|\nabla \cdot (\alpha_i v)\|_{L^2(\zeta_i)}^2 + \|\nabla \times (\alpha_i v)\|_{L^2(\zeta_i)^3}^2\}^{1/2}$$

which, in particular, implies that

$$\|\alpha_i v\|_{H^1(\theta_i \cap \Omega)^2} \le C_i \{\|\alpha_i v\|_{L^2(\theta_i \cap \Omega)^2}^2 + \|\nabla \cdot (\alpha_i v)\|_{L^2(\theta_i \cap \Omega)}^2 + \|\nabla \times (\alpha_i v)\|_{L^2(\theta_i \cap \Omega)^3}^2\}^{1/2}. \tag{3.19}$$

• **Case (B):** $\theta_i \cap \overline{K} \neq \emptyset$. In this case, since $\partial \Omega$ is a union of sets with Lipschitz-continuous boundaries and since α_i has compact support in θ_i, it is not restrictive to assume that the function $\alpha_i v$ is defined in an open subset of $\theta_i \cap \Omega$, which we shall denote by ζ_i (see Figure 3.5). In the present situation, since
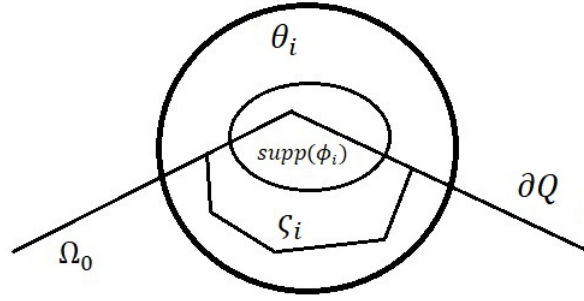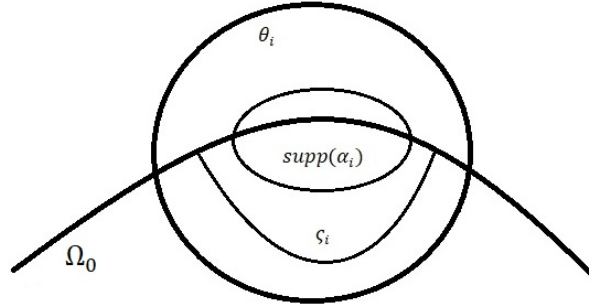

Figure 3.5: Construction of the open set $\zeta_i \subset (\theta_i \cap \Omega)$.

the domain K is smooth, we may establish that ζ_i has a $\mathcal{C}^{1,1}$ boundary and that $\mathrm{supp}(\alpha_i) \cap \Omega \subset \zeta_i$. On the other hand, as $v \in \Psi(\Omega)$, we deduce that $\alpha_i v \in L^2(\zeta_i)^2$, $\nabla \cdot (\alpha_i v) \in L^2(\zeta_i)$, $\nabla \times (\alpha_i v) \in L^2(\zeta_i)^3$ and that $(\alpha_i v) \cdot \hat{n} = 0$ in $\partial \zeta_i$. Then, applying again Lemma 3.1, we infer that $\alpha_i v \in H^1(\zeta_i)^2$ and that there exists a constant $C_i > 0$ (depending only on ζ_i) such that (3.19) holds.

Hence, (3.19) holds in both cases (A) and (B), that is, it holds for every $i \in \{1, \ldots, m\}$ and, therefore, there exists $C > 0$ (depending on Ω, $\{\theta_i\}_{i=1}^m$ and $\{\alpha_i\}_{i=1}^m$) such that

$$\|\alpha_i v\|_{H^1(\Omega)^2} \le C \{\|v\|_{L^2(\Omega)^2}^2 + \|\nabla \cdot v\|_{L^2(\Omega)}^2 + \|\nabla \times v\|_{L^2(\Omega)^3}^2\}^{1/2}.$$

Since $\nabla \cdot v = 0$ in Ω, we finally have that

$$\|\alpha_i v\|_{H^1(\Omega)^2} \le C \{\|v\|_{L^2(\Omega)^2}^2 + \|\nabla \times v\|_{L^2(\Omega)^3}^2\}^{1/2}$$

for every $v \in \Psi(\Omega)$ and $i \in \{1, \ldots, m\}$. This concludes the proof of the lemma. $\qquad \square$

Next, we recall that [61, Lemma A.2] implies that

$$\text{the map defined by } V(\Omega) \ni v \mapsto \|\nabla \times v\|_{L^2(\Omega)^3} \text{ is a norm in } V(\Omega). \tag{3.20}$$

Proof of Theorem 3.1. We now have all the ingredients to demonstrate that the bilinear form $A(\cdot, \cdot)$ is $V(\Omega)$-elliptic. Lemma 3.2 implies the existence of a constant $C_1 > 0$ (depending on Ω) such that:

$$\|v\|_{H^1(\Omega)^2} \le C_1 \{\|v\|_{L^2(\Omega)^2}^2 + \|\nabla \times v\|_{L^2(\Omega)^3}^2\}^{1/2} \quad \forall v \in V(\Omega). \tag{3.21}$$

Therefore, in order to prove the $V(\Omega)$-ellipticity of $A(\cdot, \cdot)$, it suffices to show the existence of another constant $C_2 > 0$ (also depending only on Ω) such that:

$$\|v\|_{L^2(\Omega)^2} \le C_2 \|\nabla \times v\|_{L^2(\Omega)^3} \quad \forall v \in V(\Omega). \tag{3.22}$$

For contradiction, assume that (3.22) does not hold. Then, there exists a sequence $\{v_n\} \subset V(\Omega)$ such that

$$\|v_n\|_{L^2(\Omega)^2} = 1, \quad \|\nabla \times v_n\|_{L^2(\Omega)^3} \le \frac{1}{n} \quad \forall n \in \mathbb{N}. \tag{3.23}$$

Using inequality (4.48), we see that (3.23) implies that the sequence $\{v_n\}_{n \in \mathbb{N}}$ is bounded in $V(\Omega)$ (with the standard $H^1(\Omega)^2$-norm). We may then extract a subsequence $\{v_{\varphi(n)}\}_{n \in \mathbb{N}}$ such that

$$v_{\varphi(n)} \rightharpoonup v \text{ in } H^1(\Omega)^2 \quad \text{and} \quad v_{\varphi(n)} \to v \text{ in } L^2(\Omega)^2 \quad \text{as } n \to \infty \tag{3.24}$$

for some $v \in V(\Omega)$. But, in this situation, (3.23) implies that $\nabla \times v = 0$ in Ω. Therefore, since $v \in V(\Omega)$, (3.20) allows us to conclude that $v = 0$, and hence, (3.23) contradicts (3.24). As a consequence, we conclude that the bilinear form $A(\cdot, \cdot)$ is $V(\Omega)$-elliptic, and the Lax-Milgram Theorem then ensures that the variational problem (4.103) has a unique solution.

Finally, the proofs of the statements related with the equivalence between the variational formulation (4.103) and the boundary-value problem (3.6)-(3.7) are omitted, since they can be found in [61, Section 1.5]. This concludes the proof of Theorem 3.1.

3.2 An overview of the separation of variables for biharmonic equations

In this section we survey the method of separation of variables for the biharmonic equation

$$\Delta^2 \psi = 0 \quad \text{in } \Lambda \doteq \{(y, z) \in \mathbb{R}^2 \mid y > 0 \text{ or } z > 0\} = \left\{(\rho, \theta) \in \mathbb{R}^2 \mid \rho > 0, -\frac{\pi}{2} < \theta < \pi\right\}. \tag{3.25}$$

We emphasize that, with an abuse of notation, Λ represents the domain both in cartesian and polar coordinates. In polar coordinates, equation (3.25) becomes:

$$\left(\frac{\partial^2}{\partial \rho^2} + \frac{1}{\rho}\frac{\partial}{\partial \rho} + \frac{1}{\rho^2}\frac{\partial^2}{\partial \theta^2}\right)^2 \psi(\rho, \theta) = 0 \quad \forall (\rho, \theta) \in \Lambda. \tag{3.26}$$

We here seek a solution of (3.26) having a separated-variable form $\psi(\rho, \theta) = h(\rho)g(\theta)$, for every $(\rho, \theta) \in \Lambda$, for some differentiable functions $h : (0, \infty) \to \mathbb{R}$ and $g : (-\frac{\pi}{2}, \pi) \to \mathbb{R}$. The complete description of the solutions of (3.26) in separated variables is contained in Theorem 3.2, the main result of this section. We initially follow the method employed by Stampouloglou-Theotokoglou [245], which extends the work by Michell [201], allowing the appearance of solutions of the biharmonic equation having oscillatory forms. Nevertheless, since in Theorem 3.2 we obtain more separated-variable solutions of (3.26) than in [245, Section 2], the whole (lengthy and delicate) proof is included for the sake of completeness.

36

Theorem 3.2. *Let* $\psi : \Lambda \to \mathbb{R}$ *be a solution of* (3.26) *having a separated-variable form* $\psi(\rho, \theta) = h(\rho)g(\theta)$, *for some smooth functions* $h : (0, \infty) \to \mathbb{R}$ *and* $g : \left(-\frac{\pi}{2}, \pi\right) \to \mathbb{R}$. *Then,* g *is a combination (sum, product or linear combination) of trigonometric functions, exponentials and polynomials and, therefore, it is globally bounded over* $\left(-\frac{\pi}{2}, \pi\right)$. *Moreover,* h *may take one of the following forms (for* $\rho > 0$):

$$
\begin{cases}
h(\rho) = \rho[C_1\rho^a + C_2\rho^{-a} + C_3\rho^b + C_4\rho^{-b}], \\
h(\rho) = C_1\rho^3 + C_2\rho^{-1} + \rho[C_3 + C_4\log(\rho)], \\
h(\rho) = C_1 + C_2\log(\rho) + \rho^2[C_3 + C_4\log(\rho)], \\
h(\rho) = \rho^2[C_1\cos(\mu\log(\rho)) + C_2\sin(\mu\log(\rho))] + C_3\cos(\mu\log(\rho)) + C_4\sin(\mu\log(\rho)), \\
h(\rho) = \rho[C_1\cos(\mu\log(\rho)) + C_2\sin(\mu\log(\rho))],
\end{cases}
\tag{3.27}
$$

for some $a, b, \mu > 0$ *and some arbitrary constants* $C_1, C_2, C_3, C_4 \in \mathbb{R}$.

Proof. After replacing into (3.26) the ansatz $\psi(\rho, \theta) = h(\rho)g(\theta)$, we observe that, in order for the equation to be fulfilled, the following identity must be satisfied

$$
g^{(4)}(\theta) + 2\chi(\rho)g''(\theta) + M(\rho)g(\theta) = 0 \qquad \forall(\rho, \theta) \in \Lambda, \tag{3.28}
$$

where

$$
\chi(\rho) \doteq \rho^2\frac{h''(\rho)}{h(\rho)} - \rho\frac{h'(\rho)}{h(\rho)} + 2, \qquad M(\rho) \doteq \rho^4\frac{h^{(4)}(\rho)}{h(\rho)} + 2\rho^3\frac{h'''(\rho)}{h(\rho)} - \rho^2\frac{h''(\rho)}{h(\rho)} + \rho\frac{h'(\rho)}{h(\rho)}, \tag{3.29}
$$

for every $\rho \in (0, \infty)$ such that $h(\rho) \neq 0$. By differentiating (3.28) with respect to ρ, we obtain

$$
2\chi'(\rho)g''(\theta) + M'(\rho)g(\theta) = 0 \qquad \forall(\rho, \theta) \in \Lambda. \tag{3.30}
$$

At this point, we distinguish two cases.

• **Case (I):** $\chi'(\rho) \neq 0$. In this situation, assuming that the function g is not identically null over $\left(-\frac{\pi}{2}, \pi\right)$ and, after dividing equation (3.30) by $\chi'(\rho)g(\theta)$, we infer that

$$
\frac{g''(\theta)}{g(\theta)} = -\frac{M'(\rho)}{2\chi'(\rho)} \qquad \forall(\rho, \theta) \in \Lambda, \tag{3.31}
$$

so that there exists $\lambda \in \mathbb{R}$ such that

$$
g''(\theta) - \lambda g(\theta) = 0 \qquad \forall\theta \in \left(-\frac{\pi}{2}, \pi\right). \tag{3.32}
$$

In this precise point our procedure differs from that in [245] since we do not assume that $-\lambda$ is a squared integer (a "physical number", see [245, Section 2]). The reason is that, since the angular region Λ does not cover the full range $[0, 2\pi]$ for θ, the function g may not be periodic. Nevertheless, (3.32) shows that g is a linear combination of trigonometric functions, exponentials and first-order polynomials and, therefore, it is bounded over $\left(-\frac{\pi}{2}, \pi\right)$.

Note that (3.32) implies both $g''(\theta) = \lambda g(\theta)$ and $g^{(4)}(\theta) = \lambda^2 g(\theta)$ which, inserted into (3.28), yields

$$
M(\rho) + 2\lambda\chi(\rho) + \lambda^2 = 0 \qquad \forall\rho \in (0, \infty). \tag{3.33}
$$

By combining (3.29) with (3.33) we obtain:

$$
\rho^4 h^{(4)}(\rho) + 2\rho^3 h'''(\rho) + \rho^2(2\lambda - 1)h''(\rho) + \rho(1 - 2\lambda)h'(\rho) + \lambda(4 + \lambda)h(\rho) = 0 \qquad \forall\rho \in (0, \infty). \tag{3.34}
$$

After the change of variables $t = \log(\rho)$, this equation becomes

$$
h^{(4)}(t) - 4h'''(t) + (2\lambda + 4)h''(t) - 4\lambda h'(t) + \lambda(4 + \lambda)h(t) = 0 \qquad \forall t \in \mathbb{R}. \tag{3.35}
$$

For a given $\lambda \in \mathbb{R}$, the characteristic polynomial of the ODE (3.35) reads

$$P(z) = z^4 - 4z^3 + (2\lambda + 4)z^2 - 4\lambda z + \lambda(4 + \lambda) = (z-1)^4 + 2(\lambda - 1)(z-1)^2 + (\lambda + 1)^2$$

so that $P(z) = 0$ if and only if $(z-1)^2 = 1 - \lambda \pm 2\sqrt{-\lambda}$. In the following list, according to the sign of λ, the roots $z_1, z_2, z_3, z_4 \in \mathbb{C}$ of P are computed, together with the explicit formula of the corresponding solution of the ODE (3.34).

- *Case (I.1): $\lambda < 0$, $\lambda \neq -1$.* Therefore $1 - \lambda \pm 2\sqrt{|\lambda|} > 0$, and P has four real distinct roots, given by:

$$z_1 = 1 + \sqrt{1 - \lambda + 2\sqrt{|\lambda|}}, \quad z_2 = 1 - \sqrt{1 - \lambda + 2\sqrt{|\lambda|}},$$
$$z_3 = 1 + \sqrt{1 - \lambda - 2\sqrt{|\lambda|}}, \quad z_4 = 1 - \sqrt{1 - \lambda - 2\sqrt{|\lambda|}}.$$

Hence, the solutions of (3.34) are as in $(3.27)_1$ with $a \doteq \sqrt{1 - \lambda + 2\sqrt{|\lambda|}}$, $b \doteq \sqrt{1 - \lambda - 2\sqrt{|\lambda|}}$ and any constants $C_1, C_2, C_3, C_4 \in \mathbb{R}$ such that $\chi' \neq 0$.

- *Case (I.2): $\lambda = -1$.* P has the real roots: $z_1 = 3$, $z_2 = -1$ and $z_3 = z_4 = 1$. Accordingly, solutions of (3.34) are as in $(3.27)_2$ for some arbitrary constants $C_1, C_2, C_3, C_4 \in \mathbb{R}$ such that $\chi' \neq 0$.

- *Case (I.3): $\lambda = 0$.* P has two real double roots: $z_1 = z_3 = 2$ and $z_2 = z_4 = 0$. Accordingly, solutions of (3.34) are as in $(3.27)_3$ for some arbitrary constants $C_1, C_2, C_3, C_4 \in \mathbb{R}$ such that $\chi' \neq 0$.

- *Case (I.4): $\lambda > 0$.* P has two pairs of complex-conjugate roots: $z_1 = 2 + i\sqrt{\lambda}$, $z_2 = 2 - i\sqrt{\lambda}$, $z_3 = i\sqrt{\lambda}$, $z_4 = -i\sqrt{\lambda}$. Accordingly, solutions of (3.34) are as in $(3.27)_4$, where $\mu = \sqrt{\lambda}$ and $C_1, C_2, C_3, C_4 \in \mathbb{R}$ are arbitrary constants such that $\chi' \neq 0$.

- **Case (II): $\chi'(\rho) = 0$.** Then χ is constant and, by (3.30), also M is constant: $\chi(\rho) \equiv \alpha$ and $M(\rho) \equiv \beta$ for some $\alpha, \beta \in \mathbb{R}$. Hence, if $g : (-\frac{\pi}{2}, \pi) \to \mathbb{R}$ is not identically null, from (3.28) we infer

$$g^{(4)}(\theta) + 2\alpha g''(\theta) + \beta g(\theta) = 0 \quad \forall \theta \in \left(-\frac{\pi}{2}, \pi\right), \tag{3.36}$$

whose solutions are combinations (sum, product or linear combination) of trigonometric functions, exponentials and polynomials. Furthermore, from (3.29) we obtain the following equations:

$$\begin{cases} \rho^2 h''(\rho) - \rho h'(\rho) + (2 - \alpha)h(\rho) = 0 \\ \rho^4 h^{(4)}(\rho) + 2\rho^3 h'''(\rho) - \rho^2 h''(\rho) + \rho h'(\rho) - \beta h(\rho) = 0 \end{cases} \quad \forall \rho \in (0, \infty), \tag{3.37}$$

that can be solved through the change of variables $t = \log(\rho)$. Equation $(3.37)_1$ yields the following families of solutions (for $\rho > 0$):

$$\alpha < 1 \implies h(\rho) = \rho[C_1 \cos(\sqrt{1-\alpha}\log(\rho)) + C_2 \sin(\sqrt{1-\alpha}\log(\rho))], \tag{3.38}$$
$$\alpha = 1 \implies h(\rho) = \rho[C_1 + C_2 \log(\rho)], \tag{3.39}$$
$$\alpha > 1 \implies h(\rho) = C_1 \rho^{1+\sqrt{\alpha-1}} + C_2 \rho^{1-\sqrt{\alpha-1}}, \tag{3.40}$$

where $C_1, C_2 \in \mathbb{R}$ are arbitrary constants.

Concerning $(3.37)_2$, the change of variables $t = \log(\rho)$ leads to $h^{(4)}(t) - 4h'''(t) + 4h''(t) - \beta h(t) = 0$ ($t \in \mathbb{R}$) whose characteristic polynomial is

$$H(z) \doteq z^4 - 4z^3 + 4z^2 - \beta = (z-1)^4 - 2(z-1)^2 + 1 - \beta,$$

so that $H(z) = 0$ if and only if $(z-1)^2 = 1 \pm \sqrt{\beta}$. In the following list, according to the values of β, the roots $z_1, z_2, z_3, z_4 \in \mathbb{C}$ of H are computed, together with the corresponding solutions of $(3.37)_2$.

38

- *Case (II.1):* $\beta < 0$. Here, H has two pairs of complex-conjugate roots:

$$z_1 = 1 + \sqrt{\frac{\sqrt{1-\beta}+1}{2}} + i\sqrt{\frac{\sqrt{1-\beta}-1}{2}}, \quad z_2 = 1 - \sqrt{\frac{\sqrt{1-\beta}+1}{2}} - i\sqrt{\frac{\sqrt{1-\beta}-1}{2}},$$

$$z_3 = 1 + \sqrt{\frac{\sqrt{1-\beta}+1}{2}} - i\sqrt{\frac{\sqrt{1-\beta}-1}{2}}, \quad z_4 = 1 - \sqrt{\frac{\sqrt{1-\beta}+1}{2}} + i\sqrt{\frac{\sqrt{1-\beta}-1}{2}},$$

and the general solution of $(3.37)_2$ is:

$$h(\rho) = \rho^{1+a}[C_1\cos(\mu\log(\rho)) + C_2\sin(\mu\log(\rho))] + \rho^{1-a}[C_3\cos(\mu\log(\rho)) + C_4\sin(\mu\log(\rho))] \qquad \forall \rho > 0, \quad (3.41)$$

where $a \doteq \sqrt{\sqrt{1-\beta}+1}/\sqrt{2}$, $\mu \doteq \sqrt{\sqrt{1-\beta}-1}/\sqrt{2}$ and $C_1, C_2, C_3, C_4 \in \mathbb{R}$ are arbitrary constants.

- *Case (II.2):* $\beta = 0$. Here H has two double real roots: $z_1 = z_3 = 2$ and $z_2 = z_4 = 0$. The general solution of $(3.37)_2$ is then:

$$h(\rho) = C_1 + C_2\log(\rho) + \rho^2[C_3 + C_4\log(\rho)] \qquad \forall \rho > 0, \quad (3.42)$$

where $C_1, C_2, C_3, C_4 \in \mathbb{R}$ are arbitrary constants.

- *Case (II.3):* $0 < \beta < 1$. Therefore $1 \pm \sqrt{\beta} > 0$ and H has four real distinct roots, given by:

$$z_1 = 1 + \sqrt{1+\sqrt{\beta}}, \quad z_2 = 1 - \sqrt{1+\sqrt{\beta}}, \quad z_3 = 1 + \sqrt{1-\sqrt{\beta}}, \quad z_4 = 1 - \sqrt{1-\sqrt{\beta}}.$$

Accordingly, the general solution of $(3.37)_2$ is:

$$h(\rho) = C_1\rho^{1+\sqrt{1+\sqrt{\beta}}} + C_2\rho^{1-\sqrt{1+\sqrt{\beta}}} + C_3\rho^{1+\sqrt{1-\sqrt{\beta}}} + C_4\rho^{1-\sqrt{1-\sqrt{\beta}}} \qquad \forall \rho > 0, \quad (3.43)$$

where $C_1, C_2, C_3, C_4 \in \mathbb{R}$ are arbitrary constants.

- *Case (II.4):* $\beta = 1$. Here H has the real roots: $z_1 = 1 + \sqrt{2}$, $z_2 = 1 - \sqrt{2}$ and $z_3 = z_4 = 1$. The general solution of $(3.37)_2$ is then:

$$h(\rho) = C_1\rho^{1+\sqrt{2}} + C_2\rho^{1-\sqrt{2}} + \rho[C_3 + C_4\log(\rho)] \qquad \forall \rho > 0, \quad (3.44)$$

where $C_1, C_2, C_3, C_4 \in \mathbb{R}$ are arbitrary constants.

- *Case (II.5):* $\beta > 1$. Since $1 - \sqrt{\beta} < 0 < 1 + \sqrt{\beta}$, in this case H has two real and two complex-conjugate roots, given by:

$$z_1 = 1 + \sqrt{\sqrt{\beta}+1}, \quad z_2 = 1 - \sqrt{\sqrt{\beta}+1}, \quad z_3 = 1 + i\sqrt{\sqrt{\beta}-1}, \quad z_4 = 1 - i\sqrt{\sqrt{\beta}-1}.$$

Accordingly, the general solution of $(3.37)_2$ is:

$$h(\rho) = \rho[C_1\cos(\mu\log(\rho)) + C_2\sin(\mu\log(\rho))] + C_3\rho^{1+\sqrt{\sqrt{\beta}+1}} + C_4\rho^{1-\sqrt{\sqrt{\beta}+1}} \qquad \forall \rho > 0, \quad (3.45)$$

where $\mu \doteq \sqrt{\sqrt{\beta}-1}$ and $C_1, C_2, C_3, C_4 \in \mathbb{R}$ are arbitrary constants.

From (3.38) until (3.45), the functions that simultaneously solve both the equations in (3.37) are:
– functions (3.43) with $C_3 = C_4 = 0$ and $\alpha = 2 + \sqrt{\beta}$, or with $C_1 = C_2 = 0$ and $\alpha = 2 - \sqrt{\beta}$, that coincide with (3.40), a form included in $(3.27)_1$;
– functions (3.44) with $C_3 = C_4 = 0$, that coincide with (3.40) if $\alpha = 3$, a form included in $(3.27)_1$;
– functions (3.44) with $C_1 = C_2 = 0$, that coincide with (3.39), a form included in $(3.27)_2$;
– functions (3.45) with $C_1 = C_2 = 0$, that coincide with (3.40) if $\alpha = 2 + \sqrt{\beta}$, a form included in $(3.27)_1$;
– functions (3.45) with $C_3 = C_4 = 0$, that coincide with (3.38) if $\alpha = 2 - \sqrt{\beta} < 1$, giving $(3.27)_5$. $\qquad \square$

3.3 Singular Stokes flows around a right angle

We consider here the stationary Stokes equations over the domain Λ defined in (3.25):

$$-\eta\Delta u + \nabla p = f, \quad \nabla \cdot u = 0 \quad \text{in } \Lambda. \tag{3.46}$$

The region $\Lambda \subset \mathbb{R}^2$ is open and simply-connected, with a Lipschitz boundary. The origin O of the reference system lies in its corner, as depicted in Figure 3.6.
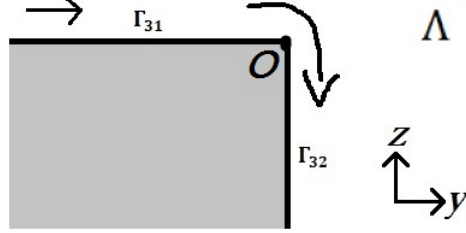

Figure 3.6: Schematic representation of the domain Λ and of the expected flow pattern.

We denote by $(u^1(y,z), u^2(y,z))$ the components of the velocity field, so that the *scalar vorticity* $\omega : \Lambda \to \mathbb{R}$ is:

$$\omega(y,z) = \frac{\partial u^2}{\partial y}(y,z) - \frac{\partial u^1}{\partial z}(y,z) \quad \forall (y,z) \in \Lambda.$$

Since Λ is simply-connected, the incompressibility condition implies the existence of a *stream function* $\psi : \Lambda \to \mathbb{R}$ such that

$$u^1(y,z) = \frac{\partial \psi}{\partial z}(y,z), \quad u^2(y,z) = -\frac{\partial \psi}{\partial y}(y,z), \quad \omega(y,z) = -\Delta \psi(y,z) \quad \forall (y,z) \in \Lambda. \tag{3.47}$$

Moreover, if we assume f to be constant, the equation of conservation of momentum in (3.46) can be rewritten as the biharmonic equation (3.25) for the stream function ψ; see, e.g., [169, Chapter 2]. Then, the pressure can be found by solving $\nabla p = f + \eta\Delta u$. In the present section, (3.25) will be tackled using the separation of variables method developed in Section 3.2, with two main targets:
– to find the boundary conditions that could be imposed on the faces of the obstacle;
– to give a precise local description of the solution obtained with these boundary conditions.

Usually, the second target is the first step if one aims to propose a variational formulation of the Stokes equation (complemented with some boundary conditions) in a *weighted* Sobolev space, following the ideas contained in [197]. However, this is beyond the scopes of this chapter. Instead, we are here interested in classifying the solutions of (3.46), according to the following characterization:

Definition 3.2. *Let $u = (u^1, u^2)$ be a solution of (3.46) in $\mathcal{C}^2(\Lambda)^2$. We say that u has a **separated-variable form** if its stream function $\psi : \Lambda \to \mathbb{R}$, defined by (3.47), has the form $\psi(\rho, \theta) = h(\rho)g(\theta)$, for some smooth functions $h : (0, \infty) \to \mathbb{R}$ and $g : \left(-\frac{\pi}{2}, \pi\right) \to \mathbb{R}$. We also say that u is:*
- *a **physical solution** if $u \in L^\infty_{\text{loc}}(\overline{\Lambda})^2$,   • a **finite-energy solution** if $u \in H^1_{\text{loc}}(\overline{\Lambda})^2$,*
- *a **singular solution** if $u \in L^\infty_{\text{loc}}(\overline{\Lambda})^2 \setminus H^1_{\text{loc}}(\overline{\Lambda})^2$.*

We emphasize that there is a small abuse of language in Definition 3.2. If the stream function has the separated-variable form $\psi(\rho, \theta) = h(\rho)g(\theta)$ (in polar coordinates), for some smooth $h : (0, \infty) \to \mathbb{R}$ and $g : \left(-\frac{\pi}{2}, \pi\right) \to \mathbb{R}$, then the components of the velocity field can be recovered through (3.47):

$$u^1(\rho, \theta) = h'(\rho)g(\theta)\sin(\theta) + \frac{h(\rho)}{\rho}g'(\theta)\cos(\theta), \quad u^2(\rho, \theta) = -h'(\rho)g(\theta)\cos(\theta) + \frac{h(\rho)}{\rho}g'(\theta)\sin(\theta), \tag{3.48}$$

for $(\rho, \theta) \in \Lambda$. But, strictly speaking, (3.48) *do not* have a separated-variable form of the kind $H(\rho)G(\theta)$. However, in order to avoid more complicated definitions, we still call it in separated-form.

We point out that one has $H^1_{loc}(\overline{\Lambda}) \subset L^p_{loc}(\overline{\Lambda})$ for all $1 \leq p < \infty$, but the embedding $H^1_{loc}(\overline{\Lambda}) \subset L^\infty_{loc}(\overline{\Lambda})$ fails since Λ is a planar domain. Therefore, not all finite-energy solutions will be physical solutions (nor the vice-versa). Since we have to deal with the singularity of vortices, we are here interested in singular solutions (physical infinite-energy solutions), namely bounded solutions of (3.46) with non-L^2 vorticity ω. In view of (3.47), this also means that the stream function ψ does not belong to $H^2_{loc}(\overline{\Lambda})$. Together with Theorem 3.2, the following result is then obtained:

Theorem 3.3. *Consider the radial component $h : (0, \infty) \to \mathbb{R}$ of the stream function of a separated-variable solution u of (3.46) in Λ. If u is a singular solution, then h is necessarily given by:*

$$h_{\mathcal{S}}(\rho) = \rho[C_1 \cos(\mu \log(\rho)) + C_2 \sin(\mu \log(\rho))] \qquad \forall \rho > 0, \tag{3.49}$$

for some coefficient $\mu \geq 0$ and arbitrary constants $C_1, C_2 \in \mathbb{R}$.

Proof. Let us write as $\psi(\rho, \theta) = h(\rho)g(\theta)$, for some smooth $h : (0, \infty) \to \mathbb{R}$ and $g : \left(-\frac{\pi}{2}, \pi\right) \to \mathbb{R}$, the stream function of a separated-variable solution u of the Stokes equations (3.46) in Λ. From Theorem 3.2 we know that h must have one of the forms in (3.27), while the function g belongs to $C^\infty\left(-\frac{\pi}{2}, \pi\right)$.

If we require that $u \in L^\infty_{loc}(\overline{\Lambda})^2$, identities (3.48) imply that

$$\limsup_{\rho \to 0} \left[|h'(\rho)g(\theta)| + \frac{1}{\rho}|h(\rho)g'(\theta)| \right] < \infty. \tag{3.50}$$

When g is not a constant function, (3.50) is equivalent to the condition

$$\limsup_{\rho \to 0} \left(|h'(\rho)| + \frac{|h(\rho)|}{\rho} \right) < \infty, \tag{3.51}$$

which immediately allows us to rule out the forms $\rho^{1-\alpha}$, $\log(\rho)$, $\rho \log(\rho)$, $\cos(\mu \log(\rho))$ and $\sin(\mu \log(\rho))$ (for any $\alpha, \mu > 0$) appearing in (3.27), since they violate (3.51). On the other hand, when g is constant, there must exist $C_1, C_2, C_3, C_4 \in \mathbb{R}$ (see the proof of Theorem 3.2) such that $h(\rho) = C_1 + C_2 \log(\rho) + \rho^2[C_3 + C_4 \log(\rho)]$, $\forall \rho > 0$, which fulfills (3.50) if and only if $C_2 = 0$. Nevertheless, as we will see in the next item, if g is constant and $h(\rho) = C_1 + \rho^2[C_3 + C_4 \log(\rho)]$, then u belongs to $H^1_{loc}(\overline{\Lambda})^2$ so that it is not a singular solution.

If $u \notin H^1_{loc}(\overline{\Lambda})^2$, then there exists $\delta > 0$ such that

$$\int_{-\frac{\pi}{2}}^{\pi} \int_0^\delta \rho(|\nabla u^1(\rho, \theta)|^2 + |\nabla u^2(\rho, \theta)|^2) \, d\rho \, d\theta$$

$$= \int_{-\frac{\pi}{2}}^{\pi} \int_0^\delta \rho \left[h''(\rho)^2 g(\theta)^2 + 2 \left(\frac{\rho h'(\rho) - h(\rho)}{\rho^2} \right)^2 g'(\theta)^2 + \left(\frac{h'(\rho)}{\rho} g(\theta) + \frac{h(\rho)}{\rho^2} g''(\theta) \right)^2 \right] d\rho \, d\theta = \infty. \tag{3.52}$$

Then, the case when g is constant and $h(\rho) = C_1 + \rho^2[C_3 + C_4 \log(\rho)]$ is ruled out. Moreover, the condition

$$\int_0^r \left(\rho h''(\rho)^2 + \frac{h'(\rho)^2}{\rho} + \frac{h(\rho)^2}{\rho^3} \right) d\rho < \infty \qquad \forall r \in (0, \infty) \tag{3.53}$$

implies that $u \in H^1_{loc}(\overline{\Lambda})^2$. This allows us to exclude the terms $\rho^{1+\alpha}$, $\rho^2 \log(\rho)$, $\rho^2 \cos(\mu \log(\rho))$ and $\rho^2 \sin(\mu \log(\rho))$ (for any $\alpha, \mu > 0$) appearing in (3.27), since they verify (3.53).

Summarizing, the only expression in (3.27) not being ruled out by criteria (3.50)-(3.52) is precisely $h_{\mathcal{S}}$ in (3.49). In this case, we infer that g cannot be constant, so that (3.51) may be used to show that

u belongs to $L^\infty_{\mathrm{loc}}(\overline{\Lambda})^2$. Indeed, $h_{\mathcal{S}}(\rho)/\rho$ and $h'_{\mathcal{S}}(\rho)$ are bounded in any interval $(0,r)$ with finite $r > 0$ so that (3.51) is verified. Moreover, when $\mu > 0$ one has that

$$\int\limits_0^1 \frac{\cos^2(\mu\log(\rho))}{\rho}\, d\rho = \int\limits_0^{+\infty} \cos^2(\mu t)\, dt = \infty \qquad \text{and} \qquad \int\limits_0^1 \frac{\sin^2(\mu\log(\rho))}{\rho}\, d\rho = \infty.$$

so that (3.52) is verified for $\delta = 1$, and then $u \notin H^1_{\mathrm{loc}}(\overline{\Lambda})^2$ for any $\mu > 0$.

If $\mu = 0$, then (3.49) reduces to $h_{\mathcal{S}}(\rho) = C_1\rho$, for every $\rho > 0$, a function that satisfies condition (3.51) and that fulfills (3.52) for $\delta = 1$ only when the associated angular function $g_{\mathcal{S}}$ does not belong to the span of $\{\cos(\theta), \sin(\theta)\}$. Within the proof of Theorem 3.2, the form $h_{\mathcal{S}}(\rho) = C_1\rho$ yields $\alpha = \beta = 1$ in Case (II) and, accordingly, $g_{\mathcal{S}}$ solves the ODE

$$g_{\mathcal{S}}^{(4)}(\theta) + 2g_{\mathcal{S}}''(\theta) + g_{\mathcal{S}}(\theta) = 0 \quad \forall \theta \in \left(-\frac{\pi}{2}, \pi\right), \tag{3.54}$$

whose general solution is given by

$$g_{\mathcal{S}}(\theta) = Q_1\theta\cos(\theta) + Q_2\theta\sin(\theta) + Q_3\cos(\theta) + Q_4\sin(\theta) \quad \forall \theta \in \left(-\frac{\pi}{2}, \pi\right), \tag{3.55}$$

for some constants $Q_1, Q_2, Q_3, Q_4 \in \mathbb{R}$. The resulting functions $\rho\cos(\theta)$ and $\rho\sin(\theta)$ are not singular so that we may choose $Q_3 = Q_4 = 0$. Then we conclude that $h_{\mathcal{S}}(\rho)g_{\mathcal{S}}(\theta)$ fulfills (3.52) and, therefore, $u \notin H^1_{\mathrm{loc}}(\overline{\Lambda})^2$ also when $\mu = 0$. $\qquad\square$

If we **drop the separated-variable assumption**, as a consequence of Theorem 3.3 we have

Corollary 3.1. *Any stream function of the kind*

$$\psi_{\mathcal{S}}(\rho, \theta) = \rho[Q_1\theta\cos(\theta) + Q_2\theta\sin(\theta)]$$
$$+ \sum_{k=1}^{\infty} \rho[C_1\cos(k\log(\rho)) + C_2\sin(k\log(\rho))][e^{k\theta}(A_1\cos(\theta) + A_2\sin(\theta)) + e^{-k\theta}(A_3\cos(\theta) + A_4\sin(\theta))], \tag{3.56}$$

for every $(\rho, \theta) \in \Lambda$ and arbitrary constants $Q_1, Q_2 \in \mathbb{R}$, yields a singular and non-separated variable solution u of (3.46), provided that the constants $A_1, A_2, A_3, A_4, C_1, C_2 \in \mathbb{R}$ (that depend on $k \in \mathbb{N}$) are properly chosen in order to ensure the convergence of the series.

Proof. From Theorem 3.3 we know that the radial component $h_{\mathcal{S}} : (0, \infty) \to \mathbb{R}$ of the stream function of a singular and separated-variable solution u of (3.46) in Λ is given by (3.49), for some coefficient $\mu \geq 0$ and arbitrary constants $C_1, C_2 \in \mathbb{R}$. Furthermore, the functions $\chi_{\mathcal{S}}$ and $M_{\mathcal{S}}$ in (3.29) are given by:

$$\chi_{\mathcal{S}}(\rho) = 1 - \mu^2, \qquad M_{\mathcal{S}}(\rho) = (1 + \mu^2)^2 \quad \forall \rho > 0.$$

That is, according to the proof of Theorem 3.2, (3.49) corresponds to the form $(3.27)_5$, which is obtained in Case (II) where $\chi'_{\mathcal{S}} \equiv 0$. In turn, the associated angular function $g_{\mathcal{S}}$ must satisfy (3.28), which reads:

$$g_{\mathcal{S}}^{(4)}(\theta) + 2(1 - \mu^2)g_{\mathcal{S}}''(\theta) + (1 + \mu^2)^2 g_{\mathcal{S}}(\theta) = 0 \quad \forall \theta \in \left(-\frac{\pi}{2}, \pi\right). \tag{3.57}$$

When $\mu > 0$, all the solutions of (3.57) may be written as

$$g_{\mathcal{S}}(\theta) = e^{\mu\theta}[A_1\cos(\theta) + A_2\sin(\theta)] + e^{-\mu\theta}[A_3\cos(\theta) + A_4\sin(\theta)] \quad \forall \theta \in \left(-\frac{\pi}{2}, \pi\right), \tag{3.58}$$

for some constants $A_1, A_2, A_3, A_4 \in \mathbb{R}$ that may depend on μ. On the other hand, when $\mu = 0$, the general solution of (3.57) is given by (3.55), for some $Q_1, Q_2, Q_3, Q_4 \in \mathbb{R}$. However, since we are only interested in singular solutions of (3.46), we take $Q_3 = Q_4 = 0$, as in the proof of Theorem 3.3. Recall that, by (3.49), the angular functions (3.58) and (3.55) (with $Q_3 = Q_4 = 0$) can only be coupled to the radial functions $\rho[C_1\cos(\mu\log(\rho)) + C_2\sin(\mu\log(\rho))]$ and ρ, respectively. If we restrict ourselves to integer values of the coefficient μ, this enables us to drop the separated-variable assumption and to find physical and infinite-energy solutions of (3.25) in the form (3.56). $\qquad\square$

3.4 Some boundary conditions leading to vortices

In this section we show that some singular solutions of (3.46) can successfully describe, both from an analytical and physical point of view, the rather chaotic dynamics of the vortex shedding pattern described in the Introduction. By adapting the first boundary condition over Γ_3 in (3.7) to the "localized" configuration in Λ, we see that the first (resp. second) component of the velocity field must vanish over the vertical face Γ_{32} (resp. horizontal face Γ_{31}):

$$u^2 = 0 \quad \text{on } \Gamma_{31} \quad \text{and} \quad u^1 = 0 \quad \text{on } \Gamma_{32}. \tag{3.59}$$

In the next two subsections we complement "by hand" (3.59) with further boundary conditions in order to build solutions of (3.46) displaying vortices. We will exhibit singular solutions $u \in \mathcal{C}^2(\overline{\Lambda} \setminus \{(0,0)\})^2$ whose streamlines qualitatively describe vortices.

3.4.1 Boundary conditions for laminar inflow

In this subsection we exhibit an example in which the boundary conditions satisfied by the singular solution of (3.25) (in separated variables) lead to the formation of vortices around the corner and over the leeward wall of the domain Λ. The mechanical description of the vortex shedding given in [210, Section 4.2.6] and [233] suggest that the flow should be laminar over Γ_{31}. Therefore, taking into account (3.59), we will seek solutions $u = (u^1, u^2)$ of (3.46) in Λ verifying

$$u^2 = \omega = 0 \quad \text{on } \Gamma_{31} \quad \text{and} \quad u^1 = 0, \ \omega = \omega_0 \quad \text{on } \Gamma_{32}. \tag{3.60}$$

We point out that boundary conditions such as (3.60) were considered by Kwon-Kweon [166, Section 2] for $\omega_0 = 0$, while our choice will be different, see (3.70) below.

We take $h_{\mathcal{S}}$ in (3.49), with $C_1 = C_2 = \mu = 1$, as the radial component of the singular stream function. Correspondingly, the angular component $g_{\mathcal{S}}$ must satisfy (3.36) with $\alpha = 0$ and $\beta = 4$:

$$g_{\mathcal{S}}^{(4)}(\theta) + 4g_{\mathcal{S}}(\theta) = 0 \quad \forall \theta \in \left(-\frac{\pi}{2}, \pi\right), \tag{3.61}$$

that is, there exist constants $A_1, A_2, A_3, A_4 \in \mathbb{R}$ such that

$$g_{\mathcal{S}}(\theta) = A_1 \cosh(\theta) \cos(\theta) + A_2 \cosh(\theta) \sin(\theta) + A_3 \sinh(\theta) \cos(\theta) + A_4 \sinh(\theta) \sin(\theta) \quad \forall \theta \in \left(-\frac{\pi}{2}, \pi\right). \tag{3.62}$$

Therefore, we take $\psi_{\mathcal{S}}(\rho, \theta) \doteq h_{\mathcal{S}}(\rho) g_{\mathcal{S}}(\theta)$ as singular solution of (3.25) and we use (3.48) to compute

$$\begin{cases} u_{\mathcal{S}}^1(\rho, \theta) = \cos(\theta)[\cos(\log(\rho)) + \sin(\log(\rho))][(A_2 + A_3)\cos(\theta)\cosh(\theta) + (A_4 - A_1)\sin(\theta)\cosh(\theta)] \\ \qquad + \cos(\theta)[\cos(\log(\rho)) + \sin(\log(\rho))][(A_1 + A_4)\cos(\theta)\sinh(\theta) + (A_2 - A_3)\sin(\theta)\sinh(\theta)] \\ \qquad + 2\sin(\theta)\cos(\log(\rho))\{[A_1\cos(\theta) + A_2\sin(\theta)]\cosh(\theta) + [A_3\cos(\theta) + A_4\sin(\theta)]\sinh(\theta)\} \\ u_{\mathcal{S}}^2(\rho, \theta) = \sin(\theta)[\cos(\log(\rho)) + \sin(\log(\rho))][(A_2 + A_3)\cos(\theta)\cosh(\theta) + (A_4 - A_1)\sin(\theta)\cosh(\theta)] \\ \qquad + \sin(\theta)[\cos(\log(\rho)) + \sin(\log(\rho))][(A_1 + A_4)\cos(\theta)\sinh(\theta) + (A_2 - A_3)\sin(\theta)\sinh(\theta)] \\ \qquad - 2\cos(\theta)\cos(\log(\rho))\{[A_1\cos(\theta) + A_2\sin(\theta)]\cosh(\theta) + [A_3\cos(\theta) + A_4\sin(\theta)]\sinh(\theta)\}, \end{cases}$$

for $(\rho, \theta) \in \Lambda$. Due to (3.59), the constants A_1, A_2, A_3, A_4 must be chosen in such a way that

$$\begin{cases} u_{\mathcal{S}}^1\left(\rho, -\frac{\pi}{2}\right) = 2\cos(\log(\rho))\left[A_2\cosh\left(\frac{\pi}{2}\right) - A_4\sinh\left(\frac{\pi}{2}\right)\right] = 0 \\ u_{\mathcal{S}}^2(\rho, \pi) = -2\cos(\log(\rho))[A_1\cosh(\pi) + A_3\sinh(\pi)] = 0, \end{cases} \tag{3.63}$$

for $\rho > 0$. Moreover, for the scalar vorticity we have

$$\omega_{\mathcal{S}}(\rho, \theta) = -\Delta \psi_{\mathcal{S}}(\rho, \theta) = -\frac{2}{\rho} \cosh(\theta) \sin(\theta)[(A_2 - A_3) \cos(\log(\rho)) - (A_2 + A_3) \sin(\log(\rho))]$$
$$-\frac{2}{\rho} \cosh(\theta) \cos(\theta)[(A_1 + A_4) \cos(\log(\rho)) + (A_4 - A_1) \sin(\log(\rho))]$$
$$-\frac{2}{\rho} \sinh(\theta) \cos(\theta)[(A_2 + A_3) \cos(\log(\rho)) + (A_2 - A_3) \sin(\log(\rho))]$$
$$+\frac{2}{\rho} \sinh(\theta) \sin(\theta)[(A_1 - A_4) \cos(\log(\rho)) + (A_1 + A_4) \sin(\log(\rho))], \quad (3.64)$$

for $(\rho, \theta) \in \Lambda$. In view of (3.60), the constants A_1, A_2, A_3, A_4 must also satisfy

$$\omega_{\mathcal{S}}(\rho, \pi) = \frac{2}{\rho} \sin(\log(\rho))[(A_4 - A_1) \cosh(\pi) + (A_2 - A_3) \sinh(\pi)]$$
$$+\frac{2}{\rho} \cos(\log(\rho))[(A_1 + A_4) \cosh(\pi) + (A_2 + A_3) \sinh(\pi)] = 0, \quad (3.65)$$

for $\rho > 0$. Thus, after combining (3.63) and (3.65), we infer that the constants must satisfy the following algebraic system in matrix form:

$$\begin{bmatrix} \cosh(\pi) & 0 & \sinh(\pi) & 0 \\ -\cosh(\pi) & \sinh(\pi) & -\sinh(\pi) & \cosh(\pi) \\ \cosh(\pi) & \sinh(\pi) & \sinh(\pi) & \cosh(\pi) \\ 0 & \cosh\left(\frac{\pi}{2}\right) & 0 & -\sinh\left(\frac{\pi}{2}\right) \end{bmatrix} \begin{bmatrix} A_1 \\ A_2 \\ A_3 \\ A_4 \end{bmatrix} = \begin{bmatrix} 0 \\ 0 \\ 0 \\ 0 \end{bmatrix}. \quad (3.66)$$

Notice that the matrix of the left-hand side of (3.66) is singular, since the first and third columns are proportional. Consequently, system (3.66) has infinitely many solutions (as expected, because we are only imposing three boundary conditions out of possible four) given by

$$A_2 = A_4 = 0, \qquad A_1 = -A_3 \tanh(\pi).$$

The resulting expressions for the singular stream function, velocity field and vorticity are given below.

- **Stream function:** $\psi_{\mathcal{S}}(\rho, \theta) = A \cos(\theta) \cosh(\theta)[\tanh(\theta) - \tanh(\pi)] \cdot \rho[\cos(\log(\rho)) + \sin(\log(\rho))]$, for $(\rho, \theta) \in \Lambda$ and any constant $A \in \mathbb{R}$.

- **Components of the velocity field:**

$$\begin{cases} u_{\mathcal{S}}^1(\rho, \theta) = A \cosh(\theta) \cos(\theta)[\cos(\theta) + \tanh(\pi) \sin(\theta)][\cos(\log(\rho)) + \sin(\log(\rho))] \\ \qquad\quad - A \sinh(\theta) \cos(\theta)[\sin(\theta) + \tanh(\pi) \cos(\theta)][\cos(\log(\rho)) + \sin(\log(\rho))] \\ \qquad\quad - 2A \cos(\theta) \sin(\theta) \dfrac{\sinh(\pi - \theta)}{\cosh(\pi)} \cos(\log(\rho)) \\ u_{\mathcal{S}}^2(\rho, \theta) = A \cosh(\theta) \sin(\theta)[\cos(\theta) + \tanh(\pi) \sin(\theta)][\cos(\log(\rho)) + \sin(\log(\rho))] \\ \qquad\quad - A \sinh(\theta) \sin(\theta)[\sin(\theta) + \tanh(\pi) \cos(\theta)][\cos(\log(\rho)) + \sin(\log(\rho))] \\ \qquad\quad + 2A \cos^2(\theta) \dfrac{\sinh(\pi - \theta)}{\cosh(\pi)} \cos(\log(\rho)), \end{cases} \quad (3.67)$$

for $(\rho, \theta) \in \Lambda$ and any constant $A \in \mathbb{R}$. Notice that $(u_{\mathcal{S}}^1, u_{\mathcal{S}}^2) \in \mathcal{C}^2(\overline{\Lambda} \setminus \{(0,0)\})^2$.

- **Vorticity:**

$$\omega_{\mathcal{S}}(\rho, \theta) = \frac{2A}{\rho} \sinh(\theta)\{\cos(\theta)[\sin(\log(\rho)) - \cos(\log(\rho))] - \tanh(\pi) \sin(\theta)[\sin(\log(\rho)) + \cos(\log(\rho))]\}$$
$$+ \frac{2A}{\rho} \cosh(\theta)\{[\sin(\theta) - \tanh(\pi) \cos(\theta)] \sin(\log(\rho)) + [\sin(\theta) + \tanh(\pi) \cos(\theta)] \cos(\log(\rho))\}, \quad (3.68)$$

44

for $(\rho, \theta) \in \Lambda$ and any constant $A \in \mathbb{R}$. As expected, the vorticity is not in $L^2(\Lambda)$. In particular, the restriction of the vorticity field to the vertical face Γ_{32} is given by:

$$\omega_{\mathcal{S}}\left(\rho, -\frac{\pi}{2}\right) = -\frac{2A}{\rho} \frac{\cosh\left(\frac{3\pi}{2}\right)}{\cosh(\pi)} [\sin(\log(\rho)) + \cos(\log(\rho))] \quad \forall \rho > 0. \tag{3.69}$$

Therefore, by selecting the value of $A = A_0 \doteq -\frac{1}{2} \frac{\cosh(\pi)}{\cosh\left(\frac{3\pi}{2}\right)}$, we infer that the velocity field $u_{\mathcal{S}}$ in (3.67) satisfies (3.46) in Λ and the boundary conditions (3.60) with

$$\omega_0(\rho) \doteq \frac{1}{\rho} [\sin(\log(\rho)) + \cos(\log(\rho))] \quad \forall \rho > 0. \tag{3.70}$$

A contour plot of $\omega_{\mathcal{S}}$ in (3.68), with $A = A_0$, is presented in Figure 3.7, where such quantity is considered in a disk of radius 0.005 around the corner (compare with the *isovorticity* plots obtained in [78]).
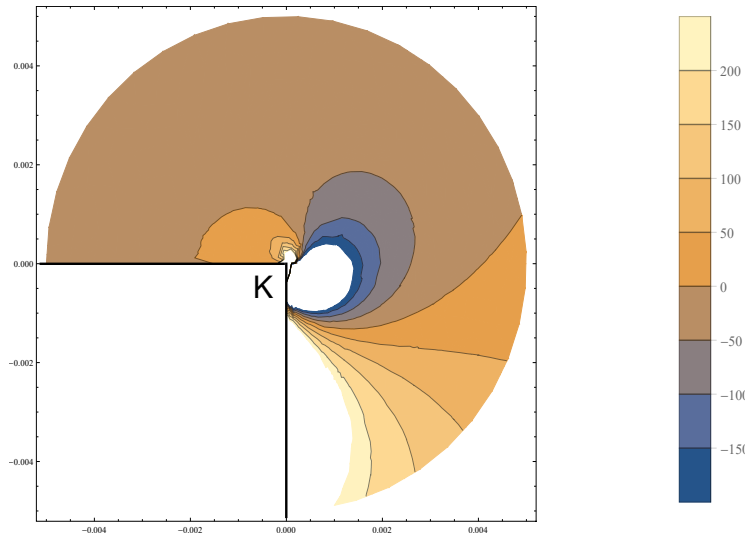
Figure 3.7: Contour plot of $\omega_{\mathcal{S}}$ in (3.68) for $A = A_0$, on a disk of radius 0.005 around the corner.

Furthermore, the streamline plot of the velocity field (3.67) (with $A = A_0$) in Figure 3.8 displays a noticeable vortex pattern around the corner (to be compared with [78, Figure 12] or [272, Figure 2]).
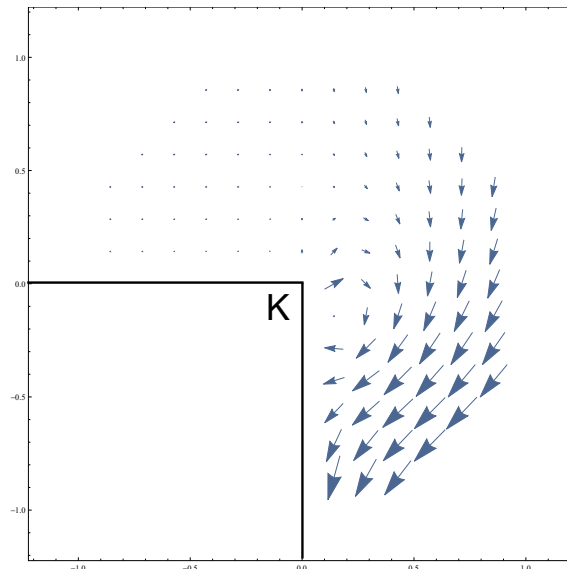

Figure 3.8: Streamline plot of $u_{\mathcal{S}} = (u_{\mathcal{S}}^1, u_{\mathcal{S}}^2)$ in (3.67) for $A = A_0$, on a disk of unitary radius.

3.4.2 Boundary conditions with oriented velocity

A further natural condition over the horizontal face Γ_{31} concerns the first component of the velocity field, which must have a positive sign in order to follow the inflow direction. In [110] (see also [166, Corollary 1.1]) such positivity condition is imposed on some given part of the boundary as a constraint for a related drag-minimization problem. Therefore, given two functions $\xi : \Gamma_{31} \to (0, \infty)$ and $\omega_0 : \Gamma_{32} \to \mathbb{R}$, and taking into account (3.59), here we seek solutions $u = (u^1, u^2)$ of (3.46) in Λ verifying

$$u^1 = \xi, \ u^2 = 0 \quad \text{on} \ \Gamma_{31} \quad \text{and} \quad u^1 = 0, \ \omega = \omega_0 \quad \text{on} \ \Gamma_{32}. \tag{3.71}$$

Explicit forms for ξ and ω_0 will be given in (3.84), in order to fit singular solutions of (3.46) into the boundary conditions (3.71). To this end, we need first to "adjust" the general expression (3.56) with some regular solution of (3.46), according to the following definition:

Definition 3.3. *We say that a solution u of* (3.46) *is* **regular** *if $u \in C^2(\overline{\Lambda})^2$.*

Clearly, a regular solution is associated to a stream function $\psi \in C^4(\overline{\Lambda})$. Following [158], we then write the solutions of (3.26) as

$$\psi(\rho, \theta) = \psi_{\mathcal{S}}(\rho, \theta) + \psi_{\mathcal{R}}(\rho, \theta) \quad \forall (\rho, \theta) \in \Lambda, \tag{3.72}$$

where $\psi_{\mathcal{S}}$ is as in (3.56) and $\psi_{\mathcal{R}} : \Lambda \to \mathbb{R}$ denotes the regular component of the stream function. The regular part $\psi_{\mathcal{R}}$ in (3.72) has much more freedom, since it only needs to "balance" $\psi_{\mathcal{S}}$ in order to match (3.71). Therefore, we consider a very simple form, we take $\psi_{\mathcal{R}}(y, z) = Ay + Bz$, for some $A, B \in \mathbb{R}$. Clearly, $\Delta^2 \psi_{\mathcal{R}} = 0$ in Λ and

$$u_{\mathcal{R}}^1(y, z) = B, \quad u_{\mathcal{R}}^2(y, z) = -A, \quad \omega_{\mathcal{R}}(y, z) = 0 \quad \forall (y, z) \in \overline{\Lambda}. \tag{3.73}$$

Notice that the dependence with respect to ρ in the series (3.56) does not vanish at the boundaries Γ_{31} and Γ_{32}. Therefore, such series cannot be equalized to a constant different from zero, and the expression $\rho[Q_1 \theta \cos(\theta) + Q_2 \theta \sin(\theta)]$ needs to act as the counterbalance part. After imposing the boundary conditions (3.71), and in view of (3.56)-(3.72)-(3.73), we see that

- $u^1\left(\rho, -\frac{\pi}{2}\right) = u_{\mathcal{R}}^1\left(\rho, -\frac{\pi}{2}\right) + u_{\mathcal{S}}^1\left(\rho, -\frac{\pi}{2}\right) = 0$, for $\rho > 0$, that is

$$B - \frac{\pi}{2}Q_2 + \sum_{k=1}^{\infty} e^{-\frac{k\pi}{2}}(A_2 + e^{k\pi}A_4)[(C_1 + kC_2)\cos(k\log(\rho)) + (C_2 - kC_1)\sin(k\log(\rho))] = 0 \quad \forall \rho > 0. \tag{3.74}$$

This implies that $B = \frac{\pi}{2}Q_2$ and $A_2(k) = -e^{k\pi}A_4(k)$, for any integer $k \geq 1$.

- $u^2(\rho, \pi) = u_{\mathcal{R}}^2(\rho, \pi) + u_{\mathcal{S}}^2(\rho, \pi) = 0$, for $\rho > 0$, that is

$$-A - \pi Q_1 - \sum_{k=1}^{\infty} e^{-k\pi}(A_3 + e^{2k\pi}A_1)[(C_1 + kC_2)\cos(k\log(\rho)) + (C_2 - kC_1)\sin(k\log(\rho))] = 0 \quad \forall \rho > 0. \tag{3.75}$$

This implies that $A = -\pi Q_1$ and $A_3(k) = -e^{2k\pi}A_1(k)$, for any integer $k \geq 1$.

- Regarding the positivity condition in (3.71), the relations derived from (3.74)-(3.75) imply that:

$$\begin{aligned} u^1(\rho, \pi) &= u_{\mathcal{R}}^1(\rho, \pi) + u_{\mathcal{S}}^1(\rho, \pi) \\ &= -\frac{A}{\pi} + 3B + \sum_{k=1}^{\infty}[(e^{-k\pi} - e^{2k\pi})A_4(k) + 2ke^{k\pi}A_1(k)][C_1(k)\cos(k\log(\rho)) + C_2(k)\sin(k\log(\rho))], \end{aligned} \tag{3.76}$$

for $\rho > 0$. Now, as stated in [222, Supplement 2], for every $a \in (-1, 1)$ and $x \in \mathbb{R}$ we have the following series

$$\sum_{k=0}^{\infty} a^k \cos(kx) = \frac{1 - a\cos(x)}{1 - 2a\cos(x) + a^2}, \qquad \sum_{k=0}^{\infty} a^k \sin(kx) = \frac{a\sin(x)}{1 - 2a\cos(x) + a^2},$$

46

and the sum of the first series is a strictly positive function in $\mathbb{R}$. This leads us to impose $-\frac{A}{\pi} + 3B = 1$ and to select the following values for the sequences of constants appearing in (3.76):

$$A_1(k) = \frac{e^{-3k\pi}}{2k}, \quad A_4(k) = C_2(k) = 0 \quad \text{and} \quad C_1(k) = 1 \quad \forall k \geq 1, \ k \in \mathbb{N}. \tag{3.77}$$

After inserting (3.77) into (3.76) we obtain:

$$u^1(\rho, \pi) = 1 + \sum_{k=1}^{\infty} e^{-2k\pi} \cos(k \log(\rho)) = \frac{1 - e^{-2\pi} \cos(\log(\rho))}{1 - 2e^{-2\pi} \cos(\log(\rho)) + e^{-4\pi}} \quad \forall \rho > 0. \tag{3.78}$$

As a particular case, we choose $A = 2\pi$ and $B = 1$, so that $Q_1 = -2$ and $Q_2 = 2/\pi$. The resulting expressions for the stream function, velocity and vorticity fields are computed below.

- **Stream function:**

$$\psi(\rho, \theta) = \rho \left[2(\pi - \theta) \cos(\theta) + \left(\frac{2\theta}{\pi} + 1 \right) \sin(\theta) \right] + \frac{\rho}{2} \cos(\theta) \sum_{k=1}^{\infty} \frac{1}{k} [e^{-k(3\pi - \theta)} - e^{-k(\theta + \pi)}] \cos(k \log(\rho)), \tag{3.79}$$

for $(\rho, \theta) \in \Lambda$. Notice that the interval of definition of θ ensures the convergence of the series of functions in (3.79).

- **First component of the velocity field:**

$$u^1(\rho, \theta) = \frac{1}{\pi} [2\theta + \sin(2\theta)] - \cos(2\theta)$$

$$+ \frac{1}{2} \cos^2(\theta) \left[\frac{1 - e^{-(\theta + \pi)} \cos(\log(\rho))}{1 - 2e^{-(\theta + \pi)} \cos(\log(\rho)) + e^{-2(\theta + \pi)}} + \frac{1 - e^{(\theta - 3\pi)} \cos(\log(\rho))}{1 - 2e^{(\theta - 3\pi)} \cos(\log(\rho)) + e^{2(\theta - 3\pi)}} - 2 \right] \tag{3.80}$$

$$+ \frac{1}{2} \cos(\theta) \sin(\theta) \left[\frac{e^{-(\theta + \pi)} \sin(\log(\rho))}{1 - 2e^{-(\theta + \pi)} \cos(\log(\rho)) + e^{-2(\theta + \pi)}} - \frac{e^{(\theta - 3\pi)} \sin(\log(\rho))}{1 - 2e^{(\theta - 3\pi)} \cos(\log(\rho)) + e^{2(\theta - 3\pi)}} \right],$$

for $(\rho, \theta) \in \Lambda$.

- **Second component of the velocity field:**

$$u^2(\rho, \theta) = 2(\theta - \pi) - \sin(2\theta) + \frac{1}{\pi} [1 - \cos(2\theta)] + \frac{1}{2} \sum_{k=1}^{\infty} \frac{1}{k} [e^{-k(\theta + \pi)} - e^{-k(3\pi - \theta)}] \cos(k \log(\rho))$$

$$+ \frac{1}{2} \cos(\theta) \sin(\theta) \left[\frac{1 - e^{-(\theta + \pi)} \cos(\log(\rho))}{1 - 2e^{-(\theta + \pi)} \cos(\log(\rho)) + e^{-2(\theta + \pi)}} + \frac{1 - e^{(\theta - 3\pi)} \cos(\log(\rho))}{1 - 2e^{(\theta - 3\pi)} \cos(\log(\rho)) + e^{2(\theta - 3\pi)}} - 2 \right] \tag{3.81}$$

$$- \frac{1}{2} \cos^2(\theta) \left[\frac{e^{-(\theta + \pi)} \sin(\log(\rho))}{1 - 2e^{-(\theta + \pi)} \cos(\log(\rho)) + e^{-2(\theta + \pi)}} - \frac{e^{(\theta - 3\pi)} \sin(\log(\rho))}{1 - 2e^{(\theta - 3\pi)} \cos(\log(\rho)) + e^{2(\theta - 3\pi)}} \right],$$

for $(\rho, \theta) \in \Lambda$. Notice again that $(u^1, u^2) \in \mathcal{C}^2(\overline{\Lambda} \setminus \{(0,0)\})^2$.

- **Scalar vorticity:**

$$\omega(\rho, \theta) = -\frac{4}{\pi \rho} [\cos(\theta) + \pi \sin(\theta)]$$

$$+ \frac{1}{\rho} \sin(\theta) \left[\frac{1 - e^{-(\theta + \pi)} \cos(\log(\rho))}{1 - 2e^{-(\theta + \pi)} \cos(\log(\rho)) + e^{-2(\theta + \pi)}} + \frac{1 - e^{(\theta - 3\pi)} \cos(\log(\rho))}{1 - 2e^{(\theta - 3\pi)} \cos(\log(\rho)) + e^{2(\theta - 3\pi)}} - 2 \right] \tag{3.82}$$

$$- \frac{1}{\rho} \cos(\theta) \left[\frac{e^{-(\theta + \pi)} \sin(\log(\rho))}{1 - 2e^{-(\theta + \pi)} \cos(\log(\rho)) + e^{-2(\theta + \pi)}} - \frac{e^{(\theta - 3\pi)} \sin(\log(\rho))}{1 - 2e^{(\theta - 3\pi)} \cos(\log(\rho)) + e^{2(\theta - 3\pi)}} \right],$$

for $(\rho, \theta) \in \Lambda$. As expected, notice that the vorticity is clearly not in $L^2(\Lambda)$. In particular, the restriction of the vorticity to the vertical face Γ_{32} is given by:

$$\omega \left(\rho, -\frac{\pi}{2} \right) = \frac{6}{\rho} - \frac{1}{\rho} \left[\frac{1 - e^{-\frac{\pi}{2}} \cos(\log(\rho))}{1 - 2e^{-\frac{\pi}{2}} \cos(\log(\rho)) + e^{-\pi}} + \frac{1 - e^{-\frac{7\pi}{2}} \cos(\log(\rho))}{1 - 2e^{-\frac{7\pi}{2}} \cos(\log(\rho)) + e^{-7\pi}} \right] \quad \forall \rho > 0. \tag{3.83}$$

47

As a consequence of these computations, we infer that the ψ (3.79) is a biharmonic function in Λ, whose velocity field (3.80)-(3.81) satisfies (3.46) in Λ and (3.71) with:

$$\begin{cases} \xi(\rho) \doteq \dfrac{1 - e^{-2\pi}\cos(\log(\rho))}{1 - 2e^{-2\pi}\cos(\log(\rho)) + e^{-4\pi}}, \\[4mm] \omega_0(\rho) \doteq \dfrac{1}{\rho}\left[6 - \dfrac{1 - e^{-\frac{\pi}{2}}\cos(\log(\rho))}{1 - 2e^{-\frac{\pi}{2}}\cos(\log(\rho)) + e^{-\pi}} - \dfrac{1 - e^{-\frac{7\pi}{2}}\cos(\log(\rho))}{1 - 2e^{-\frac{7\pi}{2}}\cos(\log(\rho)) + e^{-7\pi}} \right], \end{cases} \tag{3.84}$$

for $\rho > 0$. A contour plot of the vorticity (3.82) is presented in Figure 3.9. The chaotic dynamics of the vortex shedding process are properly illustrated and characterized by the increasing values of the vorticity (to be compared with Figure 3.7 and the *isovorticity* plots obtained in [78]).
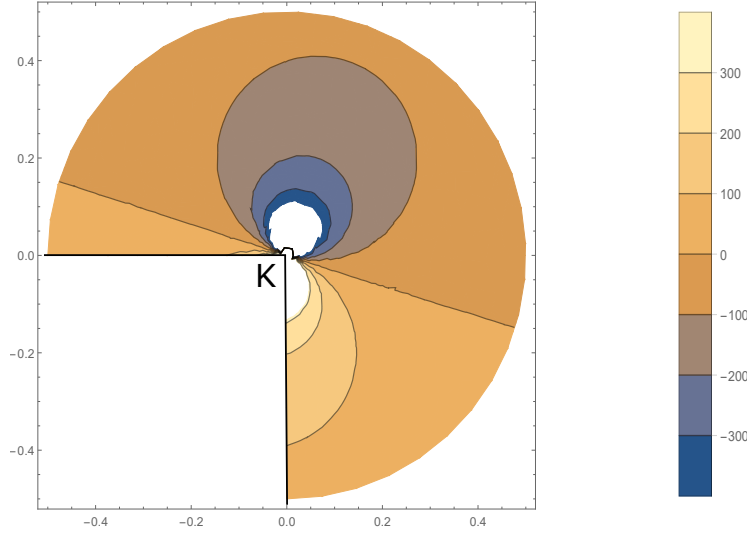
Figure 3.9: Contour plot of ω in (3.82) on a disk of radius 0.5 around the corner.

On the other hand, a streamline plot of the velocity field (3.80)-(3.81) (where the series of functions in (3.81) was numerically approximated with the sum of the ten first terms) in Figure 3.10 reproduces some of the typical geometrical patterns induced by low-Reynolds-number flows past square cylinders (see [78, Figure 10] or [272, Figure 5]).
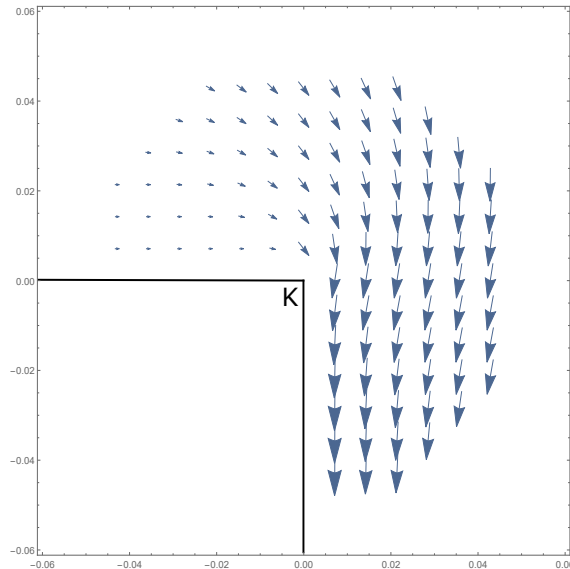
Figure 3.10: Streamline plot of $u = (u^1, u^2)$ in (3.80)-(3.81) on a disk of radius 0.05 around the corner.

Chapter 4

Steady Navier-Stokes equations in planar domains with obstacle and explicit bounds for unique solvability

Unlike the hydrodynamical model analyzed in Chapter 3, in the present chapter we consider *standard* boundary conditions for the equations of fluid mechanics (properly justified), and we study in detail some of the physical and mathematical properties of the solution that are relevant for our purposes: unique solvability, regularity, symmetry and the computation of drag and lift exerted over the obstacle.

The whole science of flight is based on the understanding and control of the *lift force*, the resistance component orthogonal to the aircraft direction of motion, see e.g. [4, Chapter 1]. The modern theory of lift, developed in the fundamental works of Kutta [165] and Zhukovsky [274] at the beginning of the 20th century (see also [4] for the English translation), relies on the principle that a cambered surface produces lift through its ability to generate vortices about itself, see Figure 4.1 for a wind tunnel experiment.
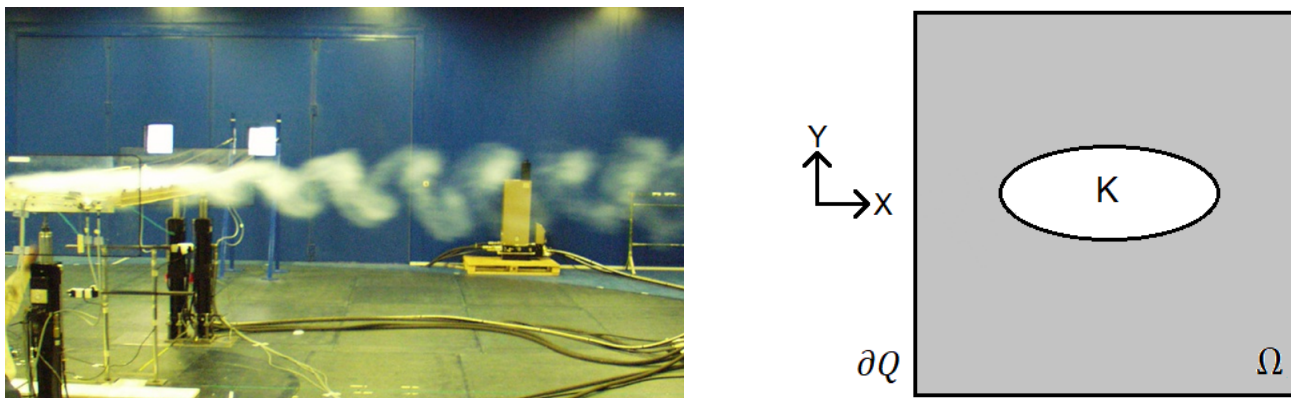
Figure 4.1: Left: vortices around a plate obtained in wind tunnel experiments at the Politecnico di Milano. Right: the planar domain Ω in (4.1) with a smooth obstacle K.

The celebrated d'Alembert paradox [179] shows that the lift is characteristic of viscous fluids so that the full evolution of aerodynamics was possible only after a precise comprehension of viscosity. Vortices in fluid dynamics appear both for turbulent flows with large Reynolds number and whenever a fluid surrounds an obstacle. The vortices generate a lift force acting on the obstacle orthogonally to the direction of the flow so that, if one considers a rigid obstacle having the shape of a 3D cylinder (the cartesian product of a planar compact set $\overline{K}$ with a bounded interval, as in the left picture of Figure 4.1), it is convenient to restrict the attention to the cross-section $\overline{K}$ of the cylinder.

In the plane $\mathbb{R}^2$ we consider an obstacle, represented by an open bounded simply connected domain K

with Lipschitz boundary ∂K, and a big squared box Q containing the obstacle and such that $\partial Q \cap \partial K = \emptyset$. More precisely, we consider the domains

$$Q = (-L, L)^2, \qquad \Omega = Q \setminus \overline{K} \qquad \left(L \gg \operatorname{diam}(K)\right), \tag{4.1}$$

where Ω should be seen as a sufficiently large (bounded) region surrounding $\overline{K}$. The boundary of Ω is split into two parts, $\partial \Omega = \partial K \cup \partial Q$, and the outward unit normal $\hat{n}$ is defined a.e. on $\partial \Omega$. This geometry appears to be the best choice to model, for instance, the motion of the wind around the cross-section of a bridge for which one needs a (squared) photo of the flow in a sufficiently large neighborhood, as in the left picture in Figure 4.1 but on a larger scale. A sketch of this geometry is illustrated in the right picture in Figure 4.1 (not in scale and with smooth ∂K).

In this chapter, which is based on the preprint [124], we provide the tools for the full theory of planar stationary flows of viscous fluids around an obstacle, assuming that they are governed by the steady Navier-Stokes equations

$$-\eta \Delta u + (u \cdot \nabla) u + \nabla p = f, \qquad \nabla \cdot u = 0 \qquad \text{in } \Omega, \tag{4.2}$$

where $u : \Omega \to \mathbb{R}^2$ is the velocity vector field, $p : \Omega \to \mathbb{R}$ is the scalar pressure, $f : \Omega \to \mathbb{R}^2$ denotes an external forcing term and $\eta > 0$ is the kinematic viscosity. To (4.2) we associate the boundary data

$$u = (U, V) \ \text{ on } \ \partial Q, \qquad u = (0, 0) \ \text{ on } \ \partial K, \tag{4.3}$$

for some given $(U, V) \in H^{1/2}(\partial Q)$ satisfying the compatibility condition (zero flux across ∂Q)

$$\int_{-L}^{L} [U(L, y) - U(-L, y)] \, dy + \int_{-L}^{L} [V(x, L) - V(x, -L)] \, dx = 0. \tag{4.4}$$

The boundary conditions (4.3) model the inflow/outflow of fluid across the boundary ∂Q with velocity (U, V), and with no-slip condition on the obstacle K where viscosity yields zero velocity of the flow. The inhomogeneous boundary datum (U, V) on ∂Q is mandatory since, as explained above, Q represents a virtual box (a planar region where the flow is analyzed) and *not* a region with rigid boundary (contrary to the obstacle). For some of our results we focus the attention on the case where $(U, V) \in \mathbb{R}^2$ is constant on ∂Q; this choice is motivated by the fact that Q is much larger than K and possible effects of the vortex shedding created by the obstacle are not detectable far away from it.

It is well-known [115] that uniqueness for (4.2)-(4.3) is ensured only whenever the data f and (U, V) are "small" compared to the viscosity η, see also Theorem 4.6 below. The proof relies on a priori bounds which lead to a contradiction if one assumes the existence of multiple solutions of (4.2)-(4.3). While in the case of homogeneous Dirichlet boundary conditions $(U, V) = (0, 0)$ the a priori bounds are straightforward, in the inhomogeneous case $(U, V) \neq (0, 0)$ they are extremely delicate because the solution of (4.2)-(4.3) is not an admissible test function and, therefore, explicit values for the bounds are not known. The standard approach is then to transform the inhomogeneous Dirichlet problem into an homogeneous problem by determining a solenoidal extension of the boundary velocity, namely one needs to find a vector field w such that

$$\nabla \cdot w = 0 \ \text{ in } \ \Omega, \qquad w = (U, V) \ \text{ on } \ \partial Q, \qquad w = (0, 0) \ \text{ on } \ \partial K. \tag{4.5}$$

This problem, whose interest and applicability go far beyond fluid mechanics, has a long story, starting from the pioneering works by Cattabriga [51] and Ladyzhenskya-Solonnikov [169, 170]; see also the book by Galdi [115, Section III.3]. Solving (4.5) is an extremely difficult task and a possible way out is to proceed in two steps. First to find an extension, not necessarily solenoidal, of the data (U, V), thereby "inverting" the trace operator for vector fields. Then to solve the Bogovskii problem [36, 37] with the resulting divergence, see Section 4.1.4: the celebrated Bogovskii formula, from 1979, yields a class of solutions by means of the Calderón-Zygmund theory of singular integrals. By using instead the Fourier

transform, Durán [90] proposed in 2012 an alternative approach that can be used to simplify some computations.

Finding explicit theoretical bounds for the critical Reynolds number, i.e. for the stability of the steady flow of a viscous fluid, constitutes a fundamental problem in fluid mechanics, see [173, Chapter III], closely related to the onset of turbulence from a laminar regime [172]. As we shall see in Section 4.2.3, in a symmetric framework the appearance of effective lift forces exerted by the fluid on the obstacle K is strictly related to non-uniqueness of solutions of (4.2)-(4.3). Therefore, for the uniqueness threshold of (4.2)-(4.3), explicit bounds are needed, as precise as possible. In turn, the uniqueness threshold is obtained through a priori bounds for the solutions of (4.5) but, so far, no such bounds are available in the literature. Obtaining explicit bounds for (4.5) and several related functional inequalities is precisely the first purpose of the present chapter.

In Section 4.1 we obtain several bounds on the relative capacity of the obstacle K with respect to Q and on some Sobolev embedding constants; moreover, we suggest a new way to bound the solenoidal extension w in (4.5). In [120], Gazzola defined the space of *web functions*, namely the subspace of $H_0^1(\Omega)$ comprising functions which only depend on the distance from the boundary $\partial\Omega$. These functions were previously introduced by Szegö [252] in a slightly different context. The main novelty in [120] was the possibility of obtaining bounds for some constants arising in variational problems, see [72, 74] and also [73] for bounds on the capacity. In our context of non simply connected domain, we cannot use web functions and we introduce instead the subset of *pyramidal functions*, see (4.9), in order to obtain bounds for the relative capacity of the obstacle. Then we need to bound the Sobolev constant for the embedding $H^1(\Omega) \subset L^4(\Omega)$, which arises naturally due to the convective term in (4.2): here we have to face both the difficulties of dealing with a non simply connected domain and of inhomogeneous boundary data, especially because we seek precise estimates. For this reason, we use an optimal Gagliardo-Nirenberg inequality by del Pino-Dolbeault [83] with some adjustments: we combine it with Hölder and Poincaré inequalities in the case of zero traces and with a delicate ad hoc argument for nonzero traces, see Theorem 4.2. Nowadays numerics can give precise bounds, but only for given specific geometries. On the contrary, our theoretical bounds are independent of the geometry; we also show that they are fairly precise, see Remark 4.1 and Corollary 4.2. For this reason, and for possible further developments, we embed our results in a general theory which goes beyond the applications given in this chapter.

The second main purpose of the present chapter is to obtain precise statements about the lift exerted by the solutions of (4.2)-(4.3) on the obstacle K. To this end, we need the bounds obtained in the first part: in particular, we use the pyramidal capacity potential in order to obtain bounds for the solutions of (4.5). The existence of symmetric solutions of the stationary Navier-Stokes equations has been proved in smooth symmetric domains in the pioneering work by Amick [7] and, subsequently, by several other authors [107, 108, 161, 184, 202]. As already mentioned, our focus is different, we connect symmetric solutions with uniqueness and with the computation of the lift. In Theorem 4.9 we study (4.2)-(4.3) in a perfectly symmetric situation, where a symmetric solution always exists and possible non-uniqueness is strictly related to the existence of asymmetric solutions. In Section 4.2.3 we define the drag and the lift, namely the forces exerted by the fluid governed by (4.2) on the bluff body represented by the obstacle K. We focus most of our attention on the lift force since it is responsible for the instability of K, as in civil engineering structures where it leads to dangerous oscillations. In regime of uniqueness, we prove that there is no lift in a symmetric situation and that the lift is small in an "almost symmetric" situation, see Theorem 4.12. This means that instability and/or non-uniqueness may appear only in asymmetric situations or with large data. Theorem 4.14 uses all the just mentioned results and gives an explicit universal bound such that, if a constant inflow velocity of the fluid is below this bound, then the obstacle is not subject to a lift force. In turn, this result also yields explicit bounds for the threshold of stability of a bluff body immersed in a viscous fluid.

While our bounds *do not* depend on the shape of the obstacle, one expects that the threshold of stability does depend on the shape. However, there is no available theory able to analyze the shape dependence of the lift, see [25] for related results about the drag. Therefore, in Section 4.2.5 we proceed

through Computational Fluid Dynamics (CFD) by using the OpenFOAM toolbox. We use an asymmetry/multiplicity principle (see Corollary 4.4) in order to compute the performance of several obstacles having the same measure but different shapes. The idea is to numerically detect non-uniqueness for (4.2)-(4.3) by finding asymmetric solutions in a symmetric framework. The obtained numerical results give strong hints on which could be the best shape yielding the largest inflow velocity (U, V) ensuring that the lift is zero. They also strengthen a conjecture by Pironneau [219, 220] claiming that the inward face should look like a "rugby ball", see in particular [219, Figure 3], in order to minimize the drag. We point out that the numerical bounds for stability cannot be compared with the theoretical ones obtained in Section 4.1, because the latter are found without assuming symmetry of the data.

Finally, we mention that the functional inequalities discussed in Section 4.1, in particular the bound of the continuity constant for the Bogovskii operator, have several applications also in different areas of mathematical physics. A whole bunch of inequalities arises both in fluid mechanics and elasticity [14, 66, 104, 151, 160], and they are all linked to each other. This is why Section 4.3 is devoted to some physical applications of our results. In Section 4.3.1 we show that the bifurcation phenomenon for the Navier-Stokes equations, related to the loss of symmetry, has a counterpart in a model of a buckled elastic plate. In Section 4.3.2 we embed our 2D results in a 3D framework where, in fact, the Navier-Stokes equations admit solutions depending only on two variables. This enables us to apply our results to the stability of suspension bridges [121]: in Corollary 4.6 we obtain an upper bound for the wind velocity ensuring that a bridge will not oscillate.

This chapter is organized as follows. In Section 4.1 we state and prove some functional inequalities with explicit constants, in particular: inequalities for the relative capacity, for the embedding $H^1(\Omega) \subset L^4(\Omega)$, and a priori bounds for (4.5). In Section 4.2 we set up the main tools for the study of (4.2)-(4.3), we analyze in detail symmetric and almost symmetric situations, we relate the appearance of lift with multiplicity of solutions; we provide numerical results giving some hints on which could be the most stable obstacle shape. Finally, Section 4.3 is devoted to some physical applications and interpretations of our results.

4.1 Functional inequalities

Although we shall deal both with scalar and vector fields (or matrices), all the functional spaces will be denoted in the same way (except for Section 4.3.2).

4.1.1 Relative capacity and pyramidal functions

Let Ω be as in (4.1). The relative capacity of K with respect to Q is defined by

$$\mathrm{Cap}_Q(K) = \min_{\substack{v \in H_0^1(Q) \\ v=1 \text{ in } K}} \int_Q |\nabla v|^2 \tag{4.6}$$

and the relative capacity potential ψ, which achieves the minimum in (4.6), satisfies

$$\Delta \psi = 0 \ \text{ in } \ \Omega = Q \setminus K, \qquad \psi = 0 \ \text{ on } \ \partial Q, \qquad \psi = 1 \ \text{ in } \ K, \qquad \mathrm{Cap}_Q(K) = \|\nabla \psi\|_{L^2(\Omega)}^2. \tag{4.7}$$

The exact value of the relative capacity is in general not known. In the next result, which has its own interest regardless of the applications considered in the present work, we give lower and upper bounds of it in a particular situation. The same idea will also be used to bound the gradients of some solenoidal extensions, see Theorem 4.5 in Section 4.1.5.

Theorem 4.1. *Consider the square $Q = (-L, L)^2$ and the rectangle $\mathcal{R} = (-a, a) \times (-d, d)$, where $a, d \in (0, L)$. Then*

$$\frac{2\pi}{\log(L) - \log\left(\sqrt{ad}\right)} \leq \mathrm{Cap}_Q(\mathcal{R}) \leq 4 \frac{(L-a)^2 + (L-d)^2}{(L-a)(L-d)} \left[\log\left(\frac{L(L-a) + L(L-d)}{a(L-a) + d(L-d)}\right)\right]^{-1}. \tag{4.8}$$

Proof. Divide the domain $Q \setminus \mathcal{R}$ into four trapezia T_1, T_2, T_3, T_4 as in the left picture in Figure 4.2.
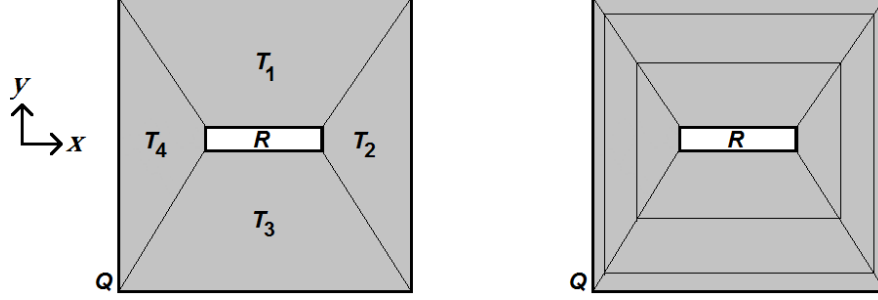

Figure 4.2: The domain $Q \setminus \mathcal{R}$ (left) and the level lines of pyramidal functions (right).

By *pyramidal function* we mean any function having the level lines as in the right picture of Figure 4.2, namely level lines parallel to ∂Q (and $\partial \mathcal{R}$) in each of the trapezia. In particular, pyramidal functions are constant on $\partial \mathcal{R}$ and constitute the following convex subset of $H_0^1(Q)$:

$$\mathcal{P}(Q) = \{u \in H_0^1(Q) \mid u = 1 \text{ in } \mathcal{R}, \ u = u(y) \text{ in } T_1 \cup T_3, \ u = u(x) \text{ in } T_2 \cup T_4\}. \tag{4.9}$$

Since $\mathcal{P}(Q) \subset H_0^1(Q)$, the relative capacity (4.6) may be upper bounded through the inequality

$$\mathrm{Cap}_Q(\mathcal{R}) \leq \min_{v \in \mathcal{P}(Q)} \int_Q |\nabla v|^2. \tag{4.10}$$

We are so led to find the minimum in (4.10) and this is equivalent to solve a classical problem in calculus of variations. Precisely, any $V^\phi \in \mathcal{P}(Q)$ is fully characterized by a (continuous) function

$$\phi \in H^1([0,1]; \mathbb{R}) \quad \text{such that} \quad \phi(0) = 1, \quad \phi(1) = 0, \tag{4.11}$$

giving the values of V^ϕ on the oblique edges of the trapezia. For instance, consider the right trapezia $T_5, T_6 \subset Q$ being, respectively, half of the trapezia T_1 and T_2, defined by

$$T_5 = \left\{(x,y) \in Q \ \middle| \ d < y < L, \ 0 < x < a + \frac{L-a}{L-d}(y-d)\right\}, \tag{4.12}$$

$$T_6 = \left\{(x,y) \in Q \ \middle| \ a < x < L, \ 0 < y < d + \frac{L-d}{L-a}(x-a)\right\}. \tag{4.13}$$

Since V^ϕ is a function of y in T_1 and a function of x in T_2, ϕ and V^ϕ are linked through the formulas

$$V^\phi(x,y) = \phi\left(\frac{y-d}{L-d}\right) \qquad \forall (x,y) \in T_5, \qquad V^\phi(x,y) = \phi\left(\frac{x-a}{L-a}\right) \qquad \forall (x,y) \in T_6. \tag{4.14}$$

Whence,

$$\frac{\partial V^\phi}{\partial y}(x,y) = \frac{1}{L-d}\phi'\left(\frac{y-d}{L-d}\right) \quad \forall (x,y) \in T_5, \qquad \frac{\partial V^\phi}{\partial x}(x,y) = \frac{1}{L-a}\phi'\left(\frac{x-a}{L-a}\right) \quad \forall (x,y) \in T_6. \tag{4.15}$$

We then seek the optimal ϕ minimizing the Dirichlet integral over Q of the pyramidal function V^ϕ.

For symmetry reasons, the contribution of $|\nabla V^\phi|$ over $T_1 \cup T_3$ is four times the contribution over T_5, whereas the contribution of $|\nabla V^\phi|$ over $T_2 \cup T_4$ is four times the contribution over T_6. By taking into

account all these facts, in particular (4.15), we infer that

$$\int_{Q\backslash\mathcal{R}} |\nabla V^\phi|^2 = 4 \int_d^L \int_0^{a+\frac{L-a}{L-d}(y-d)} \left|\frac{\partial V^\phi}{\partial y}\right|^2 dx\, dy + 4 \int_a^L \int_0^{d+\frac{L-d}{L-a}(x-a)} \left|\frac{\partial V^\phi}{\partial x}\right|^2 dy\, dx$$

$$= 4 \int_d^L \left[a + \frac{L-a}{L-d}(y-d)\right] \left|\frac{\partial V^\phi}{\partial y}\right|^2 dy + 4 \int_a^L \left[d + \frac{L-d}{L-a}(x-a)\right] \left|\frac{\partial V^\phi}{\partial x}\right|^2 dx$$

$$= 4 \int_0^1 \left(\frac{a + (L-a)s}{L-d} + \frac{d + (L-d)s}{L-a}\right) \phi'(s)^2 ds$$

$$= 4 \frac{(L-a)^2 + (L-d)^2}{(L-a)(L-d)} \int_0^1 \left[\frac{a(L-a) + d(L-d)}{(L-a)^2 + (L-d)^2} + s\right] \phi'(s)^2 ds. \tag{4.16}$$

Minimizing (4.16) among functions ϕ satisfying (4.11) yields the Euler-Lagrange equation

$$\frac{d}{ds}\left[\left(\frac{a(L-a) + d(L-d)}{(L-a)^2 + (L-d)^2} + s\right)\phi'(s)\right] = 0 \quad \Longrightarrow \quad \phi'(s) = \frac{C}{\frac{a(L-a)+d(L-d)}{(L-a)^2+(L-d)^2} + s} \qquad \forall s \in [0,1]$$

so that

$$\phi(s) = C \log\left(s + \frac{a(L-a) + d(L-d)}{(L-a)^2 + (L-d)^2}\right) + D \qquad \forall s \in [0,1],$$

for some constants C, D to be determined by imposing the conditions $\phi(0) = 1$ and $\phi(1) = 0$. We find

$$C = \left[\log\left(\frac{a(L-a) + d(L-d)}{L(L-a) + L(L-d)}\right)\right]^{-1} < 0$$

and, by inserting this into (4.16), we obtain

$$\min_{v\in\mathcal{P}(Q)} \int_Q |\nabla v|^2 = 4 \frac{(L-a)^2 + (L-d)^2}{(L-a)(L-d)} \left[\log\left(\frac{L(L-a) + L(L-d)}{a(L-a) + d(L-d)}\right)\right]^{-1}. \tag{4.17}$$

The upper bound in (4.8) follows from (4.10) and (4.17).

The lower bound in (4.8) is obtained through symmetrization. Let $\psi \in H_0^1(Q)$ be the relative capacity potential of $\mathcal{R}$ with respect to Q (see (4.7)), that is:

$$\Delta\psi = 0 \text{ in } Q \setminus \mathcal{R}, \qquad \psi = 0 \text{ on } \partial Q, \qquad \psi = 1 \text{ in } \mathcal{R}, \qquad \text{Cap}_Q(\mathcal{R}) = \|\nabla\psi\|_{L^2(Q)}^2. \tag{4.18}$$

From the maximum principle we know that $0 \leq \psi \leq 1$ in $Q \setminus \mathcal{R}$, and hence in Q. Let $Q^* \subset \mathbb{R}^2$ be the disk centered at the origin of radius $r_2 = 2L/\sqrt{\pi}$, and $\mathcal{R}^* \subset \mathbb{R}^2$ be the disk centered at the origin of radius $r_1 = 2\sqrt{ad/\pi}$ (so that $|Q^*| = |Q|$ and $|\mathcal{R}^*| = |\mathcal{R}|$). The *symmetric decreasing rearrangement* $\psi^* \in H_0^1(Q^*)$ of ψ satisfies $\psi^* = 0$ on ∂Q^*, $\psi^* = 1$ in $\mathcal{R}^*$, $\|\nabla\psi^*\|_{L^2(Q^*)} \leq \|\nabla\psi\|_{L^2(Q)}$, so that, by (4.18),

$$\text{Cap}_{Q^*}(\mathcal{R}^*) \leq \|\nabla\psi^*\|_{L^2(Q^*)}^2 \leq \text{Cap}_Q(\mathcal{R}). \tag{4.19}$$

The relative capacity potential of $\mathcal{R}^*$ with respect to Q^*, denoted by $\varphi \in H_0^1(Q^*)$, is the radial function given by

$$\varphi(\rho) = \frac{\log(\rho) - \log(r_2)}{\log(r_1) - \log(r_2)} \qquad \forall \rho \in [r_1, r_2],$$

so that

$$\text{Cap}_{Q^*}(\mathcal{R}^*) = \|\nabla\varphi\|_{L^2(\Omega^*)}^2 = \frac{2\pi}{\log(L) - \log\left(\sqrt{ad}\right)}.$$

Combined with (4.19), this concludes the proof of the lower bound. $\qquad\square$

Remark 4.1. *When $d = a$, the inequalities in (4.8) become*

$$\frac{2\pi}{\log(L) - \log(a)} \leq \mathrm{Cap}_Q(\mathcal{R}) \leq \frac{8}{\log(L) - \log(a)},$$

so that $\mathrm{Cap}_Q(\mathcal{R})$ is estimated with a fairly small error, since the ratio between the bounds is $\pi/4 \approx 0.79$.

Moreover, by using the same symmetrization method as in the proof of Theorem 4.1 we see that, for a general obstacle $K \subset Q$, one obtains the following lower bound for the relative capacity:

$$\mathrm{Cap}_Q(K) \geq \frac{4\pi}{\log(|Q|) - \log(|K|)}. \tag{4.20}$$

4.1.2 Bounds for some Sobolev constants

Let Ω be as in (4.1). We consider both the Sobolev space $H_0^1(\Omega)$ and the space of functions vanishing only on ∂K, which is a proper connected part of $\partial \Omega$ having positive 1D-measure:

$$H_*^1(\Omega) = \{v \in H^1(\Omega) \mid v = 0 \ \text{ on } \ \partial K\}.$$

This space should be seen as the closure of the space $C_c^\infty(\overline{Q} \setminus \overline{K})$ with respect to the norm $v \mapsto \|\nabla v\|_{L^2(\Omega)}$: since $|\partial K| > 0$, the Poincaré inequality holds in $H_*^1(\Omega)$, which means that $v \mapsto \|\nabla v\|_{L^2(\Omega)}$ is indeed a norm on the space $H_*^1(\Omega)$. Then we introduce the following proper subspace of $H_*^1(\Omega)$:

$$H_c^1(\Omega) = \{v \in H_*^1(\Omega) \mid v \text{ is constant on } \partial Q\}.$$

This space may be rigorously characterized by using the relative capacity potential ψ of K with respect to Q, see (4.7); it has the geometric characterization

$$H_c^1(\Omega) = H_0^1(\Omega) \oplus \mathbb{R}(\psi - 1), \quad H_0^1(\Omega) \perp \mathbb{R}(\psi - 1), \tag{4.21}$$

so that $H_0^1(\Omega)$ has codimension 1 within $H_c^1(\Omega)$ and the "missing dimension" is spanned by the function $\psi - 1$. To see this, determine the orthogonal complement of $H_0^1(\Omega)$ within $H_c^1(\Omega)$ as follows:

$$v \in H_0^1(\Omega)^\perp \iff v \in H_c^1(\Omega), \ \int_\Omega \nabla v \cdot \nabla w = 0 \ \forall w \in H_0^1(\Omega) \iff v \in H_c^1(\Omega), \ \langle \Delta v, w \rangle_\Omega = 0 \ \forall w \in H_0^1(\Omega)$$

so that v is weakly harmonic and, since $v \in H_c^1(\Omega)$, it is necessarily a real multiple of $\psi - 1$.

For later use, let us introduce

$$\mu_0 = \text{the first zero of the Bessel function of first kind of order zero} \approx 2.40483. \tag{4.22}$$

Then we define the three Sobolev constants

$$\mathcal{S} = \min_{v \in H_*^1(\Omega) \setminus \{0\}} \frac{\|\nabla v\|_{L^2(\Omega)}^2}{\|v\|_{L^4(\Omega)}^2}, \quad \mathcal{S}_0 = \min_{v \in H_0^1(\Omega) \setminus \{0\}} \frac{\|\nabla v\|_{L^2(\Omega)}^2}{\|v\|_{L^4(\Omega)}^2}, \quad \mathcal{S}_1 = \min_{v \in H_c^1(\Omega) \setminus \{0\}} \frac{\|\nabla v\|_{L^2(\Omega)}^2}{\|v\|_{L^4(\Omega)}^2}. \tag{4.23}$$

Since $H_0^1(\Omega) \subset H_c^1(\Omega) \subset H_*^1(\Omega)$, we have $\mathcal{S} \leq \mathcal{S}_1 \leq \mathcal{S}_0$. Our first result in this section provides explicit lower bounds for these embedding constants.

Theorem 4.2. *Let Ω be as in (4.1). For any $u \in H_0^1(\Omega)$ one has*

$$\|u\|_{L^4(\Omega)}^2 \leq \frac{2L}{\sqrt{3}\pi^{3/2}} \min\left\{1, \frac{\sqrt{2\pi}}{\mu_0} \sqrt{1 - \frac{|K|}{|Q|}}\right\} \|\nabla u\|_{L^2(\Omega)}^2. \tag{4.24}$$

For any $u \in H_c^1(\Omega)$ one has

$$\|u\|_{L^4(\Omega)}^2 \leq \frac{4L}{3\pi} \sqrt{1 - \frac{|K|}{|Q|} \left(1 + \sqrt{\frac{3}{8} \log\left(\frac{|Q|}{|K|}\right)}\right)^{3/2}}$$

$$\times \left[1 + \sqrt{\frac{3}{8} \log\left(\frac{|Q|}{|K|}\right)} + \frac{3\sqrt{3}}{4\sqrt{2}} \frac{|K|}{|Q| - |K|} \log^{3/2}\left(\frac{|Q|}{|K|}\right)\right]^{1/2} \|\nabla u\|_{L^2(\Omega)}^2. \tag{4.25}$$

The inequalities (4.24) and (4.25) hold both for scalar functions and for vector fields.

Proof. We first show that it suffices to prove the inequalities for scalar functions. Indeed, assume that (4.24) has been proved for scalar functions and let $u = (u_1, u_2) \in H_0^1(\Omega)$ be a vector filed. Then, by the Hölder inequality and the scalar version of (4.24), we obtain

$$\|u\|_{L^4(\Omega)}^4 \leq \left(\|u_1\|_{L^4(\Omega)}^2 + \|u_2\|_{L^4(\Omega)}^2\right)^2 \leq \frac{4L^2}{3\pi^3}\left(\|\nabla u_1\|_{L^2(\Omega)}^2 + \|\nabla u_2\|_{L^2(\Omega)}^2\right)^2 = \frac{4L^2}{3\pi^3}\|\nabla u\|_{L^2(\Omega)}^4,$$

which proves the first inequality (4.24) also for vector fields. One proceeds similarly for the second inequality in (4.24) and for (4.25). Therefore, from now on, we assume that u is a scalar function.

For scalar functions $w \in H_0^1(Q)$, we start by recalling that del Pino-Dolbeault [83, Theorem 1] obtained the optimal constant for the following Gagliardo-Nirenberg inequality in $\mathbb{R}^2$:

$$\|w\|_{L^4(Q)}^2 \leq \left(\frac{2}{3\pi}\right)^{1/4} \|\nabla w\|_{L^2(Q)}^{1/2} \|w\|_{L^3(Q)}^{3/2} \qquad \forall w \in H_0^1(Q). \tag{4.26}$$

Since functions in $H_0^1(Q)$ may be extended by zero outside Q, they can be seen as functions defined over the whole plane. We point out that (4.26) follows from a somehow "magic combination" of exponents: for general exponents, the optimal constant in the Gagliardo-Nirenberg inequality is not known, this is why the L^3-norm appears. By combining (4.26) with the following form of the Hölder inequality

$$\|w\|_{L^3(Q)}^3 \leq \|w\|_{L^2(Q)} \|w\|_{L^4(Q)}^2 \qquad \forall w \in L^4(Q),$$

we obtain

$$\|w\|_{L^4(Q)}^2 \leq \left(\frac{2}{3\pi}\right)^{1/2} \|\nabla w\|_{L^2(Q)} \|w\|_{L^2(Q)} \qquad \forall w \in H_0^1(Q). \tag{4.27}$$

Then we observe that $\cos(\frac{\pi x}{2L}) \cos(\frac{\pi y}{2L})$ is an eigenfunction of the eigenvalue problem $-\Delta v = \lambda v$ in Q under Dirichlet boundary conditions. Since it is positive, it is associated to the least eigenvalue which is then given by $\lambda = \pi^2/2L^2$. Therefore, the Poincaré inequality reads

$$\|w\|_{L^2(Q)}^2 \leq \frac{2L^2}{\pi^2} \|\nabla w\|_{L^2(Q)}^2 \qquad \forall w \in H_0^1(Q)$$

which, combined with (4.27), yields the first bound in (4.24) since any function $u \in H_0^1(\Omega)$ can be extended by 0 in K, thereby becoming a function in $H_0^1(Q)$.

In order to obtain the second bound in (4.24), we go back to (4.27) and we use the Faber-Krahn inequality, see [93, 162]. We point out that the same extension argument as above enables us to compute all the norms in (4.27) in Ω instead of Q. Therefore, we may bound the $L^2(\Omega)$-norm in terms of the gradient by using the Poincaré inequality in Ω^*, namely a disk having the same measure as Ω. Since $|\Omega| = |Q| - |K|$, the radius of Ω^* is given by

$$R = \frac{2L}{\sqrt{\pi}} \sqrt{1 - \frac{|K|}{|Q|}}$$

that we write in this "strange form" for later use. Since the Poincaré constant (least eigenvalue) in the unit disk is given by μ_0^2, see (4.22), the Poincaré constant in Ω^* is given by μ_0^2/R^2, which means that

$$\min_{w \in H_0^1(\Omega)} \frac{\|\nabla w\|_{L^2(\Omega)}}{\|w\|_{L^2(\Omega)}} \geq \min_{w \in H_0^1(\Omega^*)} \frac{\|\nabla w\|_{L^2(\Omega^*)}}{\|w\|_{L^2(\Omega^*)}} = \frac{\mu_0}{R}.$$

Therefore,

$$\|w\|_{L^2(\Omega)} \leq \frac{R}{\mu_0} \|\nabla w\|_{L^2(\Omega)} = \frac{2L}{\mu_0 \sqrt{\pi}} \sqrt{1 - \frac{|K|}{|Q|}} \|\nabla w\|_{L^2(\Omega)} \qquad \forall w \in H_0^1(\Omega)$$

which, inserted into (4.27) (with Q replaced by Ω), gives the second bound in (4.24).

Let us now prove (4.25) and we restrict our attention to functions $u \in H_c^1(\Omega) \setminus H_0^1(\Omega)$: this restriction will be justified *a posteriori* because, if we manage proving (4.25) for these functions, then it will also hold for functions in $H_0^1(\Omega)$ since the constant in (4.24) is smaller, see also Figure 4.3 below. For functions $u \in H_c^1(\Omega) \setminus H_0^1(\Omega)$, it suffices to analyze the case where $u \geq 0$ in Ω (by replacing u with $|u|$), $u = 1$ on ∂Q (by homogeneity), and we define a.e. in Q the function

$$v(x,y) = \begin{cases} 1 - u(x,y) & \text{if } (x,y) \in \Omega \\ 1 & \text{if } (x,y) \in K, \end{cases}$$

so that $v \in H_0^1(Q)$ and v satisfies (4.26). Let us put

$$A = A(u) \doteq \left(\frac{2}{3\pi}\right)^{1/2} \|\nabla v\|_{L^2(Q)} = \left(\frac{2}{3\pi}\right)^{1/2} \|\nabla u\|_{L^2(\Omega)},$$

so that (4.26) reads

$$\int_Q |v|^4 \leq A \int_Q |v|^3 \implies \int_\Omega \left[|1 - u|^4 + \frac{|K|}{|\Omega|} - A\left(|1 - u|^3 + \frac{|K|}{|\Omega|}\right) \right] \leq 0. \tag{4.28}$$

The next step consists in finding $\alpha \in (0,1)$ and $\beta > 0$ (having ratio independent of u) for which

$$(1-s)^4 - A|1-s|^3 + (1-A)\frac{|K|}{|\Omega|} \geq \alpha s^4 - \beta A^4 \qquad \forall s \geq 0. \tag{4.29}$$

Since the function $s \mapsto (1-s)^4 - A|1-s|^3 + \gamma$ is symmetric with respect to $s = 1$, for any $\gamma \in \mathbb{R}$, it suffices to find $\alpha \in (0,1)$ and $\beta > 0$ ensuring (4.29) for every $s \geq 1$. Thus, for all such α and β we define the function

$$\varphi(s) = (s-1)^4 - A(s-1)^3 - \alpha s^4 + (1-A)\frac{|K|}{|\Omega|} + \beta A^4 \qquad \forall s \geq 1,$$

and we seek $\alpha \in (0,1)$ and $\beta > 0$ in such a way that φ has a non-negative minimum value at some $s > 1$. Equivalently, we seek $\gamma > 3/4$ such that $\varphi(s)$ attains its minimum at $s_0 = 1 + \gamma A$, that is,

$$\varphi'(s_0) = A^3 \gamma^2 (4\gamma - 3) - 4\alpha(1 + \gamma A)^3 = 0 \qquad \Longleftrightarrow \qquad \alpha = \frac{A^3}{4} \frac{\gamma^2(4\gamma - 3)}{(1 + \gamma A)^3} \in (0,1),$$

which fixes α in dependence of u. By imposing $\varphi(s_0) \geq 0$, we obtain the following lower bound for β:

$$\beta \geq \frac{\gamma^3}{4} + \frac{\gamma^2(4\gamma - 3)}{4A} + \frac{A-1}{A^4} \frac{|K|}{|\Omega|}.$$

This condition is certainly satisfied if we choose

$$\beta = \frac{\gamma^3}{4} + \frac{\gamma^2(4\gamma - 3)}{4A} + \frac{1}{A^3} \frac{|K|}{|\Omega|}. \tag{4.30}$$

57

With the above choices of α and β we obtain the ratio

$$\frac{\beta}{\alpha} = \frac{4}{A^3} \frac{(1+\gamma A)^3}{\gamma^2(4\gamma - 3)} \left[\frac{\gamma^3}{4} + \frac{\gamma^2(4\gamma - 3)}{4A} + \frac{1}{A^3} \frac{|K|}{|\Omega|} \right], \tag{4.31}$$

which depends on u and on $\gamma > 3/4$; hence, we still have the freedom of choosing γ. By taking $\gamma = 1$ (which, numerically, appears to be close to the global minimum of the right-hand side of (4.31)), we obtain

$$\frac{\beta}{\alpha} = \left(1 + \frac{1}{A(u)} + \frac{4}{A(u)^3} \frac{|K|}{|\Omega|} \right) \left(1 + \frac{1}{A(u)} \right)^3, \tag{4.32}$$

where we emphasized the dependence of A on u. In order to obtain an upper bound for the ratio β/α independent of u, we use (4.20) which states that

$$A(u) \geq \sqrt{\frac{2}{3\pi} \mathrm{Cap}_Q(K)} \geq \sqrt{\frac{8}{3}} \frac{1}{\sqrt{\log\left(\frac{|Q|}{|K|}\right)}} \qquad \forall u \in H_c^1(\Omega) \text{ s.t. } u = 1 \text{ on } \partial Q, \ u \geq 0 \text{ in } \Omega.$$

Hence, from (4.32) we obtain the following uniform bound (independent of u)

$$\frac{\beta}{\alpha} \leq \left(1 + \sqrt{\frac{3}{8} \log\left(\frac{|Q|}{|K|}\right)} \right)^3 \left[1 + \sqrt{\frac{3}{8} \log\left(\frac{|Q|}{|K|}\right)} + \frac{3\sqrt{3}}{4\sqrt{2}} \frac{|K|}{|\Omega|} \log^{3/2}\left(\frac{|Q|}{|K|}\right) \right].$$

In turn, from (4.28), by replacing s with u in (4.29) and integrating, we obtain

$$\|u\|_{L^4(\Omega)}^4 \leq \frac{\beta}{\alpha} A(u)^4 |\Omega|$$

$$\leq \frac{4|\Omega|}{9\pi^2} \left(1 + \sqrt{\frac{3}{8} \log\left(\frac{|Q|}{|K|}\right)} \right)^3 \left[1 + \sqrt{\frac{3}{8} \log\left(\frac{|Q|}{|K|}\right)} + \frac{3\sqrt{3}}{4\sqrt{2}} \frac{|K|}{|\Omega|} \log^{3/2}\left(\frac{|Q|}{|K|}\right) \right] \|\nabla u\|_{L^2(\Omega)}^4,$$

for every $u \in H_c^1(\Omega)$ such that $u = 1$ on ∂Q and $u \geq 0$ in Ω. The bound (4.25) follows by taking the squared roots in the last inequality. $\square$

Several remarks about Theorem 4.2 are in order.

Remark 4.2. *The interpolation inequality by Ladyzhenskaya [168] (or [169, Lemma 1, p.8]) states that*

$$\|w\|_{L^4(\Omega)}^2 \leq \sqrt{2} \|\nabla w\|_{L^2(\Omega)} \|w\|_{L^2(\Omega)} \qquad \forall w \in H_0^1(\Omega).$$

Subsequently, Galdi [115, (II.3.9)] improved this Gagliardo-Nirenberg-type inequality by showing that

$$\|w\|_{L^4(\Omega)}^2 \leq \frac{1}{\sqrt{2}} \|\nabla w\|_{L^2(\Omega)} \|w\|_{L^2(\Omega)} \qquad \forall w \in H_0^1(\Omega).$$

Thanks to the result by del Pino-Dolbeault [83], with (4.27) we improved further the constant of this inequality by around 35%: indeed, $\sqrt{2/3\pi} \approx 0.65/\sqrt{2}$. Finally, consider the entire function $w(x, y) = (1 + x^2 + y^2)^{-1}$; by computing its norms, we see that the optimal constant in this inequality is larger than $(2\pi)^{-1/2}$, showing that (4.27) cannot be improved by more than 15%.

Remark 4.3. *The "break even" in the bound (4.24) occurs when $|K|/|Q| = 1 - \mu_0^2/2\pi \approx 0.08$: for smaller $|K|$ the first bound is better, for larger $|K|$ the second bound is better. Note that the constant in (4.24) tends to 0 whenever $|K| \to |Q|$ (the obstacle tends to fill the box) and remains uniformly bounded when $|K| \to 0$. On the contrary, the constant in (4.25) blows up when $|K| \to 0$: this is not just a consequence of our proof, also the optimal constant blows up, see Theorem 4.3 below.*

Remark 4.4. *The constant in* (4.24) *depends on the size of the surrounding box Q but it is mostly independent of the obstacle K (of its shape and of its position inside the box), it only weakly depends on its measure (in fact, its relative measure within Q); for this reason, we conjecture that it can be improved. The constant in* (4.25) *does not depend on the shape of K, nor on its position inside Q but it strongly depends on its measure; we believe that if K is close to ∂Q,* (4.25) *can be significantly improved. However, for our fluid-obstacle model to be reliable, we need to avoid "boundary effects" and maintain the obstacle K far away from ∂Q (the boundary of the photo, see the Introduction).*

Remark 4.5. *Some steps in the proof of* (4.25) *may be performed differently. For instance, one could have noticed that $\max_{A>0}(A-1)/A^4 = 27/256$, yielding a different bound for β in* (4.30). *Also the choice of $\gamma = 1$ could be slightly modified. Nevertheless, the overall (small) improvements would not justify the great effort required and the final form of* (4.25) *would have a more unpleasant form. Moreover, these variants would not improve the bounds in Section 4.2.4, see Theorem 4.14 below.*

Theorem 4.2 yields the following lower bounds for the Sobolev constants:

Corollary 4.1. *Let Ω be as in* (4.1). *Let $\mathcal{S}_0$ and $\mathcal{S}_1$ be as in* (4.23). *Then:*

$$
\mathcal{S}_0 \geq \frac{\sqrt{3}\pi^{3/2}}{2L} \max\left\{1, \frac{\mu_0}{\sqrt{2\pi}} \sqrt{\frac{\frac{|Q|}{|K|}}{\frac{|Q|}{|K|}-1}}\right\},
$$

$$
\mathcal{S}_1 \geq \frac{3\pi}{4L} \sqrt{\frac{\frac{|Q|}{|K|}}{\frac{|Q|}{|K|}-1}} \left(1 + \sqrt{\frac{3}{8}\log\left(\frac{|Q|}{|K|}\right)}\right)^{-3/2} \left[1 + \sqrt{\frac{3}{8}\log\left(\frac{|Q|}{|K|}\right)} + \frac{3\sqrt{3}}{4\sqrt{2}}\frac{1}{\frac{|Q|}{|K|}-1}\log^{3/2}\left(\frac{|Q|}{|K|}\right)\right]^{-1/2}.
$$

By dropping the multiplicative term $1/L$, the remainder of the lower bound for $\mathcal{S}_1$ in Corollary 4.1 can be treated as a function of $|Q|/|K| \in [1,\infty)$. This function vanishes like $[\log(|Q|/|K|)]^{-1}$ as $|Q|/|K| \to \infty$, see its plot in Figure 4.3 where we also compare it with the (larger) lower bound for $\mathcal{S}_0$, that becomes constant when $|Q|/|K| \approx 12.5$, see Remark 4.3.
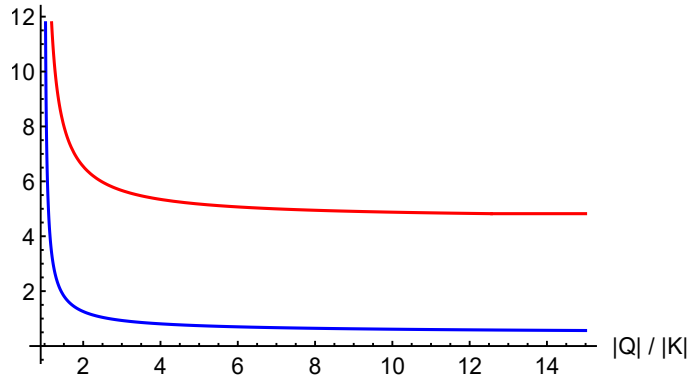
Figure 4.3: Behavior of the lower bounds for $\mathcal{S}_0$ (red) and $\mathcal{S}_1$ (blue) as functions of $|Q|/|K|$.

It is then natural to wonder whether the lower bounds obtained in Corollary 4.1 are meaningful. This can be verified through suitable upper bounds. For $\mathcal{S}_0$ we take the function $w(x,y) = \cos(\frac{\pi x}{2L})\cos(\frac{\pi y}{2L})$, defined for $(x,y) \in \overline{Q}$, so that $w \in H_0^1(Q)$ and

$$
\|w\|_{L^4(Q)}^2 = \frac{3L}{4}, \quad \|\nabla w\|_{L^2(Q)}^2 = \frac{\pi^2}{2} \quad \Longrightarrow \quad \mathcal{S}_0 \leq \frac{2\pi^2}{3L},
$$

showing that the first lower bound for $\mathcal{S}_0$ is quite accurate. An upper bound for $\mathcal{S}_1$ is given in the next statement.

Theorem 4.3. *Let Ω be as in* (4.1) *and assume that*

$$\exists\, 0 < d \le a < L \text{ such that } \mathcal{R} = (-a,a) \times (-d,d) \supset K. \tag{4.33}$$

Then

$$\mathcal{S}_1 \le \frac{2\sqrt{2}\left[(L-a)^2 + (L-d)^2\right]^2}{(L-a)(L-d)\sqrt{a(L-a)+d(L-d)}} \frac{\theta}{\sqrt{2L(2L-a-d)(d-a)^2\theta_1 + (L-a)(L-d)\left[a(L-a)+d(L-d)\right]\theta_2}},$$

where

$$\theta = \left[\log\left(\frac{L(L-a)+L(L-d)}{a(L-a)+d(L-d)}\right)\right]^{-1}, \qquad \theta_1 = (1 - 4\theta + 12\theta^2 - 24\theta^3 + 24\theta^4)\left[\frac{L(L-a)+L(L-d)}{a(L-a)+d(L-d)}\right] - 24\theta^4,$$

$$\theta_2 = (2 - 4\theta + 6\theta^2 - 6\theta^3 + 3\theta^4)\left[\frac{L(L-a)+L(L-d)}{a(L-a)+d(L-d)}\right]^2 - 3\theta^4.$$

Proof. Let $\mathcal{P}(Q)$ be as in (4.9), let $V^\phi \in \mathcal{P}(Q)$ be defined by (4.14) with

$$\phi(s) = \log\left(\frac{(L-a)^2 + (L-d)^2}{L(L-a)+L(L-d)}s + \frac{a(L-a)+d(L-d)}{L(L-a)+L(L-d)}\right) \Big/ \log\left(\frac{a(L-a)+d(L-d)}{L(L-a)+L(L-d)}\right) \qquad \forall s \in [0,1],$$

with V^ϕ extended by 1 in $\mathcal{R} \setminus K$. From (4.16) and (4.17) we know that:

$$\|\nabla V^\phi\|^2_{L^2(\Omega)} = 4\frac{(L-a)^2 + (L-d)^2}{(L-a)(L-d)}\left[\log\left(\frac{L(L-a)+L(L-d)}{a(L-a)+d(L-d)}\right)\right]^{-1}.$$

For symmetry reasons, the contribution of $|1 - V^\phi|^4$ over $T_1 \cup T_3$ is four times the contribution over the trapezium T_5 defined in (4.12), whereas the contribution of $|1 - V^\phi|^4$ over $T_2 \cup T_4$ is four times the contribution over the trapezium T_6 defined in (4.13). Then

$$
\begin{aligned}
\int_{Q\backslash\mathcal{R}} |1 - V^\phi|^4 &= 4\int_d^L \int_0^{a+\frac{L-a}{L-d}(y-d)} |1 - V^\phi(y)|^4 dx\, dy + 4\int_a^L \int_0^{d+\frac{L-d}{L-a}(x-a)} |1 - V^\phi(x)|^4 dy\, dx \\
&= 4\int_d^L \left[a + \tfrac{L-a}{L-d}(y-d)\right] |1 - V^\phi(y)|^4\, dy + 4\int_a^L \left[d + \tfrac{L-d}{L-a}(x-a)\right] |1 - V^\phi(x)|^4\, dx \\
&= 4\int_0^1 \left[a(L-d) + d(L-a) + 2(L-a)(L-d)s\right] |1 - \phi(s)|^4\, ds.
\end{aligned}
$$

Using that $V^\phi \equiv 1$ in $\mathcal{R} \setminus K$ and the change of variable $t = 1 - \phi(s)$, for $s \in [0,1]$, we then obtain

$$\|1 - V^\phi\|^4_{L^4(\Omega)} = 2\frac{a(L-a)+d(L-d)}{[(L-a)^2 + (L-d)^2]^2}\left\{2L(2L-a-d)(d-a)^2\theta_1 + (L-a)(L-d)\left[a(L-a)+d(L-d)\right]\theta_2\right\}.$$

We finally notice that if $v \in \mathcal{P}(Q)$, then $1 - v \in H^1_c(\Omega)$ with $v = 1$ on ∂Q. Therefore,

$$\mathcal{S}_1 \le \min_{v \in \mathcal{P}(Q)} \frac{\|\nabla v\|^2_{L^2(\Omega)}}{\|1 - v\|^2_{L^4(\Omega)}} \le \frac{\|\nabla V^\phi\|^2_{L^2(\Omega)}}{\|1 - V^\phi\|^2_{L^4(\Omega)}},$$

which concludes the proof. $\qquad\square$

In the case where the obstacle is a square, Theorem 4.3 enables us to evaluate the precision of the lower bound for $\mathcal{S}_1$ given in Corollary 4.1.

Corollary 4.2. *If $0 < a < L$ and $\Omega = (-L, L)^2 \setminus (-a, a)^2$, then*

$$\mathcal{S}_1 \geq \frac{1}{L} \frac{\frac{3\pi}{4} \frac{L}{a}}{\sqrt{\left(\frac{L}{a}\right)^2 - 1}} \left(1 + \frac{\sqrt{3}}{2} \log^{1/2}\left(\frac{L}{a}\right)\right)^{-3/2} \left[1 + \frac{\sqrt{3}}{2} \log^{1/2}\left(\frac{L}{a}\right)\left(1 + \frac{3}{\left(\frac{L}{a}\right)^2 - 1} \log\left(\frac{L}{a}\right)\right)\right]^{-1/2},$$

$$\mathcal{S}_1 \leq \frac{1}{L} \frac{4\sqrt{2} \frac{L}{a} \log\left(\frac{L}{a}\right)}{\sqrt{\left[2\log^4\left(\frac{L}{a}\right) - 4\log^3\left(\frac{L}{a}\right) + 6\log^2\left(\frac{L}{a}\right) - 6\log\left(\frac{L}{a}\right) + 3\right]\left(\frac{L}{a}\right)^2 - 3}}.$$

By dropping the multiplicative term $1/L$, the remainder of the lower and upper bounds for $\mathcal{S}_1$ in Corollary 4.2 can be treated as a function of $L/a \in (1, \infty)$. The ratio between the bounds tends to $4/\pi \approx 1.273$ as $L/a \to \infty$ so that, since we are interested in small obstacles compared to the size of the photo ($a \ll L$), Corollary 4.2 shows that the obtained bounds are quite precise. The plots in Figure 4.4 describe the overall behavior.
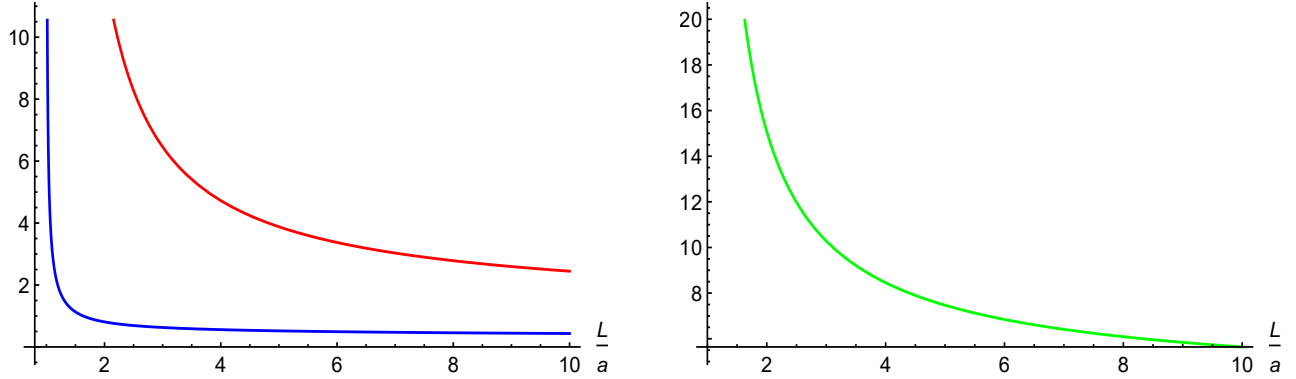
Figure 4.4: On the left: behavior of the lower and upper bounds for $\mathcal{S}_1$ from Corollary 4.2, as a function of L/a. On the right: ratio between the upper and lower bounds for $\mathcal{S}_1$ as a function of L/a.

4.1.3 Functional inequalities for the Navier-Stokes equations

In this section we quickly recall some well-known functional spaces and inequalities, by adapting them to our context. Let us introduce the two functional spaces of vector fields

$$\mathcal{V}_*(\Omega) = \{v \in H^1_*(\Omega) \mid \nabla \cdot v = 0 \text{ in } \Omega\} \quad \text{and} \quad \mathcal{V}(\Omega) = \{v \in H^1_0(\Omega) \mid \nabla \cdot v = 0 \text{ in } \Omega\},$$

which are Hilbert spaces if endowed with the scalar product $(u, v) \mapsto (\nabla u, \nabla v)_{L^2(\Omega)}$. We also introduce the trilinear form

$$\beta(u, v, w) = \int_\Omega (u \cdot \nabla)v \cdot w \qquad \forall u, v, w \in H^1(\Omega), \tag{4.34}$$

which is continuous in $H^1_*(\Omega) \times H^1_*(\Omega) \times H^1_*(\Omega)$ and satisfies (see e.g. [115, Section IX.2])

$$|\beta(u, v, w)| \leq \frac{1}{\mathcal{S}} \|\nabla u\|_{L^2(\Omega)} \|\nabla v\|_{L^2(\Omega)} \|\nabla w\|_{L^2(\Omega)} \qquad \forall u, v, w \in H^1_*(\Omega), \tag{4.35}$$

$$|\beta(u, v, w)| \leq \frac{1}{\sqrt{\mathcal{S}\mathcal{S}_0}} \|\nabla u\|_{L^2(\Omega)} \|\nabla v\|_{L^2(\Omega)} \|\nabla w\|_{L^2(\Omega)} \qquad \forall u, v \in H^1_*(\Omega), w \in H^1_0(\Omega), \tag{4.36}$$

where $\mathcal{S}$ and $\mathcal{S}_0$ are as in (4.23). Moreover,

$$\begin{aligned} \beta(u, v, w) &= -\beta(u, w, v) & \text{for any} \quad u \in \mathcal{V}_*(\Omega), \ v \in H^1(\Omega), \ w \in H^1_0(\Omega), \\ \beta(u, v, v) &= 0 & \text{for any} \quad u \in \mathcal{V}_*(\Omega), \ v \in H^1_0(\Omega). \end{aligned} \tag{4.37}$$

Since integration by parts will be performed repeatedly in the course, we recall a generalized Gauss identity from [115, Theorem III.2.2]. Since Ω in (4.1) is a bounded Lipschitz domain, its boundary $\partial\Omega$ has in a.e. point an outward unit normal $\hat{n}$. Then, for every $r, s \in (1, \infty)$ such that $\frac{1}{r} + \frac{1}{s} = 1$ one has

$$\int_\Omega u(\nabla \cdot v)\, dx + \int_\Omega \nabla u \cdot v\, dx = \langle v \cdot \hat{n}, u \rangle_{\partial\Omega} \qquad \forall u \in W^{1,s}(\Omega)\,, \ v \in E_r(\Omega), \tag{4.38}$$

where $E_r(\Omega) \doteq \{v \in L^r(\Omega) \mid \nabla \cdot v \in L^r(\Omega)\}$ and the "boundary term" $\langle \cdot, \cdot \rangle_{\partial\Omega}$ represents the duality between $W^{-\frac{1}{r}, r}(\partial\Omega)$ and $W^{\frac{1}{r}, s}(\partial\Omega)$; it is well-defined because

$$v \cdot \hat{n}|_{\partial\Omega} \in W^{-\frac{1}{r}, r}(\partial\Omega) \quad \text{and} \quad u|_{\partial\Omega} \in W^{\frac{1}{r}, s}(\partial\Omega).$$

For later use, we remark that for constant boundary data one has

$$(U, V) \in \mathbb{R}^2 \implies \|(U, V)\|_{H^{1/2}(\partial Q)} = \|(U, V)\|_{L^2(\partial Q)} = 2\sqrt{2L}\,\sqrt{U^2 + V^2}\,. \tag{4.39}$$

We now recall a combination of results by Hopf [150] and Ladyzhenskaya-Solonnikov [170], that we also state for domains Ω that are symmetric with respect to the x-axis, namely $(x, y) \in \Omega$ if and only if $(x, -y) \in \Omega$.

Proposition 4.1. *Let Ω be as in (4.1) and let $\hat{n}$ be the a.e.-defined outward unit normal to $\partial\Omega$. Let $W \in H^{1/2}(\partial\Omega)$ be such that*

$$\int_{\partial Q} W \cdot \hat{n}\, ds = \int_{\partial K} W \cdot \hat{n}\, ds = 0. \tag{4.40}$$

Then for all $\varepsilon > 0$ there exists a solenoidal extension $A_\varepsilon \in H^1(\Omega)$ satisfying

$$\nabla \cdot A_\varepsilon = 0 \ \text{in} \ \Omega, \qquad A_\varepsilon = W \ \text{on} \ \partial\Omega, \qquad |\beta(v, A_\varepsilon, v)| \le \varepsilon \|\nabla v\|_{L^2(\Omega)}^2 \quad \forall v \in \mathcal{V}(\Omega). \tag{4.41}$$

If Ω is symmetric with respect to the x-axis and $W = (W_1, W_2)$ is such that W_1 is y-even and W_2 is y-odd, then the solenoidal extension $A_\varepsilon = (A_\varepsilon^1, A_\varepsilon^2)$ can be chosen so that A_ε^1 is y-even and A_ε^2 is y-odd, with no increment of the H^1-norm.

Proof. Given $\varepsilon > 0$ and a boundary datum $W \in H^{1/2}(\partial\Omega)$ satisfying (4.40), the existence of a vector field $A_\varepsilon \in H^1(\Omega)$ verifying (4.41) is proved (e.g.) in [115, Lemma IX.4.2]; indeed, (4.40) assumes "no separated sinks and sources of fluid inside Q", see [115, Formula (IX.4.7)].

Under the symmetry assumptions given in the statement, it can be seen that the vector field

$$B_\varepsilon(x, y) \doteq \frac{1}{2}\big(A_\varepsilon^1(x, y) + A_\varepsilon^1(x, -y), A_\varepsilon^2(x, y) - A_\varepsilon^2(x, -y)\big) \qquad \text{for a.e. } (x, y) \in \Omega,$$

is y-even in its first component, y-odd in its second component and still verifies (4.41). Indeed, the solenoidal condition is readily verified, as well as the boundary condition. The H^1-bound follows from the fact that $\|B_\varepsilon\|_{H^1(\Omega)} \le \|A_\varepsilon\|_{H^1(\Omega)}$; in turn, this follows from a direct computation (and using the Young inequality) or by observing that B_ε is the "symmetrized" of A_ε. Finally, the bound on β follows by arbitrariness of v: in particular, it holds for the symmetric and/or skew-symmetric parts of any $v \in \mathcal{V}(\Omega)$. $\qquad \square$

As usual, the pressure p in (4.2) is defined up to an additive constant; therefore, we take it to have zero mean value and we introduce the space

$$L_0^2(\Omega) = \left\{ g \in L^2(\Omega) \ \Big| \ \int_\Omega g = 0 \right\}.$$

For any $g \in L_0^2(\Omega)$ we define its gradient $\nabla g \in H^{-1}(\Omega)$ as follows:

$$\langle \nabla g, \psi \rangle_\Omega = \int_\Omega g \, (\nabla \cdot \psi) \qquad \forall \psi \in H_0^1(\Omega).$$

Bogovskii [36] showed that, given any $q \in L_0^2(\Omega)$, there exists $\psi \in H_0^1(\Omega)$ such that $\nabla \cdot \psi = q$ in Ω and

$$\|\nabla \psi\|_{L^2(\Omega)} \le C_B(\Omega) \|q\|_{L^2(\Omega)}, \tag{4.42}$$

where the constant $C_B(\Omega) > 0$ depends only on Ω. Then we obtain the bound

$$\|\nabla g\|_{H^{-1}(\Omega)} = \sup_{\substack{\psi \in H_0^1(\Omega) \\ \|\nabla \psi\|_{L^2(\Omega)} = 1}} \left| \int_\Omega g \, (\nabla \cdot \psi) \right| \ge \frac{1}{C_B(\Omega)} \sup_{\substack{q \in L_0^2(\Omega) \\ \|q\|_{L^2(\Omega)} = 1}} \left| \int_\Omega g q \right| = \frac{1}{C_B(\Omega)} \|g\|_{L^2(\Omega)},$$

that is,

$$\|g\|_{L^2(\Omega)} \le C_B(\Omega) \|\nabla g\|_{H^{-1}(\Omega)} \qquad \forall g \in L_0^2(\Omega). \tag{4.43}$$

Since the purpose of the present chapter is to obtain *explicit bounds*, in the next section we give an estimate of the Bogovskii constant C_B appearing in both (4.42) and (4.43).

4.1.4 An estimate of the continuity constant for the Bogovskii operator

In this section we face the problem of estimating (explicitly) the continuity constant $C_B(\Omega) > 0$ of the Bogovskii operator, see (4.42). We will prove bounds in the case where (4.33) holds; we then denote

$$\Omega_{\mathcal{R}} = Q \setminus \overline{\mathcal{R}} \tag{4.44}$$

and we remark that $\Omega_{\mathcal{R}} = \Omega_1 \cup \Omega_2$ for some $\Omega_1, \Omega_2 \subset \Omega_{\mathcal{R}}$ that are star-shaped with respect to some disk. Indeed, as illustrated in the left picture of Figure 4.5, Ω_1 is the white region "illuminated" by the disk in the left top corner of Q, while Ω_2 is illuminated by the disk in the opposite corner of Q. Thus, in the right picture of Figure 4.5, the white region corresponds to $\Omega_1 \cap \Omega_2$.
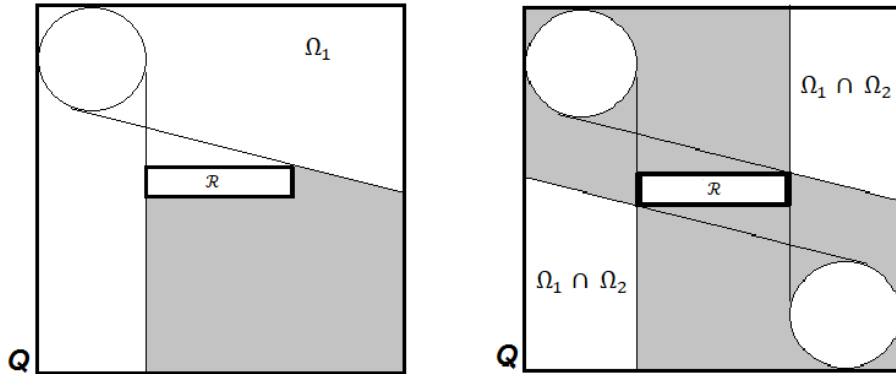
Figure 4.5: Decomposition of $\Omega_{\mathcal{R}}$ as union of two star-shaped domains.

By determining the tangent lines to the disks containing the points (a, d) and $(-a, -d)$ we find

- $\Omega_1 = [(-L, -a) \times (-L, L)] \cup [(-a, L) \times (d, L)] \cup T((a, d); (L, d); (L, d - \alpha_*))$, where, for given points $P_1, P_2, P_3 \in \mathbb{R}^2$, $T(P_1; P_2; P_3) \subset \mathbb{R}^2$ denotes the triangle with vertices in P_1, P_2 and P_3, and

$$\alpha_* \doteq \frac{L - a}{8a(L + a)} \left[(L + 3a)(L + a - 2d) - (L - a)\sqrt{(L + a - 2d)^2 + 8a(L + a)} \right] \ge 0, \tag{4.45}$$

since $a \ge d$; Ω_1 is star-shaped with respect to the disk $\left(x + \frac{L+a}{2} \right)^2 + \left(y - \frac{L+a}{2} \right)^2 < \left(\frac{L-a}{2} \right)^2$.

- $\Omega_2 = [(a, L) \times (-L, L)] \cup [(-L, a) \times (-L, -d)] \cup T((-a, -d); (-L, -d); (-L, \alpha_* - d))$. In this case, Ω_2 is star-shaped with respect to the disk $\left(x - \frac{L+a}{2}\right)^2 + \left(y + \frac{L+a}{2}\right)^2 < \left(\frac{L-a}{2}\right)^2$.

Then we put

$$\sigma \doteq |\Omega_1| = |\Omega_2| = 2L(L-a) + (L+a)(L-d) + \frac{\alpha_*}{2}(L-a), \quad |\Omega_1 \cap \Omega_2| = 2(L-a)(L-d) + \alpha_*(L-a) \quad (4.46)$$

and, for every $g \in L_0^2(\Omega_\mathcal{R})$, we define

$$\alpha_g \doteq \left\{ \|g\|_{L^2(\Omega_1)}^2 + \frac{1}{|\Omega_1 \cap \Omega_2|} \left(\int_{\Omega_1} g(z)\, dz \right) \left[\int_{\Omega_1} g(z)\, dz - 2 \int_{\Omega_1 \cap \Omega_2} g(z)\, dz \right] \right\}^{1/2},$$

$$\beta_g \doteq \left\{ \|g\|_{L^2(\Omega_2 \backslash \Omega_1)}^2 + \frac{1}{|\Omega_1 \cap \Omega_2|} \left(\int_{\Omega_2 \backslash \Omega_1} g(z)\, dz \right)^2 \right\}^{1/2}. \tag{4.47}$$

Then, by combining results from Bogovskii [36, 37] and Durán [90], we prove

Theorem 4.4. *Assume* (4.33) *and let* $\Omega_\mathcal{R}$ *be as in* (4.44). *Define* σ *as in* (4.46) *and, for* $g \in L_0^2(\Omega_\mathcal{R})$, *define* α_g *and* β_g *as in* (4.47). *Then, there exists a solution* $v \in H_0^1(\Omega_\mathcal{R})$ *of the equation* $\nabla \cdot v = g$ *in* $\Omega_\mathcal{R}$ *such that*

$$\|\nabla v\|_{L^2(\Omega_\mathcal{R})} \le 2 \left[129.35 + \frac{143.86\sqrt{\sigma}}{L-a} + \frac{45.36\sigma}{(L-a)^2} + \frac{64L^2}{(L-a)^2} \left(13.79 + 5.15\sqrt{\frac{\sigma}{L-a}} \right)^2 \right]^{1/2} (\alpha_g + \beta_g). \tag{4.48}$$

Proof. We first prove a general statement which is a quantitative version of results in [90]. We consider a bounded domain $\mathcal{O} \subset \mathbb{R}^2$ which is star-shaped with respect to a disk $\mathcal{B} \subset \mathcal{O}$ of radius $r > 0$ and let $g \in L_0^2(\mathcal{O})$. Let $d(\mathcal{O})$ denote the diameter of $\mathcal{O}$.

After translation we may assume that the disk $\mathcal{B}$ is centered at the origin of $\mathbb{R}^2$. Let $\omega \in \mathcal{C}_0^\infty(\mathbb{R}^2)$ be the standard radial mollifier whose support coincides with $\overline{\mathcal{B}}$, that is,

$$\omega(x, y) = \begin{cases} \dfrac{\ell}{r^2} \exp\left(\dfrac{r^2}{x^2 + y^2 - r^2}\right) & \text{if } x^2 + y^2 < r^2, \\ 0 & \text{if } x^2 + y^2 \ge r^2, \end{cases} \tag{4.49}$$

where $\ell > 0$ is the normalization constant such that $\|\omega\|_{L^1(\mathcal{B})} = 1$; hence,

$$\ell = \left(2\pi \int_0^1 t e^{1/(t^2-1)} dt \right)^{-1} \approx 2.14357.$$

Bogovskii [36] showed that a solution $v \in H_0^1(\mathcal{O})$ of the problem $\nabla \cdot v = g$ can be written as

$$v(z) = \int_\mathcal{O} \int_0^1 \frac{z - z'}{t^3} \omega\left(z' + \frac{z - z'}{t} \right) g(z')\, dt\, dz' \qquad \forall z \in \mathbb{R}^2. \tag{4.50}$$

Following [90], we differentiate (4.50) under the integral sign, and interpret the partial derivatives of v as operators over the function g. In other words,

$$\frac{\partial v_k}{\partial z_j}(z) = T_{kj,1}(g)(z) - T_{kj,2}(g)(z) \qquad \forall z \in \mathbb{R}^2; \ k, j \in \{1, 2\}, \tag{4.51}$$

64

where, if g is extended by zero outside $\mathcal{O}$,

$$
\begin{cases}
T_{kj,1}(g)(z) = \lim_{\varepsilon \to 0} \int_\varepsilon^1 \int_{\mathbb{R}^2} \frac{1}{t^2} \frac{\partial}{\partial z_j} \left[\left(z_k' + \frac{z_k - z_k'}{t} \right) \omega \left(z' + \frac{z - z'}{t} \right) \right] g(z') \, dt \, dz', \\[4mm]
T_{kj,2}(g)(z) = \lim_{\varepsilon \to 0} \int_\varepsilon^1 \int_{\mathbb{R}^2} \frac{z_k'}{t^2} \frac{\partial}{\partial z_j} \left[\omega \left(z' + \frac{z - z'}{t} \right) \right] g(z') \, dt \, dz',
\end{cases}
$$

for every $z \in \mathbb{R}^2$ and $k, j \in \{1, 2\}$. It is shown in [90, Theorem 3.1] that

$$
\begin{cases}
\|T_{kj,1}(g)\|_{L^2(\mathcal{O})} \leq \left(\sqrt{2} A_{kj} + 2 \widetilde{A}_{kj} \sqrt{|\mathcal{O}|} \right) \|g\|_{L^2(\mathcal{O})}, \\[3mm]
\|T_{kj,2}(g)\|_{L^2(\mathcal{O})} \leq d(\mathcal{O}) \left(\sqrt{2} B_{kj} + 2 \widetilde{B}_{kj} \sqrt{|\mathcal{O}|} \right) \|g\|_{L^2(\mathcal{O})} \qquad \text{for every } k, j \in \{1, 2\},
\end{cases}
\tag{4.52}
$$

where the constants A_{kj}, $\widetilde{A}_{kj}$, B_{kj} and $\widetilde{B}_{kj}$ are explicitly given by

$$
\begin{cases}
A_{kj} = \dfrac{1}{r} \|z_k \omega\|_{L^1(\mathcal{B})} + r \left\| \dfrac{\partial^2}{\partial z_j^2} (z_k \omega) \right\|_{L^1(\mathcal{B})} & \widetilde{A}_{kj} = \left\| \dfrac{\partial}{\partial z_j} (z_k \omega) \right\|_{L^1(\mathcal{B})}^{\frac{1}{2}} \left\| \dfrac{\partial}{\partial z_j} (z_k \omega) \right\|_{L^\infty(\mathcal{B})}^{\frac{1}{2}}, \\[5mm]
B_{kj} = \dfrac{1}{r} \|\omega\|_{L^1(\mathcal{B})} + r \left\| \dfrac{\partial^2 \omega}{\partial z_j^2} \right\|_{L^1(\mathcal{B})} & \widetilde{B}_{kj} = \left\| \dfrac{\partial \omega}{\partial z_j} \right\|_{L^1(\mathcal{B})}^{\frac{1}{2}} \left\| \dfrac{\partial \omega}{\partial z_j} \right\|_{L^\infty(\mathcal{B})}^{\frac{1}{2}},
\end{cases}
\tag{4.53}
$$

for every $k, j \in \{1, 2\}$. The constants in (4.53) admit the following upper bounds (see Section 4.4):

$$
A_{11} = A_{22} < 7.29, \qquad A_{12} = A_{21} < 3.39, \qquad \widetilde{A}_{11} = \widetilde{A}_{22} < \frac{1.19}{r}, \qquad \widetilde{A}_{12} = \widetilde{A}_{21} < \frac{0.66}{r},
$$

$$
B_{11} = B_{12} = B_{21} = B_{22} < \frac{9.75}{r}, \qquad \widetilde{B}_{11} = \widetilde{B}_{12} = \widetilde{B}_{21} = \widetilde{B}_{22} < \frac{1.82}{r^{3/2}},
$$

for every $k, j \in \{1, 2\}$. By inserting these values into (4.52) we obtain:

$$
\begin{cases}
\|T_{11,1}(g)\|_{L^2(\mathcal{O})} = \|T_{22,1}(g)\|_{L^2(\mathcal{O})} \leq \left(10.31 + \dfrac{2.38}{r} \sqrt{|\mathcal{O}|} \right) \|g\|_{L^2(\mathcal{O})}, \\[4mm]
\|T_{12,1}(g)\|_{L^2(\mathcal{O})} = \|T_{21,1}(g)\|_{L^2(\mathcal{O})} \leq \left(4.8 + \dfrac{2.38}{r} \sqrt{|\mathcal{O}|} \right) \|g\|_{L^2(\mathcal{O})}, \\[4mm]
\|T_{kj,2}(g)\|_{L^2(\mathcal{O})} \leq \dfrac{d(\mathcal{O})}{r} \left(13.79 + 3.64 \sqrt{\dfrac{|\mathcal{O}|}{r}} \right) \|g\|_{L^2(\mathcal{O})} \qquad \text{for every } k, j \in \{1, 2\}.
\end{cases}
\tag{4.54}
$$

We then recall (4.51) and apply the Young inequality to obtain

$$
\|\nabla v\|_{L^2(\mathcal{O})}^2 \leq 2 \left(\sum_{k,j=1}^2 \|T_{kj,1}(g)\|_{L^2(\mathcal{O})}^2 + \sum_{k,j=1}^2 \|T_{kj,2}(g)\|_{L^2(\mathcal{O})}^2 \right).
$$

Thanks to (4.54), we have so proved that there exists a vector field $v \in H_0^1(\mathcal{O})$ solving the equation $\nabla \cdot v = g$ in $\mathcal{O}$ and satisfying the bound

$$
\|\nabla v\|_{L^2(\mathcal{O})} \leq 2 \left[129.35 + \frac{71.93}{r} \sqrt{|\mathcal{O}|} + \frac{11.34}{r^2} |\mathcal{O}| + 2 \frac{d(\mathcal{O})^2}{r^2} \left(13.79 + 3.64 \sqrt{\frac{|\mathcal{O}|}{r}} \right)^2 \right]^{1/2} \|g\|_{L^2(\mathcal{O})}. \tag{4.55}
$$

We apply this general result to the domains Ω_1 and Ω_2 so that $d(\Omega_1) = d(\Omega_2) = 2\sqrt{2}\,L$ and $r = \frac{L-a}{2}$. We proceed as in [37], see also [115, Lemma III.3.2 and Theorem III.3.1] and decompose g as

$$g = g_1 + g_2 \ \text{ in } \ \Omega_{\mathcal{R}}, \quad g_1 \in L_0^2(\Omega_1) \text{ with supp}(g_1) \subset \overline{\Omega_1}, \quad g_2 \in L_0^2(\Omega_2) \text{ with supp}(g_2) \subset \overline{\Omega_2}.$$

The functions $g_1, g_2 : \Omega_{\mathcal{R}} \to \mathbb{R}$ are explicitly defined by

$$g_1(z) = \begin{cases} g(z) - \dfrac{\chi^*(z)}{|\Omega_1 \cap \Omega_2|} \displaystyle\int_{\Omega_1} g(z')\, dz' & \text{if } z \in \Omega_1, \\[4mm] 0 & \text{if } z \in \Omega_2 \setminus \Omega_1, \end{cases}$$

$$g_2(z) = \begin{cases} [1 - \chi^*(z)]g(z) - \dfrac{\chi^*(z)}{|\Omega_1 \cap \Omega_2|} \displaystyle\int_{\Omega_2 \setminus \Omega_1} g(z')\, dz' & \text{if } z \in \Omega_2, \\[4mm] 0 & \text{if } z \in \Omega_1 \setminus \Omega_2, \end{cases}$$

with χ^* being the characteristic function of the set $\Omega_1 \cap \Omega_2$. In view of (4.47) we then deduce

$$\|g_1\|_{L^2(\Omega_{\mathcal{R}})} = \alpha_g, \qquad \|g_2\|_{L^2(\Omega_{\mathcal{R}})} = \beta_g. \tag{4.56}$$

By (4.55), we may find two vector fields $v_1 \in H_0^1(\Omega_1)$ and $v_2 \in H_0^1(\Omega_2)$ verifying

$$\nabla \cdot v_1 = g_1 \ \text{ in } \ \Omega_1, \quad \nabla \cdot v_2 = g_2 \ \text{ in } \ \Omega_2,$$

$$\|\nabla v_k\|_{L^2(\Omega_k)} \le 2\left[129.35 + \frac{143.86\sqrt{\sigma}}{L-a} + \frac{45.36\sigma}{(L-a)^2} + \frac{64L^2}{(L-a)^2}\left(13.79 + 5.15\sqrt{\frac{\sigma}{L-a}}\right)^2\right]^{1/2} \|g_k\|_{L^2(\Omega_k)},$$

for $k \in \{1, 2\}$. Then, by extending both v_1 and v_2 by zero outside Ω_1 and Ω_2, respectively, we infer that the vector field $v \doteq v_1 + v_2 \in H_0^1(\Omega_{\mathcal{R}})$, satisfies $\nabla \cdot v = g$ in $\Omega_{\mathcal{R}}$ together with the bound (4.48), after applying (4.56). $\qquad\qquad\square$

4.1.5 Gradient bounds for solenoidal extensions

The presence of inhomogeneous boundary conditions in our physical model (4.1)-(4.2)-(4.3) constitutes a major difficulty when trying to obtain a priori bounds for the solution and a quantitative statement for its uniqueness. Furthermore, as will be apparent in the proof of Theorem 4.6 below, the fundamental step lies in the determination of a solenoidal extension v_0 of the data $(U, V) \in H^{1/2}(\partial Q)$, namely a solution of (4.5), and a bound for its norm, see (4.75). The choice of v_0 influences the explicit form of the uniqueness bound and, therefore, what is needed is precisely an explicit form of v_0. We solve this problem in two steps. First we determine an extension, not necessarily solenoidal, of the data (U, V), then we solve the Bogovskii problem with the resulting divergence. More precisely, imagine that we can determine

$$W_1 \in H_*^1(\Omega) \quad \text{such that} \quad W_1 = (U, V) \text{ on } \partial Q\,;$$

this can be done in several ways but the difficult task is to obtain explicit bounds for ∇W_1. Then one solves the Bogovskii problem

$$\nabla \cdot W_2 = -\nabla \cdot W_1 \ \text{ in } \ \Omega, \qquad W_2 \in H_0^1(\Omega)\,.$$

Finally, $v_0 = W_1 + W_2$ is the desired solenoidal extension and one then needs to find a bound for the gradient of v_0. In turn, this depends on the bound for the gradient of W_2 that can be obtained through Theorem 4.4, at least when (4.33) holds.

The purpose of the present section is to construct an explicit solenoidal extension v_0 in the particular case where $(U, V) \in \mathbb{R}^2$. Assume (4.33) and let $\Omega_{\mathcal{R}}$ be as in (4.44). Let $\mathcal{P}(Q)$ be the set of pyramidal

functions, see (4.9). For all $P^\phi \in \mathcal{P}(Q)$, characterized by a continuous function ϕ as in (4.11), we define $\Upsilon^\phi \doteq 1 - P^\phi$ extended by 0 in $\mathcal{R}$, so that

$$\Upsilon^\phi \in H^1_c(\Omega), \qquad \Upsilon^\phi = 1 \quad \text{on } \partial Q, \qquad \Upsilon^\phi \equiv 0 \quad \text{in } \mathcal{R}.$$

Then consider the vector field $W_1 = \Upsilon^\phi \left(\begin{smallmatrix} U \\ V \end{smallmatrix} \right)$ (we omit the superscript ϕ in $W_1 = W_1^\phi$), which verifies

$$\nabla \cdot W_1 = U \frac{\partial \Upsilon^\phi}{\partial x} + V \frac{\partial \Upsilon^\phi}{\partial y} \quad \text{in } \Omega, \qquad W_1 = (U,V) \quad \text{on } \partial Q, \qquad W_1 = (0,0) \quad \text{on } \partial K; \qquad (4.57)$$

we point out that $\nabla \cdot W_1 = 0$ in $\mathcal{R} \setminus K$ since $\Upsilon^\phi \equiv 0$ in $\mathcal{R} \setminus K$. Let T_5 and T_6 be the trapezia defined in (4.12)-(4.13); then, by arguing as for (4.16), we obtain

$$\|\nabla \cdot W_1\|^2_{L^2(\Omega)} = 4V^2 \int_{T_5} \left| \frac{\partial P^\phi}{\partial y} \right|^2 + 4U^2 \int_{T_6} \left| \frac{\partial P^\phi}{\partial x} \right|^2$$

$$= 4 \frac{V^2(L-a)^2 + U^2(L-d)^2}{(L-a)(L-d)} \int_0^1 \left[\frac{aV^2(L-a) + dU^2(L-d)}{V^2(L-a)^2 + U^2(L-d)^2} + s \right] \phi'(s)^2 \, ds.$$

Since we are planning to use (4.50), the bound (4.42) suggests to minimize this integral among functions ϕ satisfying (4.11); this yields the Euler-Lagrange equation

$$\frac{d}{ds} \left[\left(\frac{aV^2(L-a) + dU^2(L-d)}{V^2(L-a)^2 + U^2(L-d)^2} + s \right) \phi'(s) \right] = 0 \qquad \forall s \in (0,1),$$

so that

$$\phi(s) = C \log \left(s + \frac{aV^2(L-a) + dU^2(L-d)}{V^2(L-a)^2 + U^2(L-d)^2} \right) + D \qquad \forall s \in [0,1],$$

for some constants $C, D \in \mathbb{R}$ to be determined by the conditions $\phi(0) = 1$ and $\phi(1) = 0$. We find

$$C = \left[\log \left(\frac{aV^2(L-a)+dU^2(L-d)}{V^2 L(L-a)+U^2 L(L-d)} \right) \right]^{-1} < 0, \quad D = -C \log \left(\frac{V^2 L(L-a)+U^2 L(L-d)}{V^2(L-a)^2+U^2(L-d)^2} \right) > 0. \qquad (4.58)$$

Then, by inserting this into (4.57) and recalling (4.15), we obtain

$$\nabla \cdot W_1 = \frac{V}{L-d} \frac{1}{\log \left(\frac{V^2 L(L-a)+U^2 L(L-d)}{aV^2(L-a)+dU^2(L-d)} \right)} \frac{1}{\frac{aV^2(L-a)+dU^2(L-d)}{V^2(L-a)^2+U^2(L-d)^2} + \frac{y-d}{L-d}} \qquad \text{in } T_5,$$

$$\nabla \cdot W_1 = \frac{U}{L-a} \frac{1}{\log \left(\frac{V^2 L(L-a)+U^2 L(L-d)}{aV^2(L-a)+dU^2(L-d)} \right)} \frac{1}{\frac{aV^2(L-a)+dU^2(L-d)}{V^2(L-a)^2+U^2(L-d)^2} + \frac{x-a}{L-a}} \qquad \text{in } T_6,$$

$$\tag{4.59}$$

so that

$$\|\nabla \cdot W_1\|^2_{L^2(\Omega)} = 4C^2 \frac{V^2(L-a)^2+U^2(L-d)^2}{(L-a)(L-d)} \log \left(\frac{V^2 L(L-a)+U^2 L(L-d)}{aV^2(L-a)+dU^2(L-d)} \right) = 4|C| \frac{V^2(L-a)^2 + U^2(L-d)^2}{(L-a)(L-d)}.$$

We also have

$$\|W_1\|^4_{L^4(\Omega)} = (U^2+V^2)^2 \int_{\Omega_{\mathcal{R}}} |1 - P^\phi|^4$$

$$= 4(U^2+V^2)^2 \int_0^1 [a(L-d)+d(L-a)+2(L-a)(L-d)s] \, |1 - \phi(s)|^4 \, ds$$

$$= 2(U^2+V^2)^2(L-a)(L-d) e^{\frac{1-D}{C}} \left\{ e^{-\frac{1+D}{C}} \left[2 + 4C + 6C^2 + 6C^3 - 3C^4 \left(e^{\frac{2}{C}} - 1 \right) \right] \right.$$

$$\left. + 4 \left[\frac{a(L-d)+d(L-a)}{2(L-a)(L-d)} - \frac{aV^2(L-a)+dU^2(L-d)}{V^2(L-a)^2+U^2(L-d)^2} \right] \left[\left(1 + 4C + 12C^2 + 24C^3 + 24C^4 \right) e^{-\frac{1}{C}} - 24C^4 \right] \right\}.$$

Moreover:

$$\nabla W_1 = \begin{pmatrix} U\dfrac{\partial \Upsilon^\phi}{\partial x} & U\dfrac{\partial \Upsilon^\phi}{\partial y} \\[2ex] V\dfrac{\partial \Upsilon^\phi}{\partial x} & V\dfrac{\partial \Upsilon^\phi}{\partial y} \end{pmatrix} \implies \nabla W_1 = -\frac{\partial P^\phi}{\partial y}\begin{pmatrix} 0 & U \\ 0 & V \end{pmatrix} \text{ in } T_5\,, \quad \nabla W_1 = -\frac{\partial P^\phi}{\partial x}\begin{pmatrix} U & 0 \\ V & 0 \end{pmatrix} \text{ in } T_6\,,$$

so that, by (4.15),

$$\nabla W_1 = \frac{1}{L-d}\frac{1}{\log\left(\frac{V^2 L(L-a)+U^2 L(L-d)}{aV^2(L-a)+dU^2(L-d)}\right)}\frac{1}{\frac{aV^2(L-a)+dU^2(L-d)}{V^2(L-a)^2+U^2(L-d)^2}+\frac{y-d}{L-d}}\begin{pmatrix} 0 & U \\ 0 & V \end{pmatrix} \quad \text{in } T_5\,, \tag{4.60}$$

$$\nabla W_1 = \frac{1}{L-a}\frac{1}{\log\left(\frac{V^2 L(L-a)+U^2 L(L-d)}{aV^2(L-a)+dU^2(L-d)}\right)}\frac{1}{\frac{aV^2(L-a)+dU^2(L-d)}{V^2(L-a)^2+U^2(L-d)^2}+\frac{x-a}{L-a}}\begin{pmatrix} U & 0 \\ V & 0 \end{pmatrix} \quad \text{in } T_6\,. \tag{4.61}$$

Further explicit computations yield

$$\|\nabla W_1\|_{L^2(\Omega)}^2 = 4C^2(U^2+V^2)\frac{(L-a)^2+(L-d)^2}{(L-a)(L-d)}\left\{ e^{\frac{D}{C}}\left[\frac{a(L-a)+d(L-d)}{(L-a)^2+(L-d)^2}\frac{V^2(L-a)^2+U^2(L-d)^2}{aV^2(L-a)+dU^2(L-d)}-1\right]-\frac{1}{C}\right\}.$$

The next step is to find a suitable vector field $W_2 \in H_0^1(\Omega)$ verifying

$$\nabla \cdot W_2 = -\nabla \cdot W_1 = U\frac{\partial P^\phi}{\partial x}+V\frac{\partial P^\phi}{\partial y} \quad \text{in } \Omega, \tag{4.62}$$

together with a gradient bound for W_2. We define $g \doteq -\nabla \cdot W_1$, which belongs to $L_0^2(\Omega_\mathcal{R})$ in virtue of the Divergence Theorem. In particular, this shows

$$\int_{\Omega_1} g(z)\,dz + \int_{\Omega_2\setminus\Omega_1} g(z)\,dz = 0. \tag{4.63}$$

Notice that $\nabla \cdot W_2 = 0$ in $\mathcal{R}\setminus K$, and so, after extending by 0 in $\mathcal{R}\setminus K$, it suffices to find $W_2 \in H_0^1(\Omega_\mathcal{R})$ satisfying (4.62) in $\Omega_\mathcal{R}$. The existence of such W_2 is guaranteed by Theorem 4.4, whose gradient satisfies the estimate (4.48), with σ as in (4.46) and α_g, β_g as in (4.47). The explicit form of g allows us to go further with exact computations; in fact, by (4.63) and since g is given in the divergence form (4.59), the Divergence Theorem and the property (4.14) of pyramidal functions yield

$$\zeta_0 \doteq \int_{\Omega_1} g(z)\,dz = -\int_{\Omega_2\setminus\Omega_1} g(z)\,dz$$

$$= 2(dU-aV) + \left(C + \frac{aV^2(L-a)+dU^2(L-d)}{V^2(L-a)^2+U^2(L-d)^2}\right)\left(\frac{(L-a)^2}{\sqrt{\alpha_*^2+(L-a)^2}}\left(\frac{U\alpha_*}{L-a}+V\right)-U(L-d)\right). \tag{4.64}$$

With this particular choice of g we also have

$$\int_{\Omega_1\cap\Omega_2} g(z)\,dz = 0,$$

which allows to rule out term appearing in (4.47). Moreover, by determining the intersections of the trapezia $\{T_i\}_{i=1}^4$ with the sets Ω_1 and Ω_2, we find

$$\overline{\alpha} \doteq \alpha_g = \left\{ 4|C| \frac{V^2(L-a)^2 + U^2(L-d)^2}{(L-a)(L-d)} - C^2 V^2 \frac{L-a}{L-d} \left[\left(\frac{2a}{L-a} - \frac{aV^2(L-a) + dU^2(L-d)}{V^2(L-a)^2 + U^2(L-d)^2} \right) \frac{e^{D/C}}{e^{-D/C} - 1} - \frac{1}{C} \right] \right.$$

$$\left. - C^2 U^2 \frac{L-d-\alpha_*}{L-a} \left[\left(\frac{2d}{L-d-\alpha_*} - \frac{aV^2(L-a) + dU^2(L-d)}{V^2(L-a)^2 + U^2(L-d)^2} \right) \frac{e^{D/C}}{e^{-D/C} - 1} - \frac{1}{C} \right] + \frac{\zeta_0^2}{|\Omega_1 \cap \Omega_2|} \right\}^{1/2}, \tag{4.65}$$

$$\overline{\beta} \doteq \beta_g = \left\{ C^2 V^2 \frac{L-a}{L-d} \left[\left(\frac{2a}{L-a} - \frac{aV^2(L-a) + dU^2(L-d)}{V^2(L-a)^2 + U^2(L-d)^2} \right) \frac{e^{D/C}}{e^{-D/C} - 1} - \frac{1}{C} \right] \right.$$

$$\left. + C^2 U^2 \frac{L-d-\alpha_*}{L-a} \left[\left(\frac{2d}{L-d-\alpha_*} - \frac{aV^2(L-a) + dU^2(L-d)}{V^2(L-a)^2 + U^2(L-d)^2} \right) \frac{e^{D/C}}{e^{-D/C} - 1} - \frac{1}{C} \right] + \frac{\zeta_0^2}{|\Omega_1 \cap \Omega_2|} \right\}^{1/2}.$$

Then one defines $v \doteq W_1 + W_2$, which is an element of $H_c^1(\Omega)$ and whose gradient can be explicitly bounded in terms of the previously computed constants. We summarize these results in the following statement, providing the desired explicit form for the solenoidal extension of constant boundary data.

Theorem 4.5. *Assume* (4.33), *and for a given* $(U, V) \in \mathbb{R}^2$, *define* $\alpha_* \geq 0$ *as in* (4.45); σ *as in* (4.46); $C < 0$, $D > 0$ *as in* (4.58); $\zeta_0 \in \mathbb{R}$ *as in* (4.64); $\overline{\alpha}, \overline{\beta} \geq 0$ *as in* (4.65). *Then, there exists a vector field* $v \in H_c^1(\Omega)$ *satisfying*

$$\nabla \cdot v = 0 \quad in \quad \Omega, \qquad v = (U, V) \quad on \quad \partial Q, \tag{4.66}$$

together with the estimate

$$\|\nabla v\|_{L^2(\Omega)} \leq 2|C| \sqrt{U^2 + V^2} \sqrt{\frac{(L-a)^2 + (L-d)^2}{(L-a)(L-d)}} \sqrt{e^{\frac{D}{C}} \left[\frac{a(L-a) + d(L-d)}{(L-a)^2 + (L-d)^2} \frac{V^2(L-a)^2 + U^2(L-d)^2}{aV^2(L-a) + dU^2(L-d)} - 1 \right] - \frac{1}{C}}$$

$$+ 2\sqrt{129.35 + \frac{143.86\sqrt{\sigma}}{L-a} + \frac{45.36\sigma}{(L-a)^2} + \frac{64L^2}{(L-a)^2} \left(13.79 + 5.15\sqrt{\frac{\sigma}{L-a}} \right)^2 } \left(\overline{\alpha} + \overline{\beta} \right). \tag{4.67}$$

We point out that the bound for $\|\nabla v\|_{L^2(\Omega)}$ does not depend on the shape of the obstacle, it is obtained under the sole assumption (4.33). This result will be simplified in Section 4.2.4 where we also assume that $V = 0$.

4.2 The planar Navier-Stokes equations around an obstacle

4.2.1 Existence, uniqueness and regularity

Let us first define what is meant by weak solution of problem (4.2)-(4.3).

Definition 4.1. *Given* $f \in H^{-1}(\Omega)$ *and* $(U, V) \in H^{1/2}(\partial Q)$ *satisfying* (4.4), *we say that a vector field* $u \in \mathcal{V}_*(\Omega)$ *is a weak solution of* (4.2)-(4.3) *if* u *verifies* (4.3) *in the trace sense and*

$$\eta(\nabla u, \nabla \varphi)_{L^2(\Omega)} + \beta(u, u, \varphi) = \langle f, \varphi \rangle_\Omega \qquad \forall \varphi \in \mathcal{V}(\Omega). \tag{4.68}$$

Then we state a result which is essentially known, see e.g. [115, Section IX.4]. Nevertheless, for three important reasons give we here a proof by emphasizing several steps. First we are concerned with both nonzero forcing and boundary data, second the a priori bounds are needed in the proof of Theorem 4.11, third the quantitative bounds for uniqueness will play a crucial role in Section 4.2.4.

Theorem 4.6. *Let Ω be as in (4.1). For any $f \in H^{-1}(\Omega)$ and $(U, V) \in H^{1/2}(\partial Q)$ satisfying (4.4) there exists a weak solution $(u, p) \in \mathcal{V}_*(\Omega) \times L_0^2(\Omega)$ of (4.2)-(4.3) and any weak solution (u, p) satisfies the a priori bound*

$$\begin{cases} \|\nabla u\|_{L^2(\Omega)} \leq C_1 \left(\|(U, V)\|_{H^{1/2}(\partial Q)}^2 + \|(U, V)\|_{H^{1/2}(\partial Q)} + \|f\|_{H^{-1}(\Omega)} \right), \\ \|p\|_{L^2(\Omega)} \leq C_2 \left(\|\nabla u\|_{L^2(\Omega)}^2 + \|\nabla u\|_{L^2(\Omega)} + \|f\|_{H^{-1}(\Omega)} \right), \end{cases} \quad (4.69)$$

for some $C_1, C_2 > 0$ that depend on Ω and η. Moreover, there exists $\delta = \delta(\eta, \Omega) > 0$ such that if

$$\|(U, V)\|_{H^{1/2}(\partial Q)} + \|f\|_{H^{-1}(\Omega)} < \delta, \quad (4.70)$$

then the weak solution (u, p) of (4.2)-(4.3) is unique and also satisfies the estimate $\|\nabla u\|_{L^2(\Omega)} < \mathcal{S}_0 \eta$.

Proof. Existence of a weak solution $(u, p) \in \mathcal{V}_*(\Omega) \times L_0^2(\Omega)$ of (4.2)-(4.3) satisfying the a priori bounds (4.69) follow from [115, Theorem IX.4.1], but the proof is given here in order to show how the constants C_1 and C_2 appearing in (4.69) depend on Ω. Indeed, Proposition 4.1 ensures the existence of a solenoidal vector field $u_0 \in \mathcal{V}_*(\Omega)$ satisfying

$$u_0 = (U, V) \quad \text{on} \quad \partial Q, \quad \|\nabla u_0\|_{L^2(\Omega)} \leq M \|(U, V)\|_{H^{1/2}(\partial Q)}, \quad |\beta(v, u_0, v)| \leq \frac{\eta}{2} \|\nabla v\|_{L^2(\Omega)}^2 \quad \forall v \in \mathcal{V}(\Omega),$$

for some constant $M > 0$ depending only on Ω. Define $\xi = u - u_0$, so that $\xi \in \mathcal{V}(\Omega)$, and substitute $u = \xi + u_0$ into (4.2) to obtain

$$-\eta \Delta \xi + [(\xi + u_0) \cdot \nabla](\xi + u_0) + \nabla p = \eta \Delta u_0 + f, \quad (4.71)$$

with $\eta \Delta u_0 + f \in H^{-1}(\Omega)$. Hence, (4.71) is intended in weak sense, see (4.68); we test it with ξ and we integrate by parts over Ω in order to obtain

$$\eta \|\nabla \xi\|_{L^2(\Omega)}^2 \leq (\eta \|\nabla u_0\|_{L^2(\Omega)} + \|f\|_{H^{-1}(\Omega)}) \|\nabla \xi\|_{L^2(\Omega)} - \beta(\xi + u_0, \xi + u_0, \xi). \quad (4.72)$$

By (4.36)-(4.37) we have $\beta(\xi + u_0, \xi + u_0, \xi) = \beta(\xi + u_0, u_0, \xi)$ and the estimate

$$|\beta(\xi + u_0, u_0, \xi)| \leq \frac{\eta}{2} \|\nabla \xi\|_{L^2(\Omega)}^2 + \frac{1}{\sqrt{\mathcal{S} \mathcal{S}_0}} \|\nabla \xi\|_{L^2(\Omega)} \|\nabla u_0\|_{L^2(\Omega)}^2, \quad (4.73)$$

where we have used the definition of $\mathcal{S}$ and $\mathcal{S}_0$ given in (4.23). By plugging (4.73) into (4.72) we deduce

$$\|\nabla u\|_{L^2(\Omega)} \leq \|\nabla \xi\|_{L^2(\Omega)} + \|\nabla u_0\|_{L^2(\Omega)} \leq \frac{2}{\sqrt{\mathcal{S} \mathcal{S}_0} \, \eta} \|\nabla u_0\|_{L^2(\Omega)}^2 + 3 \|\nabla u_0\|_{L^2(\Omega)} + \frac{2}{\eta} \|f\|_{H^{-1}(\Omega)},$$

and then the inequality $\|\nabla u_0\|_{L^2(\Omega)} \leq M \|(U, V)\|_{H^{1/2}(\partial Q)}$ yields $(4.69)_1$ in the following way:

$$\|\nabla u\|_{L^2(\Omega)} \leq \frac{2M^2}{\sqrt{\mathcal{S} \mathcal{S}_0} \, \eta} \|(U, V)\|_{H^{1/2}(\partial Q)}^2 + 3M \|(U, V)\|_{H^{1/2}(\partial Q)} + \frac{2}{\eta} \|f\|_{H^{-1}(\Omega)}. \quad (4.74)$$

The a priori bound for the pressure in $(4.69)_2$ is obtained after noticing that

$$\nabla p = \eta \Delta u - (u \cdot \nabla) u + f \quad \text{in the sense of} \ H^{-1}(\Omega),$$

and applying (4.43) with some embedding inequalities.

The quantitative uniqueness statement relies on a different kind of a priori bound, based on a *given* solenoidal extension, that is,

$$v_0 \in \mathcal{V}_*(\Omega), \quad v_0 = (U, V) \quad \text{on} \quad \partial Q, \quad \|\nabla v_0\|_{L^2(\Omega)} \leq C \|(U, V)\|_{H^{1/2}(\partial Q)}, \quad (4.75)$$

where the constant $C = C(\Omega) > 0$ is independent on the boundary data, see [170]. Then we seek solutions u of (4.2)-(4.3) in the form $u = \xi + v_0$ so that $\xi \in \mathcal{V}(\Omega)$ satisfies

$$-\eta\Delta\xi + [(\xi + v_0) \cdot \nabla](\xi + v_0) + \nabla p = \eta\Delta v_0 + f, \tag{4.76}$$

with $\eta\Delta v_0 + f \in H^{-1}(\Omega)$. Hence, (4.76) is intended in weak sense, see (4.68); we test it with ξ and we integrate by parts in Ω in order to obtain

$$\eta\|\nabla\xi\|_{L^2(\Omega)}^2 \leq (\eta\|\nabla v_0\|_{L^2(\Omega)} + \|f\|_{H^{-1}(\Omega)})\|\nabla\xi\|_{L^2(\Omega)} - \beta(\xi + v_0, \xi + v_0, \xi). \tag{4.77}$$

In view of (4.36)-(4.37) we have $\beta(\xi + v_0, \xi + v_0, \xi) = \beta(\xi + v_0, v_0, \xi)$ and the estimate

$$
\begin{aligned}
|\beta(\xi + v_0, v_0, \xi)| &\leq \|\xi\|_{L^4(\Omega)}\|\nabla v_0\|_{L^2(\Omega)}(\|\xi\|_{L^4(\Omega)} + \|v_0\|_{L^4(\Omega)}) \\
&\leq \frac{\|\nabla\xi\|_{L^2(\Omega)}}{\sqrt{\mathcal{S}_0}}\|\nabla v_0\|_{L^2(\Omega)}\left(\frac{\|\nabla\xi\|_{L^2(\Omega)}}{\sqrt{\mathcal{S}_0}} + \|v_0\|_{L^4(\Omega)}\right),
\end{aligned} \tag{4.78}
$$

where we used the definition of $\mathcal{S}_0$ given in (4.23). Inserting (4.78) into (4.77) yields

$$\eta\|\nabla\xi\|_{L^2(\Omega)} \leq \frac{\|\nabla v_0\|_{L^2(\Omega)}}{\mathcal{S}_0}\|\nabla\xi\|_{L^2(\Omega)} + \frac{\|\nabla v_0\|_{L^2(\Omega)}\|v_0\|_{L^4(\Omega)}}{\sqrt{\mathcal{S}_0}} + \eta\|\nabla v_0\|_{L^2(\Omega)} + \|f\|_{H^{-1}(\Omega)}.$$

Let C be as in (4.75); if the boundary datum is small enough so that

$$C\|(U, V)\|_{H^{1/2}(\partial Q)} < \mathcal{S}_0\eta, \tag{4.79}$$

then, for the chosen extension v_0, one also has $\|\nabla v_0\|_{L^2(\Omega)} < \mathcal{S}_0\eta$ and we infer that

$$\|\nabla\xi\|_{L^2(\Omega)} \leq \frac{\dfrac{\|\nabla v_0\|_{L^2(\Omega)}\|v_0\|_{L^4(\Omega)}}{\sqrt{\mathcal{S}_0}} + \eta\|\nabla v_0\|_{L^2(\Omega)} + \|f\|_{H^{-1}(\Omega)}}{\eta - \dfrac{\|\nabla v_0\|_{L^2(\Omega)}}{\mathcal{S}_0}}. \tag{4.80}$$

This is the sought a priori bound for solutions of (4.68), up to the additive solenoidal extension v_0 of the boundary data. We emphasize that it has been obtained under the smallness assumption (4.79).

Assuming (4.79), take two weak solutions $u, v \in H_*^1(\Omega)$ of (4.2)-(4.3), with possibly different pressures that are, however, ruled out by L^2-orthogonality of the gradients with $\mathcal{V}(\Omega)$. Indeed, subtract the equations (4.68) corresponding to u and v in order to obtain

$$\eta(\nabla w, \nabla\varphi)_{L^2(\Omega)} + \beta(u, w, \varphi) + \beta(w, v, \varphi) = 0 \qquad \forall\varphi \in \mathcal{V}(\Omega),$$

where $w \doteq u - v \in \mathcal{V}(\Omega)$. By taking $\varphi = w$, defining $\xi = v - v_0$ and using (4.36) and (4.80), we derive

$$
\begin{aligned}
\eta\|\nabla w\|_{L^2(\Omega)}^2 &= -\beta(w, v, w) = \beta(w, w, v) \leq \|w\|_{L^4(\Omega)}\|\nabla w\|_{L^2(\Omega)}\|v\|_{L^4(\Omega)} \leq \frac{\|\nabla w\|_{L^2(\Omega)}^2}{\sqrt{\mathcal{S}_0}}\|v\|_{L^4(\Omega)} \\
&\leq \frac{\|\nabla w\|_{L^2(\Omega)}^2}{\sqrt{\mathcal{S}_0}}(\|\xi\|_{L^4(\Omega)} + \|v_0\|_{L^4(\Omega)}) \leq \frac{\|\nabla w\|_{L^2(\Omega)}^2}{\sqrt{\mathcal{S}_0}}\left(\frac{\|\nabla\xi\|_{L^2(\Omega)}}{\sqrt{\mathcal{S}_0}} + \|v_0\|_{L^4(\Omega)}\right) \\
&\leq \|\nabla w\|_{L^2(\Omega)}^2 \frac{\eta(\|\nabla v_0\|_{L^2(\Omega)} + \sqrt{\mathcal{S}_0}\|v_0\|_{L^4(\Omega)}) + \|f\|_{H^{-1}(\Omega)}}{\eta\mathcal{S}_0 - \|\nabla v_0\|_{L^2(\Omega)}},
\end{aligned} \tag{4.81}
$$

which shows that $w = 0$ provided that

$$\eta(2\|\nabla v_0\|_{L^2(\Omega)} + \sqrt{\mathcal{S}_0}\|v_0\|_{L^4(\Omega)}) + \|f\|_{H^{-1}(\Omega)} < \mathcal{S}_0\eta^2. \tag{4.82}$$

71

In conclusion, unique solvability of (4.2)-(4.3) is achieved whenever both (4.79) and (4.82) hold. Since the most restrictive is the latter, and since $\|v_0\|_{L^4(\Omega)} \leq \|\nabla v_0\|_{L^2(\Omega)}/\sqrt{\mathcal{S}}$, uniqueness is ensured whenever

$$\eta\left(2 + \sqrt{\frac{\mathcal{S}_0}{\mathcal{S}}}\right)\|\nabla v_0\|_{L^2(\Omega)} + \|f\|_{H^{-1}(\Omega)} < \mathcal{S}_0\eta^2. \tag{4.83}$$

In turn, by (4.75), (4.83) certainly holds if

$$\eta C \frac{2\sqrt{\mathcal{S}} + \sqrt{\mathcal{S}_0}}{\sqrt{\mathcal{S}}}\|(U,V)\|_{H^{1/2}(\partial Q)} + \|f\|_{H^{-1}(\Omega)} < \mathcal{S}_0\eta^2. \tag{4.84}$$

Therefore, an explicit expression for δ in (4.70) is given by

$$\delta(\eta, \Omega) = \min\left\{\frac{\eta}{C}\frac{\mathcal{S}_0\sqrt{\mathcal{S}}}{2\sqrt{\mathcal{S}} + \sqrt{\mathcal{S}_0}}, \mathcal{S}_0\eta^2\right\}. \tag{4.85}$$

Finally, we have to prove the gradient bound for the unique solution whenever the inequality

$$\|(U,V)\|_{H^{1/2}(\partial Q)} + \|f\|_{H^{-1}(\Omega)} < \min\left\{\frac{\eta}{C}\frac{\mathcal{S}_0\sqrt{\mathcal{S}}}{2\sqrt{\mathcal{S}} + \sqrt{\mathcal{S}_0}}, \mathcal{S}_0\eta^2\right\}$$

holds. This inequality implies (4.84) which, together with (4.75), implies

$$\|\nabla v_0\|_{L^2(\Omega)} < \eta\sqrt{\mathcal{S}\mathcal{S}_0}; \tag{4.86}$$

we point out that (4.86) slightly improves (4.79) since $\mathcal{S} \leq \mathcal{S}_0$. For the same reason, and since (4.86) holds, we may write a "slightly worse" bound than (4.80), namely

$$\|\nabla \xi\|_{L^2(\Omega)} \leq \frac{\dfrac{\|\nabla v_0\|_{L^2(\Omega)}^2}{\sqrt{\mathcal{S}\mathcal{S}_0}} + \eta\|\nabla v_0\|_{L^2(\Omega)} + \|f\|_{H^{-1}(\Omega)}}{\eta - \dfrac{\|\nabla v_0\|_{L^2(\Omega)}}{\sqrt{\mathcal{S}\mathcal{S}_0}}}.$$

Hence, recalling that $u = \xi + v_0$, by (4.83) we have that

$$\|\nabla u\|_{L^2(\Omega)} \leq \|\nabla \xi\|_{L^2(\Omega)} + \|\nabla v_0\|_{L^2(\Omega)} \leq \frac{2\eta\|\nabla v_0\|_{L^2(\Omega)} + \|f\|_{H^{-1}(\Omega)}}{\eta - \dfrac{\|\nabla v_0\|_{L^2(\Omega)}}{\sqrt{\mathcal{S}\mathcal{S}_0}}} < \mathcal{S}_0\eta.$$

This proves the gradient bound and completes the proof. $\qquad\square$

Remark 4.6. *Theorem 4.6 guarantees unique solvability of* (4.2)-(4.3) *under a smallness assumption on the data, which in turn yields the bound* $\|\nabla u\|_{L^2(\Omega)} < \mathcal{S}_0\eta$. *Conversely, the existence of such a "small" solution ensures unique solvability, see [115, Theorem IX.2.1].*

The constant δ in (4.70) depends on Ω through the embedding constants $\mathcal{S}$ and $\mathcal{S}_0$ and through the solenoidal extension constant C in (4.75). Theorem 4.6 guarantees the uniqueness of the solution whenever the data (U, V) and f are small also with respect to the kinematic viscosity η. If this smallness assumption is violated one expects multiplicity results, see [261] and also [115, Theorem IX.2.2] for a slightly more general situation: at a certain Reynolds number a bifurcation occurs.

What is left open in the proof of Theorem 4.6 is the choice of the particular solenoidal extension v_0. We can find an explicit form of v_0 in the case where the boundary data are constant (so that (4.4) is

automatically fulfilled). To this end, for $0 < d \leq a < L$, define $\sigma > 0$ as in (4.46); $\theta > 0$, $\theta_1, \theta_2 \in \mathbb{R}$ as in Theorem 4.3, and we introduce the constants

$$\gamma_1 = \left[129.35 + \frac{143.86\sqrt{\sigma}}{L-a} + \frac{45.36\sigma}{(L-a)^2} + \frac{64L^2}{(L-a)^2} \left(13.79 + 5.15\sqrt{\frac{\sigma}{L-a}} \right)^2 \right]^{1/2},$$

$$\gamma_2 = 2\sqrt{\frac{(L-a)^2 + (L-d)^2}{(L-a)(L-d)}} \left[\log\left(\frac{L(L-a) + L(L-d)}{a(L-a) + d(L-d)} \right) \right]^{-1/2},$$

$$\gamma_3 = \sqrt[4]{2\frac{a(L-a) + d(L-d)}{[(L-a)^2 + (L-d)^2]^2} \left\{ 2L(2L-a-d)(d-a)^2\theta_1 + (L-a)(L-d)\left[a(L-a) + d(L-d)\right]\theta_2 \right\}}.$$

Then, if we additionally assume that $f = 0$, Theorem 4.6 may be strengthened as follows.

Theorem 4.7. *Let Ω be as in (4.1) and assume (4.33). Define $\mu_0 > 0$ as in (4.22) and $\alpha_* \geq 0$ as in (4.45). For any $(U, V) \in \mathbb{R}^2$ there exists a weak solution $(u, p) \in \mathcal{V}_*(\Omega) \times L_0^2(\Omega)$ of (4.2)-(4.3) with $f = 0$. If, moreover,*

$$\sqrt{U^2 + V^2} < \frac{\frac{\sqrt{3}\pi^{3/2}}{2L} \max\left\{ 1, \sqrt{\frac{\mu_0^2|Q|}{2\pi(|Q|-|K|)}} \right\} \eta}{\left(2 + 12\gamma_1 \sqrt{1 + \frac{1}{2(L-a)(L-d) + \alpha_*(L-a)}} \right) \gamma_2 + \frac{\sqrt[4]{3}\pi^{3/4}}{\sqrt{2L}} \max\left\{ 1, \sqrt[4]{\frac{\mu_0^2|Q|}{2\pi(|Q|-|K|)}} \right\} \gamma_3},$$

then the weak solution of (4.2)-(4.3) is unique.

Proof. Existence of a weak solution $(u, p) \in \mathcal{V}_*(\Omega) \times L_0^2(\Omega)$ of (4.2)-(4.3) with $f = 0$ follows from Theorem 4.6, noticing that the compatibility condition (4.4) is automatically fulfilled.

Let $\mathcal{P}(Q)$ be as in (4.9), let $V^\phi \in \mathcal{P}(Q)$ be defined by (4.14) with

$$\phi(s) = \log\left(\frac{(L-a)^2 + (L-d)^2}{L(L-a) + L(L-d)} s + \frac{a(L-a) + d(L-d)}{L(L-a) + L(L-d)} \right) \Big/ \log\left(\frac{a(L-a) + d(L-d)}{L(L-a) + L(L-d)} \right) \qquad \forall s \in [0, 1],$$

with V^ϕ extended by 1 in $\mathcal{R} \setminus K$. We know that $V^\phi = 0$ on ∂Q, $V^\phi \equiv 1$ in $\mathcal{R}$, and from (4.16), (4.17) and the proof of Theorem 4.3 we also have

$$\|\nabla V^\phi\|_{L^2(\Omega)} = \gamma_2, \qquad \|1 - V^\phi\|_{L^4(\Omega)} = \gamma_3. \tag{4.87}$$

Consider the vector field $W_1 \doteq (1 - V^\phi)\left(\begin{smallmatrix} U \\ V \end{smallmatrix} \right)$, so that:

$$\nabla \cdot W_1 = -U\frac{\partial V^\phi}{\partial x} - V\frac{\partial V^\phi}{\partial y} \quad \text{in } \Omega, \qquad W_1 = (U, V) \quad \text{on } \partial Q, \qquad W_1 = (0, 0) \quad \text{on } \partial K.$$

Moreover,

$$\|\nabla W_1\|_{L^2(\Omega)}^2 = (U^2 + V^2)\|\nabla V^\phi\|_{L^2(\Omega)}^2, \qquad \|W_1\|_{L^4(\Omega)}^4 = (U^2 + V^2)^2 \|1 - V^\phi\|_{L^4(\Omega)}^4. \tag{4.88}$$

Also note that

$$|\nabla \cdot W_1|^2 = (U^2 + V^2)\left[\left(\frac{\partial V^\phi}{\partial x} \right)^2 + \left(\frac{\partial V^\phi}{\partial y} \right)^2 \right] - \left(U\frac{\partial V^\phi}{\partial y} - V\frac{\partial V^\phi}{\partial x} \right)^2 \leq (U^2 + V^2)\,|\nabla V^\phi|^2,$$

so that

$$\|\nabla \cdot W_1\|_{L^2(\Omega)}^2 \leq (U^2 + V^2)\|\nabla V^\phi\|_{L^2(\Omega)}^2. \tag{4.89}$$

73

The next step is to find a vector field $W_2 \in H_0^1(\Omega)$ verifying

$$\nabla \cdot W_2 = U \frac{\partial V^\phi}{\partial x} + V \frac{\partial V^\phi}{\partial y} \quad \text{in } \Omega, \tag{4.90}$$

together with a gradient bound. We define $g \doteq -\nabla \cdot W_1$, which belongs to $L_0^2(\Omega_{\mathcal{R}})$ in virtue of the Divergence Theorem. Notice that $\nabla \cdot W_2 = 0$ in $\mathcal{R} \setminus K$, and so, after extending by 0 in $\mathcal{R} \setminus K$, it suffices to find $W_2 \in H_0^1(\Omega_{\mathcal{R}})$ satisfying (4.90) in $\Omega_{\mathcal{R}}$. We now proceed as in Theorem 4.4 and define the two sets $\Omega_1, \Omega_2 \subset \Omega$, each one being star-shaped with respect to a disk of radius $(L-a)/2$, such that $\overline{\Omega} = \overline{\Omega_1} \cup \overline{\Omega_2}$ and $|\Omega_1 \cap \Omega_2| = 2(L-a)(L-d) + \alpha_*(L-a)$. Thus, there exists a vector field $W_2 \in H_0^1(\Omega)$ satisfying $\nabla \cdot W_2 = g$ in Ω, together with the estimate

$$\|\nabla W_2\|_{L^2(\Omega)} \le 2\gamma_1(\alpha_g + \beta_g).$$

With this particular choice of g we have

$$\int_{\Omega_1 \cap \Omega_2} g(z)\, dz = 0,$$

so that, in view of (4.63), (4.89) and the Jensen inequality, the coefficients α_g and β_g appearing in (4.47) admit the following rough estimate:

$$\alpha_g + \beta_g \le 2\sqrt{1 + \frac{1}{|\Omega_1 \cap \Omega_2|}}\, \|g\|_{L^2(\Omega)} \le 2\sqrt{U^2 + V^2}\sqrt{1 + \frac{1}{|\Omega_1 \cap \Omega_2|}}\, \|\nabla V^\phi\|_{L^2(\Omega)},$$

so that

$$\|\nabla W_2\|_{L^2(\Omega)} \le 4\gamma_1\sqrt{U^2 + V^2}\sqrt{1 + \frac{1}{|\Omega_1 \cap \Omega_2|}}\, \|\nabla V^\phi\|_{L^2(\Omega)}. \tag{4.91}$$

Therefore, we define $v_0 \doteq W_1 + W_2$, and we go back to the proof of Theorem 4.6, where the expression for δ in (4.82) now becomes

$$2\|\nabla v_0\|_{L^2(\Omega)} + \sqrt{\mathcal{S}_0}\, \|v_0\|_{L^4(\Omega)} < \mathcal{S}_0 \eta. \tag{4.92}$$

Since $v_0 = W_1 + W_2$, by the triangle inequality and (4.23) we see that (4.92) is certainly fulfilled if

$$2\|\nabla W_1\|_{L^2(\Omega)} + 3\|\nabla W_2\|_{L^2(\Omega)} + \sqrt{\mathcal{S}_0}\, \|W_1\|_{L^4(\Omega)} < \mathcal{S}_0 \eta.$$

In turn, thanks to (4.87)-(4.88)-(4.91), we see that the latter inequality is implied by

$$\sqrt{U^2 + V^2} < \frac{\mathcal{S}_0 \eta}{2\gamma_2 + 12\gamma_1\gamma_2\sqrt{1 + \frac{1}{|\Omega_1 \cap \Omega_2|}} + \gamma_3\sqrt{\mathcal{S}_0}}. \tag{4.93}$$

The proof is complete after noticing that the right-hand side of (4.93) is increasing with respect to $\mathcal{S}_0$, and using the lower bound for $\mathcal{S}_0$ given in Corollary 4.1. $\qquad\square$

Remark 4.7. *Theorem 4.7 not only gives a lower bound for δ in terms of η and Ω; since η and K are fixed, it also estimates the critical Reynolds number ensuring unique solvability of (4.2)-(4.3) with zero external forcing. Nevertheless, the method provided in the proof of Theorem 4.7 leads to an overestimation of the critical boundary velocity, since some of the inequalities employed are far from being sharp. Similar considerations, following a different approach for the computation of the critical Reynolds number ensuring the stability of a steady laminar flow, were already pointed out by Landau-Lifshitz in 1959, see [173, Chapter III]. A refined method will be used in Section 4.2.4 in the case of a constant horizontal boundary velocity, see Theorem 4.14.*

Regularity results for (4.2)-(4.3) are usually presented under the no-slip boundary condition on the whole boundary $\partial\Omega$, that is, when $U = V = 0$ on ∂Q. In this case, if $f \in L^2(\Omega)$, the regularity of a weak solution $(u, p) \in H_0^1(\Omega) \times L^2(\Omega)$ of (4.2)-(4.3) can be upgraded up to $\left[H^2(\Omega) \cap H_0^1(\Omega)\right] \times H^1(\Omega)$ whenever Ω is of class $\mathcal{C}^2$ (see [115, Theorem IX.5.2]). If Ω were a convex polygon, the same result holds, see [156]. But since we consider obstacles K having a merely Lipschitz boundary, the domain Ω may possess reentrant corners, a fact that introduces singularities in the solution, which may exhibit blow-up of the pressure and of the vorticity near the non-convex vertices, see [55]. Nevertheless, even if we remain with the minimal regularity $H^1(\Omega) \times L^2(\Omega)$, the normal component of the trace of functions in $E_r(\Omega)$ can be treated through (4.38). Furthermore, standard elliptic regularity arguments show that the solution of (4.2)-(4.3) is more regular far from K, a property that we make precise in the next statement. Since we were unable to find a unique reference for its proof, in particular because of the use of solenoidal extensions, for the sake of completeness we include it below by combining several known results adapted to the particular geometry of Ω in (4.1).

Theorem 4.8. *Let Ω be as in (4.1). For $f \in L^2(\Omega)$ and $(U, V) \in \mathbb{R}^2$, let $(u, p) \in \mathcal{V}_*(\Omega) \times L^2(\Omega)$ be a weak solution of (4.2)-(4.3). Then, for any any open set $\Omega_0 \subset \Omega$ such that $\partial\Omega \cap \partial\Omega_0 = \partial Q$ and with an internal boundary of class $\mathcal{C}^2$, one has $(u, p) \in H^2(\Omega_0) \times H^1(\Omega_0)$. Moreover, there exists a constant $C > 0$, depending on η and Ω_0, such that:*

$$\|u\|_{H^2(\Omega_0)} + \|p\|_{H^1(\Omega_0)} \leq C \left(|(U, V)|^4 + |(U, V)| + \|f\|_{L^2(\Omega)}^2 + \|f\|_{L^2(\Omega)}\right). \tag{4.94}$$

Proof. Consider a (non simply connected) $\mathcal{C}^2$-domain $\Omega_1 \subset \Omega_0$ sharing the interior boundary of Ω_0 (namely $\partial\Omega_0 \setminus \partial Q$) and such that $\partial\Omega_1 \cap \partial Q = \emptyset$. We emphasize that $\mathrm{dist}(\partial\Omega_1, \partial Q) > 0$. From (4.39) and (4.69) we know that

$$\begin{cases} \|\nabla u\|_{L^2(\Omega)} \leq C \left(|(U, V)|^2 + |(U, V)| + \|f\|_{L^2(\Omega)}\right), \\ \|p\|_{L^2(\Omega)} \leq C \left(\|\nabla u\|_{L^2(\Omega)}^2 + \|\nabla u\|_{L^2(\Omega)} + \|f\|_{L^2(\Omega)}\right), \end{cases}$$

where, from now on, $C > 0$ will denote a generic constant depending on η and Ω_1 (and therefore, on Ω_0). In particular, we have that $(u \cdot \nabla)u \in L^{3/2}(\Omega)$ with

$$\|(u \cdot \nabla)u\|_{L^{3/2}(\Omega)} \leq \|\nabla u\|_{L^2(\Omega)} \|u\|_{L^6(\Omega)} \leq C\|\nabla u\|_{L^2(\Omega)}^2 \leq C \left(|(U, V)|^2 + |(U, V)| + \|f\|_{L^2(\Omega)}\right)^2,$$

in view of the embedding $H^1(\Omega) \subset L^6(\Omega)$. Moreover, the couple (u, p) weakly solves the Stokes problem

$$-\eta\Delta u + \nabla p = f - (u \cdot \nabla)u, \qquad \nabla \cdot u = 0 \quad \text{in} \ \Omega_1.$$

Then, from [115, Theorem IV.4.1] we know that

$$\begin{aligned} \|u\|_{W^{2,3/2}(\Omega_1)} + \|p\|_{W^{1,3/2}(\Omega_1)} &\leq C \left(\|f\|_{L^{3/2}(\Omega_0)} + \|(u \cdot \nabla)u\|_{L^{3/2}(\Omega_0)} + \|\nabla u\|_{L^2(\Omega_0)} + \|p\|_{L^2(\Omega_0)}\right) \\ &\leq C \left(|(U, V)|^4 + |(U, V)| + \|f\|_{L^2(\Omega)}^2 + \|f\|_{L^2(\Omega)}\right). \end{aligned}$$

With this additional regularity of u, we infer that $(u \cdot \nabla)u \in L^2(\Omega_1)$ and, by repeating the above argument, we obtain

$$\|u\|_{H^2(\Omega_1)} + \|p\|_{H^1(\Omega_1)} \leq C \left(|(U, V)|^4 + |(U, V)| + \|f\|_{L^2(\Omega)}^2 + \|f\|_{L^2(\Omega)}\right). \tag{4.95}$$

This gives the required bound in Ω_1, namely far away from ∂Q (and from the obstacle). In order to reach ∂Q, we employ a localization argument which covers the residual domain $\Omega_* \doteq \Omega \setminus \overline{\Omega_1}$: since it is precompact, it can covered by a finite number of open disks $\{\theta_i\}_{i=1}^m$, for some $m \geq 1$:

$$\overline{\Omega_*} \subset \bigcup_{i=1}^m \theta_i.$$

By reducing the radius of the disks $\{\theta_i\}_{i=1}^m$ (if necessary), we may assume that θ_i does not intersect the internal boundary of Ω_1, for all $i \in \{1, \ldots, m\}$ (in particular, $\theta_i \cap \partial K = \emptyset$).

Next, we introduce a partition of unity subordinate to the open cover $\{\theta_i\}_{i=1}^m$, that is, we consider a family of functions $\{\phi_i\}_{i=1}^m \subset \mathcal{C}_0^\infty(\mathbb{R}^2)$ such that:

$$\phi_i \in \mathcal{C}_0^\infty(\theta_i), \qquad 0 \le \phi_i(x,y) \le 1 \quad \forall (x,y) \in \overline{\Omega_*}, \quad \forall i \in \{1, \ldots, m\}; \qquad \sum_{i=1}^m \phi_i(x,y) = 1 \quad \forall (x,y) \in \overline{\Omega_*}.$$

Therefore, we have

$$u(x,y) = \sum_{i=1}^m \phi_i(x,y) u(x,y), \qquad p(x,y) = \sum_{i=1}^m \phi_i(x,y) p(x,y) \qquad \text{for a.e. } (x,y) \in \overline{\Omega_*},$$

and it suffices to prove that $\phi_i u \in H^2(\Omega_* \cap \theta_i)$ and $\phi_i p \in H^1(\Omega_* \cap \theta_i)$, for every $i \in \{1, \ldots, m\}$. In order to achieve this, we notice that, since Q is convex and ϕ_i has compact support in θ_i, there exists a convex polygon ζ_i such that $\operatorname{supp}(\phi_i) \cap \Omega_* \subset \zeta_i$, see Figure 4.6.
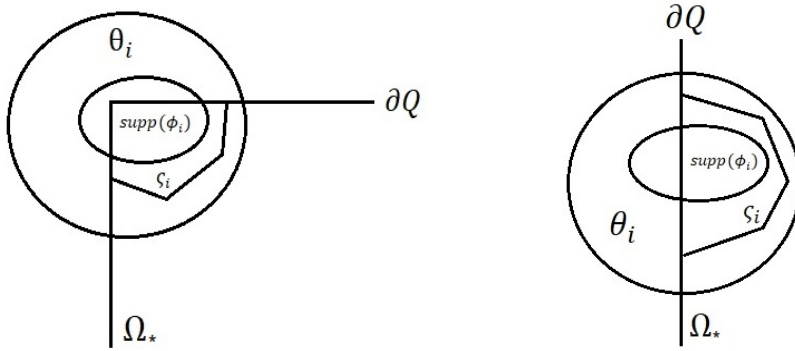

Figure 4.6: Construction of the open set $\zeta_i \subset (\theta_i \cap \Omega_*)$.

Defining $\overline{u} \doteq u - (U, V)$, one notices that $(\phi_i \overline{u}, \phi_i p) \in H_0^1(\zeta_i) \times L^2(\zeta_i)$ and $\nabla \cdot (\phi_i \overline{u}) = \nabla \phi_i \cdot \overline{u} \in H_0^1(\zeta_i)$. Thus, [115, Theorem III.3.3] guarantees the existence of a vector field $v_i \in H^2(\zeta_i) \cap H_0^1(\zeta_i)$ such that

$$\nabla \cdot v_i = \nabla \phi_i \cdot \overline{u} \quad \text{in } \zeta_i, \qquad \|v_i\|_{H^2(\zeta_i)} \le c_i \|\nabla \phi_i \cdot \overline{u}\|_{H^1(\zeta_i)}, \tag{4.96}$$

for some constant $c_i > 0$ depending only on θ_i. Since (u, p) is a solution of (4.2)-(4.3), we deduce that the pair $(\phi_i \overline{u} - v_i, \phi_i p) \in H_0^1(\zeta_i) \times L^2(\zeta_i)$ satisfies the Stokes system

$$-\eta \Delta(\phi_i \overline{u} - v_i) + \nabla(\phi_i p) = \omega_i + \eta(\Delta \phi_i)(U, V) + \eta \Delta v_i, \qquad \nabla \cdot (\phi_i \overline{u} - v_i) = 0 \qquad \text{in } \zeta_i,$$

with $\omega_i \doteq \phi_i[f - (u \cdot \nabla)u] - \eta[(\Delta \phi_i)u + 2(\nabla \phi_i \cdot \nabla)u] + p \nabla \phi_i \in L^{3/2}(\zeta_i)$ and, by bootstrapping as in Ω_1 we can deduce that $\omega_i \in L^2(\zeta_i)$. Then we apply [156, Theorem 2] to infer that $(\phi_i \overline{u}, \phi_i p) \in H^2(\zeta_i) \times H^1(\zeta_i)$ and the existence of $C_i > 0$ (depending only on θ_i) such that

$$\|\phi_i \overline{u} - v_i\|_{H^2(\zeta_i)} + \|\phi_i p\|_{H^1(\zeta_i)} \le C_i \left(\|\omega_i\|_{L^2(\zeta_i)} + \eta |(U,V)| \|\Delta \phi_i\|_{L^2(\zeta_i)} + \eta \|\Delta v_i\|_{L^2(\zeta_i)} \right).$$

In view of (4.96), this implies

$$\|\phi_i u\|_{H^2(\Omega_* \cap \theta_i)} + \|\phi_i p\|_{L^2(\Omega_* \cap \theta_i)} \le C_i \left(\|\omega_i\|_{L^2(\Omega_* \cap \theta_i)} + |(U,V)| \|\phi_i\|_{H^2(\Omega_* \cap \theta_i)} + \|\nabla \phi_i \cdot \overline{u}\|_{H^1(\Omega_* \cap \theta_i)} \right),$$

where $C_i > 0$ now denotes a constant depending on η and θ_i. By summing over $i \in \{1, \ldots, m\}$ we get

$$\|u\|_{H^2(\Omega_*)} + \|p\|_{H^1(\Omega_*)} \le \sum_{i=1}^m C_i \left(\|\omega_i\|_{L^2(\Omega_* \cap \theta_i)} + |(U,V)| \|\phi_i\|_{H^2(\Omega_* \cap \theta_i)} + \|\nabla \phi_i \cdot \overline{u}\|_{H^1(\Omega_* \cap \theta_i)} \right)$$

$$\le C \left[\|\nabla u\|_{L^2(\Omega_0)} \left(\|\nabla u\|_{L^2(\Omega_0)} + 1 \right) + \|p\|_{L^2(\Omega_0)} + \|f\|_{L^2(\Omega_0)} + |(U,V)| \right] \tag{4.97}$$

$$\le C \left(|(U,V)|^4 + |(U,V)| + \|f\|_{L^2(\Omega)}^2 + \|f\|_{L^2(\Omega)} \right),$$

after applying the Poincaré-type inequalities to $\bar{u} = u - (U, V)$, using that $\{\phi_i\}_{i=1}^m \subset \mathcal{C}_0^\infty(\mathbb{R}^2)$ and (4.69). The proof is complete after putting together (4.95) and (4.97). $\qquad\square$

Remark 4.8. *If the obstacle K has a $\mathcal{C}^2$ boundary, then the arguments of Theorem 4.8 enables to prove that weak solutions of (4.2)-(4.3) in Ω belong to $H^2(\Omega) \times H^1(\Omega)$.*

4.2.2 Symmetry and almost symmetry

Turbulence in fluids with large Reynolds number may be detected by refined numerical simulations using Computational Fluid Dynamics [109], see Figure 4.7 where the dependence of the flow on the Reynolds number is emphasized in a symmetric domain.
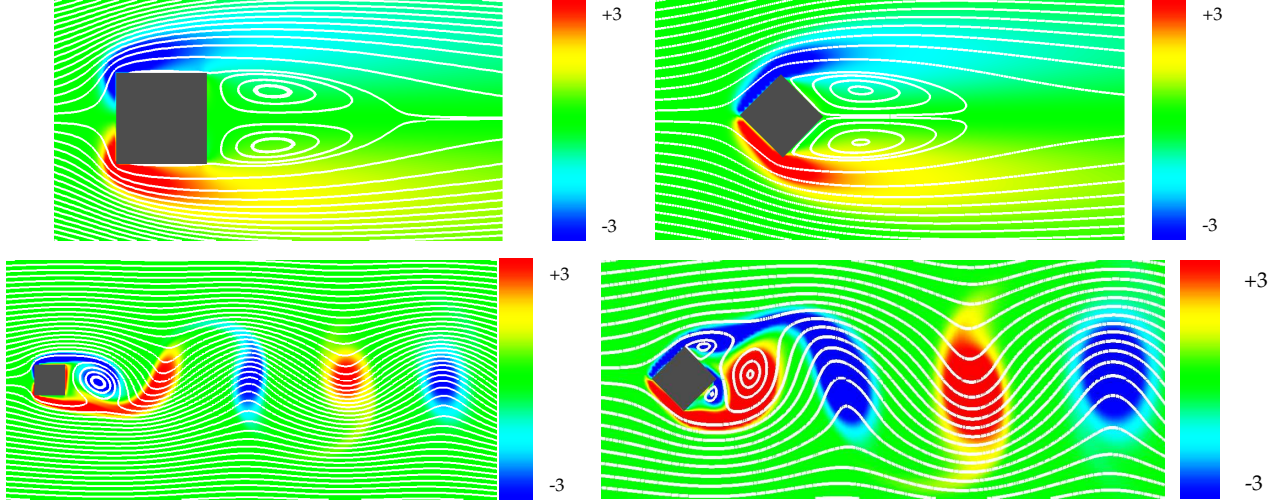

Figure 4.7: CFD simulation of a flow around a square cylinder (top line Re= 30, bottom line Re= 200) by Fuka-Brechler [109], reproduced with courtesy of the authors.

The pattern displayed in Figure 4.7 will be essential to comment the results throughout the chapter.

We consider here domains Ω being symmetric with respect to the x-axis. Moreover, we initially assume that the boundary data in (4.3) satisfy

$$U(x, -y) = U(x, y) \quad \text{and} \quad V(x, -y) = -V(x, y) \qquad \forall (x, y) \in \partial Q. \tag{4.98}$$

Concerning the source $f = (f_1, f_2) \in H^{-1}(\Omega)$, we recall that a distribution is called even (resp. odd) if its kernel contains the space of odd (resp. even) test functions. In this symmetric framework, we complement Theorem 4.6 with the following result.

Theorem 4.9. *Let Ω be as in (4.1), K being symmetric with respect to the x-axis. Suppose that $f = (f_1, f_2) \in H^{-1}(\Omega)$ and that $(U, V) \in H^{1/2}(\partial Q)$ satisfy (4.4). Assume moreover that f_1 is y-even, f_2 is y-odd, and (U, V) verifies (4.98). Then:*
• there exists (at least) one weak solution $(u_1, u_2, p) \in \mathcal{V}_*(\Omega)^2 \times L_0^2(\Omega)$ of (4.2)-(4.3) satisfying the symmetry property

$$u_1(x, -y) = u_1(x, y), \quad u_2(x, -y) = -u_2(x, y), \quad p(x, -y) = p(x, y) \qquad \text{for a.e. } (x, y) \in \Omega; \tag{4.99}$$

• if $(u_1, u_2, p) \in H^1(\Omega)^2 \times L_0^2(\Omega)$ is a weak solution of (4.2)-(4.3), then also (v_1, v_2, q) with

$$v_1(x, y) = u_1(x, -y), \quad v_2(x, y) = -u_2(x, -y), \quad q(x, y) = p(x, -y) \qquad \text{for a.e. } (x, y) \in \Omega \tag{4.100}$$

solves (4.2)-(4.3);
• if (4.70) holds, then the unique weak solution of (4.2)-(4.3) satisfies (4.99).

Proof. By Proposition 4.1, there exists a symmetric solenoidal extension $\hat{v} \in H^1(\Omega)$ of the boundary data $(U, V) \in H^{1/2}(\partial Q)$ such that

$$\begin{cases} \nabla \cdot \hat{v} = 0 \quad \text{in } \Omega, \quad \hat{v} = (U, V) \ \text{on } \partial Q, \quad \hat{v} = (0,0) \quad \text{on } \partial K \\ |\beta(z, \hat{v}, z)| \leq \dfrac{\eta}{2} \|\nabla z\|_{L^2(\Omega)}^2 \quad \forall z \in \mathcal{V}(\Omega); \quad \hat{v}_1 \text{ is } y\text{-even}, \quad \hat{v}_2 \text{ is } y\text{-odd}. \end{cases} \tag{4.101}$$

We introduce the space

$$\mathcal{Z}(\Omega) = \{v \in \mathcal{V}(\Omega) \mid v \text{ satisfies the symmetry property } (4.99)\},$$

which is a closed subspace of $\mathcal{V}(\Omega)$ and therefore it constitutes a Hilbert space under the Dirichlet scalar product. To prove the existence of a weak symmetric solution $(u, p) \in \mathcal{V}_*(\Omega) \times L_0^2(\Omega)$ of (4.2)-(4.3) amounts to show the existence of $(\hat{u}, p) \in \mathcal{Z}(\Omega) \times L_0^2(\Omega)$ such that

$$-\eta \Delta \hat{u} + (\hat{u} \cdot \nabla)\hat{u} + (\hat{u} \cdot \nabla)\hat{v} + (\hat{v} \cdot \nabla)\hat{u} + \nabla p = f + \eta \Delta \hat{v} - (\hat{v} \cdot \nabla)\hat{v} \quad \text{in } \Omega \tag{4.102}$$

in weak sense, then the solution will be given by $u = \hat{u} + \hat{v}$ and p will have the required symmetry property as a consequence of (4.102). Fix $v_0 \in \mathcal{Z}(\Omega)$ and consider the linearized version of (4.102), namely

$$-\eta \Delta \hat{u} + (v_0 \cdot \nabla)\hat{u} + (\hat{u} \cdot \nabla)\hat{v} + (\hat{v} \cdot \nabla)\hat{u} + \nabla p = f + \eta \Delta \hat{v} - (\hat{v} \cdot \nabla)\hat{v}, \quad \nabla \cdot \hat{u} = 0 \ \text{ in } \Omega.$$

By symmetric weak solution of this problem we intend a function $\hat{u} \in \mathcal{Z}(\Omega)$ such that

$$\eta(\nabla \hat{u}, \nabla \varphi)_{L^2(\Omega)} + \beta(v_0, \hat{u}, \varphi) + \beta(\hat{u}, \hat{v}, \varphi) + \beta(\hat{v}, \hat{u}, \varphi) = \langle F, \varphi \rangle_\Omega \quad \forall \varphi \in \mathcal{Z}(\Omega), \tag{4.103}$$

where $F \doteq f + \eta \Delta \hat{v} - (\hat{v} \cdot \nabla)\hat{v} \in H^{-1}(\Omega)$ is such that F_1 is y-even and F_2 is y-odd. It is quite standard for the Navier-Stokes equations to see that the bilinear form $A : \mathcal{Z}(\Omega) \times \mathcal{Z}(\Omega) \to \mathbb{R}$ defined by

$$A(v, w) = \eta(\nabla v, \nabla w)_{L^2(\Omega)} + \beta(v_0, v, w) + \beta(v, \hat{v}, w) + \beta(\hat{v}, v, w) \quad \forall v, w \in \mathcal{Z}(\Omega),$$

is continuous and coercive (for the latter property, one needs the bound in (4.101)). Therefore, the Lax-Milgram Theorem ensures the existence of a unique function $\hat{u} \in \mathcal{Z}(\Omega)$ satisfying (4.103). Whence, in view of the compact embedding $\mathcal{Z}(\Omega) \subset L^4(\Omega)$, we have constructed a compact operator $T : L^4(\Omega) \to L^4(\Omega)$ such that, for any $v_0 \in L^4(\Omega)$, $T(v_0) = \hat{u}$ is the unique symmetric solution of (4.103). Moreover, after testing (4.103) with $\varphi = \hat{u}$ and using the bound in (4.101) we obtain

$$\|\nabla \hat{u}\|_{L^2(\Omega)} \leq \frac{2}{\eta} \|F\|_{H^{-1}(\Omega)},$$

so that T actually maps the (non-empty) convex compact set $\{v \in L^4(\Omega) \mid \eta\|\nabla v\|_{L^2(\Omega)} \leq 2\|F\|_{H^{-1}(\Omega)}\}$ into itself. Then the Schauder Fixed Point Theorem ensures the existence of $\hat{u} \in \mathcal{Z}(\Omega)$ such that $T(\hat{u}) = \hat{u}$, that is, $\hat{u}$ is a weak solution of (4.102) satisfying the symmetry property (4.99). By the symmetry properties of F, we infer that the resulting pressure $p \in L_0^2(\Omega)$, which arises as a consequence of [115, Lemma III.1.1], also satisfies the symmetry property given in (4.99).

Finally, under the assumptions of the statement, one can check that also (4.100) solves (4.2)-(4.3). Thus, in case of uniqueness, the solution satisfies the symmetry property (4.99). $\qquad \square$

Remark 4.9. *Since δ in (4.85) depends increasingly on η, and therefore decreasingly on Re, Figure 4.7 is compatible with Theorem 4.6: as long as Re is small the flow is symmetric, while if Re is large, uniqueness is lost and asymmetric solutions may arise. Hence, in a symmetric framework, the existence of an asymmetric solution is a sufficient condition for non-uniqueness. Whether it is also a necessary condition is an open problem. For 2D symmetric conditions in a channel past a circular cylinder, Sahin-Owens [228, Fig.6] (see branches 1, 3, 5 therein), numerically found different symmetric solutions for suitable Reynolds numbers but for different proportions between the width of the channel and the diameter of the cylinder.*

In real life, perfect symmetry does not exist, there are no perfectly symmetric flows and any obstacle inevitably has small imperfections. It is therefore natural to wonder whether "almost symmetric" boundary data and obstacles give rise to "almost symmetric" solutions, in a suitable sense. Since we are not interested in explicit bounds, we will consider

$$(U, V) \in H^{1/2}(\partial Q) \qquad f \in L^2(\Omega).$$

Firstly, we maintain fixed the obstacle K and we perturb the boundary velocity and the external force. For any $\varepsilon > 0$, $(U, V) \in H^{1/2}(\partial \Omega)$ and $f \in L^2(\Omega)$ we denote

$$\mathcal{B}_\varepsilon(U, V, f) = \left\{ (A, B, g) \in H^{1/2}(\partial \Omega)^2 \times L^2(\Omega) \; \middle| \; \begin{array}{c} (A, B) \text{ satisfies } (4.4), \\ \|(A - U, B - V)\|_{H^{1/2}(\partial \Omega)} + \|g - f\|_{L^2(\Omega)} < \varepsilon \end{array} \right\}.$$

In this setting, we prove the following continuous dependence result.

Theorem 4.10. *Let Ω be as in (4.1), $f \in L^2(\Omega)$ and $(U, V) \in H^{1/2}(\partial \Omega)$ satisfying (4.4). There exists $\delta_0 = \delta_0(\eta, \Omega) > 0$ such that, if*

$$\|(U, V)\|_{H^{1/2}(\partial Q)} + \|f\|_{L^2(\Omega)} < \delta_0, \tag{4.104}$$

then (4.2)-(4.3) in Ω admits a unique weak solution $(u, p) \in \mathcal{V}_*(\Omega) \times L_0^2(\Omega)$ with data (U, V, f). Furthermore, there exists $\varepsilon_0 = \varepsilon_0(U, V, f) > 0$ such that, for all $\varepsilon < \varepsilon_0$ and all $(U_\varepsilon, V_\varepsilon, f_\varepsilon) \in \mathcal{B}_\varepsilon = \mathcal{B}_\varepsilon(U, V, f)$, problem (4.2)-(4.3) with data $(U_\varepsilon, V_\varepsilon, f_\varepsilon) \in \mathcal{B}_\varepsilon$ admits a unique weak solution $(u_\varepsilon, p_\varepsilon) \in \mathcal{V}_*(\Omega) \times L_0^2(\Omega)$. Furthermore, the following limit holds:

$$\lim_{\varepsilon \to 0} \sup_{(U_\varepsilon, V_\varepsilon, f_\varepsilon) \in \mathcal{B}_\varepsilon} \left(\|\nabla(u - u_\varepsilon)\|_{L^2(\Omega)} + \|p - p_\varepsilon\|_{L^2(\Omega)} \right) = 0.$$

Proof. The quantitative uniqueness statement (4.104) follows directly from (4.70), since

$$\|f\|_{H^{-1}(\Omega)} \leq \lambda^{-1} \|f\|_{L^2(\Omega)},$$

with $\lambda > 0$ the Poincaré constant of Ω. Now, let $\delta_0 = \delta_0(\eta, \Omega) > 0$ be as in (4.104). Define

$$\varepsilon_0 = \varepsilon_0(U, V, f) = \delta_0 - \|(U, V)\|_{H^{1/2}(\partial \Omega)} - \|f\|_{L^2(\Omega)} > 0$$

so that, if $0 < \varepsilon < \varepsilon_0$ and $(U_\varepsilon, V_\varepsilon, f_\varepsilon) \in \mathcal{B}_\varepsilon$, we have

$$\|(U_\varepsilon, V_\varepsilon)\|_{H^{1/2}(\partial \Omega)} + \|f_\varepsilon\|_{L^2(\Omega)} \leq \|(U_\varepsilon - U, V_\varepsilon - V)\|_{H^{1/2}(\partial \Omega)} + \|f_\varepsilon - f\|_{L^2(\Omega)} + \|(U, V)\|_{H^{1/2}(\partial \Omega)} + \|f\|_{L^2(\Omega)}$$
$$< \varepsilon + \delta_0 - \varepsilon_0 < \delta_0,$$

and problem (4.2)-(4.3) with data $(U_\varepsilon, V_\varepsilon, f_\varepsilon)$ admits a unique weak solution $(u_\varepsilon, p_\varepsilon) \in \mathcal{V}_*(\Omega) \times L_0^2(\Omega)$, see Theorem 4.6. So, fix $\varepsilon \in (0, \varepsilon_0)$ and choose any $(U_\varepsilon, V_\varepsilon, f_\varepsilon) \in \mathcal{B}_\varepsilon$. In view of Proposition 4.1, there exists a vector field $w_0 \in \mathcal{V}_*(\Omega)$ such that

$$w_0 = (U, V) - (U_\varepsilon, V_\varepsilon) \quad \text{on } \partial Q, \qquad \|\nabla w_0\|_{L^2(\Omega)} \leq C\|(U, V) - (U_\varepsilon, V_\varepsilon)\|_{H^{1/2}(\partial Q)} \leq C\varepsilon, \tag{4.105}$$

for some constant $C > 0$ depending only on Ω. Let $\xi \doteq u - u_\varepsilon - w_0$, so that $\xi \in \mathcal{V}(\Omega)$. After subtracting the equations (4.2) satisfied by (u, p, f) and $(u_\varepsilon, p_\varepsilon, f_\varepsilon)$ in Ω we infer that:

$$-\eta \Delta \xi + [(\xi + w_0) \cdot \nabla](\xi + w_0) + [(u - u_\varepsilon) \cdot \nabla]u_\varepsilon + (u_\varepsilon \cdot \nabla)(u - u_\varepsilon) + \nabla(p - p_\varepsilon) = \eta \Delta w_0 + f - f_\varepsilon, \tag{4.106}$$

with $\eta \Delta w_0 + f - f_\varepsilon \in H^{-1}(\Omega)$. Here (4.106) is intended in weak sense, see (4.68); we test it with ξ, we integrate by parts in Ω in order to obtain the upper bound (after applying (4.105)):

$$\eta \|\nabla \xi\|_{L^2(\Omega)}^2 + \beta(\xi + w_0, \xi + w_0, \xi) + \beta(u - u_\varepsilon, u_\varepsilon, \xi) + \beta(u_\varepsilon, u - u_\varepsilon, \xi) \leq \varepsilon(C\eta + 1)\|\nabla \xi\|_{L^2(\Omega)}. \tag{4.107}$$

79

After applying property (4.37) repeatedly we deduce that:

$$\beta(\xi + w_0, \xi + w_0, \xi) + \beta(u - u_\varepsilon, u_\varepsilon, \xi) + \beta(u_\varepsilon, u - u_\varepsilon, \xi) = \beta(\xi + w_0, u, \xi) + \beta(u_\varepsilon, w_0, \xi). \qquad (4.108)$$

In view of (4.35) and (4.105) we have

$$|\beta(\xi + w_0, u, \xi) + \beta(u_\varepsilon, w_0, \xi)| \leq \frac{1}{\mathcal{S}_0}\|\nabla u\|_{L^2(\Omega)}\|\nabla \xi\|_{L^2(\Omega)}^2 + \frac{C\varepsilon}{\mathcal{S}}\left(\|\nabla u\|_{L^2(\Omega)} + \|\nabla u_\varepsilon\|_{L^2(\Omega)}\right)\|\nabla \xi\|_{L^2(\Omega)},$$

inequality that, together with (4.108), can be inserted into (4.107) to yield

$$\left(\eta - \frac{1}{\mathcal{S}_0}\|\nabla u\|_{L^2(\Omega)}\right)\|\nabla \xi\|_{L^2(\Omega)} \leq \left[C\left(\frac{1}{\mathcal{S}}\left(\|\nabla u\|_{L^2(\Omega)} + \|\nabla u_\varepsilon\|_{L^2(\Omega)}\right) + \eta\right) + 1\right]\varepsilon. \qquad (4.109)$$

The uniqueness assumption ensures that $\|\nabla u\|_{L^2(\Omega)} < \mathcal{S}_0\eta$, and since $u - u_\varepsilon = \xi + w_0$, we have

$$\|\nabla(u - u_\varepsilon)\|_{L^2(\Omega)} \leq \frac{C\left[\left(\frac{\mathcal{S}_0}{\mathcal{S}} - 1\right)\|\nabla u\|_{L^2(\Omega)} + \frac{\mathcal{S}_0}{\mathcal{S}}\|\nabla u_\varepsilon\|_{L^2(\Omega)} + 2\mathcal{S}_0\eta\right] + \mathcal{S}_0}{\mathcal{S}_0\eta - \|\nabla u\|_{L^2(\Omega)}}\varepsilon. \qquad (4.110)$$

On the other hand, by subtracting the equations of conservation of momentum (4.2) satisfied by (u, p, f) and $(u_\varepsilon, p_\varepsilon, f_\varepsilon)$ in Ω we infer that:

$$\nabla(p - p_\varepsilon) = \eta\Delta(u - u_\varepsilon) + [(u_\varepsilon - u)\cdot\nabla]u_\varepsilon + (u\cdot\nabla)(u_\varepsilon - u) + f - f_\varepsilon, \qquad (4.111)$$

an identity that must also be intended in the weak sense of $H^{-1}(\Omega)$. In particular:

$$\|\nabla(p - p_\varepsilon)\|_{H^{-1}(\Omega)} \leq \eta\|\nabla(u - u_\varepsilon)\|_{L^2(\Omega)} + \|\nabla u_\varepsilon\|_{L^2(\Omega)}\|u - u_\varepsilon\|_{L^6(\Omega)} + \|\nabla(u - u_\varepsilon)\|_{L^2(\Omega)}\|u\|_{L^6(\Omega)} + \varepsilon$$

$$\leq \left[\eta + C\left(\|\nabla u\|_{L^2(\Omega)} + \|\nabla u_\varepsilon\|_{L^2(\Omega)}\right)\right]\|\nabla(u - u_\varepsilon)\|_{L^2(\Omega)} + \varepsilon,$$

where $C > 0$ is the embedding constant for $H^1(\Omega) \subset L^6(\Omega)$. From (4.43) we can deduce the existence of a constant $M > 0$ (depending only on Ω) such that $\|p - p_\varepsilon\|_{L^2(\Omega)} \leq M\|\nabla(p - p_\varepsilon)\|_{H^{-1}(\Omega)}$. This yields

$$\|\nabla(u - u_\varepsilon)\|_{L^2(\Omega)} + \|p - p_\varepsilon\|_{L^2(\Omega)} \leq \left[1 + M\left(\eta + C\left(\|\nabla u\|_{L^2(\Omega)} + \|\nabla u_\varepsilon\|_{L^2(\Omega)}\right)\right)\right]\|\nabla(u - u_\varepsilon)\|_{L^2(\Omega)} + M\varepsilon,$$

which, together with (4.110) and (4.69), completes the proof. $\qquad\square$

Theorem 4.10 is a continuous dependence result which shows, in particular, that if the first component of f is y-even, the second component of f is y-odd and the boundary data (U, V) satisfies the symmetry property (4.98), then the solution $(u_\varepsilon, p_\varepsilon)$ is "almost symmetric", since in this case (u, p) verifies (4.99). This is made precise in the following statement for which we introduce a further notation. For any function (or distribution) $\phi = \phi(x, y)$ we denote its even and odd parts by

$$\phi^E(x, y) = \frac{\phi(x, y) + \phi(x, -y)}{2}, \qquad \phi^O(x, y) = \frac{\phi(x, y) - \phi(x, -y)}{2}.$$

Then we have

Corollary 4.3. *Let Ω be as in (4.1) and K symmetric with respect to the x-axis. Let $f = (f_1, f_2) \in L^2(\Omega)^2$ with f_1 y-even and f_2 y-odd, let $(U, V) \in H^{1/2}(\partial Q)$ satisfy (4.4), (4.70) and (4.98). Then there exists $\varepsilon_0 = \varepsilon_0(U, V, f) > 0$ such that, for all $\varepsilon < \varepsilon_0$ and all $(U_\varepsilon, V_\varepsilon, f_\varepsilon) \in \mathcal{B}_\varepsilon = \mathcal{B}_\varepsilon(0, 0, 0)$, the problem*

$$-\eta\Delta v + (v\cdot\nabla)v + \nabla q = f + f_\varepsilon \quad in \ \ \Omega, \qquad v = (U + U_\varepsilon, V + V_\varepsilon) \quad on \ \ \partial Q, \qquad v = (0, 0) \quad on \ \ \partial K,$$

admits a unique weak solution $(v_1, v_2, q) \in \mathcal{V}_*(\Omega) \times L_0^2(\Omega)$ and

$$\lim_{\varepsilon\to 0} \sup_{(U_\varepsilon, V_\varepsilon, f_\varepsilon)\in\mathcal{B}_\varepsilon} \left(\|\nabla(v_1^O, v_2^E)\|_{L^2(\Omega)} + \|q^O\|_{L^2(\Omega)}\right) = 0.$$

Theorem 4.10 and Corollary 4.3 make assumptions on the fluid flow, namely on the boundary data (U, V) and on the force f. This means that *two flows having almost the same boundary data and forcing behave quite similarly.* We are now interested in a second perturbation result, by considering *the same flow conditions but with possibly different obstacles*, that is, we fix $(U, V) \in H^{1/2}(\partial Q)$ and $f \in L^2(\Omega)$, and we allow K to vary. This is the problem that occurs if an object (the obstacle) has not been manufactured with enough precision. However, this second problem is extremely more delicate and we need first to make clear what kind of imprecisions are allowed.

Definition 4.2. *Given a C^2-domain $K \subset Q$ such that $\partial K \cap \partial Q = \emptyset$, we say that the family of Lipschitz domains $\{K_\varepsilon\}_{\varepsilon>0}$ outer-approximates K as $\varepsilon \to 0$ if:*

– $K \subset K_{\varepsilon_2} \subset K_{\varepsilon_1} \subset Q$, for every $0 < \varepsilon_2 < \varepsilon_1$;

– $\mathrm{dist}_{\mathrm{H}}(\overline{K_\varepsilon}, \overline{K}) \leq \varepsilon$, for every $\varepsilon > 0$, where $\mathrm{dist}_{\mathrm{H}}$ denotes the Hausdorff distance;

– there exists a finite number of disks $\{B_1, \ldots, B_N\}$ such that, for any $\varepsilon > 0$, K_ε is contained in the union of N domains, each one being star-shaped with respect to one of these disks $(\star)$.

The first two conditions in Definition 4.2 tell us that K_ε approximates K monotonically from outside. The third condition, that we denote by $(\star)$, is a geometric assumption that yields uniform bounds for some constants depending on K_ε. We can now prove the following statement.

Theorem 4.11. *Let Ω be as in (4.1), K with C^2-boundary. Let $f \in L^2(\Omega)$ and $(U, V) \in H^{1/2}(\partial Q)$ satisfy (4.4)-(4.104), and let $(u, p) \in \mathcal{V}_*(\Omega) \times L^2_0(\Omega)$ be the unique weak solution of (4.2)-(4.3), see Theorem 4.10. For any family of Lipschitz domains $\{K_\varepsilon\}_{\varepsilon>0}$ that outer-approximates K, there exists $\varepsilon_0 > 0$ such that if $\varepsilon < \varepsilon_0$ then (4.2)-(4.3) in $\Omega_\varepsilon = Q \setminus K_\varepsilon$ admits a unique solution $(u_\varepsilon, p_\varepsilon) \in \mathcal{V}_*(\Omega_\varepsilon) \times L^2_0(\Omega_\varepsilon)$ and*

$$\lim_{\varepsilon \to 0} \left(\|\nabla(u_\varepsilon - u)\|_{L^2(\Omega_\varepsilon)} + \|p_\varepsilon - p\|_{L^2(\Omega_\varepsilon)} \right) = 0. \tag{4.112}$$

Proof. Take an (open) smooth connected domain K_0 such that $\overline{K} \subset K_0 \subset \overline{K_0} \subset Q$; we have in mind a small neighborhood of K. Let $\Omega_0 = Q \setminus K_0$ and consider a solenoidal extension $\overline{v}$ of the data in Ω_0, that is,

$$\overline{v} \in \mathcal{V}_*(\Omega_0), \qquad \overline{v} = (U, V) \text{ on } \partial Q, \qquad \|\nabla \overline{v}\|_{L^2(\Omega_0)} \leq C_0 \|(U, V)\|_{H^{1/2}(\partial Q)},$$

where $C_0 = C_0(\Omega_0) > 0$ is independent on the boundary data, see [170]. Then the function

$$v_0(x, y) = \begin{cases} \overline{v}(x, y) & \text{if } (x, y) \in \Omega_0 \\ 0 & \text{if } (x, y) \in K_0 \setminus K \end{cases}$$

is a solenoidal extension of the data (U, V) in Ω and also in Ω_ε, provided ε is small enough in such a way that $K_\varepsilon \subset K_0$. Hence, the constant C_0 can be used to compute the uniqueness threshold (4.85) (and also (4.104)) in Ω and Ω_ε, for any small enough $\varepsilon > 0$.

For all $\varepsilon > 0$ the existence of a weak solution $(u_\varepsilon, p_\varepsilon)$ of (4.2)-(4.3) in Ω_ε follows from Theorem 4.6 applied to Ω_ε. Theorem 4.10 ensures uniqueness whenever

$$\|(U, V)\|_{H^{1/2}(\partial Q)} + \|f\|_{L^2(\Omega_\varepsilon)} < \delta_\varepsilon, \tag{4.113}$$

where $\delta_\varepsilon = \delta_\varepsilon(\eta, \Omega_\varepsilon)$ is as in (4.104), but relative to Ω_ε. A careful look at the proof of Theorem 4.10 and formula (4.85) show that δ_ε depends on $\mathcal{S}^\varepsilon$ and $\mathcal{S}^\varepsilon_0$, namely the Sobolev constants defined in (4.23) but relative to Ω_ε, and on the Poincaré constant of Ω_ε (by the above construction, C_0 is independent of ε). Since K_ε outer-approximates K, one has $\mathcal{S}^\varepsilon \to \mathcal{S}$ and $\mathcal{S}^\varepsilon_0 \to \mathcal{S}_0$ as $\varepsilon \to 0$, and also the Poincaré constants converge. Therefore, by (4.104) and by continuity, we know that (4.113) holds provided ε is small enough, say $\varepsilon < \varepsilon_0$. Not only this proves the uniqueness of the solution $(u_\varepsilon, p_\varepsilon)$ but, according to Theorem 4.6, it also proves the uniform bound

$$\|\nabla u_\varepsilon\|_{L^2(\Omega_\varepsilon)} < \mathcal{S}^\varepsilon_0 \eta \leq B \qquad \forall \varepsilon > 0, \tag{4.114}$$

for some $B > 0$ (independent of ε) since $\mathcal{S}_0^\varepsilon \to \mathcal{S}_0$ as $\varepsilon \to 0$.

To complete the proof we have to show that (4.112) holds. To this end, we first claim that there exist positive constants $\{\sigma_\varepsilon\}_{\varepsilon>0}$ such that $\sigma_\varepsilon \to 0$ as $\varepsilon \to 0$ and

$$\|u\|_{H^{1/2}(\partial K_\varepsilon)} = \|u\|_{L^2(\partial K_\varepsilon)} + \left(\int_{\partial K_\varepsilon} \int_{\partial K_\varepsilon} \frac{|u(z_1) - u(z_2)|^2}{|z_1 - z_2|^2} \, ds_{z_1} \, ds_{z_2} \right)^{1/2} \le \sigma_\varepsilon \qquad \forall \varepsilon > 0. \qquad (4.115)$$

Indeed, as in the proof of Theorem 4.8, by localizing in a neighborhood of K one may deduce that $(u, p) \in H^2(\mathcal{O} \setminus \overline{K}) \times H^1(\mathcal{O} \setminus \overline{K})$, for any $\mathcal{C}^2$-domain $\mathcal{O} \subset Q$ such that $\mathcal{O} \cap \partial\Omega = \partial K$. In particular, $u \in \mathcal{C}^{0,\nu}(\overline{\mathcal{O}})$ for any $0 < \nu < 1$. Then, since u vanishes on ∂K, the uniform continuity of u in $\overline{\mathcal{O}}$ ensures the existence of positive constants $\{\theta_\varepsilon\}_{\varepsilon>0}$ such that $\theta_\varepsilon \to 0$ as $\varepsilon \to 0$ and $\|u\|_{L^\infty(\partial K_\varepsilon)} \le \theta_\varepsilon$ for every $\varepsilon > 0$. Moreover, condition $(\star)$ ensures the existence of $\Gamma > 0$ (depending on Ω but independent of ε) such that $|\partial K_\varepsilon| \le \Gamma^2$ for all $\varepsilon > 0$. By combining these two facts, we infer

$$\|u\|_{L^2(\partial K_\varepsilon)} \le \|u\|_{L^\infty(\partial K_\varepsilon)} \sqrt{|\partial K_\varepsilon|} \le \Gamma \theta_\varepsilon \qquad \forall \varepsilon > 0. \qquad (4.116)$$

Moreover, if $M > 0$ denotes the Hölder constant of u in $\overline{\mathcal{O}}$ for $\nu = 4/5$, we have

$$|u(z_1) - u(z_2)|^2 = |u(z_1) - u(z_2)|^{1/8} |u(z_1) - u(z_2)|^{15/8} \le (2\theta_\varepsilon)^{1/8} M^{15/8} |z_1 - z_2|^{3/2}$$

and, in turn,

$$\int_{\partial K_\varepsilon} \int_{\partial K_\varepsilon} \frac{|u(z_1) - u(z_2)|^2}{|z_1 - z_2|^2} \, ds_{z_1} \, ds_{z_2} \le (2M^{15}\theta_\varepsilon)^{1/8} \int_{\partial K_\varepsilon} \int_{\partial K_\varepsilon} \frac{ds_{z_1} \, ds_{z_2}}{|z_1 - z_2|^{1/2}}. \qquad (4.117)$$

Next we notice that, for every $\varepsilon > 0$, the boundary ∂K_ε can be parametrized by a Lipschitz-continuous vector field $\phi_\varepsilon : [0, 1] \to Q$ such that $\phi_\varepsilon(0) = \phi_\varepsilon(1)$; by condition $(\star)$ we know that the Lipschitz constants of ϕ_ε are uniformly bounded (independently of ε). Whence, the double integral in (4.117) is uniformly bounded, that is, there exists $\Lambda > 0$ (independent of ε) such that

$$\left(\int_{\partial K_\varepsilon} \int_{\partial K_\varepsilon} \frac{|u(z_1) - u(z_2)|^2}{|z_1 - z_2|^2} \, ds_{z_1} \, ds_{z_2} \right)^{1/2} \le \Lambda \, \theta_\varepsilon^{1/16} \qquad \forall \varepsilon > 0.$$

By combining this bound with (4.116) we obtain (4.115) with $\sigma_\varepsilon = \Gamma \theta_\varepsilon + \Lambda \theta_\varepsilon^{1/16}$.

Note that the incompressibility condition and (4.4) imply that

$$\int_{\partial\Omega_\varepsilon} u \cdot \hat{n} \, ds = \int_{\partial K_\varepsilon} u \cdot \hat{n} \, ds = 0.$$

Then, by Proposition 4.1 (applied to Ω_ε), there exists a solenoidal vector field $w_0 \in H^1(\Omega_\varepsilon)$ such that

$$w_0 = (0,0) \text{ on } \partial Q, \qquad w_0 = u|_{\partial K_\varepsilon} \text{ on } \partial K_\varepsilon, \qquad \|\nabla w_0\|_{L^2(\Omega_\varepsilon)} \le C_\varepsilon \|u\|_{H^{1/2}(\partial K_\varepsilon)}, \qquad (4.118)$$

for some constant $C_\varepsilon > 0$ that depends only on Ω_ε. From [196, Section 1.1.8], we know that condition $(\star)$ yields uniform bounds for the Lipschitz constant of the boundary and a uniform cone property. Then, by [115, Exercise II.3.5] and [115, Formula (II.4.11)], there exists $C > 0$ (depending only on the family of balls $\{B_1, \ldots, B_N\}$) such that $C_\varepsilon \le C$, for every $\varepsilon > 0$. From (4.115) and (4.118) we then obtain

$$w_0 = (0,0) \text{ on } \partial Q, \qquad w_0 = u|_{\partial K_\varepsilon} \text{ on } \partial K_\varepsilon, \qquad \|\nabla w_0\|_{L^2(\Omega_\varepsilon)} \le C\sigma_\varepsilon \qquad \forall \varepsilon > 0. \qquad (4.119)$$

From now on we follow the procedure of the proof of Theorem 4.10, taking into account that the functions involved belong to Sobolev spaces defined over different domains. For every $\varepsilon > 0$ define

82

$\xi = u - u_\varepsilon - w_0$, so that $\xi \in \mathcal{V}(\Omega_\varepsilon)$. After subtracting the equations (4.2) satisfied by (u, p, f) and $(u_\varepsilon, p_\varepsilon, f)$ in Ω_ε we infer that

$$-\eta \Delta \xi + [(\xi + w_0) \cdot \nabla](\xi + w_0) + [(u - u_\varepsilon) \cdot \nabla]u_\varepsilon + (u_\varepsilon \cdot \nabla)(u - u_\varepsilon) + \nabla(p - p_\varepsilon) = \eta \Delta w_0,$$

with $\eta \Delta w_0 \in H^{-1}(\Omega_\varepsilon)$, so that the equation is intended in weak sense, see (4.68). We test it with ξ, we integrate by parts in Ω_ε order to obtain the upper bound (after applying (4.115) and (4.119))

$$\eta \|\nabla \xi\|^2_{L^2(\Omega_\varepsilon)} + \beta_\varepsilon(\xi + w_0, \xi + w_0, \xi) + \beta_\varepsilon(u - u_\varepsilon, u_\varepsilon, \xi) + \beta_\varepsilon(u_\varepsilon, u - u_\varepsilon, \xi) \le C\eta\sigma_\varepsilon \|\nabla \xi\|_{L^2(\Omega_\varepsilon)}, \quad (4.120)$$

where $\beta_\varepsilon : H^1(\Omega_\varepsilon) \times H^1(\Omega_\varepsilon) \times H^1(\Omega_\varepsilon) \to \mathbb{R}$ denotes the trilinear form (4.34) with the integral computed over Ω_ε. Since $\xi \in \mathcal{V}(\Omega_\varepsilon)$, we have

$$\beta_\varepsilon(\xi + w_0, \xi + w_0, \xi) + \beta_\varepsilon(u - u_\varepsilon, u_\varepsilon, \xi) + \beta_\varepsilon(u_\varepsilon, u - u_\varepsilon, \xi) = \beta_\varepsilon(\xi, u, \xi) + \beta_\varepsilon(w_0, u, \xi) + \beta_\varepsilon(u_\varepsilon, w_0, \xi). \quad (4.121)$$

Since $\Omega_\varepsilon \subset \Omega$, every function in $H^1_*(\Omega_\varepsilon)$ may be extended by zero in $\overline{K_\varepsilon} \setminus K$, becoming an element of $H^1_*(\Omega)$. Therefore, $\mathcal{S}$ and $\mathcal{S}_0$, defined in (4.23) for Ω, may also be used as embedding constants in Ω_ε. By combining this fact with (4.119), we obtain the estimates

$$\left|\beta_\varepsilon(\xi, u, \xi)\right| \le \frac{1}{\mathcal{S}_0}\|\nabla u\|_{L^2(\Omega)}\|\nabla \xi\|^2_{L^2(\Omega_\varepsilon)}, \qquad \left|\beta_\varepsilon(u_\varepsilon, w_0, \xi)\right| \le \frac{C\sigma_\varepsilon}{\mathcal{S}}\|\nabla u_\varepsilon\|_{L^2(\Omega_\varepsilon)}\|\nabla \xi\|_{L^2(\Omega_\varepsilon)},$$

$$\left|\beta_\varepsilon(w_0, u, \xi)\right| \le \frac{C\sigma_\varepsilon}{\mathcal{S}}\|\nabla u\|_{L^2(\Omega)}\|\nabla \xi\|_{L^2(\Omega_\varepsilon)}. \quad (4.122)$$

We plug (4.121)-(4.122) into (4.120) to deduce that

$$\left(\eta - \frac{\|\nabla u\|_{L^2(\Omega)}}{\mathcal{S}_0}\right)\|\nabla \xi\|_{L^2(\Omega_\varepsilon)} \le C\sigma_\varepsilon \left(\eta + \frac{\|\nabla u_\varepsilon\|_{L^2(\Omega_\varepsilon)}}{\mathcal{S}} + \frac{\|\nabla u\|_{L^2(\Omega)}}{\mathcal{S}}\right).$$

We have seen above that (4.104) implies (4.70) and, in turn, Theorem 4.6 ensures $\|\nabla u\|_{L^2(\Omega)} < \mathcal{S}_0\eta$. Hence, the latter inequality yields an upper bound for $\|\nabla \xi\|_{L^2(\Omega_\varepsilon)}$ which, combined with (4.114) and (4.119), yields

$$\|\nabla(u - u_\varepsilon)\|_{L^2(\Omega_\varepsilon)} \le \|\nabla \xi\|_{L^2(\Omega_\varepsilon)} + \|\nabla w_0\|_{L^2(\Omega_\varepsilon)} \le \frac{2\mathcal{S}\eta + (1 - \mathcal{S}/\mathcal{S}_0)\|\nabla u\|_{L^2(\Omega)} + B}{\mathcal{S}_0\eta - \|\nabla u\|_{L^2(\Omega)}} \frac{C\mathcal{S}_0}{\mathcal{S}}\sigma_\varepsilon \to 0,$$

as $\varepsilon \to 0$. In order to control the pressure terms, we note that the same extension argument of $H^1_*(\Omega_\varepsilon)$ into $H^1_*(\Omega)$ proves that the embedding constant of $H^1_*(\Omega) \subset L^6(\Omega)$ bounds the corresponding embedding constant in Ω_ε. Then, as in the proof of Theorem 4.10, but applying condition $(\star)$, (4.43) and (4.114), we can deduce the existence of a constant $A > 0$, depending on η and Ω, such that

$$\|p - p_\varepsilon\|_{L^2(\Omega_\varepsilon)} \le A\left(1 + \|\nabla u\|_{L^2(\Omega)} + \|\nabla u_\varepsilon\|_{L^2(\Omega_\varepsilon)}\right)\|\nabla(u - u_\varepsilon)\|_{L^2(\Omega_\varepsilon)} \to 0 \quad \text{as } \varepsilon \to 0.$$

This shows (4.112) and completes the proof. $\qquad\square$

4.2.3 Definition and computation of drag and lift

In this section we analyze the forces of a fluid flow in Ω over the obstacle K. The stress tensor of a viscous incompressible fluid governed by (4.2) is (see [173, Chapter 2])

$$\mathbb{T}(u, p) \doteq -p\mathbb{I}_2 + \eta[\nabla u + (\nabla u)^\intercal] \quad \text{in } \Omega, \quad (4.123)$$

where $\mathbb{I}_2$ is the 2×2-identity matrix. Accordingly, the total force exerted by the fluid over the obstacle K is formally given by

$$F_K(u, p) = -\int_{\partial K} \mathbb{T}(u, p) \cdot \hat{n}\, ds, \quad (4.124)$$

83

where the minus sign is due to the fact that the outward unit normal $\hat{n}$ to Ω is directed towards the interior of K. To be precise, (4.124) makes sense only if (u, p) are regular while if $(u, p) \in \mathcal{V}_*(\Omega) \times L_0^2(\Omega)$ is a weak solution of (4.2) with $f \in L^2(\Omega)$, a generalized formula is needed. Indeed, in such case, one has $u \in L^p(\Omega)$, for every $p < \infty$ so that, in particular,

$$\mathbb{T}(u, p) \in L^2(\Omega) \subset L^{3/2}(\Omega) \quad \text{and} \quad \nabla \cdot \mathbb{T}(u, p) = (u \cdot \nabla)u - f \in L^{3/2}(\Omega). \tag{4.125}$$

Therefore, $\mathbb{T}(u, p) \in E_{3/2}(\Omega)$ and the normal component of the trace of $\mathbb{T}(u, p)$ belongs to $W^{-\frac{2}{3}, \frac{3}{2}}(\partial\Omega)$, the dual space of $W^{\frac{2}{3}, 3}(\partial\Omega)$, see (4.38). Then, we can rigorously define the force as follows.

Definition 4.3. *Let $f \in L^2(\Omega)$ and let $(u, p) \in \mathcal{V}_*(\Omega) \times L^2(\Omega)$ be a weak solution of (4.2). Then, the total force exerted by the fluid over the obstacle K is given by*

$$F_K(u, p) = -\langle \mathbb{T}(u, p) \cdot \hat{n}, 1 \rangle_{\partial K}, \tag{4.126}$$

where $\langle \cdot, \cdot \rangle_{\partial K}$ denotes the duality pairing between $W^{-\frac{2}{3}, \frac{3}{2}}(\partial K)$ and $W^{\frac{2}{3}, 3}(\partial K)$.

The classical literature [3, Introduction] defines the *drag force* as the component of F_K parallel to the incoming stream and the *lift force* as the component of F_K perpendicular to the stream. This characterization is rigorous only if the direction of the inflow velocity is constant.

Definition 4.4. *For $(U, V) \in H^{1/2}(\partial Q) \setminus \{(0, 0)\}$ such that $(U, V)/|(U, V)|$ is constant, the drag $\mathcal{D}_K(u, p)$ and the lift $\mathcal{L}_K(u, p)$, exerted by the fluid over the obstacle K, are given by*

$$\mathcal{D}_K(u, p) = F_K(u, p) \cdot \frac{(U, V)}{|(U, V)|} \quad \text{and} \quad \mathcal{L}_K(u, p) = F_K(u, p) \cdot \frac{(-V, U)}{|(U, V)|}.$$

In the case where $V = 0$ and $U \in H^{1/2}(\partial Q)$ is a strictly positive function on ∂Q, this reduces to

$$\mathcal{D}_K(u, p) = F_K(u, p) \cdot \hat{\imath} \quad \text{and} \quad \mathcal{L}_K(u, p) = F_K(u, p) \cdot \hat{\jmath}.$$

Clearly, the signs of $\mathcal{D}_K$ and $\mathcal{L}_K$ are just a matter of orientation and one could just take the absolute values, especially if one is merely interested in evaluating the strength of these forces.

The main purpose of this section is to discuss a well-known experimental fact: a bluff body immersed in a viscous fluid experiences no lift when its cross-section is symmetric with respect to the angle of attack of the fluid, as well illustrated in [217, Figure 2.6]. Moreover, any small symmetry-breaking angle of attack produces a lift on the obstacle. This was already observed by Kutta [165] in 1910 (see also [4, Chapter 12]): "With regard to dynamic lift effects, the most important types of a body immersed in a flowing fluid are long flat plates placed at an angle to the flow and slightly curved cylindrical shells, which experience lift forces even if the chord of their cross-section lies parallel to the flow".

For simplicity, we merely consider the case of constant positive horizontal data ($U \in \mathbb{R}_+$ and $V = 0$) and, if $\mathcal{B}_\varepsilon$ is as in Corollary 4.3, we prove

Theorem 4.12. *Let Ω be as in (4.1), let K be symmetric with respect to the x-axis. Assume that $U > 0$ is constant, $V = 0$, and that $f = (f_1, f_2) \in L^2(\Omega)$ is such that f_1 is y-even and f_2 is y-odd. If*

$$2\sqrt{2L}\,|U| + \|f\|_{L^2(\Omega)} < \delta_0, \tag{4.127}$$

with δ_0 as in (4.104), then the fluid governed by (4.2)-(4.3) exerts no lift over K. Moreover, there exists $\varepsilon_0 = \varepsilon_0(U, f) > 0$ such that, for all $\varepsilon < \varepsilon_0$ and all $(U_\varepsilon, V_\varepsilon, f_\varepsilon) \in \mathcal{B}_\varepsilon = \mathcal{B}_\varepsilon(0, 0, 0)$, the problem

$$-\eta\Delta v + (v \cdot \nabla)v + \nabla q = f + f_\varepsilon \text{ in } \Omega, \qquad v = (U + U_\varepsilon, V_\varepsilon) \text{ on } \partial Q, \qquad v = (0, 0) \text{ on } \partial K, \tag{4.128}$$

admits a unique weak solution $(v_\varepsilon, q_\varepsilon) \in \mathcal{V}_*(\Omega) \times L_0^2(\Omega)$ and

$$\lim_{\varepsilon \to 0} \sup_{(U_\varepsilon, V_\varepsilon, f_\varepsilon) \in \mathcal{B}_\varepsilon} |\mathcal{L}_K(v_\varepsilon, q_\varepsilon)| = 0.$$

Proof. The compatibility condition (4.4) is evidently satisfied, thus ensuring the existence of (at least) one solution $(u, p) \in \mathcal{V}_*(\Omega) \times L_0^2(\Omega)$ of (4.2)-(4.3), see Theorem 4.6. Furthermore, from (4.39) we see that (4.104) becomes (4.127) and then Theorem 4.10 ensures that the solution (u, p) is unique. Theorem 4.9 then states that (u, p) satisfies the symmetry properties (4.99).

From (4.126) and Definition 4.4 we have that

$$\mathcal{L}_K(u, p) = -\langle \mathbb{T}_2(u, p) \cdot \hat{n}, 1 \rangle_{\partial K} = \langle \mathbb{T}_2(u, p) \cdot \hat{n}, 1 \rangle_{\partial Q} - \langle \mathbb{T}_2(u, p) \cdot \hat{n}, 1 \rangle_{\partial \Omega}, \tag{4.129}$$

where

$$\mathbb{T}_2(u, p) = \left[\eta \left(\frac{\partial u_1}{\partial y} + \frac{\partial u_2}{\partial x} \right), 2\eta \frac{\partial u_2}{\partial y} - p \right]^\top.$$

By Theorem 4.8 we know that the term over ∂Q in (4.129) can be treated as an integral. On the other hand, (4.38) allows us to manage the term over $\partial \Omega$ and we obtain

$$\mathcal{L}_K(u, p) = \int_{\partial Q} \mathbb{T}_2(u, p) \cdot \hat{n} - \int_\Omega \nabla \cdot \mathbb{T}_2(u, p)$$

$$= \eta \int_{-L}^{L} \left[\frac{\partial u_1}{\partial y}(L, y) - \frac{\partial u_1}{\partial y}(-L, y) + \frac{\partial u_2}{\partial x}(L, y) - \frac{\partial u_2}{\partial x}(-L, y) \right] dy + 2\eta \int_{-L}^{L} \left[\frac{\partial u_2}{\partial y}(x, L) - \frac{\partial u_2}{\partial y}(x, -L) \right] dx$$

$$+ \int_{-L}^{L} \left[p(x, -L) - p(x, L) \right] dx + \int_\Omega \left[f_2(x, y) - u(x, y) \cdot \nabla u_2(x, y) \right] dx\, dy = 0.$$

Let us explain in detail why all the above terms vanish. In the first integral, the terms with $\frac{\partial u_1}{\partial y}$ vanish because u_1 is constant on ∂Q. For the term with $\frac{\partial u_2}{\partial x}$ in the first integral we remark that with the change of variables $y \mapsto -t$ it becomes

$$\int_{-L}^{L} \left[\frac{\partial u_2}{\partial x}(L, -t) - \frac{\partial u_2}{\partial x}(-L, -t) \right] dt$$

while, by (4.99), we know that it is also equal to the same expression with opposite sign. The second integral vanishes because (4.99) implies that $\frac{\partial u_2}{\partial y}$ is y-even and the summands cancel. The integral $\int_\Omega f_2$ vanishes because f_2 is y-odd and Ω is y-symmetric. Finally, $u \cdot \nabla u_2 = u_1 \frac{\partial u_2}{\partial x} + u_2 \frac{\partial u_2}{\partial y}$ and, again by (4.99), each summand is the product of a y-even and a y-odd function so that $u \cdot \nabla u_2$ is y-odd.

The number $\varepsilon_0 = \varepsilon_0(U, f) > 0$ can be chosen as in the proof of Theorem 4.10; then Theorem 4.6 guarantees the existence and uniqueness of a solution $(v_\varepsilon, q_\varepsilon) \in \mathcal{V}_*(\Omega) \times L_0^2(\Omega)$ of (4.128). By (4.38) and (4.126) (and by linearity), we infer

$$\mathbb{T}(v_\varepsilon, q_\varepsilon) = \mathbb{T}(v_\varepsilon - u, q_\varepsilon - p) + \mathbb{T}(u, p), \qquad F_K(v_\varepsilon, q_\varepsilon) = F_K(v_\varepsilon - u, q_\varepsilon - p) + F_K(u, p),$$

so that, by (4.129),

$$\mathcal{L}_K(v_\varepsilon, q_\varepsilon) = \mathcal{L}_K(v_\varepsilon - u, q_\varepsilon - p) = \langle \mathbb{T}_2(v_\varepsilon - u, q_\varepsilon - p) \cdot \hat{n}, 1 \rangle_{\partial Q} - \langle \mathbb{T}_2(v_\varepsilon - u, q_\varepsilon - p) \cdot \hat{n}, 1 \rangle_{\partial \Omega}.$$

By combining this with Theorem 4.10 (and by continuity of traces, see [111] or [115, Theorem II.4.3]) we obtain the statement. $\qquad \square$

Next, in the spirit of Theorem 4.11, we estimate the difference between the forces exerted by a given flow over two nearby obstacles.

Theorem 4.13. *Let Ω be as in (4.1), K with $\mathcal{C}^2$-boundary and symmetric with respect to the x-axis. Assume that $U > 0$ is constant, $V = 0$, and that $f \in L^2(\Omega)$ with f_1 y-even and f_2 y-odd; assume also that (4.127) holds. Let $\{K_\varepsilon\}_{\varepsilon>0}$ be a family of Lipschitz domains that outer-approximates K and let ε_0 be as in Theorem 4.11. For all $\varepsilon \in (0, \varepsilon_0)$ denote by $\Omega_\varepsilon = Q \setminus K_\varepsilon$ and by $(u_\varepsilon, p_\varepsilon) \in \mathcal{V}_*(\Omega_\varepsilon) \times L^2_0(\Omega_\varepsilon)$ the unique weak solution of (4.2)-(4.3) in Ω_ε. Then*

$$\lim_{\varepsilon \to 0} \mathcal{L}_{K_\varepsilon}(u_\varepsilon, p_\varepsilon) = 0.$$

Proof. Existence and uniqueness of (u, p) and $(u_\varepsilon, p_\varepsilon)$ as in the statement follow as in the proof of Theorem 4.11. Fix $\varepsilon \in (0, \varepsilon_0)$. From Theorem 4.12 we know that $\mathcal{L}_K(u, p) = 0$ and, by arguing as in that proof, we obtain

$$
\begin{aligned}
\mathcal{L}_{K_\varepsilon}(u_\varepsilon, p_\varepsilon) &= \mathcal{L}_{K_\varepsilon}(u_\varepsilon, p_\varepsilon) - \mathcal{L}_K(u, p) \\
&= \eta \int_{-L}^{L} \left[\frac{\partial (u_\varepsilon)_1}{\partial y}(L, y) - \frac{\partial u_1}{\partial y}(L, y) - \frac{\partial (u_\varepsilon)_1}{\partial y}(-L, y) + \frac{\partial u_1}{\partial y}(-L, y) \right] dy \\
&\quad + \eta \int_{-L}^{L} \left[\frac{\partial (u_\varepsilon)_2}{\partial x}(L, y) - \frac{\partial u_2}{\partial x}(L, y) - \frac{\partial (u_\varepsilon)_2}{\partial x}(-L, y) + \frac{\partial u_2}{\partial x}(-L, y) \right] dy \\
&\quad + 2\eta \int_{-L}^{L} \left[\frac{\partial (u_\varepsilon)_2}{\partial y}(x, L) - \frac{\partial u_2}{\partial y}(x, L) - \frac{\partial (u_\varepsilon)_2}{\partial y}(x, -L) + \frac{\partial u_2}{\partial y}(x, -L) \right] dx \\
&\quad + \int_{-L}^{L} \left[p_\varepsilon(x, -L) - p(x, -L) - p_\varepsilon(x, L) + p(x, L) \right] dx \\
&\quad + \int_{\Omega_\varepsilon} \left[u \cdot \nabla u_2 - u_\varepsilon \cdot \nabla (u_\varepsilon)_2 \right] + \int_{\Omega \setminus \Omega_\varepsilon} u \cdot \nabla u_2 - \int_{\Omega \setminus \Omega_\varepsilon} f_2,
\end{aligned}
\tag{4.130}
$$

and we claim that all the terms after the equality sign in (4.130) vanish as $\varepsilon \to 0$.

For the boundary integrals over ∂Q in (4.130), we fix an open set $\Omega_0 \subset \Omega_{\varepsilon_0} \subset \Omega$ having an internal boundary of class $\mathcal{C}^2$ and such that $\partial \Omega_{\varepsilon_0} \cap \partial \Omega_0 = \partial Q$; then Theorem 4.8 yields

$$(u, p), (u_\varepsilon, p_\varepsilon) \in H^2(\Omega_0) \times H^1(\Omega_0) \qquad \forall \varepsilon > 0.$$

Indeed, this choice of Ω_0 also ensures that $\Omega_0 \subset \Omega_\varepsilon$ and $\partial \Omega_\varepsilon \cap \partial \Omega_0 = \partial Q$ for all $\varepsilon > 0$ since K_ε outer-approximates K. In fact, (4.94) says more: $\|u_\varepsilon\|_{H^2(\Omega_0)}$ and $\|p_\varepsilon\|_{H^1(\Omega_0)}$ are bounded independently of ε since $\|\nabla u_\varepsilon\|_{L^2(\Omega_0)}$ and $\|p_\varepsilon\|_{L^2(\Omega_0)}$ are bounded by (4.112). Therefore, also $\|u_\varepsilon - u\|_{H^2(\Omega_0)}$ and $\|p_\varepsilon - p\|_{H^1(\Omega_0)}$ are bounded, a fact that, combined with an interpolation and with (4.112), shows that

$$u_\varepsilon \to u \text{ in } H^s(\Omega_0) \quad \forall s < 2 \quad \text{and} \quad p_\varepsilon \to p \text{ in } H^r(\Omega_0) \quad \forall r < 1, \quad \text{as } \varepsilon \to 0.$$

Then a result by Gagliardo [111] (see also [115, Theorem II.4.3]) states that

$$u_\varepsilon \to u \text{ in } H^s(\partial \Omega_0) \quad \forall s < \frac{3}{2} \quad \text{and} \quad p_\varepsilon \to p \text{ in } H^r(\partial \Omega_0) \quad \forall r < \frac{1}{2}, \quad \text{as } \varepsilon \to 0.$$

In turn, this shows that all the boundary integrals in (4.130) tend to vanish. Concerning the last line in (4.130), we notice that the first integral tends to vanish thanks to Theorem 4.11 and (4.112) while the second and third integrals tend to vanish because of the Lebesgue Theorem and because $|\Omega \setminus \Omega_\varepsilon| \to 0$ as $\varepsilon \to 0$ (since K_ε outer-approximates K).

Summarizing, all the integrals in (4.130) tend to zero as $\varepsilon \to 0$ and the result is proved. $\qquad \square$

Remark 4.10. *A careful look at the proof of Theorem 4.12 shows that the lift is due to the asymmetric part of the solution, namely $\mathcal{L}_K(u_1, u_2, p) = \mathcal{L}_K(u_1^E, u_2^O, p^E)$. Moreover, under suitable assumptions on the boundary datum $(U, V) \in H^{3/2}(\partial Q)$ (needed to prove the $H^2 \times H^1$-regularity of the solutions, see [130]), arguments similar to the ones employed in the proofs of Theorems 4.12 and 4.13 can be used to obtain the (respectively) stronger statements*

$$\lim_{\varepsilon \to 0} \sup_{(U_\varepsilon, V_\varepsilon, f_\varepsilon) \in \mathcal{B}_\varepsilon} \left| F_K(v_\varepsilon, q_\varepsilon) \right| = 0, \qquad \lim_{\varepsilon \to 0} F_{K_\varepsilon}(u_\varepsilon, p_\varepsilon) = 0.$$

This means that also the drag varies with continuity.

4.2.4 A universal threshold for the appearance of lift

In this section we restrict our attention to a simple case: we consider problem (4.2)-(4.3) assuming that K is symmetric with respect to the x-axis, that $f = 0$, $U \in \mathbb{R}_+$ and $V = 0$, thereby obtaining

$$\begin{cases} -\eta \Delta u + (u \cdot \nabla)u + \nabla p = 0, \qquad \nabla \cdot u = 0 \qquad \text{in } \Omega, \\ u = (U, 0) \ \text{ on } \ \partial Q, \qquad u = (0, 0) \ \text{ on } \ \partial K. \end{cases} \tag{4.131}$$

Note that (4.4) is satisfied and that (4.131) models an horizontal flow as in Figure 4.1.

Our purpose is to study the transition in (4.131) from uniqueness to non-uniqueness regimes (or, similarly, from symmetric to asymmetric solutions). Then, in the next section, we numerically analyze how the obtained threshold depends on the shape of the (symmetric) obstacle K.

The advantage of (4.131) is that we focus our attention on a unique parameter. Indeed, u solves (4.131) for some $\eta > 0$ and $U = 1$ if and only if $v = ku$ (for some $k > 0$) solves (4.131) for a viscosity ηk and with $U = k$. Therefore, the transition of (4.131) from the uniqueness to the non-uniqueness regimes can be studied for fixed η and variable U. In order to make sure that we are in the uniqueness regime for (4.131) (see Theorem 4.6), we use the quantitative functional inequalities obtained in Section 4.1.

So, let us revisit Theorem 4.5 in this simplified context. Previously, for $0 < d \le a < L$, define $\alpha_* \ge 0$ as in (4.45), $\sigma > 0$ as in (4.46), $\gamma_1 > 0$ as in Theorem 4.7, and we introduce the following constants:

$$C_0 = \frac{1}{\log(L) - \log(d)}, \qquad \widetilde{\zeta}_0 = 2d + \left(\frac{d}{L-d} - C_0 \right) \left(\frac{\alpha_*(L-a)}{\sqrt{\alpha_*^2 + (L-a)^2}} + d - L \right),$$

$$\widetilde{\alpha} = \left\{ 4\frac{L-d}{L-a}C_0 - \frac{(L-d-\alpha_*)C_0^2}{L-a}\left(\frac{L-d+\alpha_*}{L-d-\alpha_*}\frac{L-d}{L} + \frac{1}{C_0} \right) + \frac{\widetilde{\zeta}_0^2}{2(L-a)(L-d) + \alpha_*(L-a)} \right\}^{1/2},$$

$$\widetilde{\beta} = \left\{ \frac{(L-d-\alpha_*)C_0^2}{L-a}\left(\frac{L-d+\alpha_*}{L-d-\alpha_*}\frac{L-d}{L} + \frac{1}{C_0} \right) + \frac{\widetilde{\zeta}_0^2}{2(L-a)(L-d) + \alpha_*(L-a)} \right\}^{1/2},$$

$$\overline{\lambda_0} = C_0\sqrt{\frac{(L-a)^2 + (L-d)^2}{(L-a)(L-d)}} \sqrt{\frac{L-d}{L}\left[\frac{a(L-a) + d(L-d)}{(L-a)^2 + (L-d)^2}\frac{L-d}{d} - 1 \right] + \frac{1}{C_0}} + \gamma_1 \left(\widetilde{\alpha} + \widetilde{\beta} \right),$$

$$\overline{\lambda_1} = \left\{ \frac{2L^2(L-a)}{L-d}\left[2 - 4C_0 + 6C_0^2 - 6C_0^3 - 3C_0^4\left(\frac{d^2}{L^2} - 1 \right) \right] \right.$$

$$\left. + \frac{4dL(a-d)}{L-d}\left[(1 - 4C_0 + 12C_0^2 - 24C_0^3 + 24C_0^4)\frac{L}{d} - 24C_0^4 \right] \right\}^{1/4}.$$

Theorem 4.14. *Let Ω be as in (4.1) and assume (4.33). Define $\mu_0 > 0$ as in (4.22) and $\gamma_1 > 0$ as in Theorem 4.7. For any $U > 0$ there exists a weak solution $(u, p) \in \mathcal{V}_*(\Omega) \times L_0^2(\Omega)$ of (4.131). If, moreover,*

$$U < \frac{\dfrac{\sqrt{3}\,\pi^{3/2}}{2L}\max\left\{ 1, \sqrt{\dfrac{\mu_0^2|Q|}{2\pi(|Q| - |K|)}} \right\}\eta}{4\overline{\lambda_0} + \overline{\lambda_1}\dfrac{\sqrt[4]{3}\,\pi^{3/4}}{\sqrt{2L}}\max\left\{ 1, \sqrt[4]{\dfrac{\mu_0^2|Q|}{2\pi(|Q| - |K|)}} \right\} + 2\gamma_1\left(\widetilde{\alpha} + \widetilde{\beta} \right)}, \tag{4.132}$$

then the weak solution of (4.131) is unique. Furthermore, if K is symmetric with respect to the x-axis and (4.132) holds, then the unique solution of (4.131) exerts no lift on K.

Proof. Existence of a weak solution $(u, p) \in \mathcal{V}_*(\Omega) \times L_0^2(\Omega)$ of (4.131) follows from Theorem 4.6, noticing that the compatibility condition (4.4) is automatically fulfilled. On the other hand, by repeating the procedure of the proof of Theorem 4.5 (putting $V = 0$), we can deduce the existence of a vector field $v_0 \in H_c^1(\Omega)$ satisfying

$$\nabla \cdot v_0 = 0 \text{ in } \Omega, \quad v_0 = (U, 0) \text{ on } \partial Q,$$

together with the estimates

$$\|\nabla v_0\|_{L^2(\Omega)} \leq 2U\overline{\lambda_0}, \qquad \|v_0\|_{L^4(\Omega)} \leq U\overline{\lambda_1} + \frac{2U\gamma_1}{\sqrt{\mathcal{S}_0}} \left(\widetilde{\alpha} + \widetilde{\beta}\right). \tag{4.133}$$

In order to ensure unique solvability of (4.131) we revisit the proof of Theorem 4.6, where (4.82) becomes (4.92). In view of (4.133), inequality (4.92) is certainly satisfied whenever

$$U < \frac{\mathcal{S}_0 \eta}{4\overline{\lambda_0} + \sqrt{\mathcal{S}_0}\,\overline{\lambda_1} + 2\gamma_1 \left(\widetilde{\alpha} + \widetilde{\beta}\right)}. \tag{4.134}$$

The condition (4.132) is reached after noticing that the right-hand side of (4.134) is an increasing function of $\mathcal{S}_0$, and using the lower bound for $\mathcal{S}_0$ given in Corollary 4.1.

Finally, in the case when K is symmetric with respect to the x-axis, by combining Theorems 4.9 and 4.12, we infer that the unique solution of (4.131) exerts no lift on K. $\qquad \square$

Combined with Theorem 4.6, Theorem 4.14 states that, for a given measure of the symmetric obstacle, but regardless of its shape, there is no lift on the obstacle as long as (at least) the horizontal boundary velocity U satisfies (4.132). Hence, we have obtained

an absolute bound on the fluid velocity under which any symmetric obstacle is subject to no lift.

This bound merely depends on the viscosity of the fluid and is independent of the nature of the obstacle (a flag, any elastic body, any structure in civil engineering). If we view the fluid as the air and U as the velocity of the wind, the drag force $\mathcal{D}$ is the force directly exerted from the wind on the obstacle and, therefore, it comes from where the wind is blowing; hence it is mostly concentrated windward (the part upwind). On the contrary, the lift force $\mathcal{L}$ is an indirect force generated by an instability of the obstacle for large drag forces; this is the reason why it is oriented orthogonally to the flow and it acts downwind, on the "hidden part" of the obstacle. This situation is depicted in Figure 4.8 for a "stadium-shaped" obstacle, namely a rectangle ended by two half circles, to be compared with Figure 4.1.
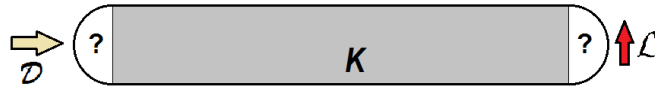

Figure 4.8: Drag $\mathcal{D}$ and lift $\mathcal{L}$ forces acting on a stadium-shaped obstacle K.

4.2.5 Multiplicity of solutions and numerical testing of shape performance

In the previous sections we gave sufficient conditions ensuring unique solvability of (4.2)-(4.3), but, as far as we are aware, there exist no sufficient conditions for the existence of multiple solutions. The first purpose of this section is precisely to give such condition in a symmetric framework, as a consequence of Theorem 4.9.

Corollary 4.4. *Let Ω be as in (4.1), K being symmetric with respect to the x-axis. Suppose that $f = (f_1, f_2) \in H^{-1}(\Omega)$ and that $(U, V) \in H^{1/2}(\partial Q)$ satisfy (4.4). Assume moreover that f_1 is y-even, f_2 is y-odd, and (U, V) verifies (4.98). If (4.2)-(4.3) admits one asymmetric solution $(u, p) \in \mathcal{V}_*(\Omega)^2 \times L_0^2(\Omega)$ (i.e., violating (4.99)), then there exist at least two more solutions of (4.2)-(4.3): its reflection (4.100) and a symmetric solution satisfying (4.99).*

Corollary 4.4 turns out to be extremely useful for numerical experiments, where one can visualize the streamlines of the solutions and determine possible asymmetries. In this section we use this principle to give hints on the shapes having better aerodynamic performances, namely, having smaller drag and lift. We choose adequately the size of the box $(-L, L)^2$ since we know from [48] that the drag decreases when L increases, and increases as the obstacle increases. In fact, this is the same monotonicity as for the Sobolev constant, see Section 4.1.2. Hence, imagine that one wishes to modify the shape of the obstacle in Figure 4.8 in such a way to lower both the drag and the lift forces: $\mathcal{D}$ has to be minimized in order to decrease as much as possible the input of energy from the wind into the obstacle whereas $\mathcal{L}$ has to be minimized in order to decrease as much as possible the vertical instability of the obstacle. As in any shape optimization problem, some common geometrical constraints need to be imposed.

$\diamond$ The total area of the obstacle is unchanged. This means that if the rectangle has thickness $2d$ then each of the two "caps" (the white semicircles in Figure 4.8) needs to have an area of $\pi d^2/2$. This constraint is needed both to ensure that the obstacle maintains its total mass and that the mass itself remains balanced on the right and the left of the barycenter of the rectangle.

$\diamond$ The obstacle is convex and symmetric with respect to the x-axis.

$\diamond$ The two caps yield a nonsmooth obstacle; this appears as a "numerical constraint", since corners give some computational difficulties and it appears unfair to compare smooth and nonsmooth obstacles.

Note that horizontal symmetry is not required and, in fact, it should not be expected as we now explain. We need to replace the two circular caps with two planar regions. A careful look at Figure 4.7 shows that, for the same Re (same line), the drag is stronger in the left picture while the lift is stronger on the right picture. Therefore, one expects that the stability might increase with asymmetry, namely in obstacles with the upwind part different from the downwind part. Since in many geographical regions the wind has mostly a constant direction, if the fluid modeled by (4.2) is the air, the obstacle K should be planned asymmetric following the expected wind direction (U, V).

In order to determine the shape performance, we fix the geometry and measure of the square and the (symmetric) obstacle. Take a square Q with edges measuring $2L = 30$ [m], and the gray rectangle of Figure 4.8 having thickness 0.25 [m] and width 3 [m]. After completing with the caps (each one having area equal to $\pi/128 \approx 0.025$ [m^2], for a total area of approximately 0.8 [m^2]), all of the considered obstacles can be enclosed by the rectangle $\mathcal{R}$ in (4.33) with $a = 1.7$ [m] and $d = 0.125$ [m]; the kinematic viscosity of air is about $\eta = 1.5 \times 10^{-5}$ [m^2/s]. With these measures, Theorem 4.14 becomes

Corollary 4.5. *Let Ω be as in (4.1) with $L = 15$ [m], and assume (4.33) with $a = 1.7$ [m], $d = 0.125$ [m]. If $V = 0$ and $U < 1.3 \times 10^{-9}$ [m/s] then the weak solution of (4.2)-(4.3) is unique and it exerts no lift on K.*

In order to determine the shape performance, we proceeded computationally by employing the Open-FOAM toolbox `http://openfoam.org`, through the use of the SIMPLE algorithm for the numerical resolution the steady-state Navier-Stokes equations in laminar regime, see [50]. In Table 4.1 we quote some numerical results obtained with the above parameters: the flow goes from left to right on the obstacles depicted in the first column.

In the first column of Table 4.1 we report the shapes of the obstacles, all having two caps of total area $\pi d^2/8$, see the above constraints. In the second column we report the numerically found critical velocity U_* for which uniqueness for (4.131) fails: due to the symmetry of the problem and to the absence of lift for $U < U_*$, see Proposition 4.12, the number U_* should be seen as the critical velocity generating lift. In the third column we report, for $U = U_*$, the *drag coefficient* $C_{\mathcal{D}}$, which is a dimensionless form of the drag $\mathcal{D}$ exerted by the fluid governed by (4.131). Given a boundary velocity U larger than all the critical velocities U_*, in the last column we report the *lift coefficient* $C_{\mathcal{L}}$, which is a dimensionless form of the lift $\mathcal{L}$ exerted by the fluid governed by (4.131). Both the drag and lift coefficients are directly proportional to the drag and lift, respectively, and for the previously specified inlet velocities, they are

Shape of the obstacle	$U_* \times 10^3$ [m/s]	$C_{\mathcal{D}}^* \times 10^6$	$C_{\mathcal{D}} \times 10^6$	$|C_{\mathcal{L}}| \times 10^6$
	3.7	0.635	139.35	72.55
	3.2	0.508	124.21	83.35
	1.9	0.239	191.33	306.62
	3.1	0.496	280.43	569.51

Table 4.1: Critical velocity U_*, drag coefficient $C_{\mathcal{D}}^*$ at critical velocity, drag $C_{\mathcal{D}}$ and lift $C_{\mathcal{L}}$ coefficients at velocity $U = 0.1$ [m/s].

computed numerically according to the following expressions (see [204, Chapter 9]):

$$C_{\mathcal{D}}^* = \frac{\mathcal{D}}{\frac{1}{2}\rho(U_*)^2 A_f}, \qquad C_{\mathcal{L}} = \frac{\mathcal{L}}{\frac{1}{2}\rho U^2 A_p}, \qquad (4.135)$$

where $\rho = 1$ [kg/m^2] is the air density, A_f is the *frontal length* (the projected length seen by an observer looking towards the object from a direction parallel to the upstream velocity), and A_p is the *planform length* (the projected length seen by an observer looking towards the object from a direction normal to the upstream velocity).

It turns out that U_* and $\mathcal{L}$ do not have the same behavior since the threshold of instability does not have the same monotonicity as the lift at $U = 0.1$ [m/s]. In fact, the most relevant results are contained in the last column: there we see the comparison between different shapes for the same flow velocity, ordered from top to bottom as the "best shape" towards the "worse shape", namely for increasing values of the lift coefficient. We tested several intermediate values of U, between U_* and $U = 0.1$ [m/s] and, as expected, for all the shapes we have noticed a clear monotonicity of the lift coefficient as U increases. Since the threshold of instability U_* has two orders of magnitude less, what really measures the performances of the shapes is the rate of increment of lift with respect to the velocity of the flow. Hence, by looking at the last column in Table 4.1 we see that, as far as the lift is concerned, the performance of the obstacle increases (lower lift) in presence of a convex angle on the upwind part and a flat face on the downwind part. Our interpretation is that the upwind part determines the separation of the flow and, therefore, the amount of energy around the obstacle. On the other hand, the downwind part quantifies how much of this energy is effectively able to lift vertically the obstacle and, hence, a flat boundary with less friction yields less lift.

Let us now turn to some numerical results which give strength to a conjecture by Pironneau [219, 220] about the optimal shape minimizing the drag. We consider a family of "rugby balls", that is, portion of ellipses glued together. More precisely, for $0 < \beta < 2\alpha$ we consider the family of functions ψ satisfying

$$\psi(x) = \alpha\sqrt{4 - x^2} - \beta, \quad 0 \le x \le \sqrt{4 - \frac{\beta^2}{\alpha^2}}, \quad \int_0^{\sqrt{4-\beta^2/\alpha^2}} \psi(x)\, dx = \frac{A}{4},$$

where A is the area of the obstacles represented in Table 4.1. The integral constraint yields

$$2\alpha \arcsin\sqrt{1 - \frac{\beta^2}{4\alpha^2}} - \beta \arcsin\sqrt{1 - \frac{\beta^2}{4\alpha^2}} = \frac{A}{4} \approx 0.2\,. \qquad (4.136)$$

Then we extend by symmetry the graph of ψ, with respect to both the axes, obtaining a rugby ball as in Figure 4.9.
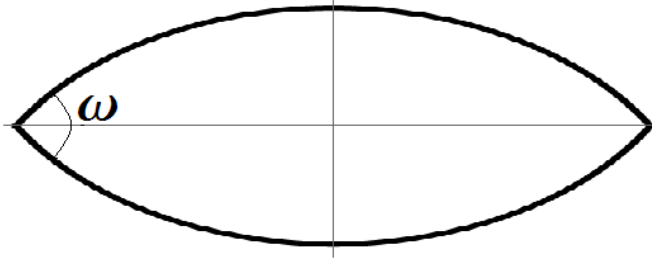
Figure 4.9: A rugby-ball-shaped obstacle.

The angle ω of the rugby ball can be computed through the derivative evaluated at the endpoint $\xi = \sqrt{4 - \beta^2/\alpha^2}$ of the interval; for instance,

$$\left\{ \begin{array}{l} \omega = \frac{2\pi}{3} \\ \omega = \frac{\pi}{2} \\ \omega = \frac{\pi}{3} \end{array} \right\} \Longleftrightarrow \left\{ \begin{array}{l} \psi'(\xi) = -\sqrt{3} \\ \psi'(\xi) = -1 \\ \psi'(\xi) = -\frac{1}{\sqrt{3}} \end{array} \right\} \Longleftrightarrow \left\{ \begin{array}{l} 4\alpha^2 = \alpha^2\beta^2 + 3\beta^2 \\ 4\alpha^2 = \alpha^2\beta^2 + \beta^2 \\ 4\alpha^2 = \alpha^2\beta^2 + \frac{\beta^2}{3} \end{array} \right\} \Longleftrightarrow \left\{ \begin{array}{l} (\alpha, \beta) \approx (0.06696, 0.00517) \\ (\alpha, \beta) \approx (0.06986, 0.00973) \\ (\alpha, \beta) \approx (0.07638, 0.02002) \end{array} \right\},$$

where the last equivalence also accounts of (4.136). For these angles we obtained the numerical results reported in Table 4.2, now ordered increasingly with respect to the second and third columns.

ω	$U_* \times 10^3$ [m/s]	$C_{\mathcal{D}}^* \times 10^6$	$C_{\mathcal{D}} \times 10^6$	$|C_{\mathcal{L}}| \times 10^6$
$2\pi/3$	13	4.09	82.87	29.94
$\pi/3$	15	5.12	84.27	34.98
$\pi/2$	17	6.17	82.24	20.69

Table 4.2: Critical velocity U_*, drag coefficient $C_{\mathcal{D}}^*$ at critical velocity, drag $C_{\mathcal{D}}$ and lift $C_{\mathcal{L}}$ coefficients at velocity $U = 0.1$ [m/s].

Table 4.2 gives strength to a conjecture by Pironneau [219, 220] claiming that, not only rugby balls lower the drag compared to other obstacles but also that the rugby balls minimizing the drag threshold are the ones having angle $\omega = 2\pi/3$.

We conclude this section by emphasizing that the second and third columns in Tables 4.1 and 4.2 suggest that the map $U_* \mapsto C_{\mathcal{D}}^*$ is increasing and superlinear. Moreover, the data from these two columns interpolate so nicely that they seem to show that "the drag force does not depend on the shape of the obstacle". This would mean that

the shape of the obstacle has the full responsibility of transforming the drag forces into lift forces.

4.3 Two connections with elasticity and mechanics

4.3.1 An impressive similitude with buckled plates

In this section we show that the bifurcation from uniqueness for the Navier-Stokes equations, related to loss of symmetry, has a counterpart in a model of a buckled elastic plate.

Consider a thin narrow rectangular plate with the two short edges hinged while the two long edges are free. In absence of forces, the plate lies horizontally flat and is represented by the planar domain $\Omega = (0, \pi) \times (-\ell, \ell)$ with $0 < \ell \ll \pi$. The plate is only subject to compressive forces along the edges, the so-called buckling loads. Following the plate model suggested by Berger [27], the nonlocal equation

modeling the deformation of the plate reads

$$\begin{cases} \Delta^2 u + \left[P - S\|u_x\|^2_{L^2(\Omega)}\right] u_{xx} = 0 & \text{in } \Omega \\ u = u_{xx} = 0 & \text{on } \{0, \pi\} \times [-\ell, \ell] \\ u_{yy} + \sigma u_{xx} = u_{yyy} + (2-\sigma)u_{xxy} = 0 & \text{on } [0, \pi] \times \{-\ell, \ell\}, \end{cases} \quad (4.137)$$

where $\sigma \in (0,1)$ is the Poisson ratio, $S > 0$ depends on the elasticity of the material composing the plate, $S\|u_x\|^2_{L^2(\Omega)}$ measures the geometric nonlinearity of the plate due to its stretching, while P is the buckling constant: one has $P > 0$ if the plate is compressed and $P < 0$ if the plate is stretched in the x-direction.

Partially hinged rectangular plates governed by (4.137) were introduced in [97] as models for the deck of suspension bridges. For the variational characterization of (4.137) we introduce the functional space

$$H^2_*(\Omega) = \{v \in H^2(\Omega) \mid v = 0 \text{ on } \{0, \pi\} \times [-\ell, \ell]\}$$

and the inner product

$$(v, w)_{H^2_*(\Omega)} = \int_\Omega \left(\Delta v \Delta w - (1-\sigma)\left(v_{xx}w_{yy} + v_{yy}w_{xx} - 2v_{xy}w_{xy}\right)\right) dx\, dy$$

with corresponding norm $\|v\|^2_{H^2_*(\Omega)} = (v, v)_{H^2_*(\Omega)}$. Since $\sigma \in (0, 1)$, this inner product defines a norm which makes $H^2_*(\Omega)$ a Hilbert space; see [97, Lemma 4.1]. The problem (4.137) is *variational* and this is the main crucial difference with (4.2): its solutions may be found as critical points of the "energy functional" defined by

$$J(v) = \frac{1}{2}\|v\|^2_{H^2_*(\Omega)} - \frac{P}{2}\|v_x\|^2_{L^2(\Omega)} + \frac{S}{4}\|v_x\|^4_{L^2(\Omega)} \qquad \forall v \in H^2_*(\Omega)\,.$$

It is proved in [96, 97] that the space $H^2_*(\Omega)$ is spanned by the eigenfunctions of the problem

$$\begin{cases} \Delta^2 u = -\lambda u_{xx} & \text{in } \Omega \\ u = u_{xx} = 0 & \text{on } \{0, \pi\} \times [-\ell, \ell] \\ u_{yy} + \sigma u_{xx} = u_{yyy} + (2-\sigma)u_{xxy} = 0 & \text{on } [0, \pi] \times \{-\ell, \ell\}, \end{cases} \quad (4.138)$$

that are given by

$$\mathcal{E}^k_m(x, y) = \varphi_{m,k}(y)\sin(mx)\,, \qquad \mathcal{O}^k_m(x, y) = \psi_{m,k}(y)\sin(mx)\,, \qquad (m, k = 1, 2, ...)\,, \qquad (4.139)$$

where $\varphi_{m,k}$ and $\psi_{m,k}$ are explicit linear combinations of $\sin(y)$, $\cos(y)$, $\sinh(y)$, $\cosh(y)$; the former are even with respect to y, while the latter are odd. Dropping this distinction, let us order increasingly the eigenvalues of (4.138) along a sequence $\{\lambda_n\}$ ($n = 1, 2, ...$) and let us denote by $\{w_n\}$ the associated sequence of normalized eigenfunctions, $\|(w_n)_x\|_{L^2(\Omega)} = 1$: the eigenvalue λ_1 is simple and w_1 has constant sign and, as a convention, we put $\lambda_0 = 0$. It is shown in [96] that $\{w_n\}$ are also eigenfunctions of the equation $\Delta^2 w_n = \Lambda_n w_n$ under the same boundary conditions.

By combining arguments from [5, 23, 96], we obtain the following statement.

Proposition 4.2. *For any $S > 0$ and $P \geq 0$, the function $u_0 = 0$ solves (4.137).*

• *If $P \in (\lambda_n, \lambda_{n+1}]$ for some $n \geq 0$ and all the eigenvalues smaller than or equal to λ_n have multiplicity 1, then (4.137) admits exactly $2n + 1$ solutions which are explicitly given by*

$$u_0 = 0\,, \qquad \pm u_j = \pm\sqrt{\frac{P - \lambda_j}{S}}\, w_j \quad (j = 1, ..., n)\,;$$

moreover, for each solution the energy is

$$J(u_0) = 0\,, \qquad J(\pm u_j) = -\frac{(P - \lambda_j)^2}{4S} \quad (j = 1, ..., n)$$

92

and the Morse index M is

$$M(u_0) = n, \qquad M(\pm u_j) = j - 1 \quad (j = 1, ..., n).$$

• *If $P \in (\lambda_n, \lambda_{n+1}]$ for some $n \geq 1$ and at least one of the eigenvalues smaller than or equal to λ_n has multiplicity larger than 1, then (4.137) admits infinitely many solutions.*

In particular, Proposition 4.2 states that (4.137) admits a unique solution whenever $P \leq \lambda_1$, whereas Theorem 4.6 states that (4.2)-(4.3) admits a unique solution whenever $\|(U, V)\|_{H^{1/2}(\partial Q)} + \|f\|_{H^{-1}(\Omega)} < \delta$.

At the value $P = \lambda_1$ a *bifurcation* in (4.137) occurs and, when P overcomes λ_1, two further solutions appear

$$\pm u_1 = \pm \sqrt{\frac{P - \lambda_1}{S}} w_1$$

and these solutions converge to u_0 as $P \searrow \lambda_1$. The counterpart of this phenomenon is the bifurcation which arises in (4.2)-(4.3) when the symmetric data overcome the critical threshold and multiple (asymmetric) solutions may appear.

As long as $\lambda_1 < P \leq \lambda_2$ only these three solutions exist and the statement about the Morse index tells us that $\pm u_1$ are stable while u_0 is unstable. Since $w_1(x, y) = \varphi(y) \sin(x)$ for some even function φ, see (4.139), the (positive) equilibrium solution of (4.137) has the shape as in Figure 4.10. The buckling load (black arrows in Figure 4.10) generates a lift (white arrow in Figure 4.10) which is orthogonal to its action. Clearly, this lift does not have the same meaning as in Section 4.2.3 but, still, we are in presence
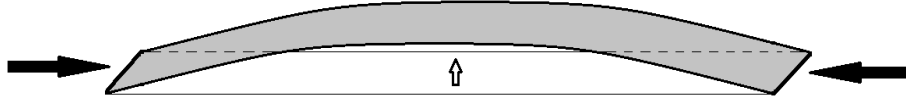

Figure 4.10: Buckling load (black) and consequent lift (white) in a partially hinged plate.

of a phenomenon where a force acting on an object has its effect in the orthogonal direction.

Letting P increase further beyond λ_2, each time P crosses an eigenvalue λ_n the number of solutions of (4.137) increases by 2, thereby their total number remains odd: the solution u_0 is symmetric, while the other solutions $\pm u_j$ are asymmetric but coupled (each asymmetric solution is coupled with its opposite), as in Theorem 4.9. The only stable solutions (with zero Morse index) are the asymmetric solutions $\pm u_1$. Since numerics (CFD) usually captures stable solutions, our feeling is that also the asymmetric solutions displayed in the second line of Figure 4.7 (large Re) are stable, while the symmetric ones are probably unstable since CFD is unable to detect them.

This pattern continues until P crosses some multiple eigenvalue, if any: in this case, the number of solutions becomes infinite because there are infinitely many possible linear combinations of the multiple eigenfunctions that solve (4.137). It is a generic property (with respect to the measures of the rectangular plate) that all the eigenvalues are simple and, in this situation, Proposition 4.2 shows that (4.137) admits a finite number of solutions (in fact, an odd number of solutions) for any $P \geq 0$. A similar result, obtained through an application of the Sard-Smale Lemma, holds for the Navier-Stokes equations: problem (4.131) admits a finite number of solutions, see Foias-Temam [100, 101], generically with respect to U and η.

4.3.2 A three-dimensional model: the deck of a bridge

The purpose of this section is to apply the results of the present chapter to a bridge model that was first suggested in the research project [125], see also [38, 127]. In the space $\mathbb{R}^3$ we consider the deck of a bridge to be a thin plate defined by

$$D = (-a, a) \times (-d, d) \times (-\Lambda, \Lambda) = K \times (-\Lambda, \Lambda), \tag{4.140}$$

where $d \ll a \ll \Lambda$. To have an idea, one could take $a = \Lambda/75$ and $d = \Lambda/1000$ (a deck of length 1km, with the width of about 13m, whose thickness is about 1m). Then we consider the region where the air surrounds the deck

$$B = (-L, L)^2 \times (-\Lambda, \Lambda) \setminus \overline{D} = \Omega \times (-\Lambda, \Lambda), \tag{4.141}$$

where $L \gg \Lambda$, for instance $L = 100\Lambda$ (100km, as a picture taken far away from the bridge). The domains B and D, as well as their intersections $\Omega = (-L, L)^2 \setminus \overline{K}$ and $K = (-a, a) \times (-d, d)$ with the plane $z = 0$, are represented in Figure 4.11 (not in scale).
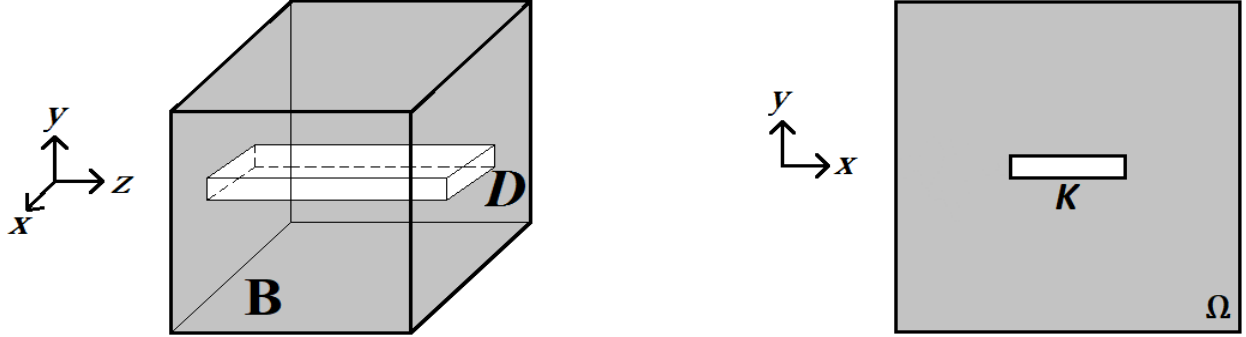

Figure 4.11: The domains B and D (left) and their intersections Ω and K with the plane $z = 0$.

The bridge is subject to a wind whose flow is governed by the Navier-Stokes equations. We model the case where the wind is blowing only in the x-direction, so that one has to analyze the planar section of this configuration, as represented in the right picture of Figure 4.11, leading us to study the planar problem of a flow around the obstacle K, governed by (4.2)-(4.3), as in Section 4.2.

In the three-dimensional configuration of the left picture in Figure 4.11, it is be convenient to decompose the boundary of B as

$$\partial B = \Sigma_1 \cup \Sigma_2 \cup \partial D,$$

where

$$\begin{aligned} \Sigma_1 &= \{(x, y, z) \in \partial B \mid x \in \{-L, L\} \} \cup \{(x, y, z) \in \partial B \mid y \in \{-L, L\} \}, \\ \Sigma_2 &= \{(x, y, z) \in \partial B \mid (x, y) \notin D, \ z \in \{-\Lambda, \Lambda\} \}. \end{aligned} \tag{4.142}$$

We then consider the three-dimensional Navier-Stokes equations in B, that is

$$-\eta \Delta v + (v \cdot \nabla)v + \nabla q = F, \quad \nabla \cdot v = 0 \quad \text{in } B, \tag{4.143}$$

for some $F \in L^2(B)$, complemented with appropriate boundary conditions. Notice that the obstacle D and the domain B are symmetric with respect to the plane $y = 0$, in the sense that $(x, y, z) \in B$ if and only if $(x, -y, z) \in B$. It is therefore natural to wonder whether symmetry and bifurcation results also hold in this 3D setting.

Proposition 4.3. *For any $F = (f_1, f_2, f_3) \in L^2(B)$ and $(U, V, W) \in H^{1/2}(\Sigma_1 \cup \Sigma_2)$ satisfying*

$$\int_{\Sigma_1 \cup \Sigma_2} (U, V, W) \cdot \hat{n} \, dA = 0, \tag{4.144}$$

there exists a weak solution $(v, q) = (v_1, v_2, v_3, q) \in H^1(B)^3 \times L_0^2(B)$ of (4.143) in B complemented with the boundary conditions

$$v = (U, V, W) \text{ on } \Sigma_1 \cup \Sigma_2, \quad v = (0, 0, 0) \text{ on } \partial D. \tag{4.145}$$

Moreover:

94

• *there exists $\gamma = \gamma(\eta, B) > 0$ such that if $\|(U, V, W)\|_{H^{1/2}(\Sigma_1 \cup \Sigma_2)} + \|F\|_{L^2(B)} < \gamma$, then the weak solution of (4.143)-(4.145) is unique;*
• *if f_1, f_3, U, W are y-even and f_2, V are y-odd, then also $(\xi_1, \xi_2, \xi_3, \pi)$ with*

$$\xi_1(x, y, z) = v_1(x, -y, z), \quad \xi_2(x, y, z) = -v_2(x, -y, z), \quad \xi_3(x, y, z) = v_3(x, -y, z), \quad \pi(x, y, z) = q(x, -y, z),$$

for a.e. $(x, y, z) \in B$, solves the problem (4.143)-(4.145);
• *if f_1, f_3, U, W are y-even, if f_2, V are y-odd and if $\|(U, V, W)\|_{H^{1/2}(\Sigma_1 \cup \Sigma_2)} + \|F\|_{L^2(B)} < \gamma$, then the weak solution of (4.143)-(4.145) is unique and satisfies the symmetry property*

$$v_1(x, y, z) = v_1(x, -y, z), \quad v_2(x, y, z) = -v_2(x, -y, z), \quad v_3(x, y, z) = v_3(x, -y, z), \quad q(x, y, z) = q(x, -y, z),$$

for a.e. $(x, y, z) \in B$.

The proof of this result is completely similar to that of Theorem 4.9 and therefore we omit it. A particular solution of (4.143) can be obtained by extending to B a solution of the corresponding planar problem in Ω, as the next result shows.

Proposition 4.4. *Let $f = (f_1, f_2) \in L^2(\Omega)$ and $(U, V) \in H^{1/2}(\partial Q)$ satisfy (4.4). Define $F(x, y, z) = (f_1(x, y), f_2(x, y), 0)$ for a.e. $(x, y, z) \in B$. There exists $\overline{\gamma} = \overline{\gamma}(\eta, B) > 0$ such that, if $\|(U, V)\|_{H^{1/2}(\partial Q)} + \|f\|_{L^2(\Omega)} < \overline{\gamma}$, then:*
• *problem (4.2)-(4.3) in Ω admits a unique weak (planar) solution $(u_1, u_2, p) \in H^1(\Omega)^2 \times L_0^2(\Omega)$;*
• *problem (4.143), complemented with the boundary conditions*

$$v = (U, V, 0) \text{ on } \Sigma_1, \quad v = (u_1, u_2, 0) \text{ on } \Sigma_2, \quad v = (0, 0, 0) \text{ on } \partial D,$$

admits a unique weak solution $(v, q) \in H^1(B)^3 \times L_0^2(B)$, which does not depend on z and is given by

$$v(x, y, z) = (u_1(x, y), u_2(x, y), 0), \qquad q(x, y, z) = p(x, y) \quad \text{for a.e. } (x, y, z) \in B. \tag{4.146}$$

Proof. Take $\overline{\gamma} = \min\{\delta, \gamma\}$, with δ as in Theorem 4.6 and γ as in Proposition 4.3. Then problem (4.2)-(4.3) in Ω admits a unique weak (planar) solution $(u_1, u_2, p) \in H^1(\Omega)^2 \times L_0^2(\Omega)$. From (4.146) we infer that $(v, q) \in H^1(B)^3 \times L_0^2(B)$ is a weak solution of (4.143), where $(U, V, 0) \in H^{1/2}(\Sigma_1)^3$ and $(u_1, u_2, 0) \in H^{1/2}(\Sigma_2)^3$ (the definition of weak solution for the 3D problem (4.143) is naturally extended from Definition 4.1). The uniqueness of such solution is guaranteed by Proposition 4.3. $\square$

The proof of Proposition 4.4, although simple, makes a connection between the uniqueness of the Navier-Stokes system in two and three dimensions. As a consequence of Theorem 4.14, and by putting together the results of the present chapter, we obtain a sufficient condition for the stability of bridges.

Corollary 4.6. *Assume that the deck of a bridge coincides with the obstacle D in (4.140) and that the wind is blowing only in the x-direction with velocity $U > 0$, in absence of external forces. If U is sufficiently small, then the bridge does not oscillate.*

To see this, it suffices to take U sufficiently small so that we fall in both the uniqueness regimes for the 2D and 3D Navier-Stokes equations, see Theorem 4.14 and Proposition 4.3. Then the unique solution of (4.143) with $F = 0$ is two-dimensional, see Proposition 4.4. In view of the symmetry of the domain, Theorem 4.14 ensures that there is no lift on any of the two-dimensional cross-sections of the deck.

4.4   Estimates for the norms of mollifiers

Let ω be the mollifier defined in (4.49) with $\ell \approx 2.14357$. In order to compute all the norms appearing in (4.53) we write the corresponding integrals over the disk $\mathcal{B}$ in polar coordinates $(\rho, \theta) \in (0, r) \times [0, 2\pi]$

and apply the change of variables $t = \frac{r^2}{r^2 - \rho^2}$, for $0 < \rho < r$. All the integrals are well-defined and we computed them numerically, finding the following bounds.

- *Bounds for the norms of zeroth-order derivatives:*

$$\|\omega\|_{L^1(\mathcal{B})} = 1; \qquad \|x\,\omega\|_{L^1(\mathcal{B})} = \|y\,\omega\|_{L^1(\mathcal{B})} = 2\ell r \int\limits_1^\infty \frac{\sqrt{t-1}}{t^{5/2}} e^{-t}\, dt < 0.31 r.$$

- *Bounds for the norms of first-order derivatives:*

$$\left\|\frac{\partial \omega}{\partial x}\right\|_{L^1(\mathcal{B})} = \left\|\frac{\partial \omega}{\partial y}\right\|_{L^1(\mathcal{B})} = \frac{4\ell}{r} \int\limits_1^\infty \sqrt{1 - \frac{1}{t}}\, e^{-t}\, dt < \frac{1.91}{r};$$

$$\left\|\frac{\partial \omega}{\partial x}\right\|_{L^\infty(\mathcal{B})} = \left\|\frac{\partial \omega}{\partial y}\right\|_{L^\infty(\mathcal{B})} = \frac{2 \times 3^{3/4}}{(1-\sqrt{3})^2} \exp\left(\frac{\sqrt{3}}{1-\sqrt{3}}\right) \frac{\ell}{r^2} < \frac{1.72}{r^2};$$

$$\left\|\frac{\partial}{\partial x}(x\omega)\right\|_{L^1(\mathcal{B})} = \frac{\ell}{2} \int\limits_0^{2\pi} \int\limits_1^\infty \left|\frac{1}{t^2} + 2\cos^2(\theta)\left(\frac{1}{t} - 1\right)\right| e^{-t}\, dt\, d\theta < 1.18;$$

$$\left\|\frac{\partial}{\partial y}(y\omega)\right\|_{L^1(\mathcal{B})} = \frac{\ell}{2} \int\limits_0^{2\pi} \int\limits_1^\infty \left|\frac{1}{t^2} + 2\sin^2(\theta)\left(\frac{1}{t} - 1\right)\right| e^{-t}\, dt\, d\theta < 1.18;$$

$$\left\|\frac{\partial}{\partial x}(x\omega)\right\|_{L^\infty(\mathcal{B})} = \left\|\frac{\partial}{\partial y}(y\omega)\right\|_{L^\infty(\mathcal{B})} = \frac{4(2\sqrt{7}-5)}{(3-\sqrt{7})^2} \exp\left(\frac{1}{\sqrt{7}-3}\right) \frac{\ell}{r^2} < \frac{1.19}{r^2};$$

$$\left\|\frac{\partial}{\partial y}(y\omega)\right\|_{L^1(\mathcal{B})} = \left\|\frac{\partial}{\partial y}(x\omega)\right\|_{L^1(\mathcal{B})} = 2\ell \int\limits_1^\infty \left(1 - \frac{1}{t}\right) e^{-t}\, dt < 0.64;$$

$$\left\|\frac{\partial}{\partial y}(y\omega)\right\|_{L^\infty(\mathcal{B})} = \left\|\frac{\partial}{\partial y}(x\omega)\right\|_{L^\infty(\mathcal{B})} = \frac{2(\sqrt{5}-1)}{(3-\sqrt{5})^2} \exp\left(\frac{2}{\sqrt{5}-3}\right) \frac{\ell}{r^2} < \frac{0.67}{r^2}.$$

- *Bounds for the norms of second-order derivatives:*

$$\left\|\frac{\partial^2 \omega}{\partial x^2}\right\|_{L^1(\mathcal{B})} = \frac{\ell}{r^2} \int\limits_0^{2\pi} \int\limits_1^\infty \left|[(t-1)\sin^2(\theta) - t]^2 - (t-1)^2 \cos^2(\theta)[2 + \cos^2(\theta)]\right| e^{-t}\, dt\, d\theta < \frac{8.75}{r^2};$$

$$\left\|\frac{\partial^2 \omega}{\partial y^2}\right\|_{L^1(\mathcal{B})} = \frac{\ell}{r^2} \int\limits_0^{2\pi} \int\limits_1^\infty \left|[(t-1)\cos^2(\theta) - t]^2 - (t-1)^2 \sin^2(\theta)[2 + \sin^2(\theta)]\right| e^{-t}\, dt\, d\theta < \frac{8.75}{r^2};$$

$$\left\|\frac{\partial^2}{\partial x^2}(x\omega)\right\|_{L^1(\mathcal{B})} = \frac{\ell}{r} \int\limits_0^{2\pi} \int\limits_1^\infty t^{3/2}\sqrt{t-1}\,|\cos(\theta)|\, \left|\left(1 - \frac{1}{t}\right)\cos^2(\theta)\left[\left(1 - \frac{1}{t}\right)(\cos^2(\theta) - 2\sin^2(\theta)) + 4\right]\right.$$

$$\left. - 3\left[1 - \left(1 - \frac{1}{t}\right)\sin^2(\theta)\right]^2\right| e^{-t}\, dt\, d\theta < \frac{6.98}{r};$$

$$\left\| \frac{\partial^2}{\partial y^2}(y\omega) \right\|_{L^1(\mathcal{B})} = \frac{\ell}{r} \int_0^{2\pi} \int_1^\infty t^{3/2}\sqrt{t-1}\, |\sin(\theta)| \left| \left(1 - \frac{1}{t}\right) \sin^2(\theta) \left[\left(1 - \frac{1}{t}\right)(\sin^2(\theta) - 2\cos^2(\theta)) + 4 \right] \right.$$

$$\left. - 3\left[1 - \left(1 - \frac{1}{t}\right)\cos^2(\theta)\right]^2 \right| e^{-t}\, dt\, d\theta < \frac{6.98}{r};$$

$$\left\| \frac{\partial^2}{\partial x^2}(y\omega) \right\|_{L^1(\mathcal{B})} = \frac{\ell}{r} \int_0^{2\pi} \int_1^\infty \frac{\sqrt{t-1}}{\sqrt{t}e^t}\, |\sin(\theta)| \left| [(t-1)\sin^2(\theta) - t]^2 - (t-1)^2 \cos^2(\theta)[\cos^2(\theta) + 2] \right| dt\, d\theta$$

$$< \frac{3.08}{r};$$

$$\left\| \frac{\partial^2}{\partial y^2}(x\omega) \right\|_{L^1(\mathcal{B})} = \frac{\ell}{r} \int_0^{2\pi} \int_1^\infty \frac{\sqrt{t-1}}{\sqrt{t}e^t}\, |\cos(\theta)| \left| [(t-1)\cos^2(\theta) - t]^2 - (t-1)^2 \sin^2(\theta)[\sin^2(\theta) + 2] \right| dt\, d\theta$$

$$< \frac{3.08}{r}.$$

Chapter 5

Conclusions and future developments

If we were forced to indicate just one main result among all the others obtained in this work, we would select Theorem 4.14, which takes into account all the remaining results and gives an explicit universal bound such that if the boundary velocity of the fluid is below this bound, then the obstacle is not subject to a lift force. In order to reach this bound, in Section 4.1 we went through several functional inequalities. Most of these inequalities are stated in literature as "there exists a constant $C > 0$ such that..." with little information (or no information at all!) on the magnitude of C. Our purpose was to give bounds, as precise as possible, on these constants. With these bounds at hand, in Section 4.2 we tackled the problem of estimating the forces exerted by a viscous fluid on a bluff body. We showed how uniqueness and symmetry play a fundamental role and, in a simple situation, we managed giving fairly precise bounds as in Theorem 4.14. As shown in Section 4.3, these bounds have important applications in physics and engineering. We believe that the results of the present work open new perspectives on fluid-structure interaction models [217], they lead to a bunch of natural questions and open problems that we list here.

• The main purpose of Chapter 2 is the determination of thresholds for the validity of the Melan equation, which is derived by considering the hangers as rigid bars, so that the deck and the cables of the suspension bridge endure the same movement. Nevertheless, this assumption is unreasonable since the hangers resist to traction but not to compression. A more complete model, involving the convexification of the cables, was then proposed in [71]. The main difficulty of this model is that the resulting energy functional is extremely complicated because it requires the convexification of unknown functions. Also, it is not clear how this model can give a precise explanation of the origin of torsional instability in terms of Poincaré maps as in [12], even though numerical evidence of the same qualitative phenomenon is given in [71]. Therefore, important mathematical work needs to be accomplished in this direction.

• In relation to Chapter 3, a natural direction of research concerns the weak formulation for the Stokes equations (and ultimately, for the Navier-Stokes equations) with the mixed and non-standard boundary conditions (3.7) in a domain with a merely Lipschitz obstacle. As mentioned in Section 3.3, this would require the use of weighted Sobolev spaces in order to describe the singularities of the solutions around concave corners, see also [79].

• In Section 4.1.2 we obtained several bounds for some embedding constants. As pointed out in Remark 4.4, we believe that they could be improved by taking into account the shape and the position of the obstacle. This would lead to a double shape/position optimization problem. We recall that, since the outer squared box Q is only virtual (it is the frame of a photo), one has the freedom of moving the obstacle inside the frame. In fact, the position of the obstacle within the flow plays a significant role, see [112] where, however, the boundary effects are important.

• As a pure functional-analytic curiosity, one could seek bounds for the embedding $H^1(\Omega) \subset L^p(\Omega)$ for any $p \geq 1$, and not just $p = 4$. For which p is our capacity approach giving better bounds? Moreover, the very same bounds could be sought in higher space dimension $n \geq 3$, where there are two crucial differences: the capacity potential behaves like $1/|x|^{n-2}$ (as the fundamental solution) and there exists

a critical exponent ($p = 2n/(n - 2)$) for the Sobolev embedding $H^1(\Omega) \subset L^p(\Omega)$. For the capacity, one should check if the pyramidal functions introduced in Section 4.1.1 still allow to obtain reliable bounds. For the critical exponent, it could be of some interest to investigate how the method developed in Section 4.1.2 allows to approximate the optimal embedding constant which, not only is known explicitly, but is independent of the domain.

• A result in the spirit of Theorem 4.14 could be of great interest also for other boundary conditions. For instance, conditions involving the pressure as in a network of pipes [30, 31, 61] or for the so-called Navier boundary conditions [205]. For the latter, we mention that they appear appropriate in many physically relevant cases [242], also for turbulent boundary layers [113, 218]. The Navier-Stokes equations under the Navier boundary conditions (with and without friction) have been studied by many authors, starting from Solonnikov-Shchadilov [244], see e.g. [2, 8, 24] and references therein; we mention in particular the work by Berselli [28] which appears relevant for our purposes since he considers flat 3D boundaries, in which cases the Navier boundary conditions reduce to combined Dirichlet-Neumann conditions.

• The evolution problem with constant data on ∂Q but with moving obstacle could be tackled from two different points of view. First, in the spirit of Galdi-Silvestre [117], one could seek periodic solutions by assuming that the obstacle is oscillating with given periodic law which maintains it far away from ∂Q: do periodic solutions exist, regardless of the magnitude of the (constant) inflow conditions? Second, in the spirit of Conca-San Martín-Tucsnak [62], one could set up a full fluid-structure interaction model. In this case, a major problem is to prevent collisions between the obstacle and ∂Q which, for our specific problem, *is not* a physical boundary. How does the non-collision condition vary with respect to the magnitude and the direction of the (constant) inflow?

• The appearance of violent lift forces creates serious problems in suspension bridges, possibly leading to disasters [121, Chapter 1]. The whole structure oscillates and both the cables and the hangers generate unexpected behaviors on the deck, such as torsional movements. It is therefore desirable to find a relationship between the fluid velocity, the resulting lift, and the attainment of the thresholds for hanger slackening and cable shortening, as obtained explicitly in [126].

• Quite interesting appears the 3D version of the stationary problem (4.2)-(4.3). By this we mean a non simply connected domain as in the right picture in Figure 4.11, which would model the deck of a bridge. As mentioned above, the functional inequalities in these domains appear quite different, as well as the computation of the lift. Indeed, a simple characterization as in Definition 4.4 is not available, since the directions orthogonal to the flow generate a plane and not just one line. Moreover, weaker embeddings are available in 3D, which yields major difficulties in regularity results. For instance, for the perturbation of the obstacle (Theorem 4.11), we used the embedding $H^2(\Omega) \subset \mathcal{C}^{0,\nu}(\overline{\Omega})$ for all $\nu < 1$ while in 3D one just has $\nu = 1/2$. Therefore, the 3D case is not just an extension of the 2D case, new issues will be needed.

• We saw in Theorem 4.9 that, in a symmetric framework (both the domain and the data), the existence of asymmetric solutions implies non-uniqueness of solutions. The multiplicity of symmetric solutions is however an open problem, see Remark 4.9. It would be extremely important (and very challenging) to have a complete picture of the bifurcation diagram for multiple solutions of (4.2)-(4.3) in dependence of the Reynolds number.

• We have seen in Remark 4.1 and Corollary 4.2 that our bounds for the relative capacity and for the Sobolev constant of the embedding $H^1(\Omega) \subset L^4(\Omega)$ are quite accurate. Therefore, possible improvements of the threshold given in Theorem 4.14 may only be achieved through a better analysis of problem (4.5).

• Let $(u, p) \in \mathcal{V}_*(\Omega) \times L_0^2(\Omega)$ be a solution of (4.2)-(4.3) with $(U, V) \in \mathbb{R}^2$. Let $u = v + w$ be the decomposition according to (4.21) so that $v \in H_0^1(\Omega)$ and $w \in \mathbb{R}(\psi - 1)$. In fact, from the boundary conditions we know more, namely

$$w = (1 - \psi) \begin{pmatrix} U \\ V \end{pmatrix} \implies \|\nabla w\|_{L^2(\Omega)}^2 = (U^2 + V^2)\|\nabla \psi\|_{L^2(\Omega)}^2 = (U^2 + V^2)\text{Cap}_Q(K) \,.$$

By (4.37) we infer that $\beta(u, u, u) = \beta(u, w, w)$ and, therefore,

$$|\beta(u, u, u)| \leq (U^2 + V^2)^2 \, \frac{\mathrm{Cap}_Q(K)^2}{\mathcal{S}_1} \, \|\nabla u\|_{L^2(\Omega)} \, .$$

Is it possible to use this inequality to improve the bounds? In particular, in Theorem 4.7.

• Is it possible to set up a theoretical shape optimization able to compute the derivative of the lift with respect to variations of the shape of the obstacle? See [25, 52] for the case of drag derivative.

Bibliography

[1] NASA Glenn Research Center. `https://www.grc.nasa.gov/www/k-12/airplane/bernnew.html`.

[2] P. Acevedo, C. Amrouche, C. Conca, and A. Ghosh. Stokes and Navier-Stokes equations with Navier boundary condition. *Comptes Rendus de l'Académie des Sciences. Série I, Mathématique*, 357:115–119, 2019.

[3] D. Acheson. *Elementary Fluid Dynamics*. Oxford University Press, 1990.

[4] J. A. Ackroyd, B. P. Axcell, and A. I. Ruban. *Early Developments of Modern Aerodynamics*. Butterworth-Heinemann, 2001.

[5] M. Al-Gwaiz, V. Benci, and F. Gazzola. Bending and stretching energies in a rectangular plate modeling suspension bridges. *Nonlinear Analysis*, 106:18–34, 2014.

[6] G. Alekseev. Mixed boundary value problems for stationary magnetohydrodynamic equations of a viscous heat-conducting fluid. *Journal of Mathematical Fluid Mechanics*, 18(3):591–607, 2016.

[7] C. Amick. Existence of solutions to the nonhomogeneous steady Navier-Stokes equations. *Indiana University Mathematics Journal*, 33(6):817–830, 1984.

[8] C. Amrouche and A. Rejaiba. L^p-theory for Stokes and Navier-Stokes equations with Navier boundary condition. *Journal of Differential Equations*, 256:1515–1547, 2014.

[9] H. Aref. Point vortex dynamics: a classical mathematics playground. *Journal of Mathematical Physics*, 48(6):065401, 2007.

[10] H. Aref, P. K. Newton, M. A. Stremler, T. Tokieda, and D. L. Vainchtein. Vortex crystals. *Advances in Applied Mechanics*, 39:1–79, 2002.

[11] T. Argentini, D. Rocchi, and A. Zasso. Aerodynamic interference and vortex-induced vibrations on parallel bridges: The Ewijk bridge during different stages of refurbishment. *Journal of Wind Engineering and Industrial Aerodynamics*, 147:276–282, 2015.

[12] G. Arioli and F. Gazzola. A new mathematical explanation of what triggered the catastrophic torsional mode of the Tacoma Narrows Bridge. *Applied Mathematical Modelling*, 39(2):901–912, 2015.

[13] G. Avalos, I. Lasiecka, and R. Triggiani. Higher regularity of a coupled parabolic-hyperbolic fluid-structure interactive system. *Georgian Mathematical Journal*, 15(3):403–437, 2008.

[14] I. Babuška and A. Aziz. Survey lectures on the mathematical foundations of the finite element method. In *The Mathematical Foundations of the Finite Element Method with Applications to Partial Differential Equations*, pages 1–359. Academic Press, 1972.

[15] M. Badra and T. Takahashi. Feedback stabilization of a simplified 1D fluid–particle system. In *Annales de l'Institut Henri Poincare - Analyse Non Linéaire*, volume 31, pages 369–389. Elsevier, 2014.

[16] M. Badra and T. Takahashi. Feedback boundary stabilization of 2D fluid-structure interaction systems. *Discrete & Continuous Dynamical Systems-A*, 37(5):2315–2373, 2017.

[17] V. Barbu, Z. Grujić, I. Lasiecka, and A. Tuffaha. Existence of the energy-level weak solutions for a nonlinear fluid-structure interaction model. In *Fluids and Waves: Recent Trends in Applied Analysis: Research Conference, May 11-13, 2006, the Universtiy of Memphis, Memphis, TN*, volume 440, pages 55–82. American Mathematical Society, 2007.

[18] V. Barbu, Z. Grujić, I. Lasiecka, and A. Tuffaha. Smoothness of weak solutions to a nonlinear fluid-structure interaction model. *Indiana University Mathematics Journal*, pages 1173–1207, 2008.

[19] C. Bardos, M. C. Lopes Filho, D. Niu, H. Nussenzveig Lopes, and E. S. Titi. Stability of two-dimensional viscous incompressible flows under three-dimensional perturbations and inviscid symmetry breaking. *SIAM Journal on Mathematical Analysis*, 45(3):1871–1885, 2013.

[20] C. W. Bardos and E. S. Titi. Mathematics and turbulence: where do we stand? *Journal of Turbulence*, 14(3):42–76, 2013.

[21] T. Bartsch and A. Pistoia. Critical points of the N-vortex Hamiltonian in bounded planar domains and steady state solutions of the incompressible Euler equations. *SIAM Journal on Applied Mathematics*, 75(2):726–744, 2015.

[22] G. Batchelor. *An Introduction to Fluid Dynamics*. Cambridge University Press, 2000.

[23] U. Battisti, E. Berchio, A. Ferrero, and F. Gazzola. Energy transfer between modes in a nonlinear beam equation. *Journal de Mathématiques Pures et Appliquées*, 108(6):885–917, 2017.

[24] H. Beirão da Veiga. Regularity for Stokes and generalized Stokes systems under nonhomogeneous slip-type boundary conditions. *Advances in Differential Equations*, 9:1079–1114, 2004.

[25] J. A. Bello, E. Fernández-Cara, J. Lemoine, and J. Simon. The differentiability of the drag with respect to the variations of a Lipschitz domain in a Navier-Stokes flow. *SIAM Journal on Control and Optimization*, 35(2):626–640, 1997.

[26] H. Bellout, J. Neustupa, and P. Penel. On the Navier-Stokes equation with boundary conditions based on vorticity. *Mathematische Nachrichten*, 269(1):59–72, 2004.

[27] H. M. Berger. A new approach to the analysis of large deflections of plates. *Journal of Applied Mechanics*, (22):465–472, 1955.

[28] L. Berselli. An elementary approach to the 3D Navier-Stokes equations with Navier boundary conditions: existence and uniqueness of various classes of solutions in the flat boundary case. *Discrete and Continuous Dynamical Systems-Series S*, 3:199–219, 2010.

[29] F. Bethuel, H. Brezis, and F. Helein. *Ginzburg-Landau Vortices*, volume 13. Springer Science & Business Media, 2012.

[30] C. Bègue, C. Conca, F. Murat, and O. Pironneau. A nouveau sur les équations de Stokes et de Navier-Stokes avec des conditions aux limites sur la pression. *Comptes Rendus de l'Académie des Sciences. Série I, Mathématique*, 304(1):23–28, 1987.

[31] C. Bègue, C. Conca, F. Murat, and O. Pironneau. Les équations de Stokes et de Navier-Stokes avec des conditions aux limites sur la pression. In *Nonlinear Partial Differential equations and their Applications, Collège de France Seminar*, volume 9, pages 179–264. Pitman, 1988.

[32] G. Birkhoff. *Hydrodynamics: a study in fact, logic and similitude*. Princeton University Press, 1950.

[33] G. Birkhoff. *Hydrodynamics: a study in fact, logic and similitude*. Princeton University Press, 1960. Second edition, revised and enlarged.

[34] D. Bloor. *The Enigma of the Aerofoil: Rival Theories in Aerodynamics, 1909-1930*. University of Chicago Press, 2011.

[35] M. Boghosian and K. Cassel. On the origins of vortex shedding in two-dimensional incompressible flows. *Theoretical and Computational Fluid Dynamics*, 30(6):511–527, 2016.

[36] M. Bogovskii. Solution of the first boundary value problem for the equation of continuity of an incompressible medium. *Doklady Akademii Nauk*, 248(5):1037–1040, 1979.

[37] M. Bogovskii. Solution of some vector analysis problems connected with operators div and grad. *Trudy Seminar S.L. Sobolev*, 80:5–40, 1980.

[38] D. Bonheure, F. Gazzola, and E. Moreira dos Santos. Mathematical study of the stability of suspended bridges: focus on the fluid-structure interactions. *Research proposal FRB 2018-J1150080-210411 BONHEURE, submitted to the Thelam Fund (Fondation Roi Baudouin, Belgium)*, Available online at: http://homepages.ulb.ac.be/~dbonheur/Thelam.pdf, March 2018.

[39] D. Bonheure, F. Gazzola, and G. Sperone. Eight(y) mathematical questions on fluids and structures. *Rendiconti Lincei - Matematica e Applicazioni*, 30:759–815, 2019.

[40] M. Borsuk and V. Kondrat'ev. *Elliptic Boundary Value Problems of Second Order in Piecewise Smooth Domains*, volume 69. Elsevier, 2006.

[41] M. Boulakia. Existence of weak solutions for an interaction problem between an elastic structure and a compressible viscous fluid. *Journal de Mathématiques Pures et Appliquées*, 84(11):1515–1554, 2005.

[42] M. Boulakia and S. Guerrero. A regularity result for a solid-fluid system associated to the compressible Navier-Stokes equations. In *Annales de l'Institut Henri Poincaré - Analyse Non Linéaire*, volume 26, pages 777–813, 2009.

[43] M. Boulakia and S. Guerrero. Regular solutions of a problem coupling a compressible fluid and an elastic structure. *Journal de Mathématiques Pures et Appliquées*, 94(4):341–365, 2010.

[44] M. Boulakia and S. Guerrero. Local null controllability of a fluid-solid interaction problem in dimension 3. *Journal of the European Mathematical Society*, 15(3):825–856, 2013.

[45] M. Boulakia and S. Guerrero. On the interaction problem between a compressible fluid and a Saint-Venant Kirchhoff elastic structure. *Advances in Differential Equations*, 22(1/2):1–48, 2017.

[46] D. Breit and S. Schwarzacher. Compressible fluids interacting with a linear-elastic shell. *Archive for Rational Mechanics and Analysis*, 228(2):495–562, 2018.

[47] Y. Brenier. Convergence of the Vlasov-Poisson system to the incompressible Euler equations. *Communications in Partial Differential Equations*, 25(3-4):737–754, 2000.

[48] D. Bresch. On bounds of the drag for Stokes flow around a body without thickness. *Commentationes Mathematicae Universitatis Carolinae*, 38(4):665–680, 1997.

[49] D. Bucur, E. Feireisl, and S. Nečasová. Boundary behavior of viscous fluids: influence of wall roughness and friction-driven boundary conditions. *Archive for Rational Mechanics and Analysis*, 197:117–138, 2010.

[50] L. Caretto, A. Gosman, S. Patankar, and D. Spalding. Two calculation procedures for steady, three-dimensional flows with recirculation. In *Proceedings of the Third International Conference on Numerical Methods in Fluid Mechanics*, pages 60–68. Springer, 1973.

[51] L. Cattabriga. Su un problema al contorno relativo al sistema di equazioni di Stokes. *Rendiconti del Seminario Matematico della Università Padova*, 31:308–340, 1961.

[52] F. Caubet and M. Dambrine. Stability of critical shapes for the drag minimization problem in Stokes flow. *Journal de Mathématiques Pures et Appliquées*, 100:327–346, 2013.

[53] T. Chacón Rebollo, V. Girault, F. Murat, and O. Pironneau. Analysis of a coupled fluid-structure model with applications to hemodynamics. *SIAM Journal on Numerical Analysis*, 54(2):994–1019, 2016.

[54] A. Chambolle, B. Desjardins, M. J. Esteban, and C. Grandmont. Existence of weak solutions for the unsteady interaction of a viscous fluid with an elastic plate. *Journal of Mathematical Fluid Mechanics*, 7(3):368–404, 2005.

[55] H. J. Choi and J. R. Kweon. The stationary Navier-Stokes system with no-slip boundary condition on polygons: corner singularity and regularity. *Communications in Partial Differential Equations*, 38(7):1235–1255, 2013.

[56] I. Chueshov. Dynamics of a nonlinear elastic plate interacting with a linearized compressible viscous fluid. *Nonlinear Analysis: Theory, Methods & Applications*, 95:650–665, 2014.

[57] I. Chueshov. Interaction of an elastic plate with a linearized inviscid incompressible fluid. *Communications on Pure & Applied Analysis*, 13(5):1759–1778, 2014.

[58] I. Chueshov, E. H. Dowell, I. Lasiecka, and J. T. Webster. Mathematical aeroelasticity: A survey. *Mathematics in Engineering, Science & Aerospace (MESA)*, 7(1):5–29.

[59] I. Chueshov and B. Schmalfuß. Stochastic dynamics in a fluid–plate interaction model with the only longitudinal deformations of the plate. *Discrete & Continuous Dynamical Systems-B*, 20(3):833–852, 2015.

[60] U. Cisotti. Sopra un paradosso e un principio in idro-aeromeccanica. *Milan Journal of Mathematics*, 1(1):39–43, 1927.

[61] C. Conca, F. Murat, and O. Pironneau. The Stokes and Navier - Stokes equations with boundary conditions involving the pressure. *Japanese Journal of Mathematics*, 20(2):279–318, 1994.

[62] C. Conca, J. San Martín, and M. Tucsnak. Existence of solutions for the equations modelling the motion of a rigid body in a viscous fluid. *Communications in Partial Differential Equations*, 25(5-6):1019–1042, 2000.

[63] P. Constantin and C. Foias. *Navier-Stokes Equations*. University of Chicago Press, 1988.

[64] M. Cooley and M. O'Neill. On the slow rotation of a sphere about a diameter parallel to a nearby plane wall. *IMA Journal of Applied Mathematics*, 4(2):163–173, 1968.

[65] M. Cooley and M. O'Neill. On the slow motion generated in a viscous fluid by the approach of a sphere to a plane wall or stationary sphere. *Mathematika*, 16(1):37–49, 1969.

[66] M. Costabel and M. Dauge. On the inequalities of Babuška-Aziz, Friedrichs and Horgan-Payne. *Archive for Rational Mechanics and Analysis*, 217:873–898, 2015.

[67] M. Coutanceau and R. Bouard. Experimental determination of the main features of the viscous flow in the wake of a circular cylinder in uniform translation. Part I - Steady flow. *Journal of Fluid Mechanics*, 79(2):231–256, 1977.

[68] M. Coutanceau and R. Bouard. Experimental determination of the main features of the viscous flow in the wake of a circular cylinder in uniform translation. Part II - Unsteady flow. *Journal of Fluid Mechanics*, 79(2):257–272, 1977.

[69] M. Coutanceau and J.-R. Defaye. Circular cylinder wake configurations: a flow visualization survey. *Applied Mechanics Reviews*, 44(6):255–305, 1991.

[70] D. Coutand and S. Shkoller. Motion of an elastic solid inside an incompressible viscous fluid. *Archive for Rational Mechanics and Analysis*, 176(1):25–102, 2005.

[71] G. Crasta, A. Falocchi, and F. Gazzola. A new model for suspension bridges involving the convexification of the cables. *ArXiv preprint 1810.02853*, 2018.

[72] G. Crasta, I. Fragalà, and F. Gazzola. A sharp upper bound for the torsional rigidity of rods by means of web functions. *Archive for Rational Mechanics and Analysis*, 164:189–211, 2002.

[73] G. Crasta, I. Fragalà, and F. Gazzola. On a long-standing conjecture by Pólya-Szegö and related topics. *Zeitschrift für angewandte Mathematik und Physik*, 56:763–782, 2005.

[74] G. Crasta and F. Gazzola. Some estimates of the minimizing properties of web functions. *Calculus of Variations*, 15:45–66, 2002.

[75] D. G. Crowdy and S. J. Brzezicki. Analytical solutions for two-dimensional Stokes flow singularities in a no-slip wedge of arbitrary angle. *Proceedings of The Royal Society of London. Series A. Mathematical, Physical and Engineering Sciences*, 473(2202):20170134, 2017.

[76] H. B. da Veiga and L. C. Berselli. Navier-Stokes equations: Green's matrices, vorticity direction, and regularity up to the boundary. *Journal of Differential Equations*, 246(2):597–628, 2009.

[77] A. G. Davenport. Buffeting of a suspension bridge by storm winds. *Journal of the Structural Division*, 88(3):233–270, 1962.

[78] R. W. Davis and E. Moore. A numerical study of vortex shedding from rectangles. *Journal of Fluid Mechanics*, 116:475–506, 1982.

[79] C. De Coster, S. Nicaise, and G. Sweers. Solving the biharmonic Dirichlet problem on domains with corners. *Mathematische Nachrichten*, 288(8-9):854–871, 2015.

[80] C. De Coster, S. Nicaise, and G. Sweers. Comparing variational methods for the hinged Kirchhoff plate with corners. *Mathematische Nachrichten*, 292(12):2574–2601, 2019.

[81] M. de Saint-Venant. Résistance des fluides: considérations historiques, physiques et pratiques relatives au problème de l'action dynamique mutuelle d'un fluide et d'un solide, spécialement dans l'état de permanence supposé acquis par leurs mouvements. *Comptes Rendus des Séances de l'Académie des Sciences, Paris*, 103:179–184, 1886.

[82] W. Dean and M. O'Neill. A slow motion of viscous liquid caused by the rotation of a solid sphere. *Mathematika*, 10(1):13–24, 1963.

[83] M. del Pino and J. Dolbeault. Best constants for Gagliardo-Nirenberg inequalities and applications to nonlinear diffusions. *Journal de Mathématiques Pures et Appliquées*, 81:847–875, 2002.

[84] B. Desjardins and M. J. Esteban. Existence of weak solutions for the motion of rigid bodies in a viscous fluid. *Archive for Rational Mechanics and Analysis*, 146(1):59–71, 1999.

[85] B. Desjardins and M. J. Esteban. On weak solutions for fluid-rigid structure interaction: compressible and incompressible models. *Communications in Partial Differential Equations*, 25(7-8):263–285, 2000.

[86] G. Diana, G. Fiammenghi, M. Belloli, and D. Rocchi. Wind tunnel tests and numerical approach for long span bridges: the Messina bridge. *Journal of Wind Engineering and Industrial Aerodynamics*, 122:38–49, 2013.

[87] G. Diana, F. Resta, M. Belloli, and D. Rocchi. On the vortex shedding forcing on suspension bridge deck. *Journal of Wind Engineering and Industrial Aerodynamics*, 94:341–363, 2006.

[88] G. Diana, D. Rocchi, T. Argentini, and S. Muggiasca. Aerodynamic instability of a bridge deck section model: linear and nonlinear approach to force modeling. *Journal of Wind Engineering and Industrial Aerodynamics*, 98(6-7):363–374, 2010.

[89] T. V. Duoc. Navier-Stokes-Oseen flows in the exterior of a rotating and translating obstacle. *Discrete & Continuous Dynamical Systems-A*, 38(7):3387–3405, 2018.

[90] R. Durán. An elementary proof of the continuity from $L_0^2(\Omega)$ to $H_0^1(\Omega)^n$ of Bogovskii's right inverse of the divergence. *Revista de la Unión Matemática Argentina*, 53(2):59–78, 2012.

[91] C. Dyrbye and S. O. Hansen. *Wind Loads on Structures*. John Wiley & Sons, 1997.

[92] I. Ekeland and R. Temam. *Convex Analysis and Variational Principles*. North-Holland, Amsterdam, 1976.

[93] G. Faber. Beweis, dass unter allen homogenen Membranen von gleicher Fläche und gleicher Spannung die kreisförmige den tiefsten Grundton gibt. *Verlag der Bayerischen Akademie der Wissenschaften*, pages 169–172, 1923.

[94] E. Feireisl. On the motion of rigid bodies in a viscous compressible fluid. *Archive for Rational Mechanics and Analysis*, 167(4):281–308, 2003.

[95] E. Feireisl. On the motion of rigid bodies in a viscous incompressible fluid. In *Nonlinear Evolution Equations and Related Topics*, pages 419–441. Springer, 2003.

[96] V. Ferreira Jr, F. Gazzola, and E. Moreira dos Santos. Instability of modes in a partially hinged rectangular plate. *Journal of Differential Equations*, 261(11):6302–6340, 2016.

[97] A. Ferrero and F. Gazzola. A partially hinged rectangular plate as a model for suspension bridges. *Discrete & Continuous Dynamical Systems-A*, 35:5879–5908, 2015.

[98] J. H. Ferziger and M. Perić. *Computational Methods for Fluid Dynamics*, volume 3. Springer, 2002.

[99] P. F. Fischer, F. Loth, S. E. Lee, S.-W. Lee, D. S. Smith, and H. S. Bassiouny. Simulation of high-Reynolds number vascular flows. *Computer Methods in Applied Mechanics and Engineering*, 196(31-32):3049–3060, 2007.

[100] C. Foias and R. Temam. Structure of the set of stationary solutions of the Navier-Stokes equations. *Communications on Pure and Applied Mathematics*, 30:149–164, 1977.

[101] C. Foias and R. Temam. Remarques sur les équations de Navier-Stokes stationnaires et les phénomènes successifs de bifurcation. *Annali della Scuola Normale Superiore di Pisa - Classe di Scienze*, 5(1):29–63, 1978.

[102] L. Föppl. Wirbelbewegung hinter einem Kreiszylinder. *Verlag der Königlich Bayerischen Akademie der Wissenschaften*, 1(1):1–18, 1913.

[103] S. Franzetti, M. Greco, S. Malavasi, and D. Mirauda. Flow induced excitation on basic shape structures. In *Vorticity and Turbulence Effects in Fluid Structure Interaction - An Application to Hydraulic Structure Design*, chapter 6, pages 131–156. WIT Press, 2006.

[104] K. Friedrichs. On the boundary-value problems of the theory of elasticity and Korn's inequality. *Annals of Mathematics*, 48:441–471, 1947.

[105] U. Frisch and A. N. Kolmogorov. *Turbulence: The Legacy of A.N. Kolmogorov.* Cambridge University Press, 1995.

[106] H. Fujita. On existence of weak solutions of the Navier-Stokes equations in regions with moving boundaries. *Journal of the Faculty of Science, University of Tokyo, Section I: Mathematics*, 17:403–420, 1970.

[107] H. Fujita. On stationary solutions to Navier-Stokes equation in symmetric plane domains under general outflow condition. *Pitman Research Notes in Mathematics Series*, pages 16–30, 1998.

[108] H. Fujita and H. Morimoto. A remark on the existence of steady Navier-Stokes flows in a certain two-dimensional infinite channel. *Tokyo Journal of Mathematics*, 25(2):307–321, 2002.

[109] V. Fuka and J. Brechler. Large eddy simulation of the stable boundary layer. In *Finite Volumes for Complex Applications VI - Problems & Perspectives*, pages 485–493. Springer, 2011. `http://artax.karlin.mff.cuni.cz/~fukav1am/sqcyl.html`.

[110] A. Fursikov and R. Rannacher. Optimal Neumann control for the two-dimensional steady-state Navier-Stokes equations. In *New Directions in Mathematical Fluid Mechanics*, pages 193–221. Springer, 2009.

[111] E. Gagliardo. Caratterizzazioni delle tracce sulla frontiera relative ad alcune classi di funzioni in n variabili. *Rendiconti del Seminario Matematico della Università di Padova*, 27:284–305, 1957.

[112] G. Galdi and V. Heuveline. Lift and sedimentation of particles in the flow of a viscoelastic liquid in a channel. *In: Free and moving boundaries, Lecture Notes in Pure and Applied Mathematics, 252*, Chapman & Hall/CRC, Boca Ratón, Florida:75–110, 2007.

[113] G. Galdi and W. Layton. Approximation of the larger eddies in fluid motions II: A model for space-filtered flow. *Mathematical Models and Methods in Applied Sciences*, 10:343–350, 2000.

[114] G. P. Galdi. Flow of a viscous liquid past an obstacle at arbitrary Reynolds number. Talk given at the Waseda University on November 8th, 2016.

[115] G. P. Galdi. *An Introduction to the Mathematical Theory of the Navier-Stokes Equations: Steady-State Problems.* Springer Science & Business Media, 2011.

[116] G. P. Galdi. On time-periodic flow of a viscous liquid past a moving cylinder. *Archive for Rational Mechanics and Analysis*, 210(2):451–498, 2013.

[117] G. P. Galdi and A. L. Silvestre. Existence of time-periodic solutions to the Navier-Stokes equations around a moving body. *Pacific Journal of Mathematics*, 223:251–267, 2006.

[118] G. P. Galdi and A. L. Silvestre. On the motion of a rigid body in a Navier-Stokes liquid under the action of a time-periodic force. *Indiana University Mathematics Journal*, pages 2805–2842, 2009.

[119] F. Gazzola. On a decomposition of the Hilbert space L^2 and its applications to Stokes problem. *Annali dell'Università di Ferrara*, 41(1):95–115, 1995.

[120] F. Gazzola. Existence of minima for nonconvex functionals in spaces of functions depending on the distance from the boundary. *Archive for Rational Mechanics and Analysis*, 150:57–76, 1999.

[121] F. Gazzola. *Mathematical Models for Suspension Bridges*. MS&A Vol. 15, Springer, 2015.

[122] F. Gazzola, M. Jleli, and B. Samet. On the Melan equation for suspension bridges. *Journal of Fixed Point Theory and Applications*, 16(1-2):159–188, 2014.

[123] F. Gazzola and P. Secchi. Inflow-outflow problems for Euler equations in a rectangular cylinder. *Nonlinear Differential Equations and Applications*, 8:195–217, 2001.

[124] F. Gazzola and G. Sperone. Steady Navier-Stokes equations in planar domains with obstacle and explicit bounds for unique solvability. Preprint.

[125] F. Gazzola and G. Sperone. Navier-Stokes equations interacting with plate equations. *Annual Report of the Politecnico di Milano PhD School*, 2017.

[126] F. Gazzola and G. Sperone. Thresholds for hanger slackening and cable shortening in the Melan equation for suspension bridges. *Nonlinear Analysis: Real World Applications*, 39:520–536, 2018.

[127] F. Gazzola and G. Sperone. Boundary conditions for planar Stokes equations inducing vortices around concave corners. *Milan Journal of Mathematics*, 87(2):1–31, 2019.

[128] F. Gazzola, Y. Wang, and R. Pavani. Variational formulation of the Melan equation. *Mathematical Methods in the Applied Sciences*, 2017. DOI: 10.1002/mma.3962.

[129] D. Gérard-Varet and M. Hillairet. Existence of weak solutions up to collision for viscous fluid-solid systems with slip. *Communications on Pure and Applied Mathematics*, 67(12):2022–2076, 2014.

[130] G. Geymonat and F. Krasucki. On the existence of the Airy function in Lipschitz domains. Application to the traces of H^2. *Comptes Rendus de l'Académie des Sciences I*, 330(5):355–360, 2000.

[131] V. Girault. Curl-conforming finite element methods for Navier-Stokes equations with non-standard boundary conditions in $\mathbb{R}^3$. In *The Navier-Stokes Equations: Theory and Numerical Methods*, pages 201–218. Springer, 1990.

[132] V. Girault and P.-A. Raviart. *Finite Element Methods for Navier-Stokes Equations: Theory and Algorithms*, volume 5. Springer Science & Business Media, 2012.

[133] O. Glass and F. Sueur. Uniqueness results for weak solutions of two-dimensional fluid–solid systems. *Archive for Rational Mechanics and Analysis*, 218(2):907–944, 2015.

[134] C. Grandmont and Y. Maday. Existence de solutions d'un problème de couplage fluide-structure bidimensionnel instationnaire. *Comptes Rendus de l'Académie des Sciences. Série I, Mathématique*, 326(4):525–530, 1998.

[135] D. Gérard-Varet. Some recent mathematical results on fluid-solid interaction. In *Lectures on the Analysis of Nonlinear Partial Differential Equations, Part III. Morningside Lectures in Mathematics 3*. International Press, Somerville, MA, 2013.

[136] G. Grimberg, W. Pauls, and U. Frisch. Genesis of d'Alembert's paradox and analytical elaboration of the drag problem. *Physica D: Nonlinear Phenomena*, 237(14-17):1878–1886, 2008.

[137] P. Grisvard. *Elliptic Problems in Nonsmooth Domains*. Pitman Advanced Publishing Program, 1985.

[138] M. D. Gunzburger, H.-C. Lee, and G. A. Seregin. Global existence of weak solutions for viscous incompressible flows around a moving rigid body in three dimensions. *Journal of Mathematical Fluid Mechanics*, 2(3):219–266, 2000.

[139] S. Hansen. Vortex-induced vibrations of structures. In *Structural Engineers World Congress 2007, Bangalore, India*, pages 2–7, 2007. `http://www.eurocodes.fi/1991/1991-1-4/background/Hansen_2007.pdf`.

[140] H. Helmholtz. Über Integrale der hydrodynamischen Gleichungen, welche den Wirbelbewegungen entsprechen. *Journal für die reine und angewandte Mathematik*, 55:25–55, 1858.

[141] M. Hillairet. Lack of collision between solid bodies in a 2D incompressible viscous flow. *Communications in Partial Differential Equations*, 32(9):1345–1371, 2007.

[142] M. Hillairet and T. Takahashi. Collisions in three-dimensional fluid structure interaction problems. *SIAM Journal on Mathematical Analysis*, 40(6):2451–2477, 2009.

[143] M. Hillairet and T. Takahashi. Blow up and grazing collision in viscous fluid solid interaction systems. In *Annales de l'Institut Henri Poincare - Analyse Non Linéaire*, volume 27, pages 291–313, 2010.

[144] J. Hoffman, J. Jansson, and C. Johnson. New theory of flight. *Journal of Mathematical Fluid Mechanics*, 18(2):219–241, 2016.

[145] J. Hoffman and C. Johnson. The mathematical secret of flight. *Normat*, 57(4):1–25, 2009.

[146] J. Hoffman and C. Johnson. Resolution of d'Alembert's paradox. *Journal of Mathematical Fluid Mechanics*, 12(3):321–334, 2010.

[147] K.-H. Hoffmann and V. N. Starovoitov. On a motion of a solid body in a viscous fluid: two-dimensional case. *Advances in Mathematical Sciences and Applications*, 9(2):633–648, 1996.

[148] K.-H. Hoffmann and V. N. Starovoitov. Zur Bewegung einer Kugel in einer zähen Flüssigkeit. *Documenta Mathematica*, 5(15-21):30, 2000.

[149] E. Hopf. Über die Anfangswertaufgabe für die hydrodynamischen Grundgleichungen. *Mathematische Nachrichten*, 4(1-6):213–231, 1950.

[150] E. Hopf. On non-linear partial differential equations. In *Lecture Series of the Symposium on Partial Differential Equations, Berkeley*, pages 1–31. University of Kansas Press, 1957.

[151] C. Horgan and L. Payne. On inequalities of Korn, Friedrichs and Babuška-Aziz. *Archive for Rational Mechanics and Analysis*, 82:165–179, 1983.

[152] A. Hundertmark, M. Lukáčová-Medviďová, and Š. Nečasová. On the weak solution of the fluid-structure interaction problem for shear-dependent fluids. In *Recent Developments of Mathematical Fluid Mechanics*, pages 291–319. Springer, 2016.

[153] C. P. Jackson. A finite-element study of the onset of vortex shedding in flow past variously shaped bodies. *Journal of Fluid Mechanics*, 182:23–45, 1987.

[154] C. Johnson. The Secret of Flight (personal blog). `https://secretofflight.wordpress.com/media/`.

[155] C. Josserand, Y. Pomeau, and S. Rica. Vortex shedding in a model of superflow. *Physica D: Nonlinear Phenomena*, 134(1):111–125, 1999.

[156] R. Kellogg and J. Osborn. A regularity result for the Stokes problem in a convex polygon. *Journal of Functional Analysis*, 21(4):397–431, 1976.

[157] G. Kirchhoff. *Vorlesungen über Mathematische Physik*. B. G. Teubner, Leipzig, 1876.

[158] V. A. Kondrat'ev. Boundary value problems for elliptic equations in domains with conical or angular points. *Trudy Moskovskogo Matematicheskogo Obshchestva*, 16:209–292, 1967.

[159] V. A. Kondrat'ev and O. A. Oleinik. Boundary-value problems for partial differential equations in non-smooth domains. *Russian Mathematical Surveys*, 38(2):1–86, 1983.

[160] A. Korn. Über die Cosserat'schen Funktionentripel und ihre Anwendung in der Elastizitätstheorie. *Acta Mathematica*, 32:81–96, 1909.

[161] M. V. Korobkov, K. Pileckas, and R. Russo. Solution of Leray's problem for stationary Navier-Stokes equations in plane and axially symmetric spatial domains. *Annals of Mathematics*, 181:769–807, 2015.

[162] E. Krahn. Über eine von Rayleigh formulierte Minimaleigenschaft des Kreises. *Mathematische Annalen*, 94(1):97–100, 1925.

[163] D. N. Ku. Blood flow in arteries. *Annual Review of Fluid Mechanics*, 29(1):399–434, 1997.

[164] H. G. Küssner. Zusammenfassender Bericht über den instationären Auftrieb von flügeln. *Luftfahrtforschung*, 13(12):410–424, 1936.

[165] M. Kutta. Über eine mit den Grundlagen des Flugsproblems in Beziehung stehende zweidimensionale Strömung. *Sitzungsberichte der Königlich Bayerischen Akademie der Wissenschaften*, 40:1–58, 1910.

[166] O. S. Kwon and J. R. Kweon. For the vorticity–velocity–pressure form of the Navier-Stokes equations on a bounded plane domain with corners. *Nonlinear Analysis: Theory, Methods & Applications*, 75(5):2936–2956, 2012.

[167] W. Lacarbonara. *Nonlinear Structural Mechanics: Theory, Dynamical Phenomena and Modeling*. Springer Science & Business Media, 2013.

[168] O. A. Ladyzhenskaya. Solution "in the large" of the nonstationary boundary value problem for the Navier-Stokes system with two space variables. *Communications in Pure and Applied Mathematics*, 12:427–433, 1959.

[169] O. A. Ladyzhenskaya. *The Mathematical Theory of Viscous Incompressible Flow*, volume 76. Gordon and Breach New York, 1969.

[170] O. A. Ladyzhenskaya and V. Solonnikov. Some problems of vector analysis and generalized formulations of boundary-value problems for the Navier-Stokes equations. *Journal of Soviet Mathematics*, 10:257–286, 1978.

[171] H. Lamb. *Hydrodynamics*. Cambridge University Press, 6th edition, 1975.

[172] L. Landau. On the problem of turbulence. *Doklady Akademii Nauk SSSR*, 44:311–314, 1944.

[173] L. Landau and E. Lifshitz. *Theoretical Physics: Fluid Mechanics*, volume 6. Pergamon Press, 1987.

[174] W. E. Langlois and M. O. Deville. *Slow Viscous Flow*. Springer Science & Business Media, 2014.

[175] A. Larsen. Advances in aeroelastic analyses of suspension and cable-stayed bridges. *Journal of Wind Engineering and Industrial Aerodynamics*, 74:73–90, 1998.

[176] I. Lasiecka and A. Tuffaha. Riccati equations arising in boundary control of fluid structure interactions. *International Journal of Computing Science and Mathematics*, 1(1):128–146, 2007.

[177] I. Lasiecka and J. T. Webster. Eliminating flutter for clamped von Kármán plates immersed in subsonic flows. *Communications on Pure & Applied Analysis*, 13(5):1935–1969, 2014.

[178] I. Lasiecka and J. T. Webster. Nonlinear plates interacting with a subsonic, inviscid flow via Kutta–Joukowski interface conditions. *Nonlinear Analysis: Real World Applications*, 17:171–191, 2014.

[179] J. le Rond d'Alembert. Theoria resistentiae quam patitur corpus in fluido motum, ex principiis omnino novis et simplissimus deducta, habita ratione tum velocitatis, figurae, et massae corporis moti, tum densitatis compressionis partium fluidi. *Berlin-Brandenburgische Akademie der Wissenschaften*, 1749.

[180] J. le Rond d'Alembert. *Essai d'une Nouvelle Théorie de la Résistance des Fluides*. David l'aîné, Paris, 1752.

[181] J. le Rond d'Alembert. Paradoxe proposé aux géomètres sur la résistance des fluides. *Opuscules Mathématiques*, 5, Mémoire XXXIV, I:132–138, 1768.

[182] J. le Rond d'Alembert. Sur la résistance des fluides. *Opuscules Mathématiques*, 8:210–230, 1780.

[183] J. Leray. Étude de diverses équations intégrales non linéaires et de quelques problèmes que pose l'hydrodynamique. *Journal de Mathématiques Pures et Appliquées*, 12:1–82, 1933.

[184] L. Li, Z. Jiang, and X. Cai. Solutions for stationary Navier-Stokes equations with non-homogeneous boundary conditions in symmetric domains of $\mathbb{R}^n$. *Journal of Mathematical Analysis and Applications*, 469(1):1–15, 2019.

[185] C. Lin. On the motion of vortices in two dimensions I. Existence of the Kirchhoff-Routh function. *Proceedings of the National Academy of Sciences of the United States of America*, 27:570–575, 1941.

[186] C. Lin. On the motion of vortices in two dimensions II. Some further properties on the Kirchhoff-Routh function. *Proceedings of the National Academy of Sciences of the United States of America*, 27:575–577, 1941.

[187] J.-L. Lions. *Quelques Méthodes de Résolution de Problèmes aux Limites Non Linéaires*. Dunod, Paris, 1969.

[188] J. Luco and J. Turmo. Effect of hanger flexibility on dynamic response of suspension bridges. *Journal of Engineering Mechanics*, 136:1444–1459, 2010.

[189] A. Majda and A. Bertozzi. *Vorticity and Incompressible Flow*, volume 27. Cambridge University Press, 2002.

[190] M. Manarini. Sui paradossi di d'Alembert e di Brillouin nella dinamica dei fluidi. *Bollettino dell'Unione Matematica Italiana*, 4(4):352–353, 1949.

[191] C. Marchioro. On the inviscid limit for a fluid with a concentrated vorticity. *Communications in Mathematical Physics*, 196(1):53–65, 1998.

[192] C. Marchioro and M. Pulvirenti. Euler evolution for singular initial data and vortex theory. *Communications in Mathematical Physics*, 91(4):563–572, 1983.

[193] C. Marchioro and M. Pulvirenti. *Mathematical Theory of Incompressible Nonviscous Fluids*. Springer-Verlag, New York, 1994.

[194] P. Maremonti. Classical solution to the Navier-Stokes system. In *Navier—Stokes Equations and Related Nonlinear Problems*, pages 147–152. Springer, 1995.

[195] E. Marušić-Paloka. Rigorous justification of the Kirchhoff law for junction of thin pipes filled with viscous fluid. *Asymptotic Analysis*, 33(1):51–66, 2003.

[196] V. Maz'ya. *Sobolev Spaces with Applications to Elliptic Partial Differential Equations*. Springer, 2011.

[197] V. Maz'ya and J. Rossmann. *Elliptic Equations in Polyhedral Domains*. Number 162. American Mathematical Society, 2010.

[198] J. Melan. *Theory of Arches and Suspension Bridges (Myron Clark, London, 1913)*, volume 2. Myron Clark Publ. Comp. London, 1913.

[199] V. Meleshko. Biharmonic problem in a rectangle. In *In Fascination of Fluid Dynamics*, pages 217–249. Springer, 1998.

[200] V. Meleshko. Selected topics in the history of the two-dimensional biharmonic problem. *Applied Mechanics Reviews*, 56(1):33–85, 2003.

[201] J. Michell. On the direct determination of stress in an elastic solid, with application to the theory of plates. *Proceedings of the London Mathematical Society*, 1(1):100–124, 1899.

[202] H. Morimoto. A remark on the existence of 2-D steady Navier-Stokes flow in bounded symmetric domain under general outflow condition. *Journal of Mathematical Fluid Mechanics*, 9(3):411–418, 2007.

[203] B. Muha and S. Čanić. Fluid-structure interaction between an incompressible, viscous 3D fluid and an elastic shell with nonlinear Koiter membrane energy. *Interfaces and Free Boundaries*, 17(4):465, 2015.

[204] B. R. Munson, T. H. Okiishi, W. W. Huebsch, and A. P. Rothmayer. *Fundamentals of Fluid Mechanics*. John Wiley & Sons, 2013.

[205] C. Navier. Mémoire sur les lois du mouvement des fluides. *Mémoires de l'Acédemie des Sciences de l'Institut de France*, 2:389–440, 1823.

[206] S. A. Nazarov, A. Stylianou, and G. Sweers. Hinged and supported plates with corners. *Zeitschrift für angewandte Mathematik und Physik*, 63:929–960, 2012.

[207] Š. Nečasová and J. Wolf. On the existence of global strong solutions to the equations modeling a motion of a rigid body around a viscous fluid. *Discrete & Continuous Dynamical Systems-A*, 36(3):1539–1562, 2016.

[208] P. Newton. *The N-vortex Problem*. Springer-Verlag, Berlin, 2001.

[209] T. H. Nguyen. Periodic motions of Stokes and Navier–Stokes flows around a rotating obstacle. *Archive for Rational Mechanics and Analysis*, 213(2):689–703, 2014.

[210] H. Oertel. *Prandtl's Essentials of Fluid Mechanics*. Springer Science & Business Media, 2004.

[211] M. O'Neill and K. Stewartson. On the slow motion of a sphere parallel to a nearby plane wall. *Journal of Fluid Mechanics*, 27(4):705–724, 1967.

[212] J. H. Ortega, L. Rosier, and T. Takahashi. Classical solutions for the equations modelling the motion of a ball in a bidimensional incompressible perfect fluid. *ESAIM: Mathematical Modelling and Numerical Analysis*, 39(1):79–108, 2005.

[213] C. W. Oseen. Über die Stokes'sche Formel und über eine verwandte Aufgabe in der Hydrodynamik. *Arkiv för Matematik, Astronomi och Fysik*, 29:1–20, 1910.

[214] F. Pacard and T. Rivière. Linear and Nonlinear Aspects of Vortices: The Ginzburg-Landau Model. In *Progress in Nonlinear Differential Equations and their Applications*, volume 39. Birkhäuser, Boston, 2000.

[215] M. P. Paidoussis. *Fluid-Structure Interactions: Slender Structures and Axial Flow*, volume 1. Academic Press, 1998.

[216] M. P. Païdoussis, S. J. Price, and E. De Langre. *Fluid-Structure Interactions: Cross-Flow-Induced Instabilities*. Cambridge University Press, 2010.

[217] M. P. Païdoussis, S. J. Price, and E. De Langre. *Fluid-Structure Interactions: Cross-Flow-Induced Instabilities*. Cambridge University Press, 2011.

[218] C. Parés. Existence, uniqueness and regularity of solution of the equations of a turbulence model for incompressible fluids. *Applicable Analysis*, 43:245–296, 1992.

[219] O. Pironneau. On optimum profiles in Stokes flow. *Journal of Fluid Mechanics*, 59:117–128, 1973.

[220] O. Pironneau. On optimum design in fluid mechanics. *Journal of Fluid Mechanics*, 64:97–110, 1974.

[221] W. Podolny. *Cable-Suspended Bridges*. In: Structural Steel Designer's Handbook: AISC, AASHTO, AISI, ASTM, AREMA, and ASCE-07 Design Standards. By R.L. Brockenbrough and F.S. Merritt, 5th Edition, McGraw-Hill, 2011.

[222] A. D. Polyanin and A. V. Manzhirov. *Handbook of Integral Equations*. Chapman & Hall/CRC, 2008.

[223] S. B. Pope. *Turbulent Flows*, volume 3. Cambridge University Press, 2000.

[224] B. Protas. Higher-order Föppl models of steady wake flows. *Physics of Fluids*, 18(11):117109, 2006.

[225] B. Protas. Vortex dynamics models in flow control problems. *Nonlinearity*, 21(9):R203, 2008.

[226] O. Reynolds. An experimental investigation of the circumstances which determine whether the motion of water shall be direct or sinuous, and of the law of resistance in parallel channels. *Philosophical Transactions of the Royal Society of London*, (174):935–982, 1883.

[227] P. G. Saffman. *Vortex Dynamics*. Cambridge University Press, 1992.

[228] M. Sahin and R. Owens. A numerical investigation of wall effects up to high blockage ratios on two-dimensional flow past a confined circular cylinder. *Physics of Fluids*, 16:1305–1320, 2004.

[229] J. San Martín, V. N. Starovoitov, and M. Tucsnak. Global weak solutions for the two-dimensional motion of several rigid bodies in an incompressible viscous fluid. *Archive for Rational Mechanics and Analysis*, 161(2):113–147, 2002.

[230] R. H. Scanlan. The action of flexible bridges under wind I: Flutter theory. *Journal of Sound and Vibration*, 60(2):187–199, 1978.

[231] R. H. Scanlan. Developments in low-speed aeroelasticity in the civil engineering field. *AIAA Journal*, 20(6):839–844, 1982.

[232] R. H. Scanlan and J. J. Tomko. Airfoil and bridge deck flutter derivatives,. *Journal of Engineering Mechanics (ASCE)*, 97:1717–1737, 1971.

[233] G. Schewe. Reynolds-number-effects in flow around a rectangular cylinder with aspect ratio 1:5. *Journal of Fluids and Structures*, 39:15–26, 2013.

[234] W. R. Sears. Airofoil theory for non–uniform motion. *Journal of Aeronautical Sciences*, 5(9):10, 1938.

[235] W. R. Sears. Some aspects of non-stationary airfoil theory and its practical application. *Journal of the Aeronautical Sciences*, 8(3):104–108, 1941.

[236] B. Semper. Finite element methods for suspension bridge models. *Computers & Mathematics with Applications*, 26:77–91, 1993.

[237] B. Semper. A mathematical model for suspension bridge vibration. *Mathematical and Computer Modelling*, 18:17–28, 1993.

[238] B. Semper. Finite element approximation of a fourth order integro-differential equation. *Applied Mathematics Letters*, 7:59–62, 1994.

[239] S. Serfaty. Coulomb Gases and Ginzburg-Landau Vortices. In *Zürich Lectures in Advanced Mathematics*. European Mathematical Society (EMS), Zürich, 2015.

[240] S. Serfaty. Mean field limits of the Gross-Pitaevskii and parabolic Ginzburg-Landau equations. *Journal of the American Mathematical Society*, 30(3):713–768, 2017.

[241] D. Serre. Chute libre d'un solide dans un fluide visqueux incompressible. Existence. *Japan Journal of Applied Mathematics*, 4(1):99, 1987.

[242] J. Serrin. Mathematical Principles of Classical Fluid Mechanics. In *Fluid Dynamics I / Strömungsmechanik I,* pp.125–263. Encyclopedia of Physics / Handbuch der Physik, Springer, 1959.

[243] A. Smith. On the stability of Föppl's vortices. *Journal of Applied Mechanics*, 40(2):610–612, 1973.

[244] V. Solonnikov and V. Shchadilov. A certain boundary value problem for the stationary system of Navier-Stokes equations. *Trudy Matematich. Instituta imeni V. A. Steklova*, 125:196–210, 1973.

[245] I. Stampouloglou and E. Theotokoglou. Additional separated-variable solutions of the biharmonic equation in polar coordinates. *Journal of Applied Mechanics*, 77(2):021003, 2010.

[246] V. N. Starovoitov. Nonuniqueness of a solution to the problem on motion of a rigid body in a viscous incompressible fluid. *Journal of Mathematical Sciences*, 130(4):4893–4898, 2005.

[247] K. Stewartson. D'Alembert's Paradox. *SIAM Review*, 23(3):308–343, 1981.

[248] J. Stoker. Hydrodynamics: a study in logic, fact, and similitude (book review). *Bulletin of the American Mathematical Society*, 57:497–499, 1951.

[249] G. G. Stokes. On the theories of the internal friction of fluids in motion, and of the equilibrium and motion of elastic solids. *Transactions of the Cambridge Philosophical Society*, 8:287–305, 1845.

[250] G. G. Stokes. On the effect of the internal friction of fluids on the motion of pendulums,. *Transactions of the Cambridge Philosophical Society*, 9:8–106, 1851.

[251] G. Sweers. A survey on boundary conditions for the biharmonic. *Complex Variables and Elliptic Equations*, 54(2):79–93, 2009.

[252] G. Szegö. Über einige neue Extremaleigenschaften der Kugel. *Mathematische Zeitschrift*, 33:419–425, 1931.

[253] T. Takahashi and M. Tucsnak. Global strong solutions for the two-dimensional motion of an infinite cylinder in a viscous fluid. *Journal of Mathematical Fluid Mechanics*, 6(1):53–77, 2004.

[254] T. Takahashi, M. Tucsnak, and G. Weiss. Stabilization of a fluid–rigid body system. *Journal of Differential Equations*, 259(11):6459–6493, 2015.

[255] S. Tang and N. Aubry. On the symmetry breaking instability leading to vortex shedding. *Physics of Fluids*, 9(9):2550–2561, 1997.

[256] G. Tarantello. Selfdual Gauge Field Vortices - an Analytical Approach. In *Progress in Nonlinear Differential Equations and their Applications*, volume 72. Birkhäuser, Boston, 2008.

[257] R. Temam. *Navier-Stokes Equations: Theory and Numerical Analysis*. North-Holland Publishing Company, 1979.

[258] T. Theodorsen. General theory of aerodynamic instability and the mechanism of flutter. *NASA Thecnical Report*, (496), 1935.

[259] S. Timoshenko. Theory of suspension bridges - Part I. *Journal of the Franklin Institute*, 235:213–238, 1943.

[260] S. Timoshenko. Theory of suspension bridges - Part II. *Journal of the Franklin Institute*, 235:327–349, 1943.

[261] M. Velte. Stabilität und Verzweigung stationärer Lösungen der Navier-Stokesschen Gleichungen beim Taylorproblem. *Archive for Rational Mechanics and Analysis*, 22:1–14, 1966.

[262] T. von Kármán. *Aerodynamics*. Cornell University Press, McGraw-Hill, 1963.

[263] T. von Kármán and M. A. Biot. *Mathematical Methods in Engineering: An Introduction to the Mathematical Treatment of Engineering Problems*. McGraw-Hill, 1940.

[264] R. von Mises. *Theory of Flight*. Dover Publications, 1959.

[265] V. Šverák. Selected Topics in Fluid Mechanics. `http://www-users.math.umn.edu/~sverak/course-notes2011.pdf`.

[266] H. Wagner. Über die Entstehung des dynamischen Auftriebes von Tragflügeln. *Zeitschrift für Angewandte Mathematik und Mechanik*, 5(1):17–35, 1925.

[267] E. Weinan. Dynamics of vortices in Ginzburg-Landau theories with applications to superconductivity. *Physica D: Nonlinear Phenomena*, 77(4):383–404, 1994.

[268] C. Williamson and R. Govardhan. Vortex-induced vibrations. *Annual Review of Fluid Mechanics*, 36:413–455, 2004.

[269] C. Williamson and R. Govardhan. A brief review of recent results in vortex-induced vibrations. *Journal of Wind Engineering and Industrial Aerodynamics*, 96(6-7):713–735, 2008.

[270] G. Wollmann. Preliminary analysis of suspension bridges. *Journal of Bridge Engineering*, 6:227–233, 2001.

[271] X. Wu, F. Ge, and Y. Hong. A review of recent studies on vortex-induced vibrations of long slender cylinders. *Journal of Fluids and Structures*, 28:292–308, 2012.

[272] S. C. Yen and C. W. Yang. Flow patterns and vortex shedding behavior behind a square cylinder. *Journal of Wind Engineering and Industrial Aerodynamics*, 99(8):868–878, 2011.

[273] A. Zebib. Stability of viscous flow past a circular cylinder. *Journal of Engineering Mathematics*, 21(2):155–165, 1987.

[274] N. Zhukovsky. On annexed vortices (in Russian). *Transactions of the Physical Section of the Imperial Society of the Friends of Natural Science, Moscow*, 13:12–25, 1906.